



GREEN SYNTHESIS OF SYMMETRICAL CARBONATE FT-IR STUDY

Adina-Elena Segneanu^{1*}, Raluca Pop¹, Ionel Balcu¹, Corina Macarie¹,
Marius Milea², Raluca Martagiu¹

¹National Institute of R&D for Electrochemistry and Condensed Matter – INCEMC– Timisoara,
144 A. P. Podeanu Street, 300569 Timisoara, Romania

²University „Politehnica” Timisoara, Faculty of Industrial Chemistry and Environment Engineering,
2 Victoriei Square, 300006 Timisoara, Romania

Abstract

An original method for the preparation of *N,N'*-bis(endo-5-norbornen-2,3-dicarboxy-imidyl) carbonate from endo-*N*-hydroxy-5-norbornen-2,3-dicarboximide in basic catalyst has been investigated. FT-IR studies performed in order to monitor the reaction allowed the identifying of the laboratory optimal conditions (reaction time, molar ratio). The method requires limited quantities of organic solvents and reagents, leading to an economical and environmental friendly process for the preparation of a new symmetrical organic carbonate.

Key words: endo-*N*-hydroxy-5-norbornen-2,3-dicarboximide, symmetrical reactive carbonates

Received: February, 2010; Revised final: July 2010; Accepted: August, 2010

1. Introduction

Within the current orientation of organic synthesis and, in general, of chemistry towards the sustainable chemical development (green chemistry), the use and expansion of non-polluting chemical technologies, and towards the environmental protection by the replacement of chemical toxic compounds, the use of the phosgene derivatives in the carbonylation reactions has been avoided.

Reactive organic carbonates with leaving groups are considered non-toxic phosgene substitutes (Segneanu et al., 2009). The increase of their reactivity is due to the electron withdrawing effect of the succinimidyl, phthalimidyl and 5-norbornen-2,3-dicarboximidyl groups, respectively. Symmetrical organic carbonates with leaving groups have been used in order to obtain important intermediates used in biochemistry and pharmaceutical industry.

The reactivity studies of succinimidyl, phthalimidyl and 5-norbornen-2,3-dicarboximidyl carbonates towards oxygen and nitrogen nucleophiles proved to be useful due to the applicability of the

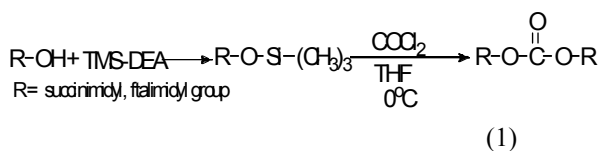
resulting compounds in avant-garde fields of chemistry, such as biochemistry and the pharmaceutical industry (Segneanu, 2006; Segneanu, 2007).

Symmetrical organic carbonates like *N,N'*-disuccinimidyl carbonate, *N,N'*-diphtalimidyl carbonate or *N,N'*-bis(5-norbornen-2,3-dicarboximidyl) carbonate were obtained from the reaction between the *N*-hydroxy compound (R-OH, where R is the succinimidyl, phthalimidyl or the 5-norbornen-2,3-dicarboximidyl group) and a silylation agent, followed by the reaction between phosgene and the silylated compound.

An alternative for the synthesis of the above-mentioned compounds is represented by the reaction between the *N*-hydroxy compounds and diphosgene in the presence of a non-polar solvent (xylene), as presented in the reaction (1) (Ogura, 1982).

The symmetrical organic carbonates have many important applications: they may be used for the insertion of a carbonyl group between amino, hydroxyl and thio groups for the synthesis of urea, carbamates, dithiocarbamates and isothiocyanates.

* Author to whom all correspondence should be addressed: e-mail: s_adinaelena@yahoo.com



They can also be used as dehydrating agents. Another important application is the peptide synthesis area, where they are used for the preparation of the reactive esters of the amino acids (Ogura, 1982).

The *N*-hydroxyimide derivatives show both a weak acid character and a nucleofuge-like behavior in the nucleophilic substitution reactions, due to their electron withdrawing effect. There are a number of studies concerning the ester derivatives of the *N*-hydroxyl compounds rather than regarding the reactions or the properties of the *N*-hydroxyimide cycles (Imajo, 1981).

The aim of this paper is to prepare a new symmetrical reactive carbonate by minimizing the pollution and reducing the quantity of chemical waste with negative impact on the environment and human health. By means of FT-IR spectroscopy, the synthesis of the *N,N'*-bis(endo-5-norbornen-2,3-dicarboximidyl) carbonate starting from the endo-*N*-hydroxy-5-norbornen-2,3-dicarboximide, a coupling reagent used in the synthesis of the peptides, both in solution- and solid-phase, was monitored.

This paper reports the investigation of new symmetrical reactive carbonate with leaving groups by an original procedure.

2. Materials and methods

The IR spectra were recorded in KBr pellets (in the case of solid compounds) and the reaction monitoring was carried out in thermostatic silicon cells of 0.137 mm thickness on a Jasco FT/IR-430 instrument. All reagents were purchased from chemical suppliers and used without further purification.

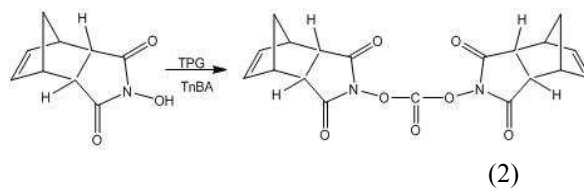
Endo-*N*-hydroxyl-5-norbornen-2,3-dicarboximide (110.8 mg, 0.618 mmol) was dissolved in tetrahydrofuran (15 mL), bis(trichloromethyl) carbonate (TPG) (60.6 mg, 0.204 mmol) and tri-*n*-butylamine (288 μ l, 2.87 mmol) was added. The reaction mixture was stirred at room temperature and then was monitored by FT-IR spectroscopy.

3. Results and discussions

The described procedure for the preparation of reactive succinimidyl and phthalimidyl carbonates was investigated (Kundu, 1994), also the results of IR monitoring of the synthesis of *N,N'*-bis(endo-5-norbornen-2,3-dicarboximidyl) carbonate were used in order to develop a new efficient synthetic route for symmetrical norbornenyl carbonates (1) starting from endo-*N*-hydroxy-5-norbornen-2,3-dicarboximide (reaction (2)).

The IR monitoring of the reaction was necessary for the identifying of the optimal laboratory

conditions (reaction time, molar ratio), and for the determination of the symmetrical norbornene carbonate formation, respectively.



The reaction occurs in a heterogeneous medium, at room temperature (25°C) due to the low solubility of the endo-*N*-hydroxy-5-norbornen-2,3-dicarboximide in THF. First, the IR spectrum of the mixture between the endo-*N*-hydroxy-5-norbornen-2,3-dicarboximide and bis(trichloromethyl) carbonate in THF was recorded, followed by the IR spectrum of the mixture of endo-*N*-hydroxy-5-norbornen-2,3-dicarboximide, bis(trichloromethyl) carbonate and tri-*n*-butylamine in THF.

The spectroscopic data obtained in the 2500-1400 cm^{-1} region (Fig. 1) led to the following statements: in the first minutes after the tri-*n*-butylamine was added in the reaction mixture (endo-*N*-hydroxy-5-norbornen-2,3-dicarboximide and bis(trichloromethyl) carbonate in THF) the pronounced decrease of the endo-*N*-hydroxyl-5-norbornen-2,3-dicarboximide absorption bands around 1720 cm^{-1} simultaneous to an increase of the 1754 cm^{-1} band and to the appearance of an intense band corresponding to the *N,N'*-bis(endo-5-norbornen-2,3-dicarboximidyl) carbonate around 1857 cm^{-1} may be observed.

The IR spectra of the reaction mixture (recorded at different moments after the reaction began) show the disappearance of the valence vibrations band of the carbonyl group from the symmetrical carbonate; their intensity is simultaneously decreasing with increasing of the reaction time. Thus, the spectrum recorded at 22 hours at room temperature after the reaction began, testifies the disappearance of the 1857 cm^{-1} band and the diminishing of the intensity of the 1754 cm^{-1} band, simultaneously to the increase of the intensity of the 2336 cm^{-1} band, confirming the total decomposition of the *N,N'*-bis(endo-5-norbornen-2,3-dicarboximidyl) carbonate (Fig. 1).

Also, a FT-IR study regarding the molar ratio influence on the synthesis of the *N,N'*-bis(endo-5-norbornen-2,3-dicarboximidyl) carbonate was performed (Fig. 2).

The performed studies on the synthesis of *N,N'*-bis(endo-5-norbornen-2,3-dicarboximidyl) carbonate showed that, when two bis(trichloromethyl) carbonate equivalents are added at room temperature, there are no changes in the intensity of the specific symmetrical norbornene carbonate bands (1754 and 1856 cm^{-1}). Also, the increase of the reaction time leads to a decrease (up to disappearance) of the corresponding absorption bands of the *N,N'*-bis(endo-5-norbornen-2,3-dicarboxi-

midyl) carbonate, confirming its decomposition as resulted from the IR spectrum recorded after a 22 hours reaction time (Fig. 2).

In order to determine the optimal conditions for the synthesis of the *N,N'*-bis-(endo-5-norbornen-2,3-dicarboximidyl) carbonate starting from endo-*N*-

hydroxy-5-norbornen-2,3-dicarboximide, bis(trichloro methyl) carbonate and tri-*n*-butylamine in THF, it was performed a comparative study of the synthesis of the symmetrical carbonate by varying the molar ratio of the reactants (Fig. 3).

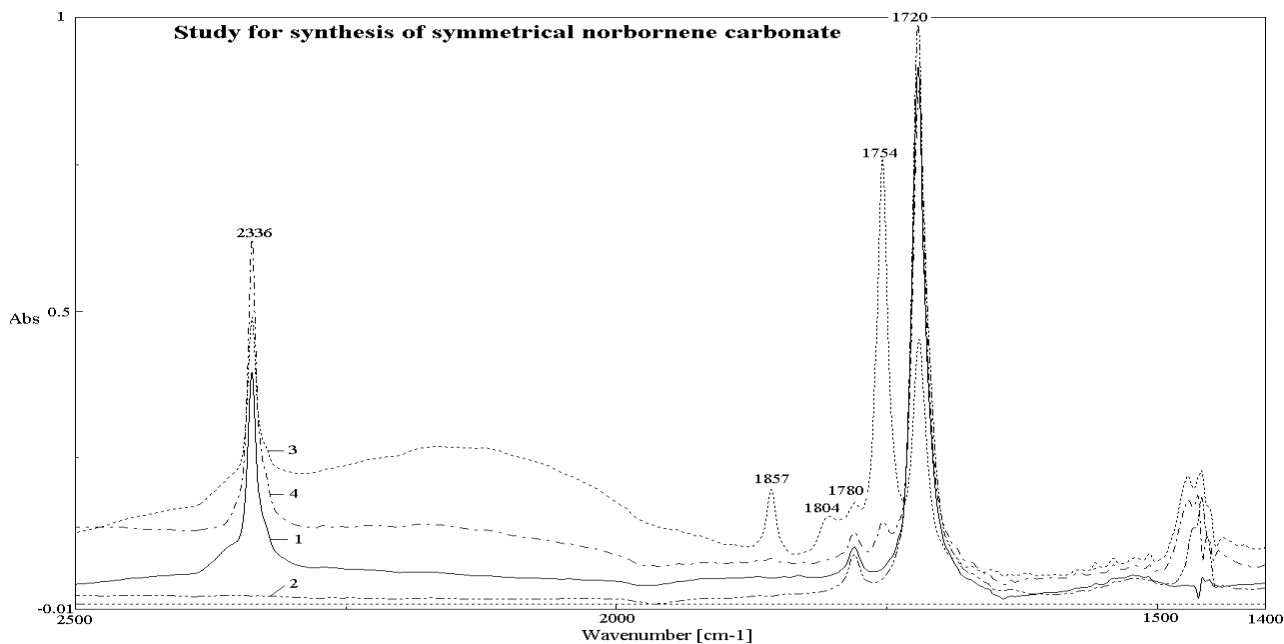


Fig. 1. FT-IR study for synthesis of symmetrical norbornene carbonate

1. The IR spectra of the endo-*N*-hydroxy-5-norbornen-2,3-dicarboximide + TPG in THF at 25°C; 2. The IR spectra of the endo-*N*-hydroxy-5-norbornen-2,3-dicarboximide + TBA in THF at 25°C; 3. The IR spectra of the endo-*N*-hydroxy-5-norbornen-2,3-dicarboximide + TPG+TBA in THF at 25°C; 4. The IR spectra of the endo-*N*-hydroxy-5-norbornen-2,3-dicarboximide + TPG+TBA in THF at 25°C, after 22 hours.

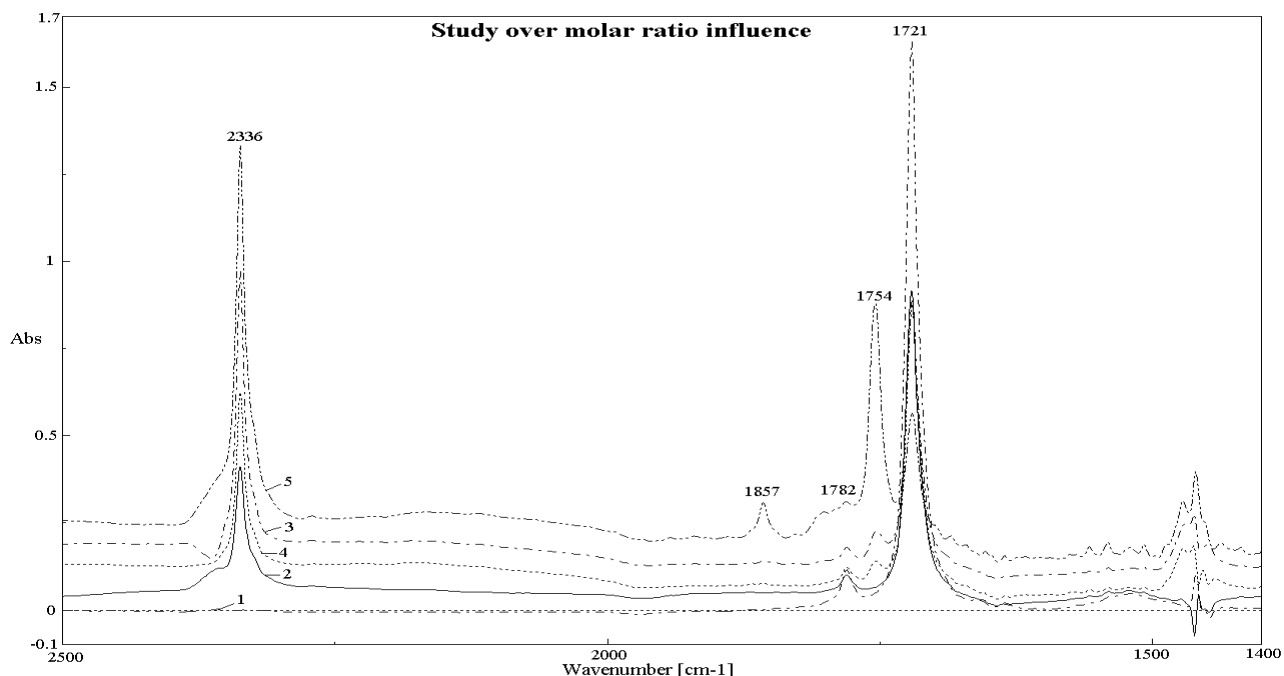


Fig. 2. Influence of condition reaction over synthesis of symmetrical norbornene carbonate – FT-IR study

1. The IR spectra of the endo-*N*-hydroxy-5-norbornen-2,3-dicarboximide in THF at 25°C; 2. The IR spectra of the endo-*N*-hydroxy-5-norbornen-2,3-dicarboximide + TPG in THF at 25°C; 3. The IR spectra of the endo-*N*-hydroxy-5-norbornen-2,3-dicarboximide + TPG+TBA in THF at 25°C; 4. The IR spectra of the endo-*N*-hydroxy-5-norbornen-2,3-dicarboximide + TPG+TBA in THF at 25°C and 22 hours; 5. The IR spectra of the endo-*N*-hydroxy-5-norbornen-2,3-dicarboximide + 2 equiv. TPG in THF at 25°C;

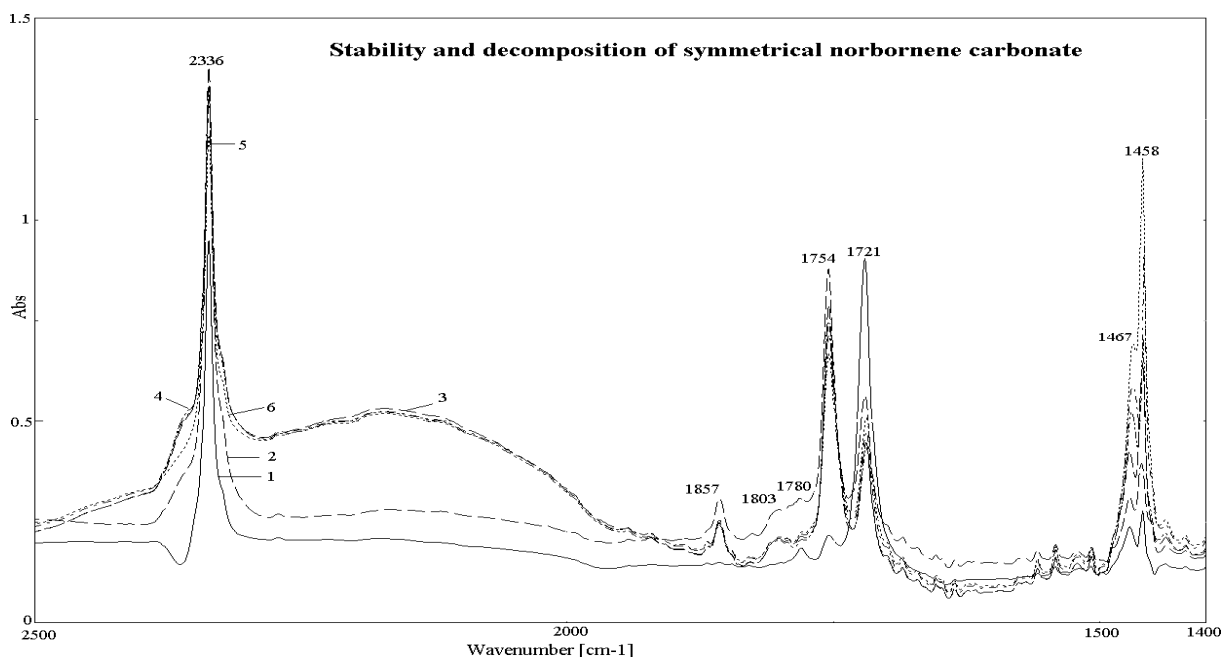


Fig. 3. Stability and decomposition of symmetrical norbornene carbonate FT-IR study

1. The IR spectra of the endo-*N*-hydroxy-5-norbornen-2,3-dicarboximide + TPG+TBA in THF at 25°C; 2. The IR spectra of the endo-*N*-hydroxy-5-norbornen-2,3-dicarboximide + 2TPG+TBA in THF at 25°C; 3. The IR spectra of the endo-*N*-hydroxy-5-norbornen-2,3-dicarboximide + 2TPG+2TBA in THF at 25°C; 4. The IR spectra of the endo-*N*-hydroxy-5-norbornen-2,3-dicarboximide + 2TPG+3TBA in THF at 25°C; 5. The IR spectra of the endo-*N*-hydroxy-5-norbornen-2,3-dicarboximide + 2TPG+4TBA in THF at 25°C; 6. The IR spectra of the endo-*N*-hydroxy-5-norbornen-2,3-dicarboximide + 2TPG+5TBA in THF at 25°C

An IR study regarding the influence of the bis(trichloromethyl) carbonate excess and the decomposition of the symmetrical norbornene carbonate was performed. The evolution of the two bands corresponding to the endo-*N*-hydroxy-5-norbornen-2,3-dicarboximide and the appearance of the specific bands of the *N,N'*-bis(endo-5-norbornen-2,3-dicarboximidyl) carbonate and its salt formed with tri-*n*-butyl amine were monitored.

The spectroscopic data recorded in the 2500-1400 cm^{-1} region (Fig. 3) corresponding to the valence vibrations of the carbonyl group, led to the following conclusions: in the first minutes of the reaction, after 1 tri-*n*-butyl amine equivalent was added, it may be observed the appearance of 1803 cm^{-1} and 1857 cm^{-1} bands, corresponding to the *N,N'*-bis(endo-5-norbornen-2,3-dicarboximidyl) carbonate. The appearance of these bands it was also observed when an excess of bis(trichloromethyl) carbonate was used.

The use of an amine excess (two or three tri-*n*-butyl amine equivalents) led to a slight decrease of the intensity of the specific symmetrical carbonate bands (Fig. 3). When a higher excess of amine was used (4 or 5 equivalents) there are no changes in the IR spectra; it can only be observed a slight decomposition of the symmetrical carbonate, highlighted by the diminished intensity of the 1803 and 1857 cm^{-1} bands, simultaneously with an increase of the intensity of the 2337 cm^{-1} band (attributed to CO_2) and of the 1467.5 and 1459 cm^{-1} bands, corresponding to the alkyl groups. The symmetrical carbonates with leaving groups are versatile

compounds that represent an attractive eco-friendly alternative for toxic traditionally phosgene substitutes.

The synthesis of norbornenyl carbonate represents the starting point for the obtaining of some new intermediates (unsymmetrical norbornenyl carbonates) useful in the peptide synthesis field, for the preparation of active esters and also in the alkoxy-carbonylation reactions for the protecting the amino groups from amines and aminoacids.

4. Conclusions

It can be observed that the reaction takes place as soon as the tri-*n*-butyl amine is added in the reaction mixture (endo-*N*-hydroxy-5-norbornen-2,3-dicarboximide and bis(trichloromethyl) carbonate dissolved in tetrahydrofuran). The performed FT-IR study for the synthesis of the *N,N'*-bis (endo-5-norbornen-2,3-dicarboximidyl) carbonate showed that using an excess of bis(trichloromethyl) carbonate doesn't influence the formation of the above-mentioned compound. The increasing of the reaction time led to the decomposition of the *N,N'*-bis (endo-5-norbornen-2,3-dicarboximidyl) carbonate.

The FT-IR study of the decomposition of *N,N'*-bis (endo-5-norbornen-2,3-dicarboximidyl) carbonate in the presence of an important amine excess showed that the valence vibrations bands of the carbonyl group from the symmetrical carbonate do not have significant changes; it may be observed only a small decrease of their intensity, due to the extend of the reaction time.

References

- Imajo H., Kurita K., Iwakura Y., (1981), Polyimides derived from bis-N-hydroxyimides. III. Polyimide-carbonates and polyimide-urethanes synthesized from bischloroformate of N,N'-dihydroxypyromellitic diimide, *Journal of Polymer Science: Part A Polymer Chemistry*, **19**, 1855–1861.
- Kundu B., Shukla M., Shukla S., (1994), A convenient method for the synthesis of mixed carbonates from alcohols, using disuccinimido carbonate. Application to alkoxycarbonylation of amino acids, *Journal of Chemical Research (S)*, **11**, 427-427.
- Ogura H., Takeda K., (1982), Imido carbonate compound, production thereof and uses thereof as reagent for forming active ester of amino acids. U.S. Patent, No. 4.341.707.
- Segneanu A., Milea M., Pintea B., Simon M., Csunderlik C., (2006), N,N'-Disuccin-imidylcarbonate, a potential reagent in fine organic synthesis of reactive asymmetrical carbonates, used to protect amino groups from aminoacids for peptides synthesis, *Revista de Chimie*, **57**, 739-742.
- Segneanu A., (2007), *The use of organic carbonates for the amino group protection and for the activation of the carboxyl group of the amino acids in the peptide synthesis*, PhD Thesis, Politehnica University of Timisoara, Romania.
- Segneanu A.E., Balcu I., Mirica M.C., Iorga A.I., Milea M., Urmosi Z., (2009), Reactive organic carbonates with leaving group for biologically active dipeptides synthesis, *Environmental Engineering and Management Journal*, **8**, 797-801.



“Gheorghe Asachi” Technical University of Iasi, Romania



HYBRID MATERIALS FOR THE REMOVAL OF ORGANIC COMPOUNDS FROM WATER

Adina-Elena Segneanu¹, Cornelia Bandas¹, Ioan Grozescu¹, Florentina Cziple², Titus Slavici³, Paula Sfirloaga^{1*}

¹National Institute for Research and Development in Electrochemistry and Condensed Matter- INCEMC Timisoara, Romania

²“Eftimie Murgu” University of Resita, Romania

³“Ioan Slavici” University of Timisoara, Romania

Abstract

Water quality is an important concern for the ecosystem state from a particular region. Since the continuous urban and economic development induces a negative impact on entire hydrological cycle, this study investigates the water quality of a Romanian lake, located in the Surduc area - Timis County. This perimeter has undergone significant economic development in the past two decades due to increased tourism potential and the number of holiday residences.

We proposed hybrid materials for the degradation of organic pollutants from the lake water. Particle size, morphology and properties of the hybrid materials are investigated by X-ray diffraction (XRD), scanning electron microscopy (SEM), energy-dispersive X-ray spectroscopy (EDX), DRUV-VIS spectroscopy and TOC determinations.

Key words: catalytic material, hypertrophication, photocatalytic activity, Z-Na

Received: January 2013; Revised final: May, 2013; Accepted: May, 2013

1. Introduction

Water quality became an integral part of environmental quality management in today's world, when clean water is essential for humans, animals and plants. The demand for clean water and sanitation (including wastewater treatment) has been steadily rising with the rapid increasing in urbanization and population within civil habitats. That fact denotes the importance of water resources in the environment and its impact on humans, animals and plants under conditions of ever increasing anthropogenic activities linked to over population (Balica et al., 2012; Dinh et al., 2012; Van et al., 2012).

Streams, rivers and lakes located in areas of urban development are often associated with increased sediment load, trash, degraded water quality, and increased flooding (Jonoski et al., 2012a,b; Moya Quiroga et al., 2013; Muste et al.,

2010; Quinn et al., 2010; Popescu et al., 2010, 2012a, b, c; Sonal et al., 2012).

Most often, accelerated development of tourist areas represent the main pollution causes for rivers and lakes in those regions. Untreated domestic wastewater, the increase of sewage quantity all contribute to water quality deterioration. The main effect is hypertrophication, since the over-enrichment of lakes and rivers with nutrients, causes toxic algae blooms, deoxygenating, foul odors, fish kills, and heavy economic losses to communities that depend on clean water for drinking, recreation or industrial use. Although there are many studies over photocatalytic methods applied in water treatment, this type of techniques continues to play an important role in water decontamination processes due to the fact that are environmental friendly (Corma et al., 2004; Ignat et al., 2011; Zhang et al., 2011). However, to increase the photonic efficiency is necessary to develop hybrid photocatalysts (Dubey et

* Author to whom all correspondence should be addressed: E-mail: s_adinaelena@yahoo.com

al., 2006; Farnandez et al., 1995; Konstantinou et al., 2004).

The aim of this study was to identify a simple and efficient method for the degradation of organic compounds from water using materials based on Z-Na-TiO₂. Also, it will establish the levels of water pollution and used materials for treat it.

2. Material and methods

Water samples were collected from three different zones of the Surduc Lake denoted by P1, P2 and P3. These individual water samples were taken and deposited in the same collection bottle and was kept at 4°C for 24 hours. Before analysis the water samples were homogenized by ultrasonic treatment and then water samples were filtered through a 0.45 µm filter.

Chemicals

Romanian zeolitic mineral from Mirsid, used as support for doped TiO₂ loading, was supplied by CEMACON Company, Romania. The diameter of grains size selected to carry out the experiments was between 315-500 µm with the mass composition 62.20% SiO₂, 11.65% Al₂O₃, 1.30% Fe₂O₃, 3.74%CaO, 0.67% MgO, 3.30% K₂O, 0.72% Na₂O and 0.28% TiO₂.

3. Experimental

3.1. Total organic carbon content

The TOC analyzer used in this study was a SHIMADZU TOC-V_{CPN} equipped with a 94 – position auto sampler. The TC principle analysis was catalytic combustion at high temperature (900°C) and for IC –acidification at 200°C (Akpan et al., 2009). The amount of water samples used for TOC analysis was 25mL and reagent used was phosphoric acid, 1:1 v/v.

3.2. Atomic Absorption Spectrometry (AAS)

The tests for determination of heavy metals contents from water samples were conducted under international standard ISO 15586:2003 (E), with equipment: Analytik Jena novAA 400G - apparatus, with a graphite furnace, equipped with autosampler MPE60 and software WinAAS 3.17.0. Examined materials: samples of water (2mL). Substances: nitric acid, ultrapure water.

The samples were treated with 5.5 mL HNO₃ 65% and subjected to digestion in a Berghof microwave oven MWS 2, using a three stages program: T1=160°C, t1= 15 min, p1= 80%. T2=210 °C, t2=15 min, p2=90% and T3, t3=15 min, p3=0%. After digestion, the sample is brought to a volume of 100 mL with ultrapure water.

3.3. Preparation of photocatalyst

The catalytic material based on natural zeolite modified with undoped TiO₂ nanocrystals was obtained by microwave-assisted hydrothermal conditions (Kitano et al., 2007). Titanium dioxide photocatalyst was previously obtained by classical sol-gel method, pure anatase phase.

The preparation of the chemically modified zeolite presumes two stages to reach acid form (H form) by using a 2M HCl solution and sodium form (Na form) with 2M NaNO₃ solution for a more efficient ion exchange. Consequently, Na forms of natural zeolite are expected to remove other cations easily in ion-exchange applications. The microwave synthesis was performed in a microwave reaction system, Multiwave 3000, produced by Anton Paar at 2.45 GHz for a continuous power of 1000 W. The temperature measurements were recorded with an IR sensor depending on solution content from autoclave. Therefore, an amount of Z-Na was mixed with 40 mL distilled water and undoped TiO₂ (2wt%), in aqueous solution under continuous stirring for 4 hours. The obtained solutions were introduced into a Teflon autoclave with a 50% degree of fullness, for 30 min to 180°C, under microwave radiations. After autoclaving, the catalytic materials (Z-Na-TiO₂) was washed with distilled water and dried at 60°C for 5 hours.

3.4. Characterization of catalytic material

The crystallinity of the prepared samples was investigated by X-Ray diffraction (XRD) using PANalytical X'PertPRO MPD Diffractometer with Cu K α radiation $\lambda = 1.5406\text{\AA}$, 2θ -step of 0.01° from 10 to 100. Scherrer equation, $d = 0.9\lambda / (B \cos \theta)$ was used to estimate grain average sizes of crystallites, where B is the half height width of the reflection peak at 2θ and λ is the wavelength of the radiation. Scherrer equation, $d = 0.9\lambda / (B \cos \theta)$ was used to estimate grain average sizes of crystallites, where B is the half height width of the reflection peak at 2θ and λ is the wavelength of the radiation. The morphology of hybrid materials was observed using an Inspect S PANalytical model scanning electron microscopy (SEM) using coupled with the energy dispersive X-ray analysis detector (EDX). The semiquantitative elemental analysis was analyzed through EDAX facility of SEM.

The light absorption properties of catalytic materials were studied by UV–VIS diffuse reflectance spectroscopy (DRUV-VIS), performed under ambient conditions using Lambda 950 Perkin Elmer with the wavelength range of 200–430 nm. The blank sample was used as the reference.

3.5. Photocatalytic degradation procedure

The photocatalytic activities of the prepared catalytic materials were assessed by application of 6W UV irradiation at room temperature for 2 hours. The volume of the reaction solution was 50mL, into which 0.05 g of photocatalyst (Z-Na and Z-Na-TiO₂)

was added. After an irradiation time of 2 h, the suspension was sampled and filtered through a 0.2 μm membrane filter. Also, the mineralization degree was assessed by monitoring total organic carbon (TOC) parameter using a SHIMADZU TOC-V_{CPN}.

4. Results and discussion

Catalytic materials based on natural zeolite modified with undoped TiO_2 (Z-Na- TiO_2) was synthesized in microwave-assisted hydrothermal conditions. X-ray diffraction, DRUV-VIS spectroscopy and SEM/EDX and TOC analysis were used for the characterization of catalytic materials. Morphological and structural analysis of the catalytic material was investigated by X-ray diffraction (XRD), scanning electron microscopy (SEM), and energy-dispersive X-ray spectroscopy (EDX).

4.1. Water analysis

Establishment of water pollution level was accomplished by two different analytic methods: TOC detection and atomic absorption spectrometry.

4.2. TOC analysis

Measurement of TOC is a much more fast method to determine the organic matter content in water and wastewater, which is directly related to total organic content. Organic, inorganic and total carbon content was measured from the water samples. The results are shown in the Table 1.

From TOC analysis results can be determine the average of organic content of the lake water which is 21.31 mg/L. According to the date base values of TOC higher than 20 mg/L corresponds to polluted water (Table 2).

4.3. Atomic absorption spectrometry (AAS)

The evaluation of the metals contents (As, Cu, Pb, Zn, Cd, Fe and Ni) from water samples was performed through atomic absorption spectroscopy. The results of the analysis are presented in Table 3.

From the results obtained in Table 2 it can be seen that in water samples was found only two metals: iron and zinc in concentrations much lower than national and international regulation for drinking water: 200 $\mu\text{g/L}$ for Fe and 5000 $\mu\text{g/L}$ (Clesceri, 1996; Law 458, 2002; Law 311, 2004; Statutory Instruments, 2007).

4.4. Characterization of catalytic material

4.4.1. X-ray diffraction analysis

Fig. 1a and b described XRD patterns of catalytic materials i.e., Z-Na and Z-Na- TiO_2 . For comparison, the XRD pattern of the natural zeolite (Z-Na) is also shown in Fig. 1a. The presented results revealed that the natural zeolite used is mostly clinoptilolite (2theta: 10°; 22.5°; 30°) (Bowman, 2003; Kowalczyk et al., 2006; Korkuna et al., 2006).

It can be seen that the main peak positions of natural zeolite (clinoptilolite) are unchanged, indicating that the structure of natural zeolite has a good thermal stabilization, after the microwave-assisted hydrothermal treatment.

4.4.2. DRUV-VIS spectroscopy

DRUV-VIS patterns are examined to determine the light absorption quantification and absorption wavelength range correlated with band gap energy. Fig. 2 presents an intense absorption maximum at ~260 nm, which can be assigned to isolated titanium with tetrahedral coordination. Another absorption range found in the range of 300–370 nm indicates that some titanium is also in an octahedral environment (Dabici et al., 2011).

Table 1. Results of TOC analyses

| Water Sample | TOC (mg/L) | TC (mg/L) | IC (mg/L) |
|--------------|------------|-----------|-----------|
| P1 | 20.78 | 21.56 | 0.7808 |
| P2 | 21.27 | 21.81 | 0.5452 |
| P3 | 21.89 | 22.27 | 0.3800 |

Table 2. Levels of TOC in various water streams (SIST ISO 8245, 1999; Clesceri et al., 1996)

| Type of water | TOC (mg/L) | Type of water | TOC (mg/L) | Type of water | TOC (mg/L) |
|-------------------|------------|----------------|------------|---------------|------------|
| High purity water | <0.01 | Seawater | <1 | Surface water | <10 |
| Ground water | <1 | Drinking water | <4 | Wastewater | >20 |

Table 3. Concentration of metals detected by AAS analysis

| Water Sample | As ($\mu\text{g/L}$) | Cu ($\mu\text{g/L}$) | Ni ($\mu\text{g/L}$) | Pb ($\mu\text{g/L}$) | Cd ($\mu\text{g/L}$) | Fe ($\mu\text{g/L}$) | Zn ($\mu\text{g/L}$) |
|--------------|------------------------|------------------------|------------------------|------------------------|------------------------|------------------------|------------------------|
| P1 | * | * | * | * | * | 67.56 | 22.42 |
| P2 | * | * | * | * | * | 52.64 | 24.24 |
| P3 | * | * | * | * | * | 46.88 | 15.47 |

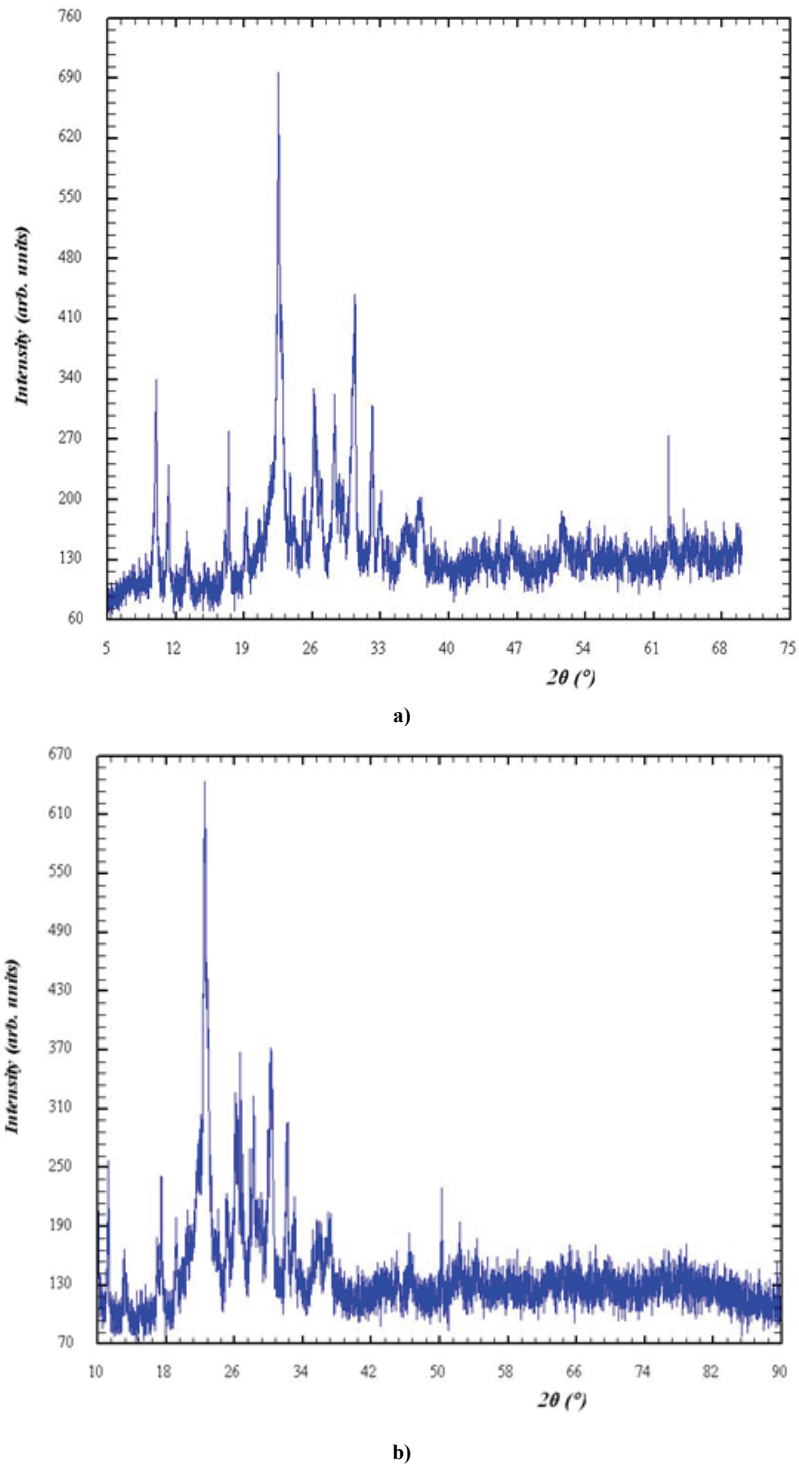


Fig. 1. a) XRD patterns of Z-Na material, b) XRD patterns of Z-Na-TiO₂ materials

For the catalytic material modified with undoped TiO₂ the absorption bands intensity is higher in UV domain, because the anatase form of undoped TiO₂ with the band gap energy about 3.2 eV strongly adsorbs in this domain. The SEM images (Fig. 3a, b) show the lamellar texture of clinoptilolite, according to the literature data (Kowalczyk et al., 2006).

The TiO₂ particles are distributed randomized and form cluster agglomerate groups on the surface

and in site of zeolite channels. At a larger magnification (mag. 12.000X), it is obvious that the TiO₂ nanocrystals (spherical form) are non-uniformly distributed on the zeolite surface.

EDX results, that provided a semiquantitative elemental analysis of the surface, indicate that Ti was present on the zeolite surface. Also, this natural zeolite contains the major elements such as Na, Si, Al, Ca, K and Mg as can be seen from the EDX spectra (Figs. 3c, d).

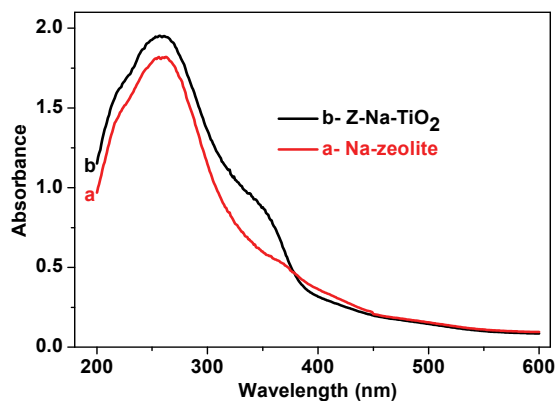


Fig. 2. DRUV-VIS spectra of catalytic materials (a) Na-Z- and (b) Z-Na-TiO₂

4.5. Photocatalytic activity

The prepared catalytic materials, Na-Z and Z-Na-TiO₂ were used to degrade and mineralize organic compounds under ultraviolet light irradiation for 2 h, and the results are presented in Figs. 4-6.

The performance of the photocatalytic activities of materials was determined comparatively for the degradation of organic compounds from water samples (P1-P3) by photocatalysis and photolysis under 6W UV irradiation at wavelengths of 254-365 nm at room temperature, after 2 hours of illumination. In comparison the Z-Na material was tested for degradation of pollutants from water.

The volume of the reaction solution was 50mL, into which 0.05 g of photocatalyst (Z-Na and Z-Na-TiO₂) was added. After irradiation time of 2 h, the suspension was sampled and filtered through a 0.2 μm membrane filter. Also, the mineralization degree was assessed by monitoring the removal efficiency expressed by total organic carbon (TOC) parameter reduction. It can be observed from the Figs. 4-6 that by comparison with other catalytic material tested (Z-Na), the hybrid material based on TiO₂ presents a good photocatalytic activity.

5. Conclusions

This study has demonstrated the photocatalytic efficiency of hybrid materials obtained through microwave-assisted hydrothermal synthesis. The performance of the photocatalytic activities of materials was determined comparatively for the degradation of organic compounds from real water (Surduc Lake, Romania) from three different areas, by photocatalysis and photolysis under 6W UV irradiation at wavelengths of 254-365 nm at room temperature, after 2 hours of illumination. In comparison the Z-Na material was tested for degradation of pollutants from water.

Thus, materials based on Na-Z and Z-Na-TiO₂ was used to degrade and mineralize organic compounds from water samples under ultraviolet light. The performance of the photocatalytic activities of materials was determined comparatively by photocatalysis and photolysis.

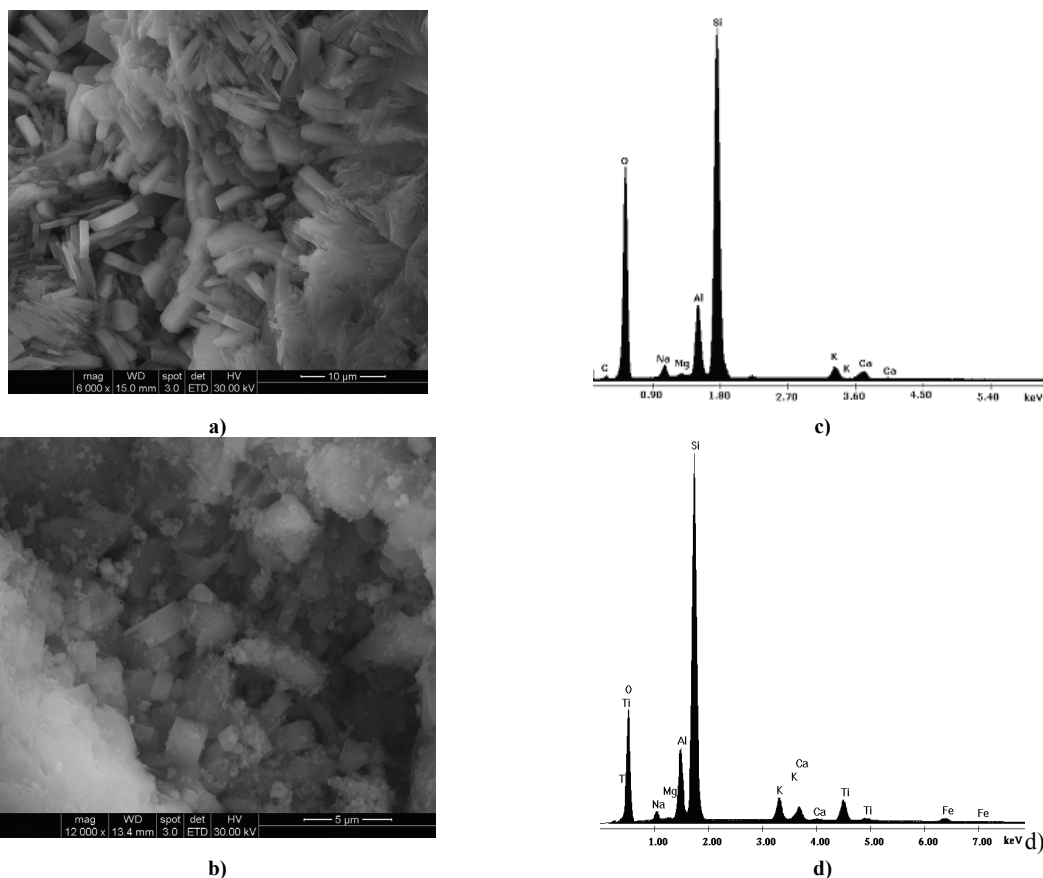


Fig. 3. SEM morphology for Z-Na-TiO₂ (a and b) and elemental analysis of Z-Na-TiO₂ (c and d)

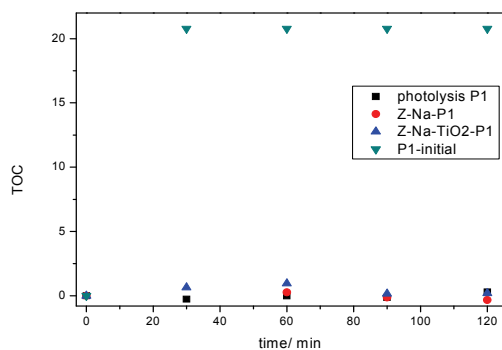


Fig. 4. Variation in time of removal efficiency expressed by total organic carbon (TOC) reduction for P1

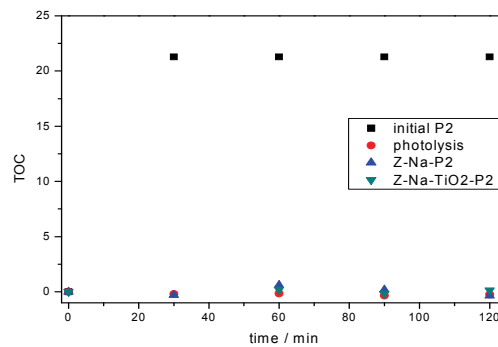


Fig. 5. Variation in time of removal efficiency expressed by total organic carbon (TOC) reduction for P2

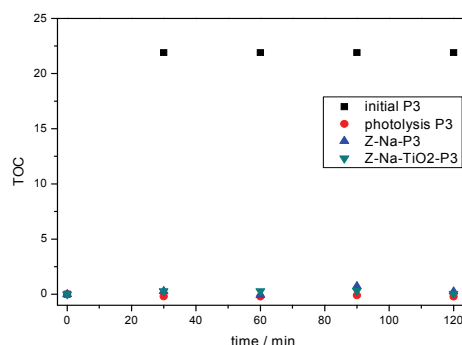


Fig. 6. Variation in time of removal efficiency expressed by total organic carbon (TOC) reduction for P3

Acknowledgements

This work was supported by PN II No: 49/2012 BIOSIM. The authors thanks to Daniel Boc for TOC analysis.

References

Akpan U.G., Hameed B.H., (2009), Parameters affecting the photocatalytic degradation of dyes using TiO₂-based photocatalysts: A review, *Journal of Hazardous Materials*, **170**, 520–529.

Balica S. F., Popescu I., Beevers L., Wright N.G., (2013), Parametric and physically based modelling techniques for flood risk and vulnerability assessment: a comparison, *Journal of Environmental Modelling & Software*, **41**, 84-92

Bowman R.S., (2003), Applications of surfactant-modified zeolites to environmental remediation, *Microporous and Mesoporous Materials*, **61**, 43-56.

Clesceri L.S., Eaton A.D., Greenberg A.E., (1996), *Standard Methods for the Examination of Water and Wastewater, 19th Edition Supplement*, American Public Health Association, American Water Works Assoc., Water Environment Federation, Washington, DC.

Corma H., Garcia A., (2004), Zeolite based photocatalysts, *Chemical Communications*, 1443–1459.

Dabici A., Sfirloaga P., C. Lazau, C. Bandas (Ratiu) C., Misca C., Vaszilcsin N., (2011), Effect of natural zeolite functionalized with TiO₂ for Enterococcus faecalis removal from water, *Digest Journal of Nanomaterials and Biostructures*, **6**, 1325-1332.

Dinh N.Q., Balica S., Popescu I., Jonoski A., (2012), Climate change impact on flood hazard, vulnerability and risk of the Long Xuyen Quadrangle in the Mekong Delta, *Journal of River Basin Management*, **10**, 103-120.

Dubey N., Rayalu S.S, Labhsetwar N.K., Naidu R.R., Chatti R.V, Devotta S., (2006), Photocatalytic properties of zeolite-based materials for the photoreduction of methyl orange, *Applied Catalysis A: General*, **303**, 152–157.

Farnandez G., Lassaleta V.M., Jimenez A., Justo A.R., Gonzalez-Elipe, (1995), Preparation and characterization of TiO₂ photocatalyst supported on various rigid supports (glass, quartz and stainless steel). Comparative studies of photocatalytic activity in water purification, *Applied catalysis B: Environmental*, **7**, 49-63.

Ignat M., Revenco L.M., Pascaru A.R., Popovici E., (2011), Functionalized Zeolitic Materials with Photocatalytic Properties, *Acta Chemica Iasi*, **19**, 21-34.

Jonoski A., Almoradie A., Khan K., Popescu I., Anel S.J., (2012a), Google Android Mobile Phone Applications for Water Quality Information Management, *Journal of Hydroinformatics*, DOI 10.2166/hydro.2012.147.

Jonoski A., Alfonso L., Almoradie A., Popescu I., van Anel S.J., Vojinovic Z., (2012b), Mobile phone applications in the water domain, *Environmental Engineering and Management Journal*, **11**, 919-930.

- Kitano M., Matsuoka M., Ueshima M., Anpo M., (2007), Recent developments in titanium oxide-based photocatalysts, *Applied Catalysis A*, **325**, 1–14.
- Konstantinou I.K., Albanis T.A., (2004), TiO₂-assisted photocatalytic degradation of azo dyes in aqueous solution: kinetic and mechanistic investigations, *Applied Catalysis B Environmental*, **49**, 1-14.
- Korkuna O., Lebeda R., Skubiszewska-Zieba J., Vrublevska T., Gunko V.M., Ryczkowski J., (2006), Structural and physicochemical properties of natural zeolites: clinoptilolite and mordenite, *Microporous and Mesoporous Materials*, **87**, 243.
- Kowalczyk P.M., Sprynskyy A.P., Terzyk M., Lebedynets M., Namiesnik J., Buszewski B., (2006), Porous structure of natural and modified clinoptilolites, *Journal of Colloid and Interface Science*, **297**, 77–85.
- Law 458, (2002), Law no. 458/2002 on drinking water quality, *Romanian Official Monitor*, Part I, No. 552, 29 July 2002.
- Law 311, (2004), Law 311/2004 amending and supplementing Law no. 458/2002 on drinking water quality, *Romanian Official Monitor*, No. 582, 30 June 2004.
- Liu Z.F., Liu Z.C., Wang Y., Li Y. B., Qu L.E., Ya J., Huang P.Y., (2012), Photocatalysis of TiO₂ nanoparticles supported on natural zeolite, *Materials Technology: Advanced Performance Materials*, **27**, 267-271.
- Moya Quiroga V., Popescu I., Solomatine D., Bociort L., (2013), Cloud and cluster computing in uncertainty analysis of integrated flood models, *Journal of Hydroinformatics*, **15**, 55-70.
- Muste M., Quinn P.F., Hewett C.J.M., Popescu I., Basu N.B., Kumar P., Franz K., Merwade V., Arnold W., Potter, K., (2010), *Initiation of the Upper Mississippi River Basin Observatory*, Proc. ASCE, Innovations in Watershed Management under Land Use and Climate Change, **39**, 1270–1281.
- Popescu I., Jonoski A., van Andel S.J., Onyari E., Moya Quiroga V.G., (2010), Integrated modelling for flood risk mitigation in Romania: case study of the Timis-Bega river basin, *International Journal of River Basin Management*, **8**, 269-280.
- Popescu I., Jonoski A., Bhattacharya B., (2012a), Experiences from online and classroom education in hydroinformatics, *Hydrology and Earth System Sciences*, **16**, 3935-3944.
- Popescu I., Archetti F., van Andel S.J., Giordani I., (2012b), Lennis: A user centric, web services based system to retrieve, analyze and deliver environmental and health information, *Environmental Engineering and Management Journal*, **11**, 889-897.
- Popescu I., Jonoski A., Bociort A., (2012c), Decision Support Systems for flood management in the Timis Bega catchment, *Environmental Engineering and Management Journal*, **11**, 2305-2311.
- Quinn P., Hewett C., Popescu I., Muste M., (2010), Towards New Types of Water-centric Collaboration: Instigating the Upper Mississippi River Basin Observatory Process, *Water Management*, **163**, 39–51.
- SIST ISO 8245, (1999), Water quality-Guidelines for the determination of total organic carbon (TOC) and dissolved organic carbon (DOC), International Organization for Standardization, Geneva, 1-11.
- Sonal T., Kataria H. C., (2012), Physico-Chemical Studies of Water Quality of Shahpura Lake, Bhopal (M.P) with Special Reference to Pollution Effects on Ground Water of its Fringe Areas, *Current World Environment*, **7**, 139-144.
- Statutory Instruments. (2007), S.I. No.106, European Communities (Drinking Water) Regulations, On line at: <http://www.attorneygeneral.ie/esi/2007/B25111.pdf>
- Van P.D.T, Popescu I., van Griensven A., Solomatine D., Trung N.H., Green A., (2012), A study of the climate change impacts on fluvial flood propagation in the Vietnamese Mekong Delta, *Hydrology and Earth System Sciences*, **16**, 4637–4649.
- Zhang G., Choi W., Kim S. H., Hong S. B., (2011), Selective photocatalytic degradation of aquatic pollutants by titania encapsulated into FAU-type zeolites, *Journal of Hazardous Materials*, **188** 198–205.



MICROWAVES EFFECT OVER BIOMASS HYDROLYSIS

Ionel Balcu, Adina-Elena Segneanu*, Marius Constantin Mirica, Mirela Ioana Iorga, Corina Macarie, Raluca Martagiu

National Institute of R&D for Electrochemistry and Condensed Matter Timisoara– INCEMC, 144 Aurel Paunescu Podeanu, 300569 Timisoara, Romania

Abstract

Changing fuel consumption to a more ecological environmentally alternative is replacing fossil fuels with fuels generated from renewable resources. Ethanol, a renewable fuel, can be produced mainly from crops, lignocellulosic biomass and different other environmental wastes. Although ethanol has been produced mainly from crops, there is a great interest in using cheaper lignocellulosic materials as a feedstock for ethanol production.

The aim of this paper is study of dilute acid hydrolysis of different types of biomass using the microwaves radiation. Acid hydrolysis of biomass will be accomplished in a speedwave TMMVS-2 system, at 130-170°C, for 35 minutes, at high pressure. Dilute-acid hydrolysis is a cheap and fast process to obtain sugar from lignocelluloses materials.

The suggested method offers multiple advantages: an important decrease of energy consumption, reducing of reaction time and reaction temperature optimization by the microwave generator.

The resulting compounds were analysed by HPLC chromatography and UV-VIS spectroscopy.

Key words: dilute-acid hydrolysis, ethanol, lignocellulosic biomass, microwave, renewable fuel

1. Introduction

Fossil fuels available on earth will be exhausted within the foreseeable future. The worldwide depletion midpoint for conventional oil is expected to be reached in the next years, and a decline in the oil reserves/production ratio will commence (Ciubota-Rosie et al., 2008; Gavrilescu M., 2008). The forest and agriculture industry can supply renewable biomass that can be valuable in providing electrical/heat energy, transport fuels or chemical feedstock (Lako et al., 2008; Gavrilescu D., 2008; Shulga et al., 2008). Softwoods are the dominating source of lignocellulosic material in the northern hemisphere (Kishi and Fujita, 2008; Lăzăroiu et al., 2008; Palm and Zacchi, 2003).

Biomass is a complex material made up of three major organic fractions as follows: 30%–55% cellulose, 10%–40% hemicellulose, and 15%–30% lignin.

Biomass also contains smaller amounts of minerals (ash) and various so-called extractives (Fig. 1).

Lignocellulosic materials are renewable, largely unused, and abundantly available sources of raw materials for the production of fuel ethanol. Lignocellulosic materials can be obtained at low cost from a variety of sources (agricultural and forestry residues, domestic wastes, municipal solid waste, waste paper, and crop residue resources (e.g. sugar cane bagasse, corn cobs and corn stover).

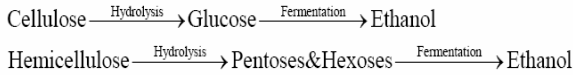
These materials contain sugars polymerized in form of cellulose and hemicellulose, which can be liberated by hydrolysis and subsequently fermented to ethanol (Taherzadeh and Karimi, 2007).

The main environmental advantages of fuel ethanol are its sustainability in using a renewable resource as a feedstock, thus promoting independence of fossil fuel, and maintaining the level of greenhouse gas (CO₂) (Demirbas, 2005).

* Author to whom all correspondence should be addressed: e-mail: s_adinaelena@yahoo.com; Phone: +40721072589

The carbohydrate polymers in the lignocellulosic materials need to be converted to simple sugars before fermentation, through a process called hydrolysis. There are several possible methods to hydrolyze lignocelluloses, the most commonly applied method can be classified in two groups: chemical hydrolysis and enzymatic hydrolysis.

Cellulose and hemicelluloses can be converted to ethanol, while lignin remains as a by-product:



A generally simplified representation of the process for ethanol production from lignocellulosic materials by chemical hydrolysis is shown in Fig. 2. The lignocellulosic raw materials are milled initially to sizes of a few millimeters, and then they are hydrolyzed to obtain fermentable sugars. Several by-products may be formed or released in this step. If highly toxic hydrolyzates are then formed, a detoxification stage is necessary prior to fermentation. The hydrolyzates are then fermented to ethanol in bioreactors. The ethanol is distilled to 90-95% purity by distillation. If fuel ethanol is desired, it should be further dehydrated to >99% by e.g. molecular sieves, to enable its blending with gasoline (Taherzadeh and Karimi, 2007).

2. Experimental

The analysis of lignocellulosic materials depends on the method of analysis and also on the sample preparation. The analysis of hydrolyzate and fermentation broths based on lignocellulosic hydrolyzates is not straightforward, since the solution contains a complex array of sugars, phenolic compounds, organic acids, furans, and other degradation products.

Table 1 presents the main crop waste composition from agriculture or forestry used for ethanol production (Purwadi, 2006).

Table 1. The main crop waste composition used in the biofuel production process

| Lignocellulosic biomass | Cellulose (%) | Hemicellulose (%) | Lignin (%) |
|-------------------------|---------------|-------------------|------------|
| Hardwood | 40-45 | 24-40 | 18-25 |
| Softwood | 45-50 | 25-35 | 25-35 |
| Corn straws | 45 | 35 | 15 |
| Rice straws | 32.1 | 24 | 18 |
| Sugarcane waste | 33.4 | 30 | 18.9 |
| Wheat straws | 30 | 50 | 15 |
| Leaves | 15-20 | 80-85 | 0 |
| Switchgrass | 45 | 31.4 | 12 |

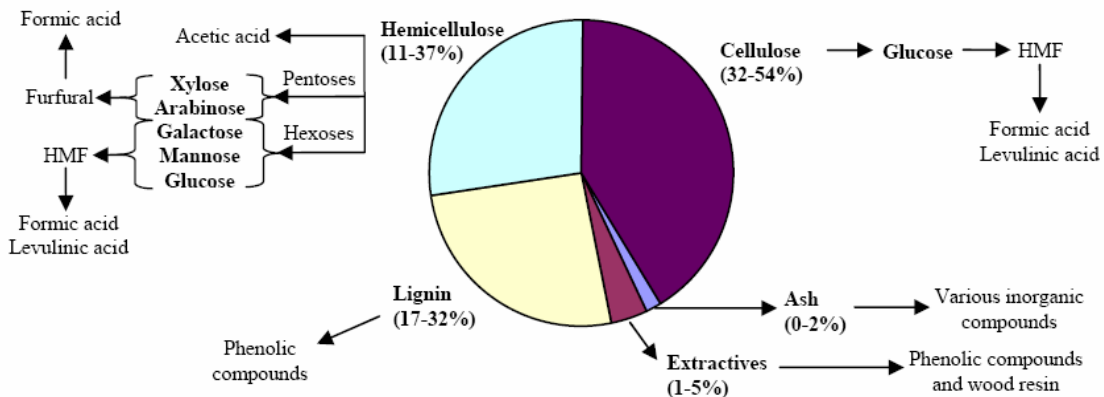


Fig. 1. Composition of lignocellulosic materials and their potential hydrolysis products

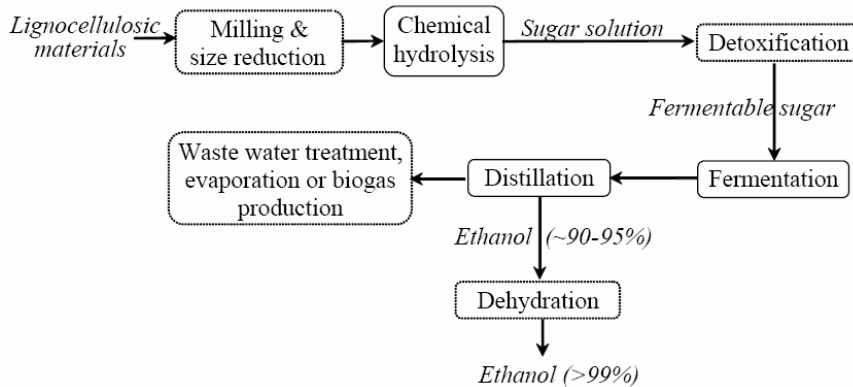


Fig. 2. Biofuel production process from lignocellulosic biomass

It was used the hydrolysis method with dilute acid due to the major advantage of high reaction rate which allows a continuous processing.

2.1. Raw material

The raw materials (sawdust) was first reduced of a few millimeters by destroying its cell structure to make it more accessible to further chemical or biological treatment, and then they are hydrolyzed to obtain fermentable sugars. The biomass was formed by: poplar, oak, robinia obtained from: wood processing (wood chips) and the crumbling of the wood wastes.

2.2. Experimental setup

For biomass acid hydrolysis was used a Microwaves speedwaveTMMVS-2 system in the temperature interval 130-170oC, for 35 minutes at pressure.

The chemical composition of the sawdust after pretreatment (acid hydrolysis) was determined by high-performance liquid chromatography (HPLC). This equipment was formed from a quaternary pump, JASCO PU-2089, autosampler JASCO AS-2055 Plus, and light scattering detector ELSD 300 (Soft Corporation, USA). Analysis column was a Tracer Extrasil NH2 (Teknokroma, Spain), with dimensions of 15 x 0.56 cm. As eluent was used the mixture acetonitrile-water 75:25 in isocratic medium, flow 1 mL/min at ambient temperature, the chromatograms were processed using a Chrompass program.

2.3. Acid hydrolysis

Hydrolysis was performed using 0.15g sawdust (poplar, oak, robinia), 1 mL H₂SO₄ 72% and 28 mL distilled water and shake for 15 minutes on a magnetic stirrer. The suspension is placed in the reactor which is shut, and it's placed in the microwave, where it heats up to 150°C for 5-10 minutes.

The hidrolizate is filtered, washed with distilled water, the volumes are bringing together with the washing water and they are stored in a refrigerator until the HPLC analysis.

Solid residues obtained after acid hydrolysis of biomass were subjected to drying using a laboratory drying stove with adjustable temperature. These samples were maintained at 105°C until constant mass (2 hours).

Acid hydrolysis was made in microwaves speedwaveTMMVS-2. The working program of the oven was performed in three stages:

- I. 120°C for 10 min., the microwave system power of 50%;
- II. 130°C for 5 min, the microwave system power of 50%;
- III. 150°C for 10 min, at the same power of the microwave system.

HPLC analysis was performed for the solution obtained after pretreatment so as for those resulted after sulfuric acid hydrolysis of pretreated sawdust, to observe the composition of sugars in those solutions.

Physical-chemical characterization of the compounds resulted with acids and acid hydrolysis pretreatment, have been concretized by determination of:

- soluble and insoluble lignin;
- total sugars content (these carbohydrates are polysaccharides constructed primarily of glucose, xylose, arabinose, galactose and mannose monomeric subunits);
- biomass total solids content.

3. Results and discussion

A representation of hydrolysis reaction kinetics in diluted sulfuric acid is shown in Fig. 3.

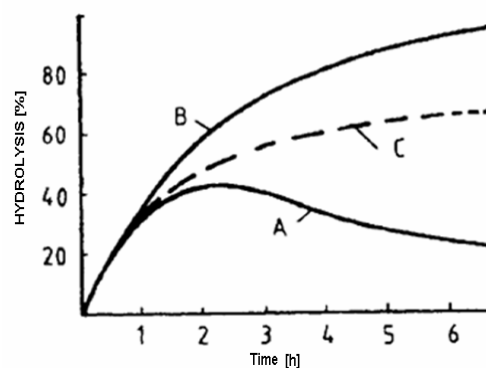


Fig. 3. Diluted acid hydrolysis of cellulose to glucose
A: kinetic hydrolysis according to the literature; B: ideal kinetic hydrolysis (no degradation); C: real kinetic hydrolysis

Despite significant efforts to identify reliable standard methods for use in characterising lignocellulosic feedstocks for conversion to fuels, a review of the literature on biomass conversions indicated that a range of methods are currently in use for polysaccharide acid hydrolysis and monosaccharide analyses.

In order to achieve quantitative analysis by HPLC method, it took a calibration with known amounts of carbohydrates. The calibration was done for fructose and glucose which are the most important carbohydrates resulting from pretreatment and enzymatic hydrolysis of biomass.

For xylose calibration (Table 2), was used the intern standard method, the standard compound is mannitol. Xylose concentration was variable to obtain concentrations between 0.1 and 0.4. A chromatogram is shown in Fig. 4. From the calibration graph was obtained a linear dependence of which equation was presented in Fig. 5.

Glucose calibration was done in a similar way, except that no internal standard was used for calibration and calculation was based on glucose

peaks area at different concentrations. Fig. 6 is an example of calibration chromatogram, and Fig. 7

represents the calibration graph that shows in this case, too, a linear dependence.

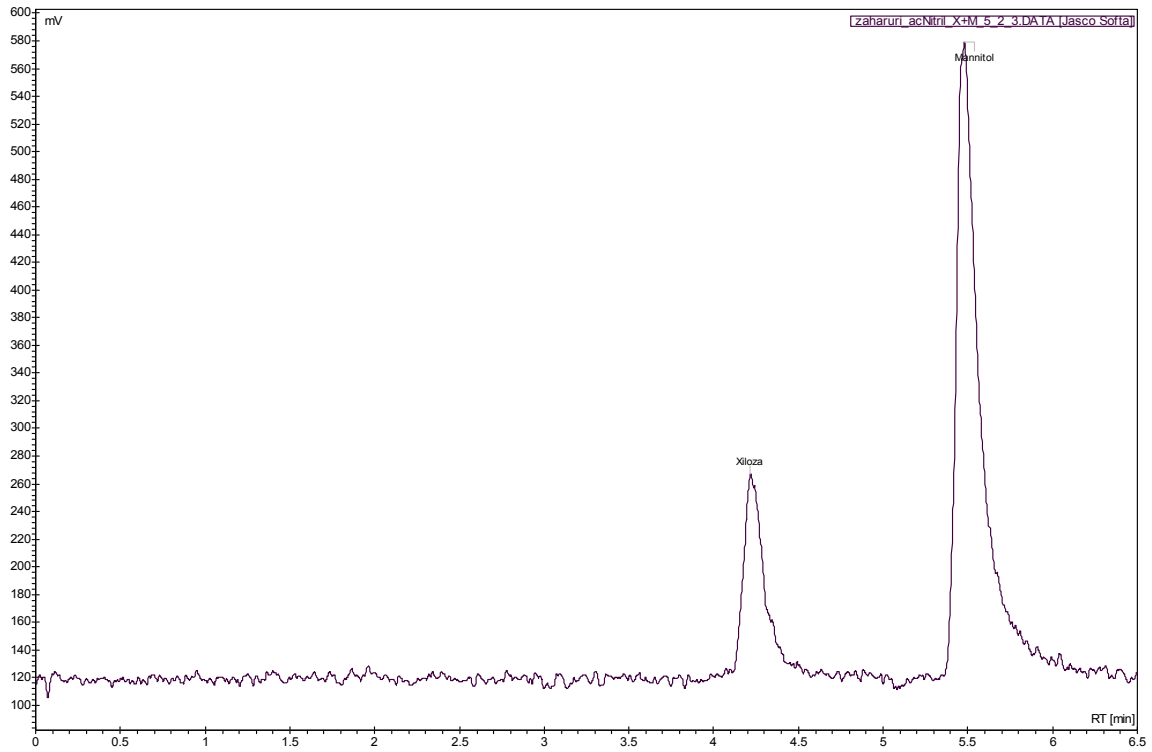


Fig. 4. HPLC chromatogram of sample 4 from xylose calibration with mannitol as internal standard (2 mg/mL xylose, 5 mg/mL mannitol)

Table 2. The xylose calibration results with Liquid Scintillator Detector (LSD)

| Sample | Concentration (mg/mL) | Peak area (mV·min) |
|--------|-----------------------|--------------------|
| 1 | 1 | 7.4 |
| 2 | 2 | 20.7 |
| 3 | 3 | 30.5 |
| 4 | 4 | 41.8 |
| 5 | 5 | 52.1 |

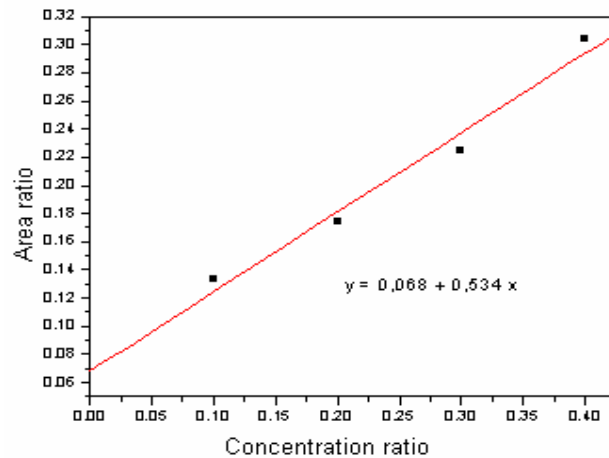


Fig. 5. Xylose calibration diagram using mannitol as internal standard

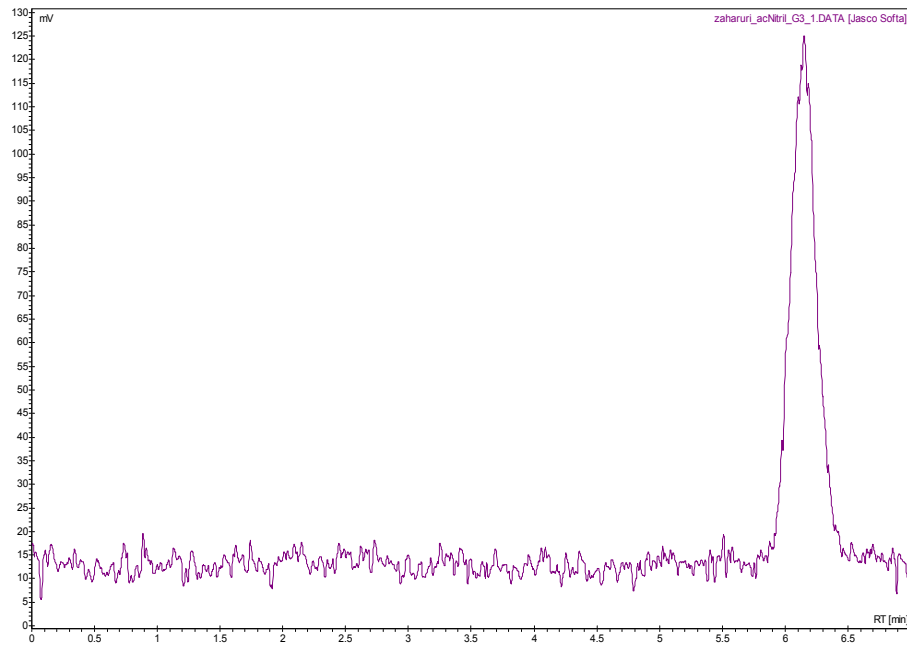


Fig. 6. HPLC chromatogram of sample 3 (mg/mL) from glucose calibration

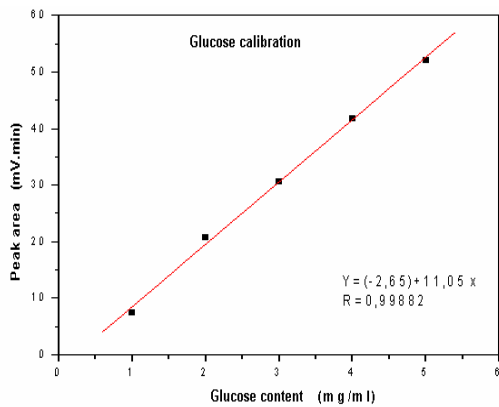


Fig. 7. Glucose calibration diagram

To illustrate the effect of temperature over pretreated biomass hydrolysis, for each enzymes, in Fig. 9 is presented the evolution of the released glucose in the first 7 hours of reaction, for two essences (aspen and fir).

4. Conclusions

From the experimental data, we can draw the following conclusions:

- the ozonization process is highly efficient to remove the pollutant organic compounds from aqueous solutions, even the most persistent ones, toxic, which can be found in waste water, having a great effect on marine ecosystems;

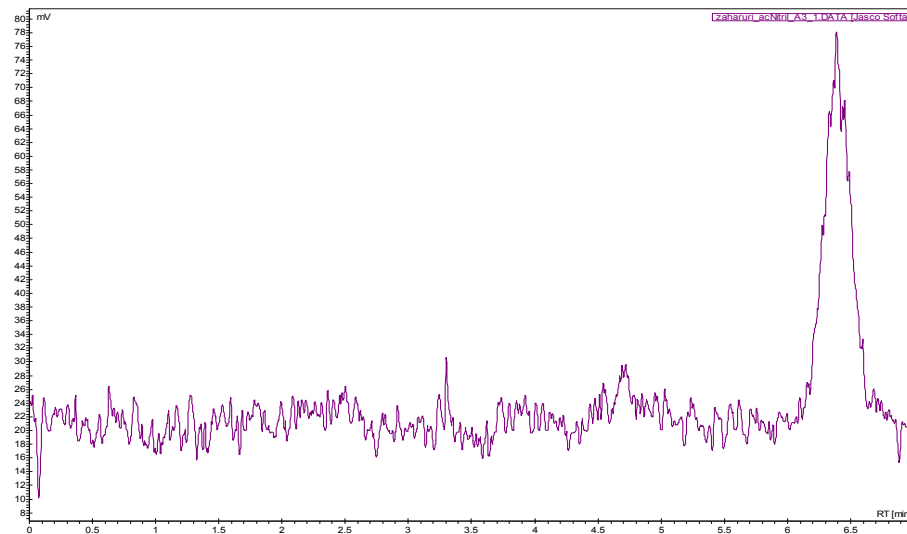


Fig. 8. HPLC chromatogram of the pretreated oak sawdust hydrolysis product, 24 hours reaction time, catalyzed by Accelerase 1000, at 40°C

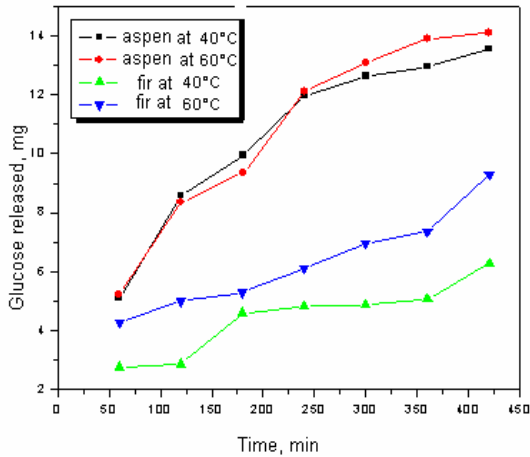


Fig. 9. The temperature dependence of fir and poplar sawdust hydrolysis pretreated with 0,84% H₂SO₄, catalyzed by Accelerase 1000 as cellulase complex

- the efficiency of the oxidation products can be improved by using catalytic systems as Me_xO_y/Al₂O₃;
- from the catalytic systems studied, the most effective proved to be the catalyst 10 Cu;
- the oxidation process with ozone follows a radicalic mechanism in alkaline environment, or by a direct attack of the ozone molecules on the pollutant;
- the presence of catalytic systems favours the formation of the OH radicals, indifferent of the pH of the solution;
- by following the quantity of intermediate oxidative products trough the parameter CCO_C showed that in presence of catalyst the maximum of their concentration is much lower then in the process with out a catalyst, and moved to smaller reaction times, which denotes that in parallel with ONF oxidation process, the oxidation of the formed intermediate products is continued.

References

- Gavrilescu D., (2008), Energy from biomass in pulp and paper mills, *Environ Eng Manag J*, **7**, 537-546.
- Gavrilescu M., (2008), Biomass power for energy and sustainable development *Environ Eng Manag J*, **7**, 617-640.
- Ciubota-Rosie C., Gavrilescu M., Macoveanu M., (2008), Biomass – an important renewable source of energy in Romania, *Environ Eng Manag J*, **7**, 559-568.
- Hameed B.H., Rahman A.A., (2008), Removal of phenol from aqueous solutions by adsorption onto activated carbon prepared from biomass material, *Journal of Hazardous Materials*, **160**, 576-581.
- Ion R.M., (1994), The photochemical conversion application on ecological systems, *Solar Energy for sustainable development*, **3**, 81.
- Ion R.M., Brezoi D.V., (2006), Au/TiO₂ nanoparticles for phenol derivatives photodegradation, *Revista Romana de Mecanica Fina, Optica si Meatronica*, **31**, 227-231.
- Ion R.M., Ureche A., (1995), Industrial Pollutants and photochemical ways for their inactivation, *Solar Energy for sustainable development*, **1**, 12.
- Ion R.M., Ureche-Fotea A., (1995), Photochemical inactivation of industrial pollutants, *Solar Energy for sustainable development*, **1**, 15.
- Kumar S.R., Murty H.R., Gupta S.K., Dikshit A.K., (2009), An overview of sustainability assessment methodologies, *Ecological Indicators*, **9**, 189-212.
- Kishi H., Fujita A., (2008), Wood-based epoxy resins and the ramie fiber Reinforced composites, *Environ Eng Manag J*, **7**, 517-523.
- Lakó J., Hancsók J., Yuzhakova T., Marton G., Utasi A., Rédey A., (2008), Biomass – a source of chemicals and energy for sustainable development, *Environ Eng Manag J*, **7**, 499-509.
- Lăzăroiu G., Mihăescu L., Prisecaru T., Oprea I., Pișă I., Negreanu G., Indrieș R., (2008), Combustion of pitcoal-wood biomass brichettes in a boiler test facility, *Environ Eng Manag J*, **7**, 595-601.
- Shulga G., Betkers T., Brovkina J., Aniskevicha O., Ozolinš J., (2008), Relationship between composition of the lignin-based interpolymer complex and its structuring ability, *Environ Eng Manag J*, **7**, 397-400.

New series of asymmetrical carbonates used in peptide synthesis

A.-E. SEGNEANU, M. MILEA^a, I. GROZESCU*

National Institute of Research & Development for Electrochemistry and Condensed Matter – INCEMC Timisoara, Romania, 300569, 144 Aurel Paunescu Podeanu

^aUniversity „Politehnica” P-ta Victoriei nr.1, Timisoara, Romania

In many preparations of delicate organic compounds, some specific parts of their molecules cannot survive the required reagents or chemical environments. Then, these parts, or groups, must be protected. The organic reactive carbonates are used especially as alkoxycarbonyl-type (carbamate) groups for protection of the amino function in amino acids. These protection groups are widely used in peptide synthesis because of their tendency to suppress racemisation of optically active centers. This paper presents the synthesis of new asymmetrical reactive carbonates with leaving group from the corresponding symmetrical carbonates and different type of alcohols, by an original procedure, as an alternative to the traditional method which employs toxic and dangerous reagents (phosgene and its chlorinated derivatives), as well as the applicability of these derivatives to the synthesis of bioactive compounds with many utilizations in pharmaceuticals and food industries. The synthesis of asymmetrical primary-, secondary- and tertiary-alkyl phthalimidyl carbonates from *N,N'*-diphtamidylcarbonates (DPC) can be performed in one step reaction and with good yields. For the structure elucidations of final products was used the yield of these reactive carbonates depends on the alcohols reactivity, on the hindering factor and on the stability of the final product.

(Received January 14, 2012; accepted June 6, 2012)

Keywords: Asymmetrical carbonates, Peptide synthesis, Phthalimidyl carbonates, Amino-protection groups

1. Introduction

The global interest in sustainable chemical development (green chemistry) imposed the establishing and adoption of measures for the reduction of the negative effects of chemical compounds on the environment and human health. Thus, the resolution regarding the synthesis of products as a result of molecular transformations, which imply low energy consumption, reduction of the formation of waste and the use of solvents and toxic or dangerous reagents, was adopted in the European Union in 2003 [1].

Within the current orientation of organic synthesis and, in general, of chemistry towards to the sustainable chemical development (green chemistry), to the use and expansion of non-polluting chemical technologies, and towards to the environmental protection by the replacement of chemical toxic compounds, the use of the phosgene derivatives in the carbonylation reactions has been avoided. The development of a new reagents and techniques, the synthesis of the smallest peptides, have received considerable attention recently because the need for green, economic, robust, scalable and reliable processes for organic synthesis applications in the pharmaceutical and fine chemical industries.

The need to identify and develop new organic reactive carbonates is very important in fine organic synthesis because these compounds present extremely many applications especially in the peptide synthesis.

In the peptides synthesis, alkoxycarbonyl amino-protecting group (carbamate) from a symmetric carbonate

and primary, secondary or tertiary alcohols are used. The use of some mixed phthalimidyl carbonates is an alternative option for the *N*-protecting amino acids. The protection of functional groups is directly accomplished by converting the particular group into a stable derivative, from which the original group can be regenerated without affecting the synthesized molecule. A good yield for the deprotecting step is mandatory [5].

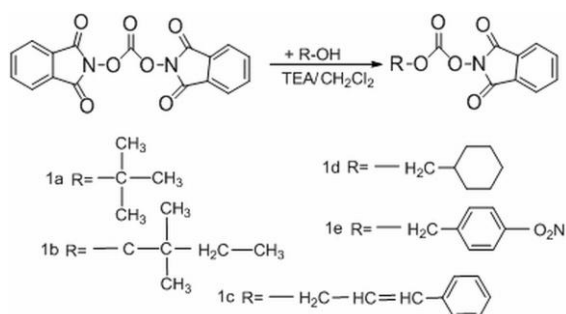
Organic reactive carbonates are interesting target since their conventional production involves the use of toxic phosgene [9]. These compounds have numerous potential applications for synthesis of different important organic molecules (functionalized carbonates, pharmaceutical and cosmetic intermediaries, lubricants, solvents etc). Carbonates production by a clean process, possesses properties of non-toxicity and biodegradability, make these compounds as true green reagent to be used in syntheses that prevent pollution at the source.

Organic carbonates are considered an option for classical synthetic ways which takes place in the presence of toxic compounds [4,6].

The coproduct, dioxide is nontoxic, an advantage over phosgene and carbon monoxide, and easy to handle and to store, but much less reactive [2]. However, the implementation of safer technologies justifies the assessment of chemical reactions based on carbon dioxide as it can be viewed as a renewable raw material.

The preparation of some new asymmetrical reactive carbonate with leaving groups (tert-buthyl-*N*-phthalimidylcarbonate (a), 2-methyl-2-buthyl-*N*-

phtalimidylcarbonate (b), cinnamyl-*N*-phtalimidylcarbonate (c), cyclohexyl-methyl-*N*-phtalimidylcarbonate (d), 4-nitro-benzyl-*N*-phtalimidylcarbonate (e)) by an original procedure will be investigated.



Scheme 1. Reaction for obtaining asymmetrical carbonates.

2. Experimental

2.1. Materials

All reagents were purchased from chemical suppliers and used without further purification.

N,N'-diphtalimidylcarbonate was synthesized according Ref 8 and 9.

2.2. Synthesis of asymmetrical carbonates

To a solution of alcohol (1.52 mmols) in CH₂Cl₂ (10 ml), diphtalimidyl carbonate (1.52 mmols) and triethylamine (TEA) (1.52 mmols) were added by drops. The reaction mixture is maintained under stirring at room temperature for 24 hours, and then is washed with citric acid (5% excess to the amine stoichiometric ratio) and the unreacted *N*-hydroxyphtalimide was then filtered. The filtrate is washed with saturated NaCl solution. The organic layer is dried on MgSO₄, filtered and then the solvent evaporated. The residue is recrystallized from CHCl₃/heptanes.

2.3. Characterisation

2.3.1. FT-IR spectroscopy

The IR spectra of solid compounds were recorded in KBr pellets and the reaction monitoring was carried out in thermostatic silicon cells of 0.137 mm thickness on a Jasco FT/IR-Vertex 70 instrument.

2.3.2. Mass spectroscopy

Mass spectrometry was conducted on a High Capacity Ion Trap Ultra (HCT Ultra, PTM discovery) mass

spectrometer from Bruker Daltonics, Bremen, Germany. HCT MS is interfaced to a PC running the CompassTM 1.2 integrated software package, which include the HystarTM 3.2.37 and Esquire 6.1.512 modules for instrument controlling and chromatogram/spectrum acquisition, and Data Analysis 3.4.179 portal for storing the ion chromatograms and processing the MS data.

To identify and analysis the purity of the final products, samples were dissolved in 1.5 ml HPLC grade methanol. In this way, the samples were carried significant evidence. The samples were maintained at room temperature for 24 hours, and then were evaporated in Speed Vac Concentrator (Thermo Electron Corporation, Milford, MA USA).

Infusion into mass spectrometer (ESI HCT Ultra, Bruker Daltonics, Germany) was performed by the robot NanoMate (Advion Biosciences, UK). The robot is an automatic injection device electrospray chip. 20 μl of sample was pipetted into microtitre plate wells, containing 96 holes.

Then the robot's software was chosen to test wells and was given command of infusion through silicon chip (chip contains 400 holes) in the mass spectrometer. It was measured in positive ionization technique, the amount of gas (nebuliser) of 50 psi and temperature spectrometer source 200°C. Robot parameters were set as follows: pipette robotic arm to aspirate 10 ml of sample and 2 ml of air, gas pressure was 0.30 psi, and the voltage of 1.40 kV (low voltage it was chosen to prevent fragmentation at source).

2.3.3. RMN spectroscopy

The ¹H-NMR and ¹³C-NMR were recorded on a Bruker DPX at 200 MHz in DMSO-*d*₆, with TMS as reference.

The values of coupling constants are normal for vicinal couplings (CH-CH, CH-NH): 6.5 - 7 Hz.

Detailed IR, MS, ¹H-NMR and ¹³C-NMR spectra are available from the authors.

3. Results and discussions

First, starting from the preparation of mixed succinimidyl carbonates according Ref 8 and 9 was investigated the most appropriate conditions for the synthesis of phtalimidyl asymmetrical carbonates in heterogeneous medium using different types of alcohols (Scheme 1). It was demonstrated that symmetrical carbonate (*N,N*-succinimidylcarbonate) can react efficiently with alcohols and amine (TEA) in the molar ratio carbonate: alcohol: amine = 1,1:1:1,1. The reactions we carried out in acetonitrile at room temperature for 4 hours.

The procedure for the preparation of a new series of asymmetrical carbonates starting to phtalimidyl carbonate and different types of alcohols, used in peptide synthesis, was investigated.

It was found that under this same reaction conditions, the mixed carbonates were obtained in very low yield and major product was *N*-hydroxyphthalimide result from symmetrical carbonates decomposition. It has shown that is necessary to change the reaction medium with another solvent in which the *N,N*-diphthalimidyl-carbonate is insoluble. To facilitate the isolation and removal of the coproduct, (*N*-hydroxy-phthalimide) was chosen as reaction medium dichloromethane. To increase the yields of was necessary to determinate the optimal conditions (reaction time, molar ratio) of these types of mixed carbonates by FT-IR spectroscopy. Thus, it was developed a chemoselective, convenient and efficient synthetic procedure for preparation of phthalimidyl asymmetrical carbonates in good yields.

It was prepared five asymmetric carbonates from *N,N*-diphthalimidylcarbonate and alcohols (benzyl and aliphatic type with electron attractive groups) and TEA in a molar ratio 1:1:1. The reactions occurs in a heterogeneous medium, at room temperature (25°C) due to the low solubility of the symmetric carbonate (*N,N*-diphthalimidyl-carbonate) in dichloromethane.

The new asymmetrical reactive phthalimidylcarbonates with leaving groups (tert-butyl-*N*-phthalimidylcarbonate (a), 2-methyl-2-butyl-*N*-phthalimidylcarbonate (b), cinnamyl-*N*-phthalimidylcarbonate (c), cyclohexylmethyl-*N*-phthalimidylcarbonate (d), 4-nitro-benzyl-*N*-phthalimidylcarbonate (e)) were analyzed by FT-IR, mass spectrometry, ¹H-NMR and ¹³C-NMR.

Tert-butyl-N-phthalimidylcarbonate - 1a, white solid, 70,8%, IR $\nu(\text{cm}^{-1})$: 1734.1(C=O); 1761.1(C=O); 1774.6(C=O); 1795.8(C=O); 1805.4(C=O); 1807.3(C=O); 1851.7(C=O); ¹H-NMR(CDCl₃, DMSO): δ 0.85(m); 3.8(s); 7.87(m); ¹³C-NMR(CDCl₃, DMSO): 25.4(C3); 54.6; 123.7; 131.5; 132.2(C3); 153.6(C2); 161(C1); MS (EI) *m/z*: 89.6; 114.4; 123.3; 157.3; 213.2; 229.2; 245.2; 263.2 [Calc. for C₁₃H₁₃NO₅: requires M, 263.13. Found: 263.2 (M+)].

2-Methyl-2-butyl-N-phthalimidylcarbonate - 1b, white solid, 63,2%; IR $\nu(\text{cm}^{-1})$: 1701.7(C=O); 1720(C=O); 1734.3(C=O); 1759.4(C=O); 1770.7; 1788(C=O); 1799.6(C=O); 1817(C=O); ¹H-NMR (CDCl₃, DMSO): δ 0.88(t); 1.2(d); 7.88(m); ¹³C-NMR(CDCl₃, DMSO): 25.4(C3); 123.7; 132.5; 153.6; 161; MS (EI) *m/z*: 143.3; 157.2; 171.2; 220.2; 233.2; 250.2; 277.2, 279.2, 289.2 [Calc. for C₁₅H₁₅NO₅: requires M, 289.13. Found: 289.2 (M+)].

Cinnamyl-N-phthalimidylcarbonate - 1c, white solid, 74.1%; IR $\nu(\text{cm}^{-1})$: 1734.1(C=O); 1763(C=O); 1772.6(C=O); 1784.2(C=O); 1838.2(C=O); 1849.8(C=O); 1871(C=O); ¹H-NMR(CDCl₃, DMSO): δ 1.23(s); 2.4(d); 3.8(d); 5.25(d); 7.16(m); 7.85(m); ¹³C-NMR(CDCl₃, DMSO): 21.3(C3); 54.6; 123.3; 125.7; 129; 132; 138.4; 153.6; 167; MS (EI) *m/z*: 114.3; 158.2; 190.1; 229.1; 265.3; 279.2; 293.2; 312.3; 323.1 [Calc. for C₁₈H₁₃NO₅: requires M, 323.13. Found: 323.1 (M+)].

Cyclohexylmethyl-N-phthalimidylcarbonate - 1d, white solid, 60.1%; IR $\nu(\text{cm}^{-1})$: 1734.7(C=O); 1761.2(C=O); 1774.6(C=O); 1803.5(C=O); 1807.3(C=O); ¹H-NMR(CDCl₃, DMSO): δ 0.9(t); 1.4(m); 1.52(m); 1.61(m); 3.8(d); 7.9(m); ¹³C-NMR(CDCl₃, DMSO): 25.5(C3); 26.1; 31.3; 34.2; 54.6; 123.7; 129.1; 132.2; 153.6; 161; MS (EI) *m/z*: 114.4; 160.2; 207.2; 235.2; 250.3; 263.2;

279.2; 300.3; 303.2 [Calc. for C₁₆H₁₇NO₅: requires M, 303.13. Found: 303.2 (M+)].

4-Nitro-benzyl-N-phthalimidylcarbonate - 1e, white solid, 68.5%; IR $\nu(\text{cm}^{-1})$: 1737.9(C=O), 1751.4(C=O); 1768.8(C=O); 1770.7(C=O); 1788(C=O); 1817(C=O); 1821(C=O); 1822.8(C=O), 1834.3(C=O); ¹H-NMR(CDCl₃, DMSO): δ 2.34(m); 3.05(d); 3.8(d); 7.11(d); 7.85(m); ¹³C-NMR(CDCl₃, DMSO): 41.3; 124; 129; 135.4; 138.3; 156; 169.7; MS (EI) *m/z*: 265.3; 279.2; 292.3; 337.4; 342.2 [Calc. for C₁₆H₁₀N₂O₇: requires M, 342.13. Found: 342.2 (M+)].

4. Conclusion

The optimal conditions (reaction time, molar ratio) of these types of mixed carbonates were determinate by FT-IR spectroscopy. It was developed a convenient synthesis procedure for the one step preparation of a new series of asymmetrical carbonates from *N,N*-diphthalimidyl-carbonate and different aromatic and aliphatic alcohols in good yields (60-70.8%). The reactive organic carbonates yield depends on alcohol reactivity, hindering factor and stability of final product.

This synthetic procedure represents an easier and eco-friendly alternative for preparation of new key intermediaries use for protection of amino group from amines and amino-acids and than in peptide synthesis, compounds with biological activity, useful in pharmaceutical industry.

Acknowledgements

This study was supported by National Multipartner Grant - PN II – project nr. **32-129/01.10.2008** - Study On The Preparation Of Some Reactive Organic Carbonates With Leaving Group With Applications In The Synthesis Of Biologically Active Dipeptides – Conda.

References

- [1] P. T. Anastas, J. C. Warner, Green Chemistry: Theory and Practice, Oxford University Press, New York (1998).
- [2] M. Aresta, E. Quaranta, Carbon Dioxide: A Substitute for Phosgene, CHEMTECH **27**, 32 (1997).
- [3] A. K. Ghost, T. T. Duong, S. P. McKee, W. J. Thompson, Tetrahedron Lett., **32** (20), 2781 (1992).
- [4] M. A. Pacheco, C. L. Marshall. Review of Dimethyl Carbonate Manufacture and its Characteristics as a Fuel Additive, Energy & Fuels, **11**, 2 (1997).
- [5] R. V. N. Pillai, Photoremovable Protecting Groups in Organic Synthesis, Synthesis, International Journal of Methods in Synthetic Organic Chemistry, **1**, 1-2 (1980).
- [6] F. Rivetti, The Role of Dimethyl Carbonate in the Replacement of Hazardous Chemicals, C. R. Acad. Sci. Paris Série IIC Chimie, **3**, 497 (2000).
- [7] A. E. Segneanu, M. Milea, M. Simon, C. Csunderlik, Revista de Chimie, **58** (6), 542 (2007).

- [8] A. E. Segneanu, Ed. Politehnica Timisoara, seria 2: Chimie, nr. **1** (2007).
- [9] A. G. Shaikh, S. Sivaram, Organic Carbonates, American Chemical Society, Chemical Reviews, **96**, 3, 951 (1996).
- [10] P. Tundo, New Developments in Dimethyl Carbonate Chemistry, Pure and Applied Chemistry, **73**, 1117 (2001).
- [11] A. E. Segneanu, I. Balcu, M. C. Mirica, M. I. Iorga, M. Milea, Z. Urmosi, Environmental Engineering and Management Journal, **8**(4), 797 (2009).
- [12] A. E. Segneanu, M. Milea, I. Grozescu, Optoelectron. Adv. Mater. – Rapid Commun. **6**(1-2), 197 (2012).

*Corresponding author: ioangrozescu@gmail.com



ANTICORROSIVE PROTECTION SYSTEM BASED ON NANOCOMPOSITES

Ionel Balcu*, Adina-Elena Segneanu, Marius Constantin Mirica, Mirela Ioana Iorga, Corina Amalia Macarie, Iuliana Popa

National Institute of R&D for Electrochemistry and Condensed Matter, INCEMC – Timisoara, 144, Aurel Păunescu Podeanu, Timișoara, Romania

Abstract

Corrosion control, using inhibitors like, polymerisable porphyrins and multifunctional nanocomposites, is extremely useful in many environments. Phosphogypsum is a waste product resulted from the process of obtaining the phosphoric acid and it can be also used as corrosion inhibitor; in a mixture with other coating materials.

Two types of modified porphyrin: Na₄TFP Ac - dissolved in KOH and H₂SO₄ and H₂TPP - dissolved in benzonitrile, were tested. The structure characterization of phosphogypsum was analyzed through SEM and X-ray diffraction. The efficiency of the complex multifunctional system was investigated in the salt spray chamber, using diverse exposure conditions. The corrosion resistance was studied by cyclic voltammetry, in 20% Na₂SO₄ electrolyte solution. The multifunctional nanocomposites used as coating systems improve the anti-corrosion properties of electrodes.

Key words: corrosion, nanocomposites, phosphogypsum, porphyrins, voltammetry

1. Introduction

Corrosion occurs because metals tend to return to their more stable state, which caused surface deterioration and changes on structural metal properties. A corrosion inhibitor may be defined, in general terms as a substance which, when added in a small concentration to an environment, effectively reduces the corrosion rate of a metal exposed to certain conditions (Epstein 1997).

Inhibition is an economic corrosion control alternative to stainless steels and alloys, coatings or non-metallic composites (Liu 1999). Corrosion control by the use of inhibitors is extremely useful in many environments. Polymerisable porphyrins and multifunctional nanocomposites can be used alone as coating compositions or as part of a coating system (MacDiarmid, 1997; Rahmini, 2004; Sathiyarayanan, 2007).

Advantageously, they may be combined with other materials for this purpose, including known coating materials, compositions or precursors of such materials.

One of these materials, currently being deposited as waste product, is the phosphogypsum. Phosphogypsum (calcium sulphate) is a naturally occurring part of the process of creating phosphoric acid (P₂O₅), an essential component of many modern fertilizers. For every ton of phosphoric acid made, from the reaction of phosphate rock with acid, commonly sulphuric acid, some four to five tons of phosphogypsum are created. A couple of billion tons of phosphogypsum already exist worldwide and about 30 million tons are produced, as by-product, annually.

There are three options for managing phosphogypsum: disposal or dumping; stacking; use in agriculture, construction or landfill.

2. Experimental

Two types of modified porphyrin were tested (dissolved in two different solutions and mixed with phosphogypsum)

a) 0.2 g of Na₄TFP Ac porphyrin (C₄₄H₂₆N₄Na₄O₁₂S₄ × H₂O) dissolved in 40 mL 10% KOH, mentioned from this point forward as **system I**.

* Author to whom all correspondence should be addressed: e-mail: ionel_balcu@yahoo.com; Phone/Fax: +40 256-222 119 /+40 256-201 382

b) 0.2 g of Na₄TFP Ac porphyrin (C₄₄H₂₆N₄Na₄O₁₂S₄ × H₂O) dissolved in 40 mL 10% H₂SO₄, mentioned from this point forward as **system II**.

c) 0.2 g of H₂TPP porphyrin (5, 10, 15, 20 tetrakis 4 phenyl-21H, 23H) dissolved in benzonitrile, mentioned from this point forward as **system III**.

The cyclic voltammetry measurements were conducted between -1,000 and 2,500 mV potentials at a sweep rate of 100 mV/s.

The working electrode is a FeC electrode, with 0,13 cm² active surface, (coated or uncoated); platinum counter electrode with 0.31 cm² active surface and saturated calomel electrode, (SCE), as reference electrode; all of which connected to a PGZ 402 Dynamic EIS Voltalab, (Fig. 1) from Radiometer Copenhagen. 20% Na₂SO₄ solution was used as base electrolyte.



Fig. 1. The PGZ 402 Dynamic EIS Voltalab

Before each experiment, the working electrode was polished with a series of wet sandings of different grit sizes (320, 400, 600, 800, 1000 and 1200). After polishing, the carbon-steel electrode was washed with ultrapure water and dried at room temperature and then the active part was immersed in porphyrin solution for 5 minute and 60 minute (mentioned later on as exposure time).

3. Results and discussion

Figs. 2, 3, 4 and 5 show the cyclic voltammograms for the uncoated, respectively coated according to system I, II and III, FeC electrode, 20% Na₂SO₄ solution as base electrolyte and 25°C temperature; and 5 minute exposure time.

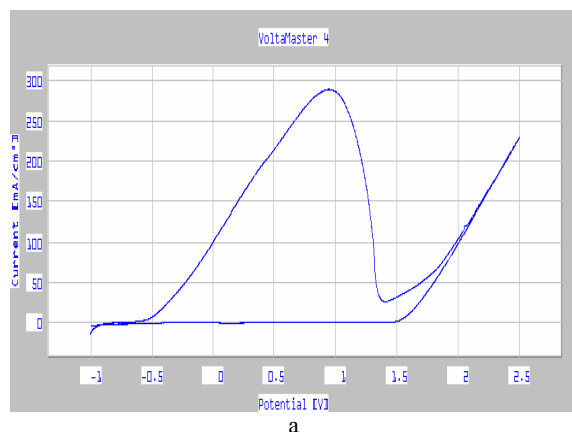
The notations present in the table: i_{peak}^{\rightarrow} - peak current density; $\epsilon_{peak}^{\rightarrow}$ - peak potential i_{peak}^{\leftarrow} - peak current density $\epsilon_{peak}^{\leftarrow}$ - peak potential ϵ_{O_2} - oxygen generation potential; ϵ_{pas} - passivation potential; i_{pas} - passivation current.

Variation of i_{peak}^{\leftarrow} is correlated with type of porphyrin systems. For Na₄TFPac both in NaOH and H₂SO₄ solutions, exhibits a decrease of i_{peak}^{\leftarrow} value and increase of i_{peak}^{\rightarrow} in benzonitrile solution, of porphyrin system III.

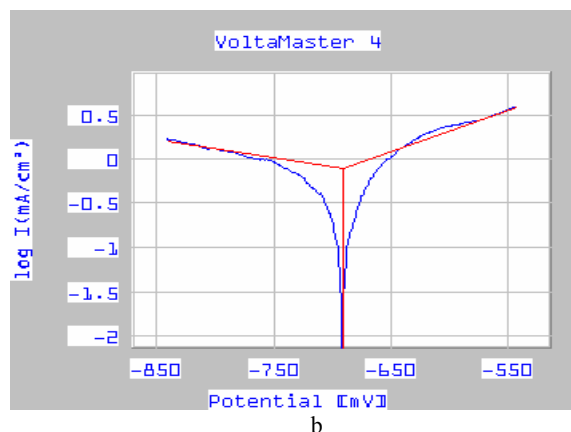
The peak potential ($\epsilon_{peak}^{\leftarrow}$) shows a similar evolution: decreased values for system I and II and increase values for system III.

There is no variation of oxygen generation potential (ϵ_{O_2}). Passivation potential (ϵ_{pas}) and passivation current depend on the coating systems: decreased for system I and II and increased systems: decreased for system I and II and increased about 20% for porphyrin system III). These results indicate that corrosion rate depends on porphyrin system type used. For system I, there is a corrosion rate increase of about 25%; 15 % for system II and 1000 % for system III, indicating that the surfaces of FeC coated with H₂TPP form a passive corrosion protection layer. The following Figs.: 6, 7, 8 and 9, with the same coating systems, (I, II and III, described earlier), but at a 60 minute exposure time presents voltammograms obtained using 20% Na₂SO₄ base electrolyte; 100 mV/s polarization rate, 25°C temperature. For Na₄TFPac both in NaOH and H₂SO₄ solutions, variation of i_{peak}^{\leftarrow} , exhibits an increase and a decrease for benzonitrile. Peak potential: decreased values for all 3 systems. There is no variation of ϵ_{O_2} . Passivation potential (ϵ_{pas}) and passivation current also decreases for all 3 systems.

A corrosion rate increase of about 20% is observed for system I, 30% for system II and 3000 % for systems III.



a



b

Fig. 2. Uncoated FeC electrode, a – cyclic voltammograms; b –Tafel tests

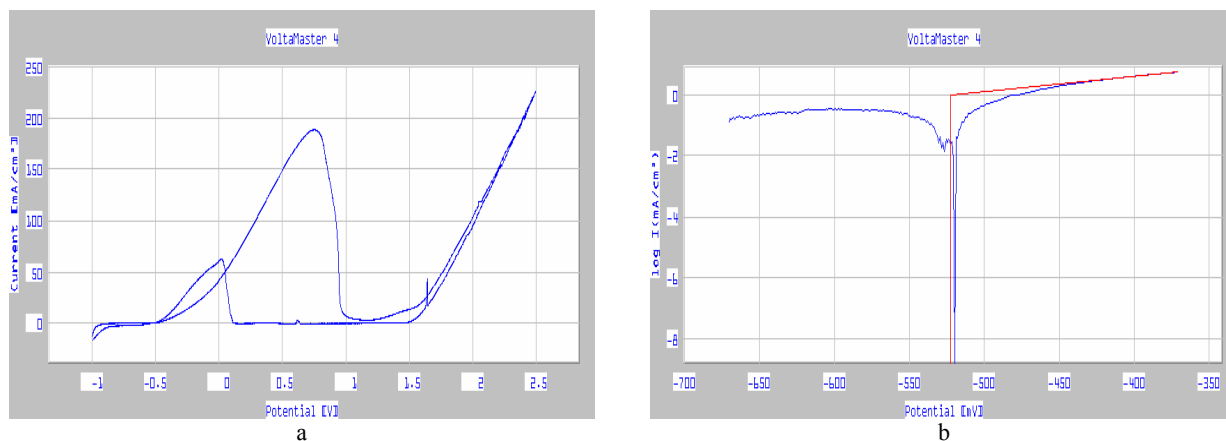


Fig. 3. Coated FeC electrode; system I; a - cyclic voltammograms; b -Tafel tests

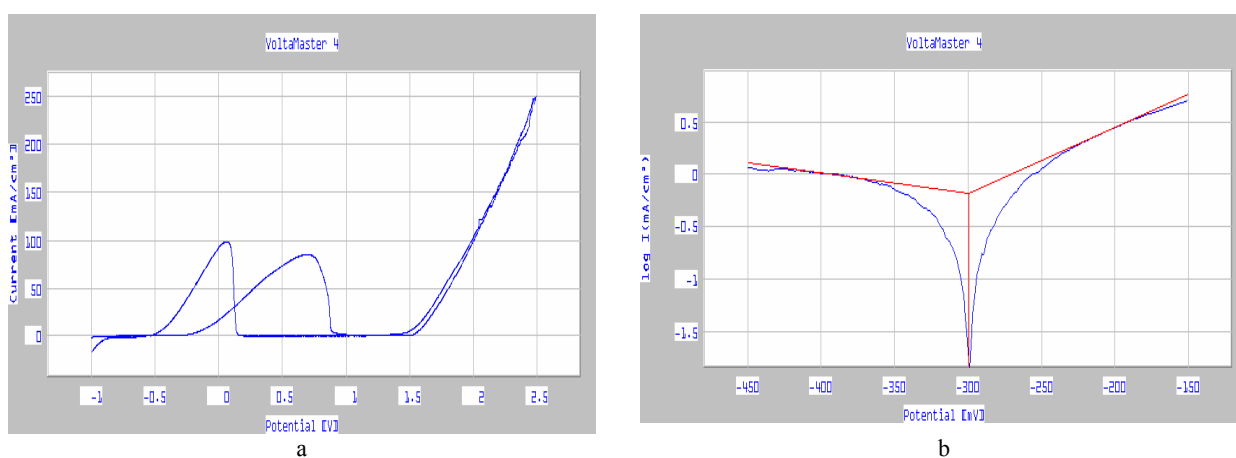


Fig. 4. Coated FeC electrode; system II; a – cyclic voltammograms; b –Tafel tests

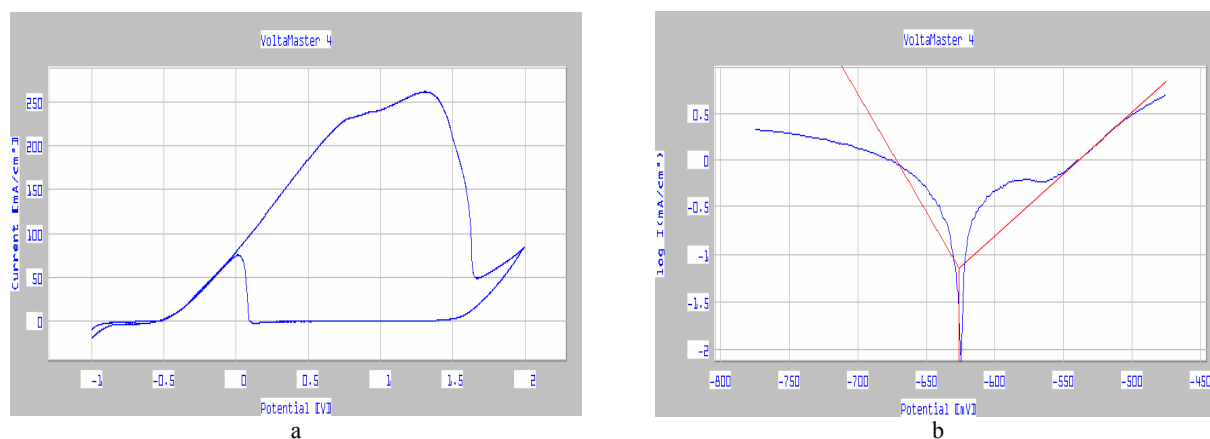


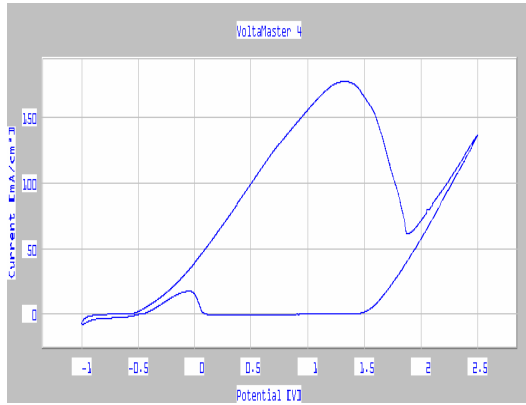
Fig. 5. Coated FeC electrode according to system III; a – cyclic voltammograms; b –Tafel tests

Table 1. Results of cyclic voltammograms 2a, 3a, 4a, 5a

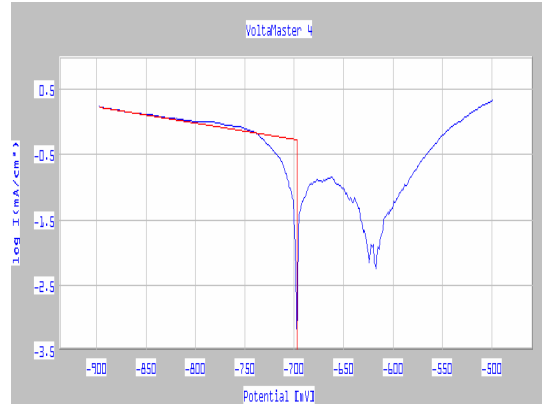
| Parameters | Electrodes | | | |
|--|------------|----------|-----------|------------|
| | Uncoated | System I | System II | System III |
| i_{peak}^{\rightarrow} [mA/cm ²] | 290 | 190 | 90 | 280 |
| $\epsilon_{pic}^{\rightarrow}$ [mV] | 900 | 750 | 600 | 1300 |
| i_{peak}^{\leftarrow} [mA/cm ²] | - | 60 | 100 | 85 |
| $\epsilon_{peak}^{\leftarrow}$ [mV] | - | 50 | 100 | 50 |
| ϵ_{O_2} [mV] | 1500 | 1500 | 1500 | 1500 |
| ϵ_{pas} [mV] | 1350 | 900 | 850 | 1600 |
| i_{pas} [mA/cm ²] | 25 | 8 | 0 | 50 |

Table 2. Results of Tafel test 2b, 3b, 4b, 5b

| Parameters | Electrodes | | | |
|---------------------------------|------------|----------|-----------|------------|
| | Uncoated | System I | System II | System III |
| i_{cor} [mA/cm ²] | 0.7666 | 0.9792 | 0.6506 | 0.0718 |
| v_{cor} [mm/year] | 8.99 | 11.48 | 7.63 | 0.842 |
| Rp | 50.91 | 129.51 | 59.57 | 47.67 |
| C | 0.9962 | 0.9996 | 0.9997 | 1.000 |

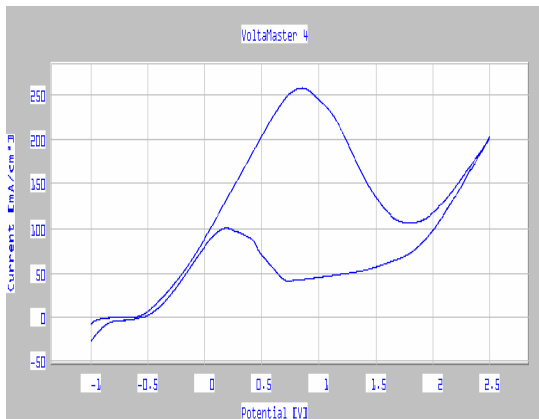


a

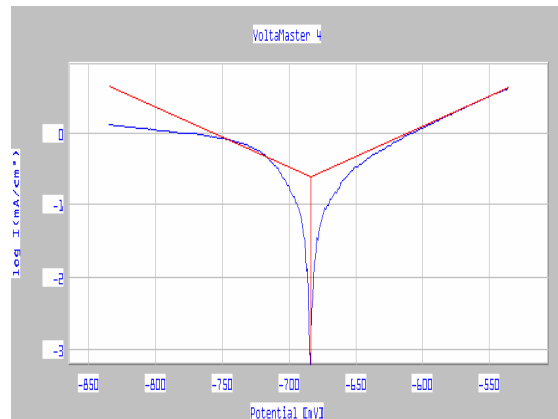


b

Fig. 6. Uncoated FeC electrode, a – cyclic voltammograms; b –Tafel tests

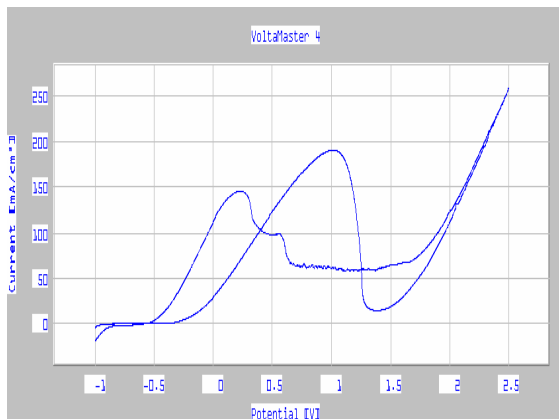


a

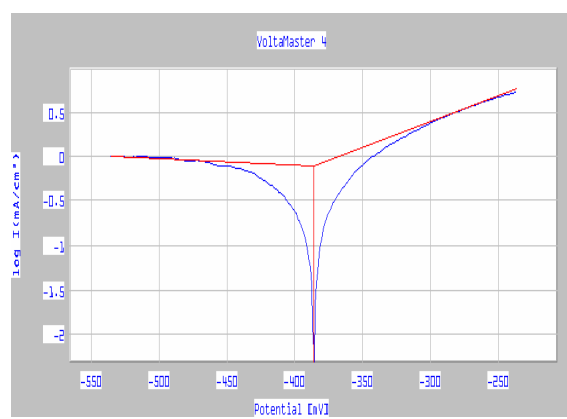


b

Fig. 7. Coated FeC electrode; system I; a - cyclic voltammograms; b -Tafel tests



a



b

Fig. 8. Coated FeC electrode; system II; a - cyclic voltammograms; b -Tafel tests

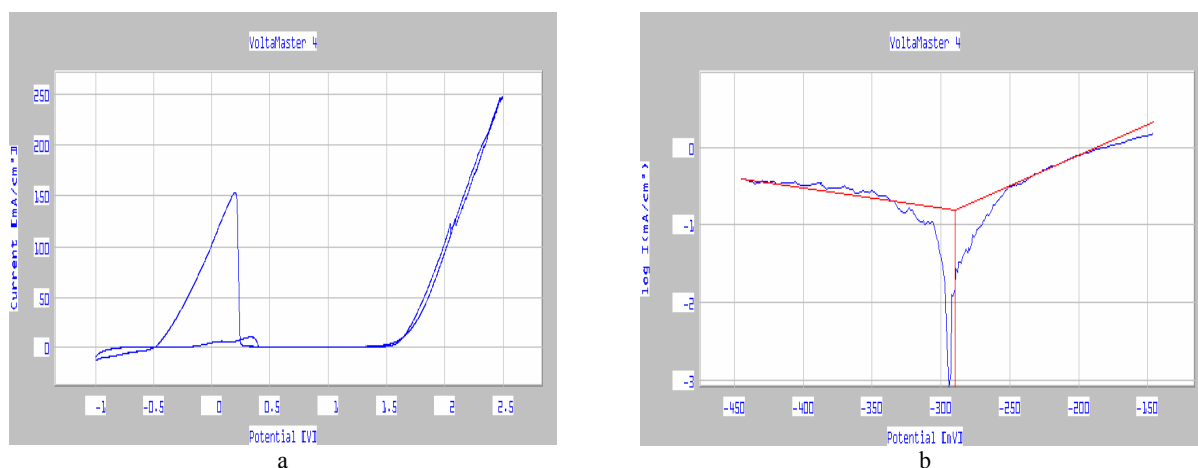

Fig. 9. Coated FeC electrode; system III; a - cyclic voltammograms; b -Tafel tests

Table 3. Results of cyclic voltammograms 8a, 9a, 10a, 11a

| Parameters | Electrodes | | | |
|---|------------|----------|-----------|------------|
| | Uncoated | System I | System II | System III |
| $i_{\text{peak}}^{\rightarrow}$ [mA/cm ²] | 180 | 255 | 195 | 160 |
| $\epsilon_{\text{peak}}^{\rightarrow}$ [mV] | 1300 | 800 | 1050 | 200 |
| $i_{\text{peak}}^{\leftarrow}$ [mA/cm ²] | 20 | 75 | 150 | - |
| $\epsilon_{\text{peak}}^{\leftarrow}$ [mV] | -100 | 190 | 250 | - |
| ϵ_{O_2} [mV] | 1500 | 1500 | 1500 | 1500 |
| ϵ_{pas} [mV] | 1750 | - | 1200 | 210 |
| i_{pas} [mA/cm ²] | 60 | 80 | 10 | 0 |

Table 4. Results of Tafel tests 6b, 7b, 8b, 9b

| Parameters | Electrodes | | | |
|--|------------|----------|-----------|------------|
| | Bare | System I | System II | System III |
| i_{cor} [mA/cm ²] | 0.509 | 0.242 | 0.759 | 0.1522 |
| v_{cor} [mm/year] | 5.966 | 2.835 | 8.898 | 1.785 |
| R_p | 122.86 | 143.45 | 54.46 | -40.69 |
| C | 0.9986 | 1.000 | 0.998 | 0.9964 |

4. Conclusions

The best results was obtained for system III (H₂TPP in benzonitrile) even for a short intent time (5 minutes)- decreased corrosion rate of about 20 time compared to with bare electrode. Increasing of intent time show a significant improving - decreasing of corrosion rate about 20 times comparing with bare electrode. The multifunctional nanocomposites (porphyrin systems) used in this study as coating systems improve the anti-corrosion properties of carbon-steel electrodes.

References

- Epstein A.J., Jasty S.G., (1997), Corrosion protection of iron/steel by emeraldine base polyaniline, *US Patent* 5972518.
- Liu L., Levon K., (1999), Undoped Polyaniline/Surfactant Complex for Corrosion Prevention, *NASA CR*.
- MacDiarmid A.G., Ahmad N., (1997), Prevention of corrosion with polyaniline, *US Patent* 5645890.
- Rahimi A., (2004), Inorganic and Organometallic Polymers, *Iranian Polymer Journal*, **13**, 149-164.
- Sathiyarayanan S., Azim S., Venkatachari G., (2007), Preparation of polyaniline-TiO₂ composite and its comparative corrosion protection performance with polyaniline, *Synthetic Metals*, **157**, 205–213.



REACTIVE ORGANIC CARBONATES WITH LEAVING GROUP FOR BIOLOGICALLY ACTIVE DIPEPTIDES SYNTHESIS

Adina-Elena Segneanu^{1*}, Ionel Balcu¹, Marius Constantin Mirica¹,
Mirela Ioana Iorga¹, Marius Milea², Zoltan Urmosi¹

¹National Institute of R&D for Electrochemistry and Condensed Matter – INCEMC–Timisoara, 144 A. P. Podeanu,
300569 Timisoara, Romania

²University „Politehnica” Timisoara, Faculty of Industrial Chemistry and Environment Engineering, 2 P-ța Victoriei,
300006, Timisoara, Romania

Abstract

The aim of this present paper is investigation of the reactions of preparation of unsymmetrical reactive carbonates from the corresponding symmetrical carbonates and different type of alcohols. The asymmetrical carbonates represent alternative reagents (mild, efficient) for alkoxycarbonylation of amines and amino-acids. The synthesized compounds were characterized by spectroscopic and chromatographic methods. A general method for preparation of asymmetrical carbonates was develop from *N,N'*-disuccinimidylcarbonate. The yield of this reactive carbonates depends by alcohols reactivity, hindered factor and stability of final product.

Key words: alkoxycarbonylation, leaving group, *N,N'*-disuccinimidylcarbonate

1. Introduction

Problems regarding the increase in population density, global climate changes and the dwindling of natural resources are reflected on all the scientific fields. In chemistry, the underlying principles of sustainable chemical development (green chemistry) imposed the necessity for the identification of new methods concerning the reduction of reagents and energy consumption in the chemical processes, the reduction of emissions of toxic chemical products into the environment, the extension of the use of renewable resources.

Thus, reactive organic carbonates are an ecological alternative to halogenated compounds, reagents like phosgene and its reactive chlorinated derivatives (chloroformates, diphosgene, triphosgene) in alkoxycarbonylation and carbonylation reactions.

As carbonic acid esters, reactive organic carbonates have numerous applications in fine organic chemistry: intermediates in the synthesis of other derivatives of carbonic acid (asymmetric carbonates, polycarbonates, carbamates, ureas) and in peptide synthesis. There are many fundamental and applicative scientific studies on the physical and chemical properties (reactivity, stability of molecule) of reactive organic carbonates (Ghost, 1994).

A special interest has been allocated to the relatively high reactivity of these carbonic acid derivatives towards nucleophilic reagents in organic syntheses. (Nájera, 2002).

In peptide synthesis, reactive organic carbonates are employed especially for the protection of amino groups, by converting it into a carbamate-type derivative through an alkoxycarbonylation reaction, and for the activation of carboxyl groups by

* Author to whom all correspondence should be addressed: e-mail: s_adinaelena@yahoo.com; Phone: 0721072589

converting it into a reactive ester (Shaikh et al., 1996). For the protection of the amino function in amino acids alkoxy-carbonyl-type (carbamate) groups are preferred, which minimize the racemisation of optically active centres.

The classical synthesis of carbamates takes place in the presence of toxic compounds such as phosgene and its reactive chlorinated derivatives (chloroformates, diphosgene, and triphosgene).

This paper proposes the synthesis of a series of reactive organic carbonate by an original procedure, as an alternative to the traditional method which employs toxic and dangerous reagents (phosgene and its chlorinated derivatives), as well as the applicability of these derivatives to the synthesis of bioactive compounds with many utilizations in pharmaceuticals and food industries.

2. Materials and methods

Melting points were determined in a Boetius apparatus (Carl Zeiss Jena). The *IR spectra* were recorded in KBr pellet for solid compounds and the reaction monitoring was carried out in thermostated silicon cells of 0.137 mm thickness on a Jasco FT/IR-430 instrument. TLC analyses were carried out on pre-coated plates silica gel 60 F254 (Merk). (Eluent: dichloromethane:ethyl ether= 3:7). Spot visualization was achieved by exposing the plates under a UV 254 lamp.

Mass spectrometry was conducted on a High Capacity Ion Trap Ultra (HCT Ultra, PTM discovery) mass spectrometer from Bruker Daltonics, Bremen, Germany. HCT MS is interfaced to a PC running the CompassTM 1.2 integrated software package, which includes the HystarTM 3.2.37 and Esquire 6.1.512 modules for instrument controlling and chromatogram/ spectrum acquisition, and Data Analysis 3.4.179 portal for storing the ion chromatograms and processing the MS data.

The ¹H-NMR and ¹³C-NMR were recorded on a Bruker DPX at 200 MHz in DMSO-*d*₆, with TMS as reference. The values of coupling constants are normal for vicinal couplings (CH-CH, CH-NH): 6.5 - 7 Hz. Detailed IR, ¹H-NMR and ¹³C-NMR spectra are available from the authors.

All reagents were purchased from chemical suppliers and used without further purification.

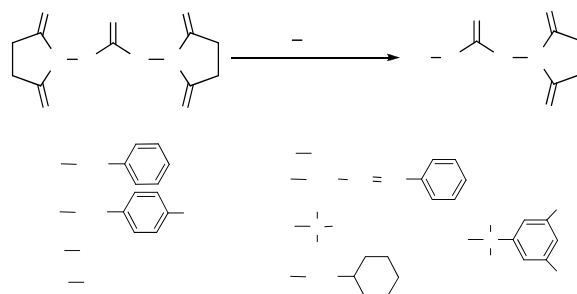
3. Results and discussions

Investigation on described procedure for preparation of reactive succinimidyl carbonates (Kundu et al., 1994) and using the results of IR reaction monitoring for benzyl-*N*-succinimidylcarbonate (Z-OSu) has been developed a new efficient synthetic route for various mixed succinimidyl carbonates (1) from *N,N'*-disuccinimidylcarbonate (Scheme 1).

The synthesis of reactive succinimidyl carbonates (1) was done by a different procedure

from the literature (molar ratio, reaction time) (Segneanu, 2007).

Thus to obtain compounds **1**, symmetrical carbonate was treated with alcohols and amine (TEA) in the molar ratio carbamate: diamine = 1,1:1:1,1. The reactions we carried out in acetonitrile at room temperature for 4 hours.



Scheme 1. Synthesis of asymmetric carbonates from *N,N'*-disuccinimidylcarbonate

Following our protocol was achieved asymmetrical carbonates **1a-i** from the in yields between 60-82,8% (Table 1).

Table 1. Preparation of mixed succinimidyl carbonates

| Compound | η (%) | TLC | Mp ($^{\circ}$ C) | IR (cm^{-1}) |
|-----------|------------|------|--------------------|------------------|
| 1a | 70.5 | 0.11 | 78-81 | 1816, 1783, 1727 |
| 1b | 66.8 | 0.55 | 87-89 | 1815, 1793, 1742 |
| 1c | 64.1 | 0.58 | - | 1814, 1784, 1725 |
| 1d | 75.0 | 0.61 | - | 1811, 1796, 1740 |
| 1e | 62.0 | 0.69 | 84.5-86.5 | 1833, 1785, 1736 |
| 1f | 69.4 | 0.12 | 168-171 | 1786, 1740 |
| 1g | 82.8 | 0.21 | 91-94 | 1817, 1788, 1736 |
| 1h | 68.5 | 0.19 | 72-75 | 1807, 1774, 1734 |
| 1i | 60.0 | 0.36 | 99-101 | 1832, 1786, 1736 |

4. Experimental

N,N'-disuccinimidylcarbonate (563 mg, 2.2 mmol) was dissolved in acetonitrile (15 mL), alcohol (1.1 equiv.) and tri-*n*-butylamine (1.1 equiv.) was added. The reaction mixture was stirred at room temperature for 4 hours. After vacuum solvent evaporation, the residue was dissolved in ethyl acetate (20 mL) and the solution was three time washed with 20% citric acid solution (5 mL), 5% NaHCO₃ solution (5 mL) and saturated NaCl solution (5 mL). The organic phase was dried (MgSO₄) and concentrated to dryness. The residue was crystallized from ethyl acetate-hexane.

Benzyl-*N*-succinimidylcarbonate (Z-OSu) – **1a**. MS (m/z): 81,7, 88,7, 115,4, 161,2, 173,3, 189,3, 233,2, 249,2; ¹H-RMN (DMSO): 7,44s, 7,39s, 5,39s, 5s, 2,80s; ¹³C-RMN (DMSO): 169,7(C₁), 151,2(C₂), 133,7(C₅) 129,0(C₆), 72,2(C₄), 25,3(C₃).

4-Nitro-benzyl-*N*-succinimidylcarbonate
(Z(NO₂)-OSu) – 1b. MS (m/z): 97,4, 139,0, 152,0, 160,0, 205,1, 221,2, 232,1, 261,1, 274,4, 294,3

2-Ethoxyethyl-*N*-succinimidylcarbonate – 1c.
¹H-RMN (DMSO): 4,44t, 3,65t, 3,48q, 2,8s, 1,13t
¹³C-RMN (DMSO): 169,7(C₁), 151,3(C₂), 70,2(C₄), 67,0(C₅), 65,6(C₆), 25,3(C₃), 14,9(C₇).

β-Phenylethyl-*N*-succinimidylcarbonate – 1d.
¹H-RMN (CDCl₃): 7,3 m, 4,5 t, 3,05 t, 2,79 s, 2,64 s
¹³C-RMN (CDCl₃): 168,7(C₁), 151,4(C₂), 136,1(C₆), 128,7(C₇), 71,5(C₄), 34,7(C₅), 25,4(C₃).

Diphenylethyl-*N*-succinimidylcarbonate – 1e.
MS (m/z): 211, 204, 184, 183, 168, 167, 165, 155, 154, 152, 142, 115, 107, 105, 100, 98, 88, 78, 70, 53, 52; ¹H-RMN (CDCl₃, DMSO): 7,42m, 6,87s, 2,79 s.

¹³C-RMN (CDCl₃, DMSO): 169,4(C₁), 150,5(C₂), 138,2(C₅), 128,6(C₆), 83,5(C₄), 25,3(C₃).

Cinnamyl-*N*-succinimidylcarbonate-1f. MS (m/z): 107,5, 117,4, 135,3, 149,2, 163,3, 180,3, 205,2, 217, 3, 234,2, 259, 2, 275,3.

Tert-buthyl-*N*-succinimidylcarbonate (Boc-OSu)-1g. MS (m/z): 100,5, 116,3, 155,2, 183,1, 197,2, 215, 05.

Cyclohexylmethyl-*N*-succinimidylcarbonate-1h. MS (m/z): 81,7, 89,6, 99,5, 114,4, 123,3, 157,3, 157,3, 171,2, 185,1, 203,1, 213, 2, 227, 3.

α, α-dimethyl-3,5-dimethoxybenzyl-*N*-succinimidylcarbonate (DdZ-OSu)-1i. MS (m/z): 196, 181, 165, 149, 142, 115, 100, 98, 88, 86, 70, 55, 54, 53; ¹H-RMN (CDCl₃, DMSO): 6,63s, 6,28s, 4,73s, 3,76s, 2,84s, 1,47d; ¹³C-RMN (CDCl₃, DMSO): 160,2(C₁), 153,0(C₂), 103,5(C₇), 97,6(C₉), 78,9(C₄), 550(C₁₀), 31,71(C₅), 25,5(C₃).

Detailed ¹³C-RMN for Benzyl-*N*-succinimidylcarbonate (Z-OSu) (1a), ¹H-NMR spectra for 2-Ethoxyethyl-*N*-succinimidylcarbonate (1c) and β-Phenylethyl-*N*-succinimidylcarbonate (1d) and are illustrated in Figs. 1, 2 and 3.

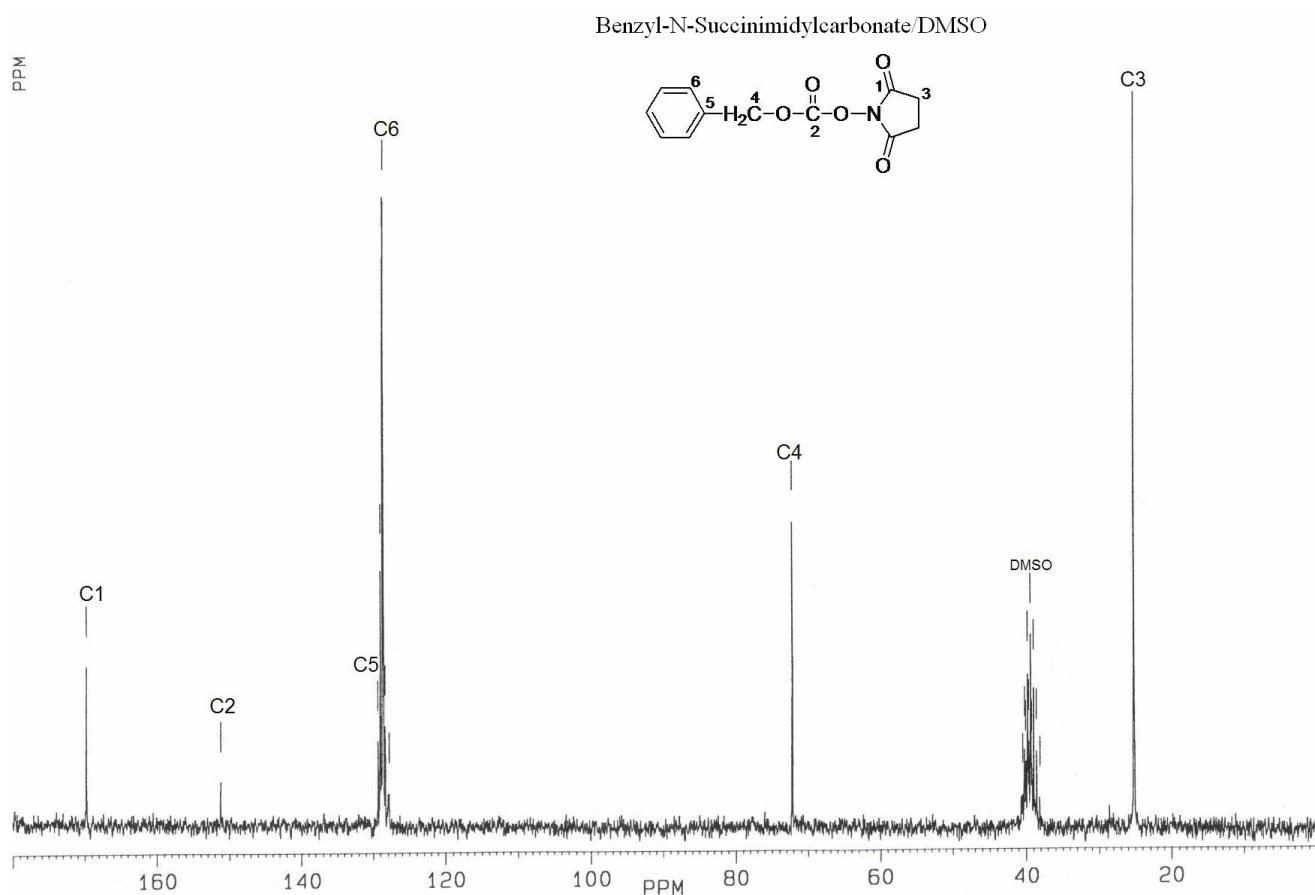


Fig. 1. ¹³C-RMN spectra of Benzyl-*N*-succinimidylcarbonate (Z-OSu) (1a)

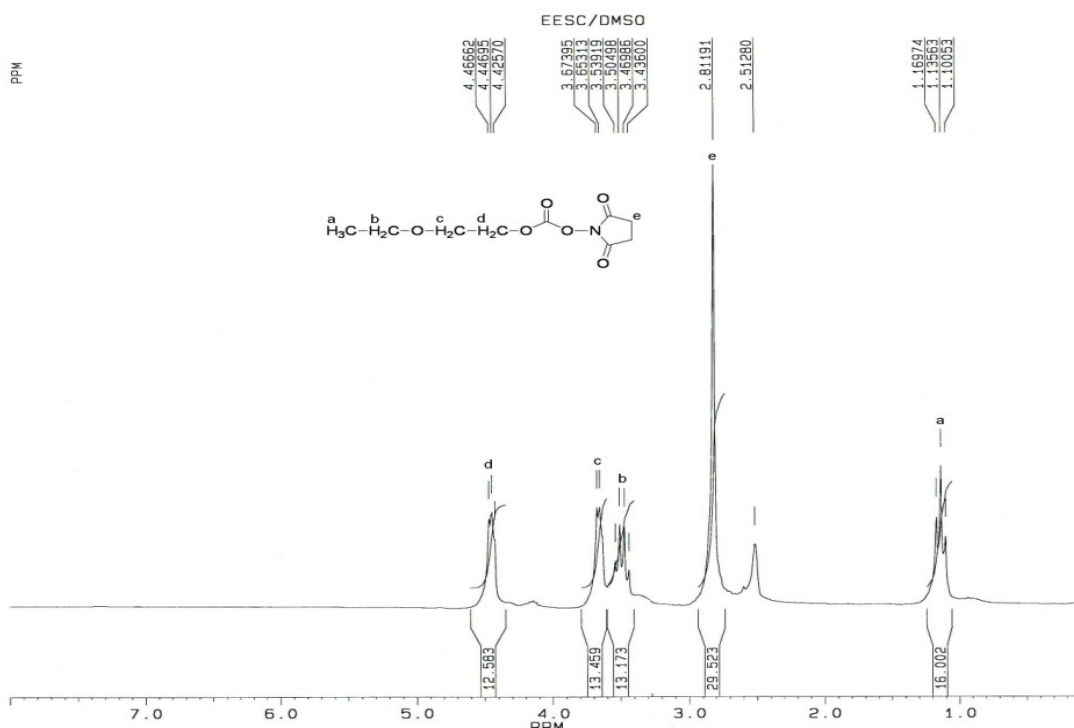


Fig. 2. ¹H-NMR spectra for 2-Ethoxyethyl-N-succinimidylcarbonate (1c)

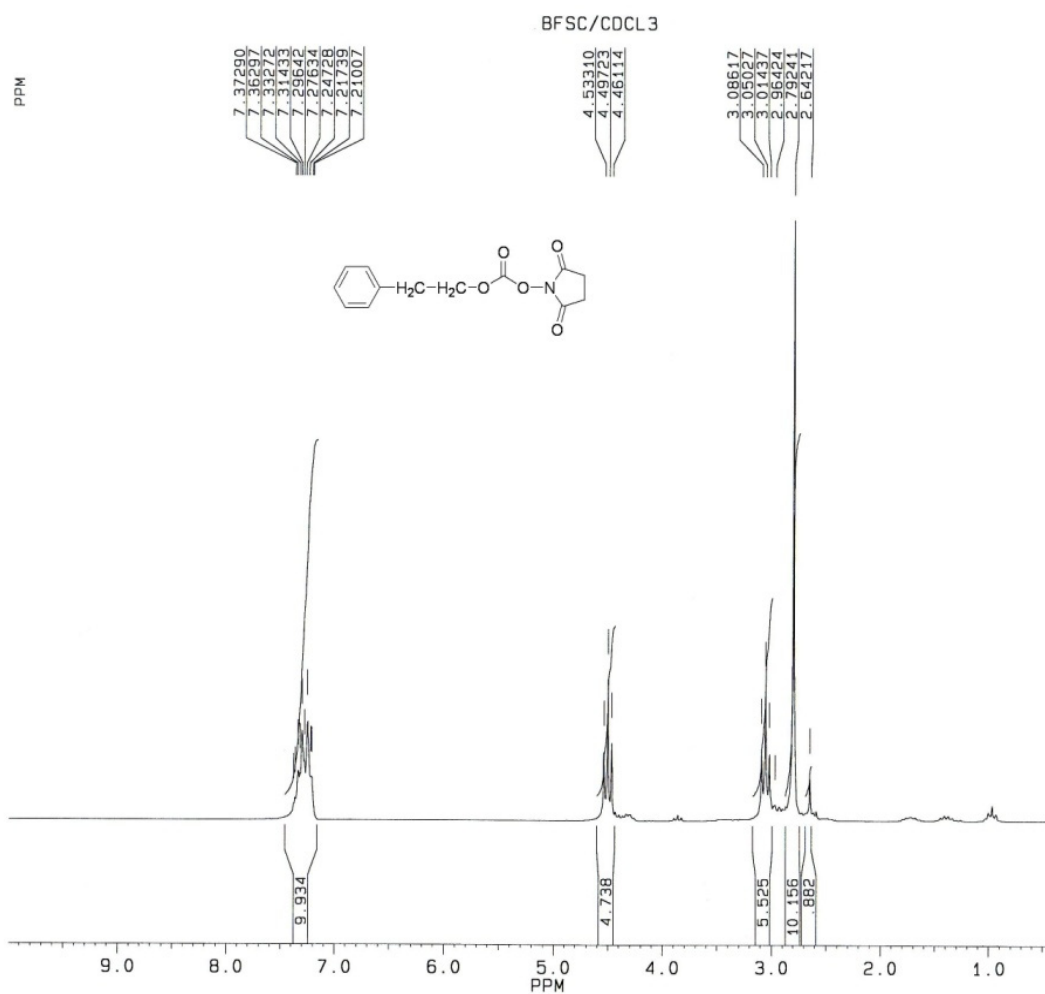


Fig. 3. ¹H-NMR spectra β -Phenylethyl-N-succinimidylcarbonate (1d)

5. Conclusions

Comparative with synthesis method describe in literature, after the IR monitoring reaction and establishment the laboratory optimal conditions (reaction time, molar ratio) we have developed a convenient synthesis procedure for the preparation of a series of mixed carbonates from *N,N'*-disuccinimidylcarbonate and different aromatic and aliphatic alcohols.

The reactive organic carbonates yield depends on alcohol reactivity, hindered factor and stability of final product.

The yield of α, α -dimethyl-3,5-dimethoxybenzyl-*N*-succinimidylcarbonate is acceptable due the low stability of this compound and also, because the tertiary alcohol (α, α -dimethyl-3,5-dimethoxy-benzyl alcohol) is characterized by an relative low stability (sterically hindered).

References

- Ghost A.K., Duong T.T., McKee S.P., Thompson W.J., (1992), *N,N'*-disuccinimidyl carbonate: a useful reagent for alkoxy-carbonylation of amines, *Tetrahedron Letter*, **32**, 2781-2784.
- Kundu B., Shukla A., Guptasarma P., (2002), Manipulation of unfolding-induced protein aggregation by peptides selected for aggregate-binding ability through phage display library screening, *Biochemical and Biophysical Research Communications*, **291**, 903-907.
- Nájera C., (2002), *From α -Amino Acids to Peptides: All You Need for the Journey*, *Synlett*, **9**, 1388-1403.
- Segneanu A., (2007), *Using Organic Carbonates for protecting Aminic Groups and Activation of Carboxylic Groups of Aminoacids during Peptides Synthesis* (in Romanian), Politehnica Timisoara Press, Romania.
- Shaikh A.G., Sivaram S., (1996), Organic Carbonates, American Chemical Society, *Chemical Reviews*, **96**, 951-976.



NON-FERROUS HEAVY METAL METALLURGY WASTEWATER TREATMENT BY THE ELECTRO-FLOTO-COAGULATION METHOD

Marius Constantin Mirica, Mirela Ioana Iorga*, Adina Segneanu, Ionel Balcu, Doru Buzatu, Cristian Vaszilcsin

National Institute for R&D in Electrochemistry and Condensed Matter, INCEMC,
144 Dr. Aurel Paunescu Podeanu St., 300569 Timisoara, Romania

Abstract

Electroflotocoagulation is used for the treatment of liquid wastes of various origins, containing suspended matter. The metal hydroxide formed by electrochemical metallic ions generation acts to aggregate the colloidal impurities, and the hydrogen bubbles evolved at the cathode allow flotation of foam containing the impurities. The aggregates formed (containing the impurities) and lifted above the solution can then be removed. Electroflotocoagulation (simultaneous electrocoagulation and electroflotation) is studied as partially treatment method for non-ferrous heavy metals metallurgy wastewater (levigates). A pilot scale reactor for electroflotocoagulation is proposed. Different parameters are studied: pH variation during the process, anodic and cathodic current densities, cell voltage, energy consumption, hydrogen evolution etc.

Key words: electroflotocoagulation, environment protection, levigate, metallurgy wastewater

1. Introduction

Considering the latest regulation in environment protection, the impact of industry over natural environment must be significantly diminished. An important pollution source is industrial wastewater, particularly metallurgy wastewater.

Coagulation is an effective technique for the treatment of liquid wastes of various origins, especially in the presence of suspended matter. Coagulation agents (usually Fe or Al cations) determine the flocculation by decreasing the zeta potential of the suspended entities (Chen, 2004; Hansen et al., 2007; Holt et al., 1999; Racoviteanu, 2003).

Flotation is the process of gas bubbles adhering to suspended entities surfaces, therefore increasing their buoyancy and determining them to ascend (Chen, 2004; Khelifa et al., 2005).

It is possible to generate Fe or Al cations using sacrificial anodes to induce flocculation and to use the hydrogen evolved at the counter-electrode to lift the formed flocs. This method is called electroflotocoagulation (Chen, 2004; Escobar et al.,

2006). Electroflotocoagulation was studied as an intermediary stage for metallurgy wastewater (levigates) treatment, aimed at removing the fine solid particles in suspension (colloids).

A pilot scale reactor for electroflotocoagulation was build and tested in both synthetic and real electrolyte solution.

2. Experimental

A pilot reactor of 2 dm³ volume was build. The height of the pilot scale reactor is the same with the proposed industrial reactor, thus the translation to industrial scale is easy done by multiplying the other two axes, maintaining a good similarity.

Reactor's dimensions are: length: 100 mm, width: 20 mm, working height: 1000 mm.

The cathode is made of Fe. It is a fixed flat surface of 1000 mm² (10 x 100 mm).

The anode is removable and consists of a wire of 3 mm diameter and 100 mm length.

The pilot installation for non-ferrous heavy metal metallurgy wastewater treatment is presented in Fig. 1.

* Author to whom all correspondence should be addressed: e-mail: mirela.iorga@incemc.ro; Fax 0256 201382

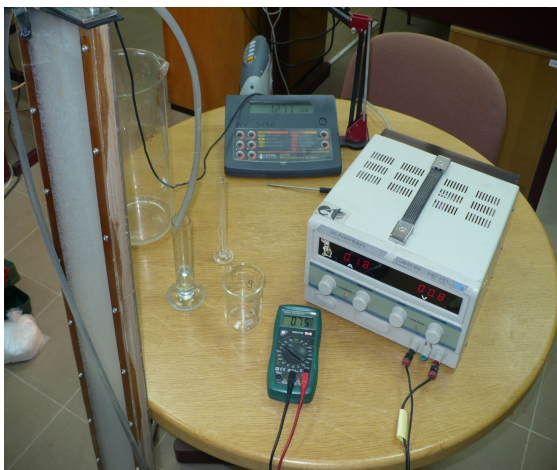


Fig. 1. Pilot installation for non-ferrous heavy metal metallurgy wastewater treatment

For the first part of the experiment, a synthetic solution was used for electrolysis.

The solution's composition was: 20% NaCl, 1000 ppm Na₂SO₄ (Khelifa et al., 2005). NaOH was also added up to pH 12.7. The solution was electrolyzed for 120 min. at an anodic current density of 50, 150, 250, 350, 450, 550 A/m², respectively. Two anode materials were used: Fe and Al.

The following parameters were observed during electrolysis and measured every 10 minutes: pH, cell voltage, foam layer thickness, evolved hydrogen volume.

For the second part of the experiment, a real solution was used for electrolysis. The solution's composition was unknown. However the real solutions are very complex (an example of such solution is 0.07 mg/L As; 0.02 mg/L Ba; 0.003 mg/L Cd; <0.005 mg/L Cr; 0.08 mg/L Cu; <0.05 mg/L Hg; 0.01 mg/L Mo; <0.004 mg/L Ni; 0.33 mg/L Pb; 0.01 mg/L Sb; <0.5 mg/L Se; 0.16 mg/L Zn; 1.4 mg/L chlorides; <10 mg/L fluorides; 3.6 mg/L sulphates).

The measured solution's pH was 13.5. The solution was electrolyzed for 360 min. at an anodic current density of 250 A/m². Two anode materials were used: Fe and Al. The following parameters were observed during electrolysis and measured every 10 minutes: pH, cell voltage, foam layer thickness.

3. Results and Discussion

The results of the experiment are presented in Table 1 – for synthetic solution and Al electrode, Table 2 – for synthetic solution and Fe electrode, Table 3 – for real solution and Al electrode and Table 4 – for real solution and Fe electrode.

For the synthetic solution for both Al and Fe anodes:

- the pH remained constant during the experiment;
- the volume of evolving H₂ was constant during the experiment;

- the cell voltage (and thus the energy consumption) was quickly stabilized and remained constant during the experiment;
- the foam layer thickness remained under 10 mm during the experiment.

For the real solutions:

- the pH remained constant during the experiment for both Al and Fe anodes;
- the foam layer thickness remained under 10 mm during the experiment for both Al and Fe anodes;
- in case of Fe anode, the cell voltage increased by a factor of approximately 1.2, then remained constant;
- in case of Al anode, the cell voltage increased by a factor of approximately 19, then remained constant.

The abrupt increase in cell voltage in case of Al anode as opposed to Fe anode is due to the flocs quick apparition at anode surface, thus blocking the anode surface.

Fig. 2 presents a blocked Al anode and Fig. 3 presents an unblocked Fe anode.



Fig. 2. Blocked Al anode

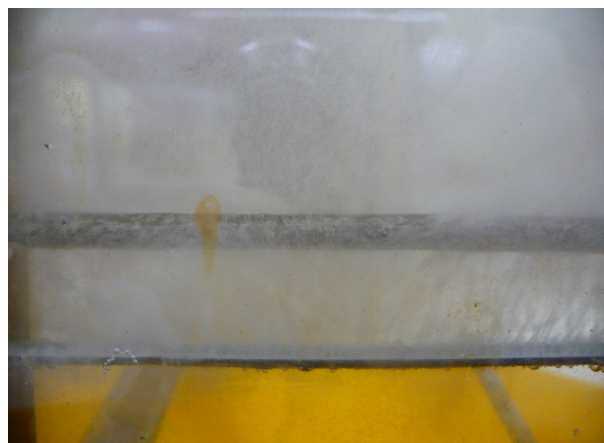


Fig. 3. Unblocked Fe anode

A solution for this problem could be to conduct the electrolysis at a much lower current density so that the aluminum ions are generated at a much lower speed and are dispersed before clogging the anode. However this will proportionally increase the duration of the process and needs to be further experimented.

Table 1. Synthetic solution, Al electrode

| $\tau = 120 \text{ min, Al anode, } i = 50 \text{ A/m}^2$ | | | | | | | | | | | | | |
|--|-------|-------|-------|-------|-------|-------|-------|-------|-------|-------|-------|-------|-------|
| $\tau [\text{min}]$ | 0 | 10 | 20 | 30 | 40 | 50 | 60 | 70 | 80 | 90 | 100 | 110 | 120 |
| pH | 12.67 | 12.79 | 12.80 | 12.80 | 12.79 | 12.78 | 12.76 | 12.75 | 12.73 | 12.74 | 12.75 | 12.75 | 12.75 |
| $V \text{H}_2 [\text{mL}]$ | 0 | 9 | 20 | 30 | 42 | 53 | 65 | 78 | 89 | 101 | 110 | 121 | 133 |
| $U [\text{V}]$ | 0.55 | 0.63 | 0.65 | 0.65 | 0.66 | 0.66 | 0.67 | 0.67 | 0.67 | 0.67 | 0.67 | 0.67 | 0.67 |
| $\Delta_{\text{foam}} [\text{mm}]$ | 0 | 4 | 4 | 4 | 4 | 4 | 4 | 4 | 4 | 4 | 4 | 4 | 4 |
| $\tau = 120 \text{ min, Al anode, } i = 150 \text{ A/m}^2$ | | | | | | | | | | | | | |
| $\tau [\text{min}]$ | 0 | 10 | 20 | 30 | 40 | 50 | 60 | 70 | 80 | 90 | 100 | 110 | 120 |
| pH | 12.66 | 12.80 | 12.81 | 12.80 | 12.78 | 12.77 | 12.75 | 12.73 | 12.72 | 12.73 | 12.76 | 12.77 | 12.76 |
| $V \text{H}_2 [\text{mL}]$ | 0 | 17 | 33 | 47 | 65 | 85 | 103 | 119 | 136 | 154 | 173 | 187 | 205 |
| $U [\text{V}]$ | 0.69 | 0.74 | 0.75 | 0.74 | 0.74 | 0.75 | 0.75 | 0.75 | 0.75 | 0.75 | 0.75 | 0.75 | 0.75 |
| $\Delta_{\text{foam}} [\text{mm}]$ | 0 | 2 | 3 | 3 | 3 | 3 | 3 | 3 | 3 | 3 | 3 | 3 | 3 |
| $\tau = 120 \text{ min, Al anode, } i = 250 \text{ A/m}^2$ | | | | | | | | | | | | | |
| $\tau [\text{min}]$ | 0 | 10 | 20 | 30 | 40 | 50 | 60 | 70 | 80 | 90 | 100 | 110 | 120 |
| pH | 12.66 | 12.80 | 12.81 | 12.80 | 12.78 | 12.77 | 12.75 | 12.73 | 12.72 | 12.73 | 12.76 | 12.77 | 12.76 |
| $V \text{H}_2 [\text{mL}]$ | 0 | 17 | 33 | 47 | 65 | 85 | 103 | 119 | 136 | 154 | 173 | 187 | 205 |
| $U [\text{V}]$ | 0.69 | 0.74 | 0.75 | 0.74 | 0.74 | 0.75 | 0.75 | 0.75 | 0.75 | 0.75 | 0.75 | 0.75 | 0.75 |
| $\Delta_{\text{foam}} [\text{mm}]$ | 0 | 2 | 3 | 3 | 3 | 3 | 3 | 3 | 3 | 3 | 3 | 3 | 3 |
| $\tau = 120 \text{ min, Al anode, } i = 350 \text{ A/m}^2$ | | | | | | | | | | | | | |
| $\tau [\text{min}]$ | 0 | 10 | 20 | 30 | 40 | 50 | 60 | 70 | 80 | 90 | 100 | 110 | 120 |
| pH | 12.69 | 12.69 | 12.70 | 12.71 | 12.70 | 12.71 | 12.70 | 12.69 | 12.69 | 12.69 | 12.69 | 12.69 | 12.69 |
| $V \text{H}_2 [\text{mL}]$ | 0 | 33 | 67 | 101 | 136 | 172 | 207 | 242 | 278 | 315 | 350 | 386 | 421 |
| $U [\text{V}]$ | 0.85 | 0.91 | 0.92 | 0.92 | 0.92 | 0.92 | 0.93 | 0.93 | 0.93 | 0.93 | 0.93 | 0.93 | 0.93 |
| $\Delta_{\text{foam}} [\text{mm}]$ | 0 | 4 | 4 | 4 | 4 | 4 | 4 | 4 | 4 | 4 | 4 | 4 | 4 |
| $\tau = 120 \text{ min, Al anode, } i = 450 \text{ A/m}^2$ | | | | | | | | | | | | | |
| $\tau [\text{min}]$ | 0 | 10 | 20 | 30 | 40 | 50 | 60 | 70 | 80 | 90 | 100 | 110 | 120 |
| pH | 12.67 | 12.69 | 12.70 | 12.70 | 12.69 | 12.68 | 12.67 | 12.67 | 12.66 | 12.66 | 12.67 | 12.67 | 12.66 |
| $V \text{H}_2 [\text{mL}]$ | 0 | 41 | 84 | 126 | 170 | 213 | 258 | 302 | 347 | 389 | 432 | 476 | 519 |
| $U [\text{V}]$ | 0.92 | 0.97 | 0.97 | 0.98 | 0.98 | 0.98 | 0.99 | 0.99 | 0.98 | 0.98 | 0.98 | 0.98 | 0.98 |
| $\Delta_{\text{foam}} [\text{mm}]$ | 0 | 4 | 4 | 4 | 4 | 4 | 4 | 4 | 4 | 4 | 4 | 4 | 4 |
| $\tau = 120 \text{ min, Al anode, } i = 550 \text{ A/m}^2$ | | | | | | | | | | | | | |
| $\tau [\text{min}]$ | 0 | 10 | 20 | 30 | 40 | 50 | 60 | 70 | 80 | 90 | 100 | 110 | 120 |
| pH | 12.66 | 12.69 | 12.70 | 12.69 | 12.68 | 12.68 | 12.67 | 12.67 | 12.68 | 12.68 | 12.67 | 12.68 | 12.67 |
| $V \text{H}_2 [\text{mL}]$ | 0 | 51 | 111 | 172 | 231 | 289 | 347 | 403 | 458 | 511 | 565 | 617 | 670 |
| $U [\text{V}]$ | 1.02 | 1.06 | 1.07 | 1.08 | 1.07 | 1.07 | 1.08 | 1.08 | 1.08 | 1.08 | 1.07 | 1.07 | 1.07 |
| $\Delta_{\text{foam}} [\text{mm}]$ | 0 | 4 | 4 | 4 | 4 | 4 | 4 | 4 | 4 | 4 | 4 | 4 | 4 |

Table 2. Synthetic solution, Fe electrode

| $\tau = 120 \text{ min, Fe anode, } i = 50 \text{ A/m}^2$ | | | | | | | | | | | | | |
|--|-------|-------|-------|-------|-------|-------|-------|-------|-------|-------|-------|-------|-------|
| $\tau [\text{min}]$ | 0 | 10 | 20 | 30 | 40 | 50 | 60 | 70 | 80 | 90 | 100 | 110 | 120 |
| pH | 12.77 | 12.80 | 12.82 | 12.83 | 12.85 | 12.84 | 12.83 | 12.82 | 12.81 | 12.81 | 12.80 | 12.81 | 12.81 |
| $V \text{H}_2 [\text{mL}]$ | 0 | 0 | 0 | 0 | 0 | 0 | 0 | 0 | 0 | 0 | 0 | 0 | 0 |
| $U [\text{V}]$ | 0.84 | 0.83 | 0.81 | 0.81 | 0.80 | 0.79 | 0.79 | 0.78 | 0.79 | 0.79 | 0.78 | 0.78 | 0.78 |
| $\Delta_{\text{foam}} [\text{mm}]$ | 0 | 2 | 2 | 3 | 4 | 4 | 4 | 4 | 5 | 5 | 5 | 5 | 5 |
| $\tau = 120 \text{ min, Fe anode, } i = 150 \text{ A/m}^2$ | | | | | | | | | | | | | |
| $\tau [\text{min}]$ | 0 | 10 | 20 | 30 | 40 | 50 | 60 | 70 | 80 | 90 | 100 | 110 | 120 |
| pH | 12.77 | 12.80 | 12.82 | 12.83 | 12.85 | 12.84 | 12.83 | 12.82 | 12.81 | 12.81 | 12.80 | 12.81 | 12.81 |
| $V \text{H}_2 [\text{mL}]$ | 0 | 0 | 0 | 0 | 0 | 0 | 0 | 0 | 0 | 0 | 0 | 0 | 0 |
| $U [\text{V}]$ | 0.84 | 0.83 | 0.81 | 0.81 | 0.80 | 0.79 | 0.79 | 0.78 | 0.79 | 0.79 | 0.78 | 0.78 | 0.78 |
| $\Delta_{\text{foam}} [\text{mm}]$ | 0 | 2 | 2 | 3 | 4 | 4 | 4 | 4 | 5 | 5 | 5 | 5 | 5 |

| $\tau = 120 \text{ min, Fe anode, } i = 250 \text{ A/m}^2$ | | | | | | | | | | | | | |
|--|-------|-------|-------|-------|-------|-------|-------|-------|-------|-------|-------|-------|-------|
| $\tau [\text{min}]$ | 0 | 10 | 20 | 30 | 40 | 50 | 60 | 70 | 80 | 90 | 100 | 110 | 120 |
| pH | 12.76 | 12.77 | 12.79 | 12.80 | 12.80 | 12.79 | 12.80 | 12.80 | 12.79 | 12.80 | 12.80 | 12.79 | 12.80 |
| $V H_2 [\text{mL}]$ | 0 | 0 | 0 | 0 | 0 | 0 | 0 | 0 | 0 | 0 | 0 | 0 | 0 |
| $U [V]$ | 1.16 | 1.14 | 1.11 | 1.09 | 1.09 | 10.8 | 1.08 | 1.09 | 1.08 | 1.08 | 1.08 | 1.08 | 1.08 |
| $\Delta_{\text{foam}} [\text{mm}]$ | 0 | 2 | 3 | 5 | 5 | 5 | 6 | 6 | 6 | 6 | 6 | 6 | 6 |
| $\tau = 120 \text{ min, Fe anode, } i = 350 \text{ A/m}^2$ | | | | | | | | | | | | | |
| $\tau [\text{min}]$ | 0 | 10 | 20 | 30 | 40 | 50 | 60 | 70 | 80 | 90 | 100 | 110 | 120 |
| pH | 12.76 | 12.77 | 12.79 | 12.80 | 12.80 | 12.79 | 12.80 | 12.80 | 12.79 | 12.80 | 12.80 | 12.79 | 12.80 |
| $V H_2 [\text{mL}]$ | 0 | 0 | 0 | 0 | 0 | 0 | 0 | 0 | 0 | 0 | 0 | 0 | 0 |
| $U [V]$ | 1.16 | 1.14 | 1.11 | 1.09 | 1.09 | 10.8 | 1.08 | 1.09 | 1.08 | 1.08 | 1.08 | 1.08 | 1.08 |
| $\Delta_{\text{foam}} [\text{mm}]$ | 0 | 2 | 3 | 5 | 5 | 5 | 6 | 6 | 6 | 6 | 6 | 6 | 6 |
| $\tau = 120 \text{ min, Fe anode, } i = 450 \text{ A/m}^2$ | | | | | | | | | | | | | |
| $\tau [\text{min}]$ | 0 | 10 | 20 | 30 | 40 | 50 | 60 | 70 | 80 | 90 | 100 | 110 | 120 |
| pH | 12.72 | 12.73 | 12.77 | 12.77 | 12.75 | 12.75 | 12.74 | 12.74 | 12.75 | 12.74 | 12.73 | 12.74 | 12.74 |
| $V H_2 [\text{mL}]$ | 0 | 0 | 0 | 0 | 0 | 0 | 0 | 0 | 0 | 0 | 0 | 0 | 0 |
| $U [V]$ | 1.38 | 1.36 | 1.33 | 1.32 | 1.32 | 1.32 | 1.31 | 1.32 | 1.31 | 1.32 | 1.32 | 1.32 | 1.31 |
| $\Delta_{\text{foam}} [\text{mm}]$ | 0 | 2 | 3 | 4 | 6 | 6 | 7 | 7 | 7 | 7 | 7 | 7 | 7 |
| $\tau = 120 \text{ min, Fe anode, } i = 550 \text{ A/m}^2$ | | | | | | | | | | | | | |
| $\tau [\text{min}]$ | 0 | 10 | 20 | 30 | 40 | 50 | 60 | 70 | 80 | 90 | 100 | 110 | 120 |
| pH | 12.72 | 12.73 | 12.77 | 12.77 | 12.75 | 12.75 | 12.74 | 12.74 | 12.75 | 12.74 | 12.73 | 12.74 | 12.74 |
| $V H_2 [\text{mL}]$ | 0 | 0 | 0 | 0 | 0 | 0 | 0 | 0 | 0 | 0 | 0 | 0 | 0 |
| $U [V]$ | 1.38 | 1.36 | 1.33 | 1.32 | 1.32 | 1.32 | 1.31 | 1.32 | 1.31 | 1.32 | 1.32 | 1.32 | 1.31 |
| $\Delta_{\text{foam}} [\text{mm}]$ | 0 | 2 | 3 | 4 | 6 | 6 | 7 | 7 | 7 | 7 | 7 | 7 | 7 |

Table 3. Real solution, Al electrode

| $\tau = 360 \text{ min, Al anode, } i = 250 \text{ A/m}^2$ | | | | | | | | | | | | | |
|--|-------|-------|-------|-------|-------|-------|-------|-------|-------|-------|-------|-------|-------|
| $\tau [\text{min}]$ | 0 | 10 | 20 | 30 | 40 | 50 | 60 | 70 | 80 | 90 | 100 | 110 | 120 |
| pH | 13.53 | 13.84 | 13.83 | 13.81 | 13.78 | 13.77 | 13.75 | 13.77 | 13.80 | 13.83 | 13.85 | 13.87 | 13.88 |
| $U [V]$ | 1.65 | 19.14 | 29.4 | 31.4 | 31.4 | 31.4 | 31.4 | 31.4 | 31.4 | 31.4 | 31.4 | 31.4 | 31.4 |
| $\Delta_{\text{foam}} [\text{mm}]$ | 0 | 5 | 5 | 5 | 5 | 5 | 5 | 5 | 5 | 5 | 5 | 5 | 5 |
| $\tau [\text{min}]$ | 130 | 140 | 150 | 160 | 170 | 180 | 190 | 200 | 210 | 220 | 230 | 240 | 250 |
| pH | 13.89 | 13.89 | 13.89 | 13.88 | 13.87 | 13.85 | 13.85 | 13.83 | 13.85 | 13.85 | 13.85 | 13.84 | 13.78 |
| $U [V]$ | 31.4 | 31.4 | 31.4 | 31.4 | 31.4 | 31.4 | 31.3 | 31.3 | 31.3 | 31.3 | 31.3 | 31.3 | 31.3 |
| $\Delta_{\text{foam}} [\text{mm}]$ | 5 | 5 | 5 | 5 | 5 | 5 | 4 | 4 | 4 | 4 | 4 | 4 | 4 |
| $\tau [\text{min}]$ | 260 | 270 | 280 | 290 | 300 | 310 | 320 | 330 | 340 | 350 | 360 | - | - |
| pH | 13.74 | 13.74 | 13.79 | 13.81 | 13.82 | 13.83 | 13.84 | 13.84 | 13.84 | 13.84 | 13.84 | - | - |
| $U [V]$ | 31.3 | 31.3 | 31.3 | 31.3 | 31.3 | 31.3 | 31.3 | 31.3 | 31.3 | 31.3 | 31.3 | - | - |
| $\Delta_{\text{foam}} [\text{mm}]$ | 4 | 4 | 4 | 4 | 4 | 4 | 4 | 4 | 3 | 3 | 3 | - | - |

Table 4. Real solution, Fe electrode

| $\tau = 360 \text{ min, Fe anode, } i = 250 \text{ A/m}^2$ | | | | | | | | | | | | | |
|--|-------|-------|-------|-------|-------|-------|-------|-------|-------|-------|-------|-------|-------|
| $\tau [\text{min}]$ | 0 | 10 | 20 | 30 | 40 | 50 | 60 | 70 | 80 | 90 | 100 | 110 | 120 |
| pH | 13.56 | 13.75 | 13.82 | 13.84 | 13.85 | 13.86 | 13.85 | 13.83 | 13.82 | 13.83 | 13.84 | 13.85 | 13.86 |
| $U [V]$ | 2.33 | 2.01 | 2.51 | 2.54 | 2.71 | 2.78 | 2.81 | 2.79 | 2.79 | 2.78 | 2.74 | 2.72 | 2.72 |
| $\Delta_{\text{foam}} [\text{mm}]$ | 0 | 6 | 6 | 6 | 6 | 6 | 6 | 6 | 6 | 6 | 6 | 6 | 6 |
| $\tau [\text{min}]$ | 130 | 140 | 150 | 160 | 170 | 180 | 190 | 200 | 210 | 220 | 230 | 240 | 250 |
| pH | 13.86 | 13.86 | 13.86 | 13.87 | 13.87 | 13.87 | 13.88 | 13.88 | 13.88 | 13.88 | 13.88 | 13.89 | 13.89 |
| $U [V]$ | 2.73 | 2.76 | 2.83 | 2.83 | 2.83 | 2.83 | 2.83 | 2.83 | 2.83 | 2.83 | 2.83 | 2.83 | 2.83 |
| $\Delta_{\text{foam}} [\text{mm}]$ | 5 | 4 | 4 | 4 | 4 | 4 | 4 | 4 | 4 | 4 | 4 | 4 | 4 |
| $\tau [\text{min}]$ | 260 | 270 | 280 | 290 | 300 | 310 | 320 | 330 | 340 | 350 | 360 | - | - |

| | | | | | | | | | | | | | |
|------------------------------|-------|-------|-------|-------|-------|-------|-------|-------|-------|-------|-------|---|---|
| <i>pH</i> | 13.90 | 13.91 | 13.92 | 13.93 | 13.93 | 13.93 | 13.94 | 13.94 | 13.94 | 13.94 | 13.94 | - | - |
| <i>U [V]</i> | 2.83 | 2.83 | 2.83 | 2.83 | 2.83 | 2.83 | 2.84 | 2.84 | 2.84 | 2.84 | 2.84 | - | - |
| <i>Δ_{foam} [mm]</i> | 4 | 4 | 4 | 4 | 4 | 4 | 4 | 4 | 4 | 4 | 4 | - | - |

4. Conclusions

Electroflotocoagulation can be used at industrial scale for non-ferrous heavy metal metallurgy wastewater (levigates) treatment as an intermediary step for colloids removal.

Depending on the specific solution composition and pH, the anodic material and electrolysis parameters (anodic current density, duration of electrolysis etc.) can be easily experimentally determinate using the proposed pilot reactor.

References

- Chen G., (2004), Electrochemical technologies in wastewater treatment, *Separation and Purification Technology*, **38**, 11–41.
- Escobar C., Soto-Salazar C., Ines Toral M., (2006), Optimization of the electrocoagulation process for the removal of copper, lead and cadmium in natural waters and simulated wastewater, *Journal of Environmental Management*, **81**, 384-391.
- Hansen H.K., Nunez P., Raboz D., Schippacasse I., Grandon R., (2007), Electrocoagulation in wastewater containing arsenic: Comparing different process designs, ScienceDirect, *Electrochimica Acta*, **52**, 3464-3470.
- Holt P., Barton G., Mitchell C., (1999), *Wastewater treatment by electrocoagulation*, The Third Annual Australian Environmental Engineering Research Event, Castlemaine, Victoria, 23-26 November 1999.
- Khelifa A., Moulay S., Naceur A.W., (2005), Treatment of metal finishing effluents by the electroflotation technique, *Desalination*, **181**, 27-33.
- Racovițeanu G., (2003), *Theory of water cleaning and filtration* (in Romanian), Matrix Rom, Bucharest.



IRON OXIDES FROM ELECTROFILTER ASH FOR WATER TREATMENT (ARSENIC REMOVAL)

Ionel Balcu^{1*}, Adina Segneanu¹, Marius Mirica¹, Mirela Iorga¹,
Catalin Badea², Iuliana Firuta Fitigau¹

¹National Institute of R&D for Electrochemistry and Condensed Matter – INCEMC, 144 Aurel Paunescu Podeanu, 300569 Timisoara, Romania

²„Politehnica” University of Timisoara, 2 Piata Victoriei, Timisoara – Romania

Abstract

Arsenic (As)-contaminated drinking water is a major problem around the world. The removal efficiency depends strongly on the size of Fe₃O₄ sorbents. Fe₃O₄ prepared in laboratory is more efficient in the removal of As and is also more easily recovered from column of magnetic separator than the commercial materials. This would be beneficial in a water treatment system because the As-contaminated Fe₃O₄ could be flushed from the column permitting reuse of the separator system. The dispersed Fe₃O₄ nanocrystals can be removed from the solution through interactions with a magnetic column. The 20 nm commercially made nanocrystals were permanently retained in the column and could not be recovered, while the laboratory prepared nanocrystals were able to be recovered when the magnetic field was turned off.

Key words: absorption spectrometer, arsenic removal, iron oxides

1. Introduction

The thermoelectric power stations ash from our country, evacuates million tons of ash annually. Thermoelectric ashes are used in cement industry, construction materials (buildings, bricks, light aggregates) or backfill materials. The dry ashes can also be considerate as a veritable binder that can be used in layers of shape, foundation or base, roadwork execution. It is necessary a physical-chemical and morphostructural characterization of the ashes resulted in the burn processes of the thermoelectric power stations (Nicolescu, 1978).

Thermoelectric ashes are considered environmental wastes because are obtained in big quantities and are needed large land surfaces for their storage.

A number of studies regarding thermoelectric ash characterization and valorification as appendix to Portland cements based on puzzolanic activity of

ashes were done, but valorification of this waste is still an unresolved problem (Voina, 1981). The chemical composition of ash was determinate on the sample previous calcinated at 800°C and the obtained results are (%): SiO₂ – 51.6; Al₂O₃ – 20.1; Fe₂O₃ – 10.6; CaO – 10.8; MgO – 1.9; Na₂O – 1.2; K₂O – 0.3.

Long-term exposure to carcinogenic arsenic, may cause lung, bladder, kidney and skin cancer as well as pigmentation changes. Generally, acute and chronic poisoning may cause nausea, dryness of the mouth and gastro-intestinal symptoms (Tuutijarvi et al., 2009). Countries such as Bangladesh, India, Vietnam, Mexico, Argentina, Chile, Hungary, Romania, and the United States face significant challenges in meeting the newly lowered standards for As in drinking water (Mayo et al., 2007).

Arsenic is an element found in the environment but without any essential biological functions and is toxic for almost all organisms. It is a very volatile toxic metal that generated a highest attention in the class of metallic pollutants. In Table 1

* Author to whom all correspondence should be addressed: e-mil: ionel_balcu@yahoo.com; Phone: +40752197758

are shown the chemical forms of arsenic in water. The fact that arsenic is situated in the periodic table below phosphorous involves a similar chemical behavior; arsenic and phosphorous coexists in natural sources and also interferes in biological phosphor dependent mechanisms (phosphorilation). There are proves that the organisms has developed their own methylation mechanisms to isolate and 'detoxificate' arsenic into organoarsenic derivates. The incorporation of arsenic in zwitterions of arsenic like arsenobetaine and arsenocoline, can serve to the double purpose of detoxification and osmoregulation analogous to some sulphur compounds. The toxicity of arsenic is similar to that of plumb and mercury.

Table 1. The arsenic chemical formulas in samples of water

| Compound | Chemical formula |
|---------------------------|------------------|
| Arsenate (V) | $H_2 As O_4$ |
| Arsenite (III) | $As (OH)_3$ |
| Arsin | $As H_3$ |
| Monomethylarsenate (MMA) | $CH_3 AsO_2 OH$ |
| Dimethylarsenate | $(CH_3)_2 AsOO$ |
| Dimethylarsin(DMA) | $(CH_3)_2 As H$ |
| Trimethylarsin (TMA) | $(CH_3)_3 As$ |
| Trimethylarsinoxid (TMAO) | $(CH_3)_3 AsO$ |

The hard metals and their salts that are very stable are toxic and dangerous for aquatic creatures. The contamination of surface waters is accomplished by the waste water from the mills that are using those substances in their production process. The biological treatment of this water can be compromised because many microorganisms are destructed by that class of pollutes and inhibits the methanic fermentation process of mud.

The environmental problem draw the attention of the worldwide experts because is an international project.

2. Experimental

The X ray diffraction spectra were performed by X'Pert PRO MPD equipment from PANalytical, with Cu anodic tube and PIXcel detector, on 2theta 10-100 domain, voltage of 45 kW and current intensity of 30 mA. X'ray diffraction represents an undestructive technique of analysis, the sample is seated on a silicon standard support and then is gently pressed, the equipment sample support spin with a rate of 1 rot/sec.

2.1. Experimental proceeding sol-gel method

Work steps description:

a. Precursor preparation – the precursors are prepared thereby: depending on the state of aggregation the solid reagents used as precursors are weighted using an analytical balance and in the case of liquid reagents it's measured their volume and then we prepared the samples.

b. Sample stirring - the sample can be agitated using a magnetic or mechanic stirrer. The precursors were added drop by drop with continuous stirring.

c. The addition of the doping precursor – the doping precursor is added over the solution obtained in the previous step (if necessary).

d. pH- adjustment – we determined the initial pH. The pH adjustment was realized compared with the final pH assess by the reaction conditions.

e. Solvent evaporation – the solvent evaporation (if necessary) can be accomplished at room temperature or using a rotary evaporator (in the organic solvents case).

f. Products separation- to remove the byproducts using centrifuging and filtering.

g. Washing and drying - the washing (if necessary) can be done using filter paper with distilled water and alcohol until the soluble substances are completely removed and the drying can be made in a drying chamber at previously established temperature.

h. Heat treatment- to crystallize via calcination at the given temperature.

In Fig. 1, the experimental proceeding for the sol-gel method is presented.

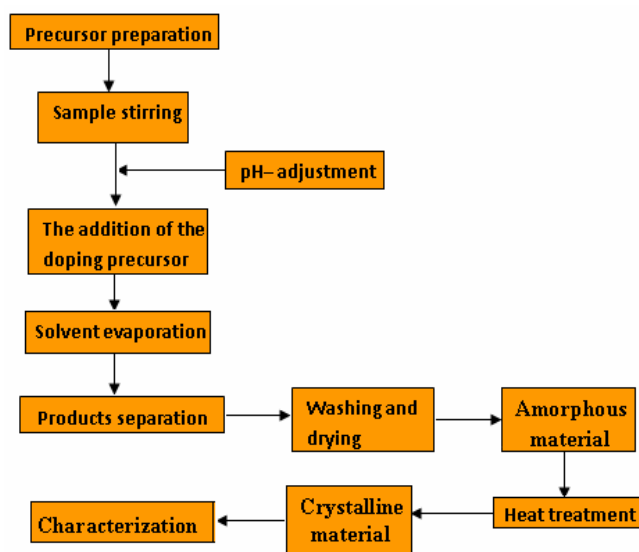


Fig. 1. Experimental setting up for the sol-gel method

2.2. Experimental - Baleyage SEM electronic microscopy

Sample characteristics:

- the samples have to be conductors;
- the non-conducting samples are covered with a thin layer of an conductor metal (Au, Ag, Pt).

The sample that have to be analyzed (pill, powder, plates, etc) is seated on a double adhesive carbon band on the equipment stub. After that the sample is introduced in the microscope chamber in vacuum (fine vacuum or preliminary vacuum).

• For imagistic: the sample is set to the corresponding parameters (pressure, voltage, magnification and spot) and then is baleyated on the interest surface;

- To collect EDAX spectrum: the sample is set to the corresponding parameters (voltage, spot, WD-working distance).

2.3. Hydrothermal method

The hydrothermal method is an essential method for nanoferrite synthesis. Hydrothermal synthesis can be defined as a method of synthesis of single crystals which depends on the solubility of minerals in hot water under high pressure. The crystal growth is performed in an apparatus consisting of a steel pressure vessel called autoclave, in which a nutrient is supplied along with water. A gradient of temperature is maintained at the opposite ends of the growth chamber so that the hotter end dissolves the nutrient and the cooler end causes seeds to take additional growth.

Possible advantages of the hydrothermal method over other types of crystal growth include the ability to create crystalline phases which are not stable at the melting point. Also, materials which have a high vapor pressure near their melting points can also be grown by the hydrothermal method. The method is also particularly suitable for the growth of large good-quality crystals while maintaining good control over their composition. Disadvantages of the method include the need of expensive autoclaves, good quality seeds of a fair size and the impossibility of observing the crystal as it grows.

3. Results and discussions

The CET thermoelectric power station – Timisoara South ash has been morphologically (Imagery- SEM Inspect S FEI Company), elementary (EDAX Inspect S FEI Company) and X-ray diffraction (X'Pert Pro MPD - Panlitical) analyzed. From SEM images (Fig. 2) it is observed that the ash has a pronounced heterogeneous character, areas with agglomerated powder are alternating with micro and spherical nanostructures areas. For EDAX analysis was chosen two structures and a 'flake' respectively.

The ash elementary quantitative analysis on the three chosen areas is visualized in Fig. 3.

Fig. 3 shows a different composition of the aggregate ash. In the aggregate ash SiO_2 predominates in the alpha quartz structure (Fig. 7), CaSO_4 anhydrous partial crystallized (diffuse spectrum with noise) (Fig. 8) and Al_2O_3 (Fig. 9) resulting from X-ray diffraction (Fig. 4) after comparison with base data (Division of Geological and Planetary Sciences - California Institute of Technology USA) and small quantities of iron; the 'flakes' contain more elements as Si, Al, Ca, O, S and the microspheres a large quantity of iron.

The elements quantification of ash aggregate, 'flake' and sphere are shown in Table 2-c.

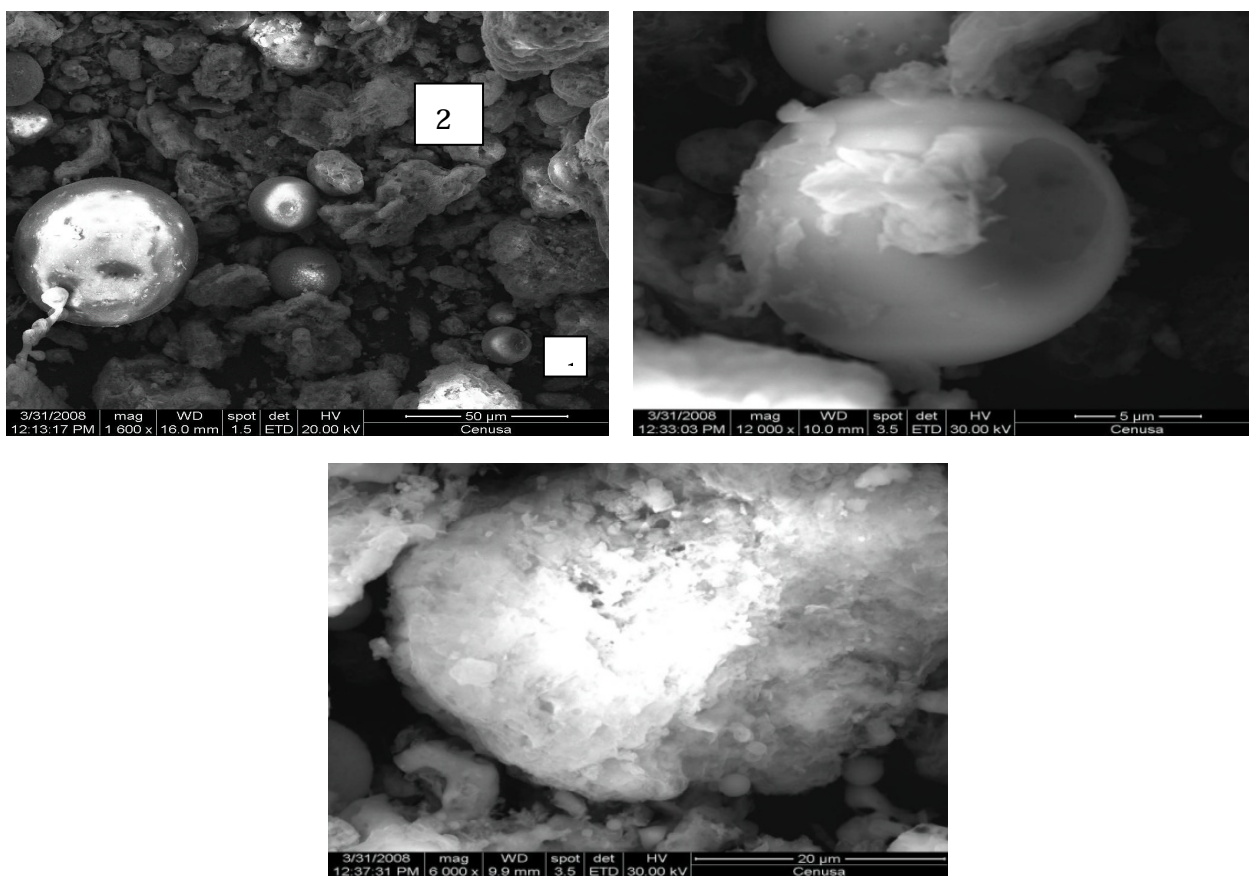


Fig. 2. SEM images of ash from South Timisoara CET (1.600X) - in the left side- images for the area noted with 1, with 2 respectively for a higher magnitude (12.000X, 6000X respectively).

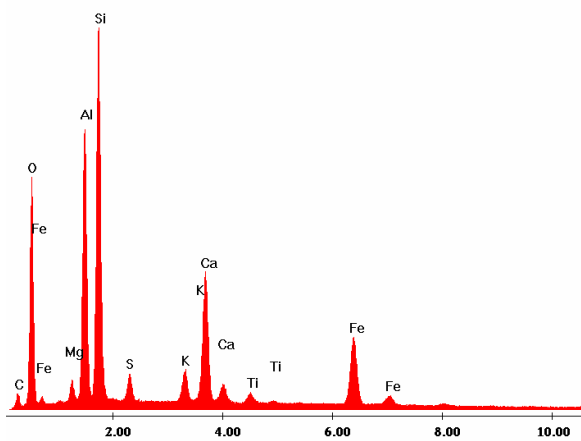
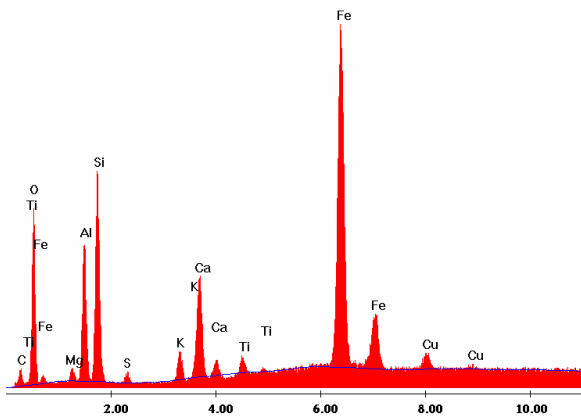
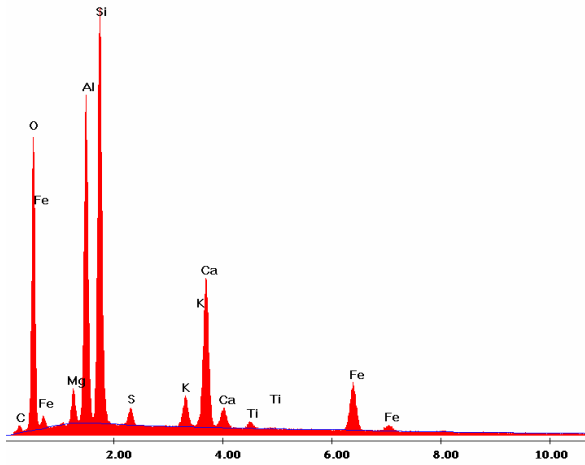


Fig. 3. EDAX spectrums of South Timisoara CET ash; the first from above, showing the ash's general view, the second the view from area 1 and the third the view for area 2.

Considering the high content of iron and remark that is magnetic (Fe_3O_4 probably it couldn't be determinate from the X-ray diffraction spectrum because we work with copper cathode tube) it was tried a magnetic separation of South Timisoara CET ash.

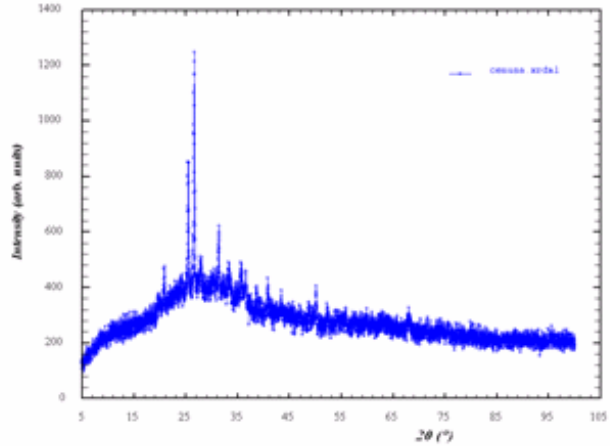


Fig. 4. X-ray diffraction spectrum of South Timisoara CET ash

The ash was analyzed morphologically and elementally, before and after the separation process as shown in Figs. 5, 6, 10 and Tables 2a, 2b, 2c. Comparing the samples before and after separation, the number of microspheres is higher in the later one. After the magnetic process the separated part of the ash contained a much more iron as seen in Fig.10.

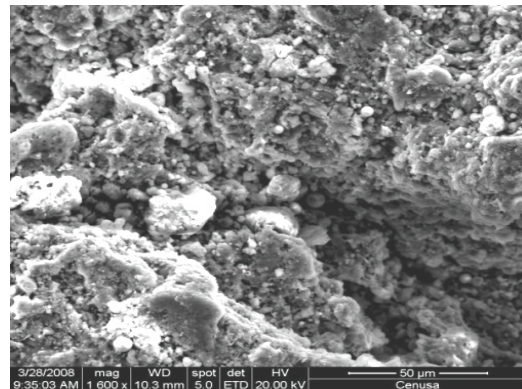


Fig. 5. SEM image of ash from South Timisoara CET before separation

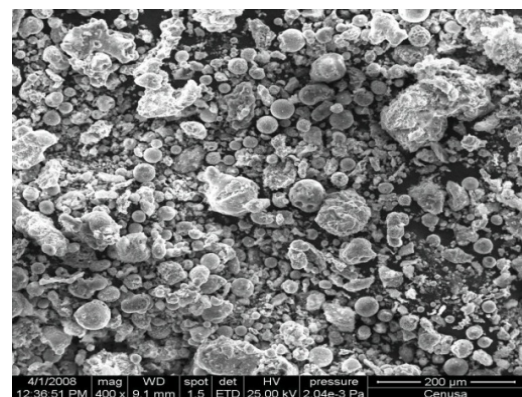


Fig. 6. SEM image of ash from South Timisoara CET after separation

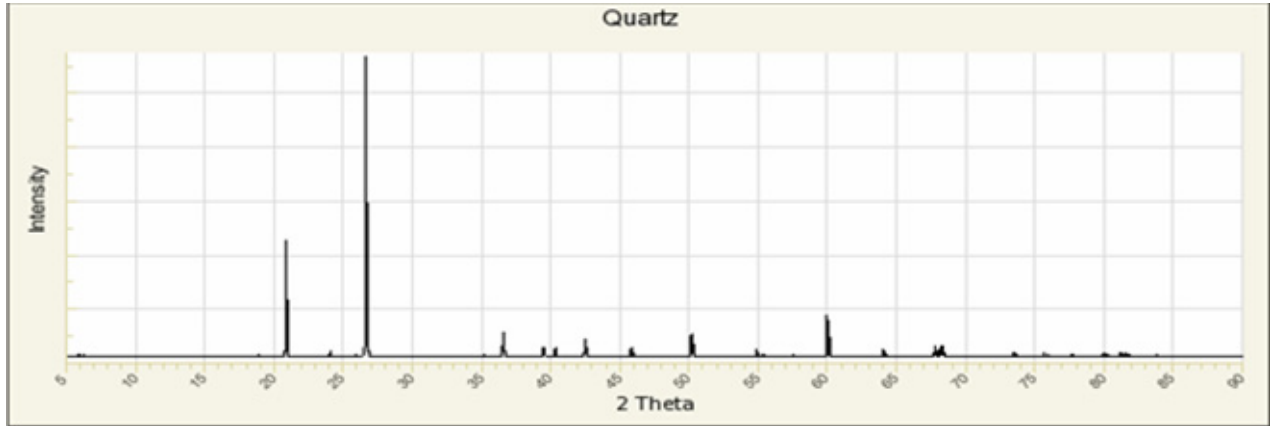


Fig. 7. X –ray diffraction spectrum of alpha quartz SiO₂

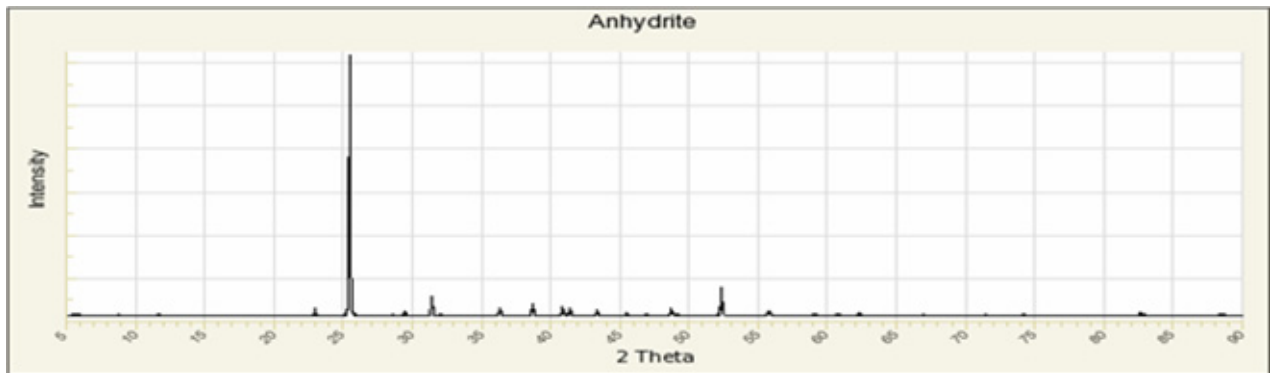


Fig. 8. X –ray diffraction spectrum of partial crystallized anhydrous CaSO₄

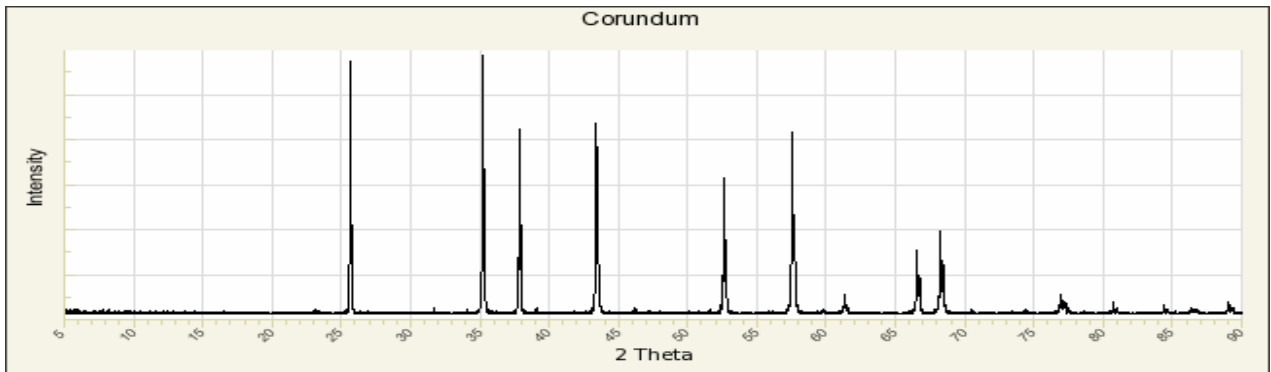


Fig. 9. X –ray diffraction spectrum of Al₂O₃

Table 2.a. Ash quantification

| <i>Elem</i> | | <i>Wt %</i> | <i>At %</i> | <i>K - Ratio</i> | <i>Z</i> | <i>A</i> | <i>F</i> |
|-------------|---|-------------|-------------|------------------|----------|----------|----------|
| O | K | 37.18 | 53.87 | 0.0938 | 1.0423 | 0.2420 | 1.0007 |
| Mg | K | 1.67 | 1.59 | 0.0070 | 1.0026 | 0.4141 | 1.0097 |
| Al | K | 16.06 | 13.80 | 0.0848 | 0.9736 | 0.5367 | 1.0102 |
| Si | K | 28.69 | 23.68 | 0.1464 | 1.0026 | 0.5083 | 1.0012 |
| S | K | 0.57 | 0.41 | 0.0030 | 0.9955 | 0.5370 | 1.0028 |
| Sn | L | 1.09 | 0.21 | 0.0085 | 0.7807 | 0.9932 | 1.0045 |
| Ca | K | 5.38 | 3.11 | 0.0456 | 0.9759 | 0.8641 | 1.0059 |
| Ba | L | 2.26 | 0.38 | 0.0182 | 0.7651 | 1.0435 | 1.0092 |
| Fe | K | 7.12 | 2.96 | 0.0623 | 0.8949 | 0.9775 | 1.0000 |
| Total | | 100.00 | 100.00 | | | | |

Table 2.b. "Flake" area quantification

| <i>Elem</i> | <i>Wt %</i> | <i>At %</i> | <i>K - Ratio</i> | <i>Z</i> | <i>A</i> | <i>F</i> |
|-------------|-------------|-------------|------------------|----------|----------|----------|
| C K | 12.00 | 19.67 | 0.0185 | 1.0398 | 0.1479 | 1.0005 |
| O K | 41.13 | 50.62 | 0.0862 | 1.0251 | 0.2044 | 1.0005 |
| Mg K | 1.23 | 1.00 | 0.0044 | 0.9883 | 0.3594 | 1.0081 |
| Al K | 13.05 | 9.52 | 0.0612 | 0.9603 | 0.4848 | 1.0080 |
| Si K | 18.28 | 12.82 | 0.0853 | 0.9892 | 0.4710 | 1.0017 |
| S K | 1.32 | 0.81 | 0.0071 | 0.9831 | 0.5448 | 1.0037 |
| K K | 1.34 | 0.68 | 0.0105 | 0.9378 | 0.8185 | 1.0131 |
| Ca K | 5.42 | 2.66 | 0.0453 | 0.9597 | 0.8671 | 1.0048 |
| Ti K | 0.50 | 0.20 | 0.0048 | 0.8816 | 0.9121 | 1.0091 |
| Fe K | 5.27 | 2.02 | 0.0504 | 0.8877 | 0.9928 | 1.0000 |
| Total | 100.00 | 100.00 | | | | |

Table 2.c. Sphere quantification

| <i>Elem</i> | <i>Wt %</i> | <i>At %</i> | <i>K - Ratio</i> | <i>Z</i> | <i>A</i> | <i>F</i> |
|-------------|-------------|-------------|------------------|----------|----------|----------|
| C K | 12.45 | 23.92 | 0.0214 | 1.0662 | 0.1615 | 1.0004 |
| O K | 28.62 | 41.28 | 0.0653 | 1.0511 | 0.2167 | 1.0011 |
| Mg K | 1.14 | 1.08 | 0.0029 | 1.0131 | 0.2474 | 1.0042 |
| Al K | 9.07 | 7.76 | 0.0307 | 0.9843 | 0.3420 | 1.0046 |
| Si K | 11.94 | 9.81 | 0.0476 | 1.0140 | 0.3926 | 1.0018 |
| S K | 0.52 | 0.37 | 0.0028 | 1.0076 | 0.5355 | 1.0049 |
| K K | 1.15 | 0.68 | 0.0093 | 0.9661 | 0.8182 | 1.0207 |
| Ca K | 4.06 | 2.34 | 0.0356 | 0.9885 | 0.8686 | 1.0213 |
| Ti K | 0.77 | 0.37 | 0.0068 | 0.9065 | 0.9220 | 1.0469 |
| Fe K | 28.02 | 11.58 | 0.2558 | 0.9121 | 0.9955 | 1.0053 |
| Cu K | 2.27 | 0.82 | 0.0189 | 0.8861 | 0.9428 | 1.0000 |
| Total | 100.00 | 100.00 | | | | |

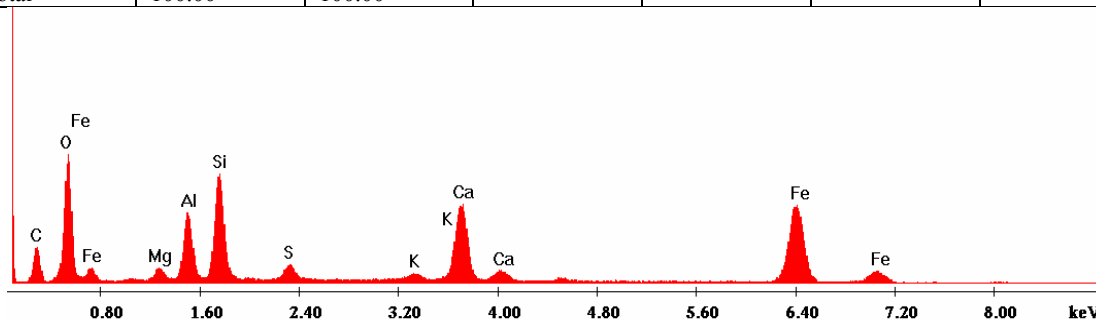


Fig. 10. EDAX Spectrum ash from South Timisoara CET after separation

4. Conclusions

This paper suggests that Fe_3O_4 nanocrystals and magnetic separation offer a promising method for arsenic removal and the iron oxides from powerplant electrofilter ash can be reused.

For obtaining of monostructured iron oxides we used two comparative methods: hydrothermal and sol-gel method. Analysis of electrofilter ash structure was realized using X-ray diffraction.

The arsenic level from waste water will be monitored using an atomic absorption spectrometer (NovAA 400 Analytik Jena).

References

- Mayo J.T., Yavuz C., Yean S., Cong L., Shipley H., Yu W., Falkner J., Kan A., Tomson M., Colvin V.L., (2007) The effect of nanocrystalline magnetite size on arsenic removal, *Science and Technology of Advanced Materials*, **8**, 71–75.
- Neamtu, N. Rujenescu, I. Lazau, D. Becherescu (2002), *Use of thermoelectric plant ashes in concrete tiles*, University's day 8th international conference, Targu Jiu, May 24-26.
- Nicolescu L., (1978), *Cenușa de termocentrală în construcții*, Ceres Printing House, București.
- Tuutijarvi T., Lu J., Sillanpaa M., Chen G. (2009), As(V) Adsorption on maghemite nanoparticle, *Journal of Hazardous Materials*, **166**, 1415-1420.
- Voina N.I., (1981), *Theory and practice of using the thermoelectric plant ashes (in Romanian)*, Tehnica Printing House, București.

CHARACTERISATION OF TRUFFLES USING ELECTROCHEMICAL AND ANALYTICAL METHODS

A.E. SEGNEANU^{a*}, P. SFIRLOAGA^a, I. DAVID^b, I. BALCU^a, I. GROZESCU^{a,c}

^aNational Institute of Research & Development for Electrochemistry and Condensed Matter INCCEM Timisoara, Romania, 144 Dr. A. P. Podeanu, 300569 Timisoara, Timis, Romania,

^bBanat University of Agricultural Sciences and Veterinary Medicine Timisoara, Calea Aradului nr. 119, 300645 Timisoara, jud. Timis, Romania, fax. 0256200296

^cAurel Vlaicu University Arad, B-dul Revoluției nr. 77, 310130 Arad, Romania,

This paper aims to investigate a comparative study on two types of truffles: *Tuber magnatum pico* and *Tuber melanosporum* using different analytical methods. In this investigation we have determined the antioxidant activity of truffles by an electrochemical method (cyclic voltammetry), the content of total organic carbon and heavy metals. Moreover, it was comparative examined the morphology and elemental composition by scanning electron microscopy and EDAX to estimate the diversity of this two different types of truffles.

(Received November 7, 2011; Accepted February 15, 2012)

Keywords: Truffle, Cyclic voltammograms, Electrochemical methods, Scanning electron microscopy

1. Introduction

Truffles (*Tuber spp.*) are hypogean fungus, which form symbiotic relationships with compatible host tree species (beech, poplar, oak, birch, hornbeam, hazel, and pine) (1). Although it is one of the world's most expensive foods, truffles are very popular in French and Italian cuisine, due to their unique aroma and flavour, delicious taste and highly nutritional value. Mushrooms, and especially edible mushroom species were also among the healthy food because are the best sources of other essential nutrients (protein, amino acids, fatty acids, minerals and carbohydrates). Truffles are known for their antioxidant, immuno-modulating effects and antitumor activity in humans (2-3).

Growth of truffles depends on many factors such as rainy season and its timing, soil characteristics, water availability, and climatic conditions. Truffles grow in temperate, moist climates throughout the world; they like warm, dry summers, cool, wet winters and alkaline (limestone) soil (1).

The white truffle (*Tuber magnatum pico*) is a hypogean fungus, living entirely underground, ensconced among the roots trees, and those among the oaks are the most sought. It is found from October 1 through December 31, in the vicinity of oaks, lime trees and poplars. It is known for its luscious, heady aroma. The black truffle (*Tuber melanosporum*) commonly known as the “black diamond of cuisine” is considered the most aromatic, while white truffle (*Tuber magnatum*) from Italy is considered the finest because of its complex aroma, and it is also the rarest and the most expensive. White truffles are softer and more perishable than black truffles, and are almost always served raw (they cannot tolerate the heat of cooking) (5).

For this reason, there are necessary to develop a method of conservation to preserve intact the unique aroma and the flavor of truffles.

* Corresponding author: s_adinaelena@yahoo.com

2. Experimental section

Reagents and Analytes

The truffles were harvested from Romanian natural population only. The fruiting bodies of truffles were cleaned and preserved in pressure nitrogen atmosphere. Small sample of truffles were analyzed.

- Cyclic voltammetry

Examined material: sample of preserved truffles (*Tuber magnatum pico*) and (*Tuber melanosporum*) substances: solvents (methylic alcohol); equipment: Radiometer PGZ-402 Universal Dynamic Pulse Voltammetry EIS equipped with VoltaMaster software 4. The working parameters were experimental established (the base electrolyte and pH). The base electrolyte is composed of 0.1 M phosphate buffer solutions (PBS) at different pH's (2.8 and 8).

For voltammetric studies were used 8.83 g of white truffle extracted in 20 mL MeOH with stirring for 3 hours at room temperature. A volume of 3 ml of truffles extract were dissolved in 10 ml of base electrolyte (PBS solution) and then were recorded cyclic voltammograms.

The antioxidant activity of *Tuber magnatum pico* and *Tuber melanosporum* was analyzed by cyclic voltammetry using the following parameters:

- two working electrodes were used: nickel and platinum plate
- The cyclic voltammograms for nickel electrode were recorded in the potential range of -250 ÷ 1200mV and for platinum plate electrode in the potential range of -250÷1400mV/s at different polarization rate: 25mV/s, 50mV/s, 100mV/s, at room temperature.

Electrochemical cell was equipped with three electrodes, namely:

- reference electrode: Ag/AgCl;
- auxiliary electrode: platinum wire with 0.25cm² active surface;
- working electrode: nickel with surface of 0.2 cm² and platinum plate with surface of 0.8 cm²;

- Atomic absorption spectrometry (AAS)

The tests for determination of heavy metals contents from truffles were conducted under international standard ISO 15586:2003 (E), on equipment: Analytik Jena novAA 400G - apparatus, with a graphite furnace, equipped with autosampler MPE60 and software WinAAS 3.17.0.

Examined materials: samples of truffles (0.2541 g) weighed on a Sartorius analytical balance, with an accuracy of ± 0.0001 g.; Substances: nitric acid, ultrapure water. The samples is treated with 5.5 mL HNO₃ 65% and subjected to digestion in a Berghof microwave oven MWS 2, using a three stages program: T₁=160°C, t₁= 15 min, p₁= 80%. After digestion, the sample is brought to a volume of 100 mL with ultrapure water.

- Total organic carbon content

The TOC analyzer used in this study was a SHIMADZU TOC-V_{CPN} equipped with a 94 – position auto sampler. The TC principle analysis was catalytic combustion at high temperature (900°C) and for IC –acidification at 200°C.

Examined materials: samples of truffles (0.301 g) weighed on a Sartorius analytical balance, with an accuracy of ± 0.0001 g. Substances: phosphoric acid, 1:1 v/v (Merck).

- Scanning electron microscopy (SEM/EDAX)

To highlight the morphology and elemental composition of two types of truffles were analyzed by scanning electron microscopy (SEM) using Inspect S PANalytical model coupled with the energy dispersive X-ray analysis detector (EDX).

3. Results and disscution

Studies for determination of natural sources of antioxidants compounds (phenolic and flavonoids) are very important due to the positive biological effects on human health and welfare.

These compounds function as free radical scavengers, initiator of the complexes of pro-oxidant metals, reducing agents and quenchers of singlet oxygen formation (6-10).

Previous research demonstrate that there is a direct correlation between electrochemical activity and antioxidant activity (11).

The present paper aims to investigate the electrochemical activity of the two type of truffles.

- *Comparative evaluation of Tuber magnatum pico and Tuber melanosporum antioxidant activity of through electrochemical methods*

The cyclic voltammograms indicate the influence of pH and reversible oxidation process of *Tuber magnatum pico*. The cyclic voltammograms of *Tuber magnatum pico* in phosphate buffer solutions at different pH's and different polarization rate are presented in the figures below.

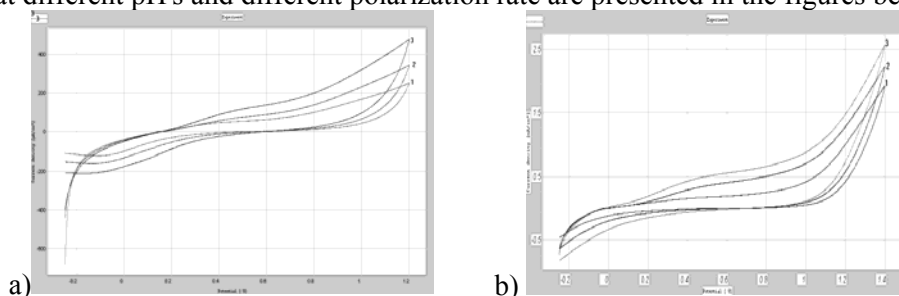


Fig. 1. Cyclic voltammograms of: a) *Tuber melanosporum*, b) *Tuber magnatum pico* on platinum plate electrode; pH=2.8; scan rate of: 1- 25mV/s; 2- 50 mV/s; 3- 100 mV/s

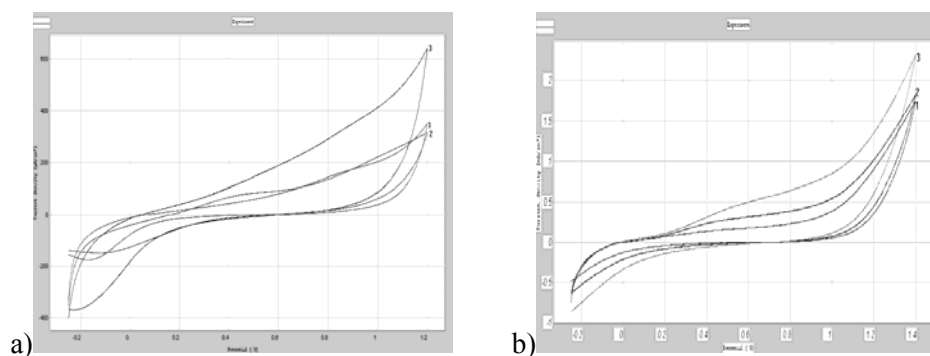


Fig. 2. Cyclic voltammograms of: a) *Tuber melanosporum*, b) *Tuber magnatum pico* on platinum plate electrode; pH= 8; scan rate of: 1- 25mV/s; 2- 50 mV/s; 3- 100 mV/s

Table 1. *Tuber melanosporum* - cyclic voltammograms results on platinum plate electrode

| pH | 2.8 | | | 8 | | |
|---|--------|--------|---------|--------|--------|---------|
| | 25mV/s | 50mV/s | 100mV/s | 25mV/s | 50mV/s | 100mV/s |
| i_{pic}^{\rightarrow} (mA/cm ²) | 46.48 | 75.87 | 120.3 | 16.7 | 23.7 | 34.8 |
| $\epsilon_{pic}^{\leftarrow}$ (V) | - | - | - | -170.2 | -275.5 | -371.4 |
| | 0.5 | 0.5 | 0.5 | 0.9 | 0.9 | 0.9 |
| | - | - | - | 0.16 | 0.16 | 0.16 |

Table 2. *Tuber magnatum pico* - cyclic voltammograms results on platinum plate electrode

| pH | 2.8 | | | 8 | | |
|---|--------|--------|---------|--------|--------|---------|
| | 25mV/s | 50mV/s | 100mV/s | 25mV/s | 50mV/s | 100mV/s |
| i_{pic}^{\rightarrow} (mA/cm ²) | 18.05 | 39.16 | 520 | 16 | 29.36 | 49.59 |
| $\epsilon_{pic}^{\leftarrow}$ (V) | 0.5 | 0.5 | 0.5 | 0.5 | 0.5 | 0.5 |

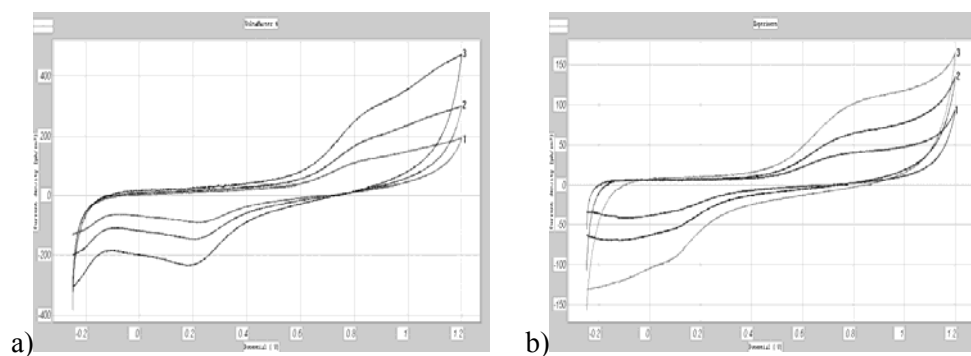


Fig. 3. Cyclic voltammograms of: a) *Tuber melanosporum*, b) *Tuber magnatum pico* on nickel electrode at pH=2.8; scan rate of: 1 - 25mV/s; 2- 50 mV/s; 3 - 100 mV/s

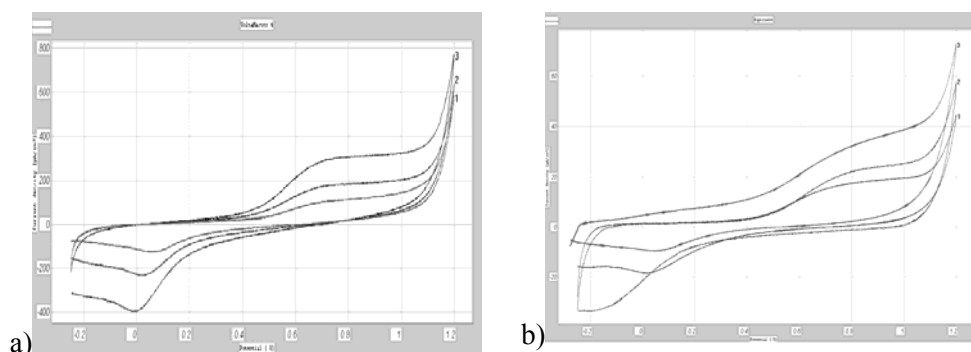


Fig. 4. Cyclic voltammograms of: a) *Tuber melanosporum*; b) *Tuber magnatum pico* on nickel electrode at pH= 8; scan rate of: 1- 25mV/s; 2- 50 mV/s; 3- 100 mV/s

Table 3. *Tuber melanosporum* - cyclic Voltammograms results on nickel electrode

| pH | 2.8 | | | 8 | | |
|---|--------|--------|---------|--------|--------|---------|
| Scan rate | 25mV/s | 50mV/s | 100mV/s | 25mV/s | 50mV/s | 100mV/s |
| i_{pic}^{\rightarrow} (mA/cm ²) | 113.9 | 166 | 268.8 | 103.7 | 168.3 | 281 |
| | -88.61 | -137.7 | -221.5 | -123 | -228 | -397.8 |
| $\epsilon_{pic}^{\leftarrow}$ (V) | 0.8 | 0.8 | 0.8 | 0.8 | 0.8 | 0.8 |
| | 0.23 | 0.23 | 0.23 | 0.06 | 0.03 | 0.003 |

Table 4. *Tuber magnatum pico* - cyclic Voltammograms results on nickel electrode

| pH | 2.8 | | | 8 | | |
|---|--------|--------|---------|--------|--------|---------|
| Scan rate | 25mV/s | 50mV/s | 100mV/s | 25mV/s | 50mV/s | 100mV/s |
| i_{pic}^{\rightarrow} (mA/cm ²) | 40.57 | 65 | 103.7 | 32.56 | 22.6 | 18.07 |
| | -40.84 | -68.03 | -92.61 | -9.32 | -18.07 | -32.06 |
| $\epsilon_{pic}^{\leftarrow}$ (V) | 0.8 | 0.8 | 0.8 | 0.8 | 0.8 | 0.8 |
| | 0.07 | 0.07 | 0.07 | 0.07 | 0.04 | 0.01 |

Comparative study of the both types of truffles releases that the cyclic voltammograms of recorded on platinum plate electrode, in acid media show that a single irreversible process occurs and the intensity of anodic peak increases with the scan rate.

In basic media, cyclic voltammograms recorded for *Tuber melanosporum* present a reversible process occurs, and only minor differences appear on the anodic current density with increasing the scan rate of both types of truffles. The reduction peak it is more pronounced with decreasing the scan rate. Instead for the cyclic voltammograms of both types of truffles recorded on the nickel electrode in both reaction media, a reversible process can be noticed in which the anodic peak intensity is much higher for the *Tuber melanosporum* at all three scan rates and is increasing with the increasing of scan rate while for the current density of the cathodic peak it is much higher with the decrease of rate. From the cyclic voltammograms on nickel electrode at pH = 2.8 it appears that a reversible oxidation process occurs for all three polarization rate: 25, 50 and

100 mV/s, with the appearance of anodic peak around 0.8V. Instead it can see a slight shift of cathodic peak potential to positive values with increasing polarization rate. When a pH=8 solution was used, the reversible oxidation process appears for all three different polarization rate, but here the reduction peak is more pronounced with decreasing the polarization rate. For the cyclic voltammograms recorded on platinum electrode for all three pH only one irreversible process occurs, where the oxidation peak intensity increases with the polarization rate increasing.

4. Characterization of *truffles samples* through analytical methods

Atomic absorption spectrometry analysis

The actual state of atomic absorption spectrometry of two types of truffles as the method of determining As, Cu, Pb, Zn, Mn, Fe and Ni is described on the basis of literature data.

Table 5. The metals content (mg/g) from the truffles samples:

| No | Sample | As | Cu | Pb | Zn | Mn | Fe | Ni |
|----|----------------------------|----|-------|----|-------|-------|--------|-------|
| 1. | <i>Tuber magnatum pico</i> | * | * | * | 39.67 | 2.32 | 68.67 | 0.581 |
| 2. | <i>Tuber melanosporum</i> | * | 7.242 | * | 34.08 | 2.414 | 523.58 | 0.569 |

* below the detection device

From the results obtained it can see that in *Tuber magnatum pico* and *Tuber melanosporum* metals such Zn, Mn, Fe, and small amounts of Ni were found.

- **Total organic carbon analysis**

Table 6. Results of the TOC analysis

| Sample no. | Area | CNV | Abs C (µg) | Conc (mg) | Weight (mg) | Volume |
|------------|-------|-------|------------|-----------|-------------|--------|
| 1 | 200.1 | 200.1 | 2420 | 2.420 | 35.80 | 35 µL |
| 2 | 347.1 | 347.1 | 4201 | 4.201 | 34.10 | 34 µL |

Sample 1. *Tuber magnatum pico*; Sample 2.- *Tuber melanosporum*

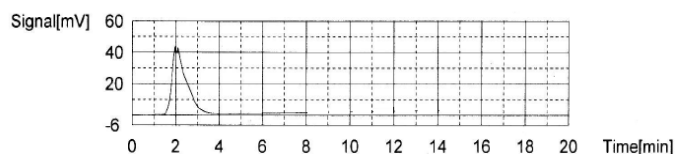


Fig. 5. *Tuber magnatum pico* - TOC measurement

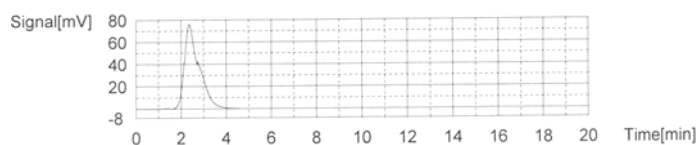


Fig. 6. *Tuber melanosporum* - TOC measurement

Total Carbon analysis

Table 7. Results of the TC analysis.

| Sample no. | Dilution. | Density (mg/µl) | Result (mg) |
|------------|-----------|-----------------|----------------------------------|
| 1 | 1.000 | 1.000 | TOC:2.420; TC:2.420; IC:0.000 |
| 2 | 1.000 | 1.000 | TOC:4.188; TC:4.201; IC: 0.01265 |

From TOC analysis results that, the sample 2, *Tuber melanosporum* contain practically much more carbon than the sample of *Tuber magnatum pico*.

- **Scanning electron microscopy (SEM/EDAX)**

To highlight the morphology and elemental composition of two types of truffles were analyzed by scanning electron microscopy and EDAX. We made a comparative study between the *Tuber magnatum pico* and *Tuber melanosporum*. The results are shown follow figures.

From the SEM images (Figure 7. (a)) it can be observed the surface topography on the *Tuber magnatum pico*. This shows a fibrous structure with a thickness about few μm . EDAX analysis provided a semi quantitative elemental analysis of the surface indicating the elements of the study material. Thus, it can be observed that for sample of *Tuber melanosporum* (Figure 8. (b)) the corresponding carbon peak is much higher than in the *Tuber magnatum pico*, keeping most of the components of this material.

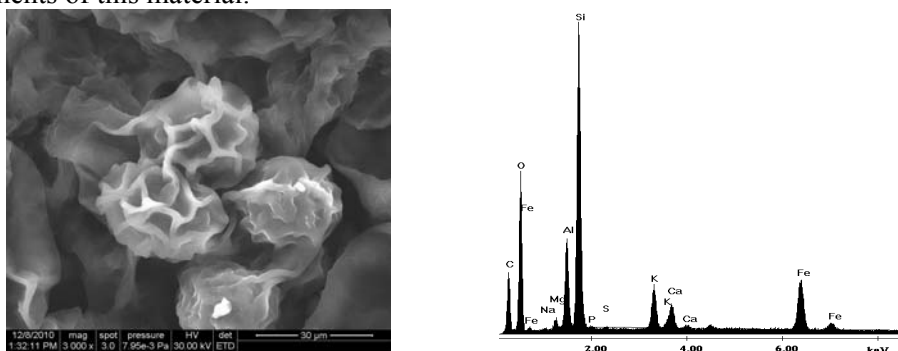


Fig. 7. (a) *Tuber magnatum pico* - SEM morphology; (b) EDX spectra for elemental analysis

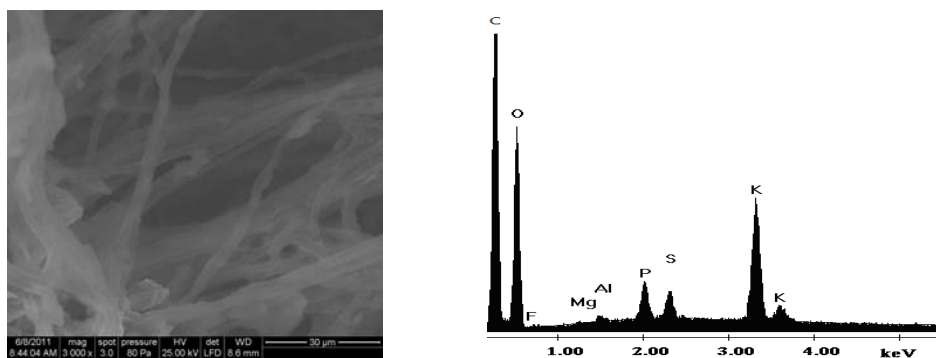


Fig. 8. (a) *Tuber melanosporum* - SEM morphology; (b) EDX spectra for elemental analysis.

5. Conclusion

The results of the present investigation indicated that the electrochemical evaluation of antioxidant activity of both types of truffles shows an dependence of the oxidation process by the pH and the nature of electrode. Reversible oxidation process of both types of truffles samples occurs better in acid medium reaction and the oxidation peak is more pronounced on the nickel electrode than for the platinum plate electrode.

The comparative electrochemical study of both truffles in different conditions (medium reactions, electrodes, different scan rates) demonstrates that the sample of *Tuber melanosporum* shows a higher antioxidant activity than *Tuber magnatum pico*.

Further studies should be performed on the isolation and identification of the antioxidant components in two types of truffles.

The analytical methods used to characterize the samples revealed that the two types of truffles shows different morphologies and composition. The sample of *Tuber melanosporum* contains a high amount of carbon and Fe than *Tuber magnatum pico*. The content of the other metals in both truffles samples determinate by atomic absorption spectrometry and EDX analysis is approximately the same.

References

- [1] Beetz, A.; Kustudia, M. Mushroom Cultivation And Marketing, Horticulture Production Guide, ATTRA Publication IP 087. 2004
- [2] Liu, G.; Wang, H.; Zhou, B.; Guo, X.; Hu, X. Journal of Medicinal Plants Research, , **4**(12), 1222-1227 (2010).
- [3] Ameer, A.; A. Al-Laith, Journal of Food Composition and Analysis, **23**, 15–22 (2010).
- [4] Culleré, L.; Ferreira, V.; Chevret, B.; Venturini, M. E.; Sánchez-Gimeno, A. C.; Blanco, D. Food Chemistry, **122**, 300–306 (2010).
- [5] Seki, H.; Suzuki, A. Journal of Colloid and Interface Science, **190**, 206–211 (1997).
- [6] Gao, J.M.; Zhang, A.L.; Chen, H.; Liu, J.K. Chemistry and Physics of Lipids, **131**, 205–213 (2004).
- [7] Sawaya, W. N.; AL-Shalhat, A.; AL-Sogair, A.; AL-Mohammad, M. Journal of Food Science, **50**(2), 450–453 (1985).
- [8] Bokhary, H.A.; Parvez, S. Journal of Food Composition and Analysis, **6**, 285-293 (1993).
- [9] Alho, H.; Leinonen, J. Methods in Enzymology, **299**, 3-15 (1999).
- [10] Omer, E.A.; Smith, D.L.; Wood, K.V.; El-Menshawhi, B.S. Plant Foods for Human Nutrition, **45**, 247-249 (1994).
- [11] Gazdik, Z.; Krska, B.; Adam, V.; Saloun, J.; Pokorna, T.; Reznicek, V.; Horna, A.; Kizek, R. Sensors, **8**, 7564-7570 (2008).

COMPARATIVE STUDY ON ENZYMATIC HYDROLYSIS OF CELLULOSE

A.E. SEGNEANU^a, C. MACARIE^a, M. UNGUREANU^b, I. BALCU^a,
V. GHERMAN^b, I. GROZESCU^{a*}

^aNational Institute for Research and Development in Electrochemistry and
Condensed Matter, Timisoara, 144 A.P. Paunescu, 300569, Timisoara, Romania,

^bPolitehnica University of Timisoara, Timisoara, Romania

Identification and optimization of strains with high enzyme activity able to overcome constraints imposed by the cellulosic structure represents an important step in the development of new biotechnologies for bioethanol. This paper aims to reveal the advantages and disadvantages of the cellulase enzymes derived from two completely different microorganisms: *Trichoderma reesei*, a very known cellulase producer and *Butyrivibrio fibrisolvens*, a ruminal bacteria. Both organisms were inoculated under the same conditions (strict anaerobic, Sabouraud dextrose agar media, pH and temperature). The cellulose degradation was investigated by the time evolution of cellulase activity and the amount of reducing sugar released (glucose as standard) from carboxymethyl cellulose.

(Received July 2, 2013; Accepted August 5, 2013)

1. Introduction

The enzymatic hydrolysis of cellulose still represents an important step of the bioethanol production's cost. The identification of a highly efficiency cellulolytic enzymes (cellulases) with a high specific activity, will have a major impact on the availability of cost competitive biofuels market.¹⁻⁸ Although it is well known that physical properties of cellulose affects the rate of the enzymatic degradation process, recent studies aim to develop an innovative biotechnology based on suitable cellulolytic microorganisms capable to produce a complex and efficient enzyme system, being able to ensure a coordinate and a very efficient hydrolysis of hemicellulose and cellulose, from different lignocellulosic substrates.²⁻¹²

Under the enzymatic attack occurs the depolymerisation of cellulose in easily fermentable saccharides. Usually, the microorganisms which degrade cellulose, also degrade hemicellulose.⁸⁻²⁰

There are a great diversity of microorganisms for lignocellulose degradation: *Trichoderma*, *Aspergillus*, *Clostridium*, *Humicola*, *Talaromyces*, *Acrophialophora*, *Thermoascus*, *Bacillus* and *Penicillium* species.¹²⁻²⁵

Comparative studies on the efficiency of aerobic and anaerobic microorganisms had proved that not only 5-10 % of cellulose is degraded in nature under anaerobic conditions, but there are many differences between these two types of cellulolytic microorganisms.^{1,23-30} The best known strict anaerob microorganism is *Clostridium thermocellum*, but the main disadvantage consists in that it is necessary high temperature for cellulose degradation.^{2,3}

Researchers have paid special attention on anaerobic and, facultative, on anaerobic cellulolytic microorganisms isolated from a rumen microbial environment, because it is well known that cellulolytic rumen microorganisms (bacteria, fungi, etc) can convert the carbohydrates, from cellulose and other several types of biomasses, in carbon and energy sources. Even the

* Corresponding author: ioangrozescu@gmail.com

complex mechanism of cellulolysis system is not yet complete elucidated, has been studied intensively the competitive and synergic interaction between rumen microbes.^{4-6, 23, 25-29}

Most of the rumen cellulolytic microbes are: bacteria species (*Pseudomonas aeruginosa*, *Bacillus*, *Micrococcus*, *Streptococcus*, *Fibrobacter succinogenes*, *Ruminococcus flavefaciens*, and *Ruminococcus albus*), while the fungi isolated were species of *Fusarium*, *Penicillium*, *Aspergillus* and *Mucor*.^{5,6}

Studies on biodegradation of lignocellulose biomass under the action of rumen bacteria can represent an promising step for the development of an innovating biotechnology for bioethanol production.^{23, 25-29}

This paper investigate the cellulolysis efficiency of enzymes isolated from an rumen bacteria *Butyrivibria fibrisolvens* in comparison with an industrially important cellulolytic filamentous fungus, *Trichoderma reesei*.

2. Experimental

Materials and instruments

All the reagents are analytical grade. Folin-Ciocalteu reagent, 3,5-dinitrosalicylic acid (DNS), sodium hydroxide, potassium sodium tartrate, copper sulphate, glacial acetic acid, glucose, 3,5- dinitrosalicylic acid (DNS), phenol, sodium sulphite and sodium carbonate were obtained from Merck. The bovine serum albumin BSA, carboxymethyl cellulase (CMC) are from Fluka.

The microorganism used for inoculation of culture media were: *Butyrivibrio fibrisolvens*. The culture inoculation was carried out in sterile conditions in Laminar Flow Advanced Bio Safety Cabinet, BIOQUELL Medical Limited, England.

3. Experimental procedure

Estimation of protein concentration was determinated by Lowry method using bovine serum albumin (BSA) as the standard. This chromogenic procedure is inexpensive, easy to perform, very sensitive and highly reproducible, but the major disadvantage is because its accuracy depends on the pH of the solution.³¹⁻³²

A) Different dilutions of BSA solutions are prepared by mixing stock BSA solution (1 mg/ mL) and water in the test tube as given in the table 1. The final volume in each of the test tubes is 2 mL. The BSA range volume is 0.02 to 0.2 mL.

B) The alkaline cooper reagent was prepared by mixing 0.5 mL of 0.5% cupric sulfate with 0.5 mL of 2% sodium potassium tartrate, followed by the addition of 50 mL of 2% sodium carbonate in 0.1 N NaOH. The mixture was then allowed to incubate at room temperature for 10-15 minutes.

C) There were taken portions from the standard solution of Bovine serum albumin (BSA) and placed into 10 tubes by filling with distilled water to 0.2 mL, 5mL of alkaline copper reagent and 0.5mL Folin-Ciocalteu reagent were added in this order.

D) Calibration solution of albumin bovine serum (BSA) in distilled water (1 mg/mL).

The samples were mixed and the color was allowed to develop for 30 minutes at room temperature and the absorbance measured at 660 nm against a blank obtained under the same condition, by replacing the BSA solution with distilled water. For safety determination two samples have been made in parallel. The results are being presented in the table 1.

Table 1. BSA solution calibration with Lowry method.

| Nr. crt. | BSA solution (mL) | Distilled water (mL) | Extinction | Protein quantity (mg) |
|------------|-------------------|----------------------|------------|-----------------------|
| 1. (blank) | - | 0,20 | - | 0,00 |
| 2. | 0,02 | 0,18 | 0,0496 | 0,02 |
| 3. | 0,04 | 0,16 | 0,0957 | 0,04 |
| 4. | 0,06 | 0,14 | 0,1442 | 0,06 |
| 5. | 0,08 | 0,12 | 0,2022 | 0,08 |
| 6. | 0,10 | 0,10 | 0,2538 | 0,10 |
| 7. | 0,12 | 0,08 | 0,2838 | 0,12 |
| 8. | 0,14 | 0,06 | 0,3342 | 0,14 |
| 9. | 0,16 | 0,04 | 0,3562 | 0,16 |
| 10. | 0,18 | 0,02 | 0,4349 | 0,18 |
| 11. | 0,20 | - | 0,4169 | 0,20 |

The plot of the extinction depending on the protein amount shows a straight form. This dependence may be expressed by the next equation:

$$E = b \cdot C_p$$

where:

E = the extinction

b = the slope

C_p = the protein amount, (mg)

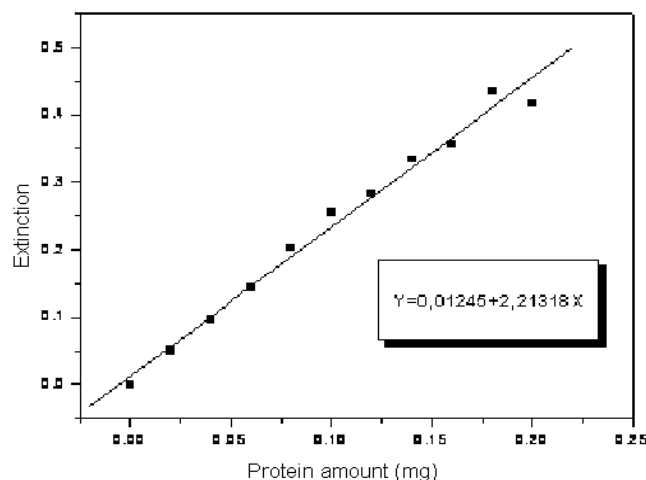


Fig. 1. Calibration curve of BSA solution by Lowry method

Simultaneously have performed an estimate of a protein concentration from an unknown solution

A volume of 2 mL sample, 0,2 mL distilled water, 5 mL copper alkaline reagent and 0,5 mL Folin-Ciocalteu reagent were added into a test tube and left ageing for 30 minutes at the room temperature. After this, the extinction was determined at 660 nm against a blank obtained in the same condition but replacing the sample with distilled water. For a safety determination two samples have been made in parallel.

The protein content of the sample was determined with the relationship:

$$C = \frac{1}{2,21318} \cdot E \cdot 5 \cdot F \text{ (mg/ml)}$$

Where: 5 = sample dilution at 1 mL

F = the dilution factor of enzymatic solution

Evaluation of Cellulase Activity using the carboxymethylcellulase as substrate was performed by Miller method with 3,5-dinitro-salicylic acid (DNS).

D-glucose standards were prepared in 0,05 M sodium acetate buffer pH 4.8 at concentration between 0.25 and 1.5 mg/mL (Table 2) and the reaction was carried out with a reagent solution composed from: 1,0 g DNS, 200 mg phenol, 50 mg of sodium sulphite and adjusted to volume with 1% NaOH.

Table 2. Preparation of standard glucose solutions.

| Glucose solution (mL) | Sodium acetate buffer solution 0,05 M, pH 4,8 (mL) | Dilution | Concentration (mg/mL) |
|-----------------------|--|----------|-----------------------|
| 1,0 | 2,3 | 1 :3,3 | 1,5 |
| 1,0 | 3,0 | 1 :4 | 1,25 |
| 1,0 | 4,0 | 1:5 | 1,0 |
| 1,0 | 5,7 | 1:6,7 | 0,75 |
| 1,0 | 9,0 | 1:10 | 0,5 |
| 1,0 | 19,0 | 1:20 | 0,25 |

Glucose standard curve

Determination of the calibration curve for glucose solution required the next procedure:

- the blank sample contains: 0.4 mL acetate buffer solution (0,05 M, pH 4.8), 0.4 mL distilled water and 1.2 mL DNS solution;
- glucose sample was prepared from 0.4 mL standard glucose solution dissolved in 0.4 mL distilled water and was added 1.2 mL DNS solution;

The both obtained samples were boiled for 15 minutes and then cooled at room temperature and absorbance at 540 nm was determined.

The standard curve for glucose standards (Figure 2) has a linear form described by the following equation:

$$E = a + b \cdot C_G$$

where:

E= absorbance

C_G = concentration of glucose, mg/mL

a = origin ordinate

b = slope

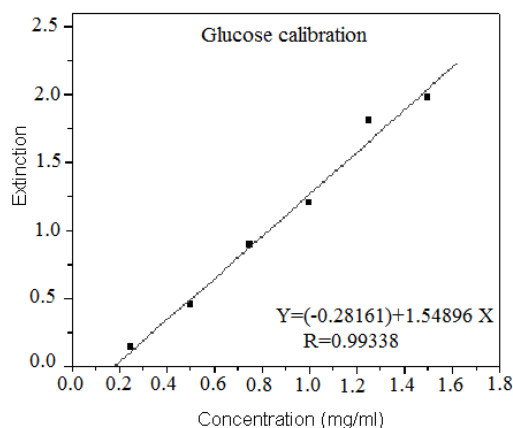


Figure 2. D-glucose calibration curve

The amount of glucose expressed as mg glucose from the sample was determined from the calibration curve using the following relation:

$$C_G = \frac{(E_p - E_M)}{1,54896} \cdot \text{sample dilution} \cdot V [\text{mg glucose}]$$

where: V- total volume (1,5 mL).

Cellulase preparation from *Trichoderma reesei*

The *Trichoderma reesei* was inoculated on a Sabouraud dextrose agar media prepared from 200 mL of potato extract and 2 g cellulose/l, in serum bottle sealed with rubber stoppers. The serum bottles were autoclaved (20 min, 120°C, 1 atm pressure) and then flushed with nitrogen. The culture was grown in anaerobic condition, ten days at 30°C. Then was prelevated samples for enzymatic activity assay and for protein assay.

Cellulase preparation from *Butyrivibrio fibrisolvens*

The *Butyrivibrio fibrisolvens* was inoculated on a Sabouraud dextrose agar media prepared from 200 mL of potato extract and 2 g cellulose/l, in serum bottle sealed with rubber stoppers. The serum bottles were autoclaved (20 min, 120°C, 1 atm pressure) and then flushed with nitrogen. The culture was grown in anaerobic conditions, ten days at 30°C.

Determination of cellulase activity

The 1 mL sample was added to 0.5 mL of 2% carboxymethyl cellulose (CMC). The mixture was incubated in a water bath at 50°C for 30 minutes. Comparative was prepared a blank sample consisting from 1.0 mL cellulase solution and 0.5 mL substrate solution CMC 2%. The evaluation of the enzymatic activity was determined in basis of the remaining unreacted glucose and is expressed in units. A unit is the amount of enzyme from 1mL enzyme solution which releases 1 mol of reducing sugars (glucose as standard) in a minute at 30°C.

The calculation formula of the activity is:

$$A_{\text{CMC}} = \frac{\text{mg glucose} \cdot 1000}{180 \cdot 1,0 \cdot 30} \quad [\text{U/ml}]$$

4. Results and discussions

According to the literature, *Butyrivibrio fibrisolvens* is an anaerobic, butyric acid forming bacteria which produce an multi-enzyme complex with predominantly xylanase activity.^{1-6,23,25-29} This study is important in terms to investigate the enzymatic activity of the pure *Butyrivibrio* species isolated and particularly, their cellulolytic enzyme activity by comparison with a well known cellulolytic microorganism, *Trichoderma reesei*. Was chosen this widely used fungus *Trichoderma reesei*, for cellulase production, because of its ability to produce significant quantities of enzymes.

The specific activity of pure cellulase-producing strains was carried out using traditional technique in strict aerobic condition by determination of the amount of reducing sugar released (glucose as standard) from carboxymethyl cellulose.

The results of the enzyme activity per time are presented in the Tables 3 and 4 and figures 3 and 4.

Tabelul 3. Cellulasic activity and total protein content in the *Trichoderma reesei* culture

| Time [h] | Carbon source | Glucose (mg) | Activity [U/mL] | Protein [mg/mL] |
|----------|----------------------|--------------|-----------------|-----------------|
| 24 | Cellulose 5 [g/L] | 6,06 | 1,122 | 0,964 |
| 48 | | 5,90 | 3,520 | 0,998 |
| 144 | | 4,19 | 7,760 | 1,039 |

Table 4. Cellulasic activity and total protein content in the *Butyrivibrio fibrisolvens* culture

| Time [h] | Carbon source | Glucose (mg) | Activity [U/mL] | Protein [mg/mL] |
|----------|----------------------|--------------|-----------------|-----------------|
| 24 | Cellulose 2 [g/L] | 7,972 | 9,885 | 0,495 |
| 48 | | 5,338 | 30,90 | 0,529 |
| 144 | | 3,477 | 0,644 | 0,664 |

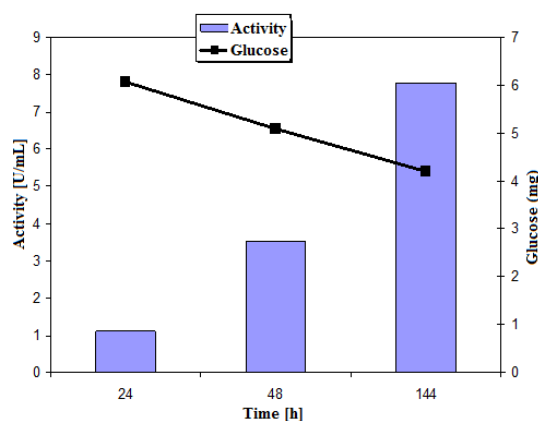


Fig. 3. The evolution in time of the cellulase produced by *Trichoderma reesei* and of the glucose quantity.

Analysis of experimental showed that the both microorganisms growth occurs fast on the Sabouraud dextrose agar media. The evolution of the cellulosic activity present several features for each microorganism investigated. For instance, *Trichoderma reesei* stains showed a continuous increase of the cellulosic activity throughout the monitored period, yielding a value of 7.76 U/mL after 144 hours (Figure 3). These results are comparable to those reported in the literature³⁰⁻³³, which give higher values for cellulase activity of *Trichoderma reesei* cultures after 7 days, and the can be difference can be attributed to the type of the culture media which ensure the mantainance of the pH value at a specific value. The total protein concentration exhibit only a mild variation. Evolution of the amount of glucose indicate a slight decrease until at value of 4.19 mg after 144 hours, which shows that there is still required condition for further enzymes production.

The rumen cellulolytic bacteria, *Butyrivibrio fibrisolvens*, acted in different way. It was found that the maximum enzyme production was 30,90 U/mL and was optimum at 48 h, then have showed a dramatic decrease in enzyme production level was detected at day six (0,644 U/mL) (Figure 4). In contrast, the protein concentration recorded present a steady growth, which shown that the culture media used was appropriate from the point of view of ensuring the required nutritional factors. After six days, was retrieved aproximative half o the glucose amount from day one (24 hour), which demonstrates that there were growth resources of biomass, however this fact is not important in given condition because it was of interest only in the production of cellulase.

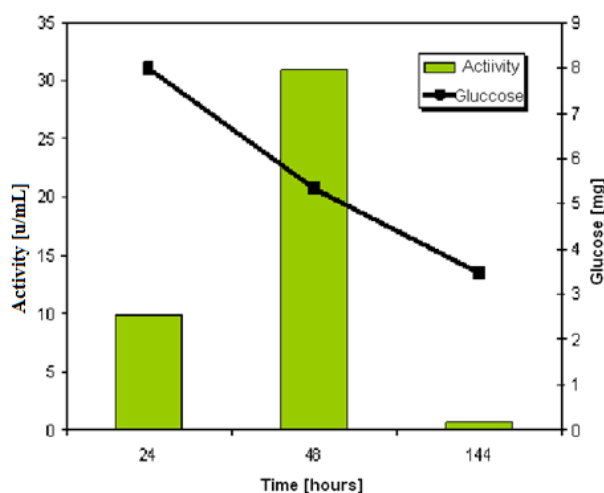


Fig. 4. The evolution in time of the cellulase produced by *Butyrivibrio fibrisolvens* and of the glucose quantity

The results obtained has been suggested that enzymatic activity of the cellulolytic bacteria start present an early rate exponential (until the second day), unlike the industrial fungus, whose enzyme production increases slowly. Further studies are necessary to optimise the culture conditions (pH, temperature, carbon sources and nitrogen sources) to achieve the maximum yield of the cellulase activity.

5. Conclusions

The purpose of this study was a comparative analysis of enzymatic activity of two type of microorganisms, inoculated on the same culture condition. *Butyrivibrio* species isolated in this experiment can be considered as a higher source of cellulolytic enzyme. The results of this investigation have suggested that this cellulolytic ruminal bacteria endowed with the capacity to digest native insoluble cellulose and relatively high specific growth rates, the must be regarded as a very promising solution for industrial enzymatic hydrolysis step.

References

- [1] J. Perez, C. J. Muñoz-Dorado, T. de la Rubia, C. J. Martínez, *Int Microbiol.*, **5**, 53 (2002).
- [2] W.H Schwarz, *Applied Microbiology and Biotechnology*, **56**(5-6), 634 (2001).
- [3] J. Miron, D. Ben-Ghedalia, M. Morrison, *Journal of Dairy Science*, **84**(6), 1294 (2001).
- [4] S.B.Oyeleke, T.A. Okusanmi, *African Journal of Biotechnology*, **7**(10), 1503 (2008),
- [5] R. Singh, M. Singh, S. Nayyar, *Indian Journal of Animal Sciences* **75**(11), 1295 (2005),
- [6] C.G. Orpin, *Applied Biochemistry and Biotechnology*, **9**(4), 327 (1984).
- [7] S. B., Leschine, *Ann. Rev. Microbiol.* **49**, 399 (1995).
- [8] D. Matt, Sweeney and Feng Xu, *Biomass Converting Enzymes as Industrial Biocatalysts for Fuels and Chemicals: Recent Developments, Catalysts*, **2**, 244 (2012),
- [9] S.L. Li, J.S. Lin, Y.H. Wang, Z.K. Lee, S.C. Kuo, I.C. Tseng, S.S. Cheng, *Bioresource Technology* **102**(18), 8682 (2011),
- [10] R.B. Hespell, R. Wolf, R.J. Bothast, *Applied and Environmental Microbiology*, **53**(12), 2849 (1987).
- [11] M. Ali, H. Suzuki, T. Fukuba, X. Jiang, H. Nakano, T. Yamane, *Journal of Bioscience and Bioengineering*, **99**(2), 181 (2005)
- [12] L.R. Lynd, P.J. Weimer, Zyl Van, W.H., I.S. Pretorius, *Microbiology and Molecular Biology Reviews*, **66** (3), pp. 506-577. (2002),
- [13] M.E. Vega-Sánchez, P.C. Ronald, *Current Opinion in Biotechnology*, **21**(2), 218 (2010),
- [14] S. Haruta, Z. Cui, Z. Huang, M. Li, M. Ishii, Y. Igarashi *Appl. Microbiology and Biotechnology*, **59**(4-5), 529 (2002),
- [15] S. Kato, S. Haruta, Z.J. Cui, M. Ishii, Y. Igarashi, *FEMS Microbiology Ecology*, **51**(1), 133 (2004)
- [16] R.H. Doi, A. Kosugi, *Nature Reviews Microbiology*, **2**(7), 541 (2004)
- [17] L.R. Lynd, W.H. Van Zyl, J.E. McBride, M. Laser, *Current Opinion in Biotechnology*, **16**(5), 577 (2005),
- [18] L.R. Lynd, P.J. Weimer, W.H. Van Zyl, I.S. Pretorius, *Microbiology and Molecular Biology Reviews*, **66**(3), 506 (2002),
- [19] L.O. Shengde Zhou, *Ingram Biotechnology Letters*, **23**(18), 1455 (2001),
- [20] P. Ronan, C. William Yeung, J. Schellenberg, R. Sparling, G.M. Wolfaardt, M. Hausner, *Bioresource Technology*, **129**, 156 (2013).
- [21] K., Brenner, L. You, F.H. Arnold, *Trends in Biotechnology*, **26**(9), 483 (2008)
- [22] W. Wang, L. Yan, Z. Cui, Y. Gao, Y. Wang, R. Jing, *Bioresource Technology*, **102**(19), 9321 (2011).

- [23] D.O. Krause, , C.S. McSweeney and, R. J. Forster Molecular ecological methods to study fibrolytic ruminal bacteria: Phylogeny, competition, and persistence. In: Bell, C.R., (1999)
- [24] C.A. Macarie, A.E. Segneanu, I. Balcu, R. Pop, G. Burtica, V.D. Gherman, *Low Carbon Economy*, **2**, 224-229, (2011),
- [25] N.V. Zyabreva, , E.P. Isakova, V.V. Biryukov, *Applied Biochemistry and Microbiology*, **37**(4), 363 (2001)
- [26] S. Koike, Y. Kobayashi, *Asian-Aust. J. Anim. Sci.*, **22**(1), 131 (2009),
- [27] J. B. Russell, R. E. Muck, P. J. Weimer, *FEMS Microbiol Ecol* 67, pp.183–197. (2009),
- [28] M.A. Cotta and, R.L. Zeltwanger *Applied and Environmental Microbiology*, **61**, 4396 (1995).
- [29] Krushna Chandra Das, Wensheng Qin, *Open J. of Animal Sciences* **2**, 224 (2012).
- [30] B. Nidetzky, W. Steiner, M. Hayn, Marc Claeysens, *Biochem.J.* **298**, 705 (1994),
- [31] M. Dashtban, M. Maki, K. T. Leung, C. Mao, W. Qin, *Critical Reviews in Biotechnology*, **30**(4), 302 (2010),
- [32] T. K. Ghose, Measurement of cellulase activities, *Pure & Appl. Chem.*, **59**(2), 257 (1987),
- [33] C.A. Macarie, A.E. Segneanu, I. Grozescu, G. Burtica, *Digest Journal of Nanomaterials and Biostructures* **7**(4), 1577 (2012).



“Gheorghe Asachi” Technical University of Iasi, Romania



A NEW PHOTO-FENTON PROCEDURE APPLIED IN OXIDATIVE DEGRADATION OF ORGANIC COMPOUNDS FROM WASTEWATER

Cristina Orbeci¹, Ion Untea^{1*}, Rodica Stanescu¹,
Adina Elena Segneanu², Mihaela Emanuela Craciun¹

¹Politehnica” University of Bucharest, Faculty of Applied Chemistry and Materials Science,
1-7 Gh. Polizu Street, 011061 Bucharest, Romania

²National Institute of Research and Development for Electrochemistry and Condensed Matter, Timisoara,
144 A. P. Podeanu Street, 300569 Timisoara, Romania

Abstract

This paper presents a new photo-Fenton procedure applied in oxidative degradation of organic pollutants using 4-chlorophenol (4-CP) as low biodegradable testing compound. The homogeneous photo-Fenton process was modified by using a photo-catalytic reactor equipped with a steel wire mesh which acts as source for Fe²⁺ catalyst generation into reaction medium and as heterogeneous catalyst, by iron oxy-hydroxyl compounds formation on the surface. The oxidation process was evaluated by measuring the organic substrate concentration changes using COD, TOC, HPLC and LC-MS analyses, in correlation with modification of solution pH and Fe^{2+/3+} concentration as function of reaction time. The oxidation rate is higher at the beginning of the process and then slows down, being controlled by the nature of the intermediate oxidation products and by the change of Fe(III)/Fe(II) molar ratio into the solution. The new photo-Fenton procedure is simple but effective, combining the advantages of homogeneous and heterogeneous photo-Fenton processes.

Key words: 4-chlorophenol; in situ Fe²⁺ catalyst generation; oxidation; photo-Fenton process

Received: September, 2011; *Revised final:* January 2012; *Accepted:* January, 2012

1. Introduction

The chlorophenols are common persistent organic contaminants, which show low biodegradability, posing serious risks to the environment once discharged into natural water (Du et al., 2006).

The AOPs (Advanced Oxidation Processes) can be successfully used in wastewater treatment to degrade the persistent organic pollutants, the oxidation process being determined by the very high oxidative potential of the HO[•] radicals generated into the reaction medium by different mechanisms (Pera-Titus et al., 2004). AOPs can be applied to fully or partially oxidize pollutants, usually using a combination of oxidants.

Photo-chemical and photo-catalytic advanced oxidation processes including UV/H₂O₂, UV/O₃, UV/H₂O₂/O₃, UV/H₂O₂/Fe²⁺ (Fe³⁺), UV/TiO₂ and UV/H₂O₂/TiO₂ can be used for oxidative degradation of organic contaminants. A complete mineralization of the organic pollutants is not necessary, being more worthwhile to transform them into biodegradable aliphatic carboxylic acids followed by a biological process (Orbeci et al., 2010; Wang and Wang, 2007).

The efficiency of the various AOPs depends both on the rate of generation of the free radicals and the extent of contact between the radicals and the organic compound. Also, the pH has a significant role determining the efficiency of Fenton and photo-Fenton oxidation processes (Gogate and Pandit, 2004).

* Author to whom all the correspondence should be addressed: e-mail: i.untea@yahoo.com; Phone: +40727792523

The optimum pH range in the case of homogeneous photo-Fenton process is 2.5-4, a correction of solution pH being necessary. Also, at the end of the oxidation process, iron precipitation and catalyst separation and recovery are necessary. These disadvantages can be avoided using heterogeneous photo-Fenton procedure by active iron species immobilization on small particulate solid supports. In this case, different iron-containing catalysts can be used, such as the iron bulk catalysts (iron oxy-hydroxyl compounds: hematite, goethite, magnetite) or iron supported catalysts (zeolites, clays, bentonite, glass, active carbon, polymers etc.) (Duarte and Madeira, 2010; Feng et al., 2005; He et al., 2005; Leland and Bard, 1987; Nie et al., 2008; Ortiz de la Plata et al., 2010; Vinita et al., 2010).

In the case of the heterogeneous photo-Fenton process, a relevant fraction of the incident UV radiation can be lost via scattering, due to particulate solid support suspended into the reaction medium. As a consequence, the photo-Fenton process may be seriously affected (Herney-Ramirez et al., 2010). Also, the solution pH affects the Fe leaching from the support, at pH values less than 3 a higher amount of Fe being released into the solution (Duarte and Madeira, 2010; Herney-Ramirez et al., 2010). By using a zero-valent iron with iron oxide composite catalysts, the oxidation process proceed via hydroxyl radicals generated from $\text{Fe}^{2+}(\text{surf})$ species and H_2O_2 in a Fenton like mechanism. The $\text{Fe}^{2+}(\text{surf})$ species are formed by electron transfer from Fe^0 to Fe^{3+} at the interface metal/oxide (Moura et al., 2005, 2006). The experimental data obtained by Nie et al. (2008) indicate that hydrogen peroxide provides a driving force in the electron transfer from Fe^{2+} to Fe^{3+} , while the degradation of organic pollutants increases the electron transfer at the interface of Fe^0 /iron oxide due to their reaction with hydroxyl radicals.

The degradation of organic pollutants using photo-Fenton processes occurs by intermediates oxidation products formation. In the case of phenol oxidation by Fenton's reagent, a series of intermediates were identified, corresponding mainly to ring compounds and short-chain organic acids (Assadi and Eslami, 2010; Zazo et al., 2005). Most significant among the former were catechol, hydroquinone, and *p*-benzoquinone; the main organic acids were maleic, acetic, oxalic, and formic, with substantially lower amounts of muconic, fumaric, and malonic acids. Oxalic and acetic acid appeared to be fairly refractory to the Fenton oxidation process.

In the Fenton process, carboxylic acids like acetic and oxalic acid may be formed as end products during the degradation of phenol while in photo-Fenton process, both these acids were identified during the early stages of phenol degradation and were oxidized almost completely at the end of the process (Kavitha and Palanivelu, 2004). Studying the degradation of 4-chlorophenol by an electrochemical advanced oxidation process, Wang and Wang (2007) have proposed the following possible pathway: (a) 4-chlorophenol dechlorination to phenol; (b)

hydroxylation of phenol to hydroquinone; (c) dehydrogenation of hydroquinone to benzoquinone; (d) the oxidation of benzoquinone (with aromatic ring cleavage) to aliphatic carboxylic acids such as maleic acid, fumaric acid, malonic acid; (e) the oxidation of maleic and fumaric acids to oxalic acid, formic acid and finally, to carbon dioxide and water. The main intermediates products detected by HPLC analyses were chlorocatechol and benzoquinone after 60 min reaction time and aliphatic carboxylic acids after 120 min reaction time. Benzoquinone and hydroquinone-like intermediates such as catechol, hydroquinone and 4-chlorocatechol can reduce the ferric ion to ferrous ion and the oxidation process becomes faster (Du et al., 2006).

The aim of this study is to evaluate a new photo-Fenton procedure as a suitable advanced oxidation process to degrade 4-chlorophenol, as low biodegradable testing compound, in aqueous solutions. The proposal of a new photo-Fenton procedure refers to using a photo-catalytic reactor equipped with a steel wire mesh (cylindrical shape, centrally and coaxially positioned) as a precursor of photo-catalytic active iron species.

2. Experimental

The laboratory experiments were achieved using a photo-catalytic reactor with continuous recirculation equipped with a steel wire mesh (cylindrical shape, diameter of 70 mm, height of 350 mm, wire thickness of 0.23 mm, 30 mesh/cm²) and a high pressure mercury lamp, power of 120 W, centrally and coaxially positioned (Fig. 1).

The experiments were performed at $30 \pm 2^\circ\text{C}$ using synthetic solutions of 4-chlorophenol (analytical grade reagent from Merck) with initial concentration of 186 mg 4-CP/L (initial COD of 360 mg O₂/L). The used amount of hydrogen peroxide (solution stock of 30% w/w, analytical reagent from SC COMCHIM SA) was calculated at H₂O₂/4-CP stoichiometric ratio of 1.5. The photo-catalytic reactor volume was 1.5 L, total solution volume 4.0 L and the recirculation flow rate 1.5 L/min.

The efficiency of the oxidation process was evaluated by monitoring the organic substrate concentration changes using COD, TOC, HPLC and LC-MS analyses, in correlation with modification of solution pH and $\text{Fe}^{2+/3+}$ concentration as function of reaction time.

The solution samples, collected at different reaction times, were stabilized by MnO₂ addition for a quick decomposition of unreacted H₂O₂ and then were filtered. For COD analysis, the samples were corrected in terms of pH using NaOH solution 40% (w/w) for Fe ions precipitation, and then were filtered. Chemical oxygen demand analyses (COD) were performed through a standard method using a Digestor DK6. Total organic carbon (TOC) analyses were performed using a Multi N/C 2100 Analytikjena TOC-analyzer.

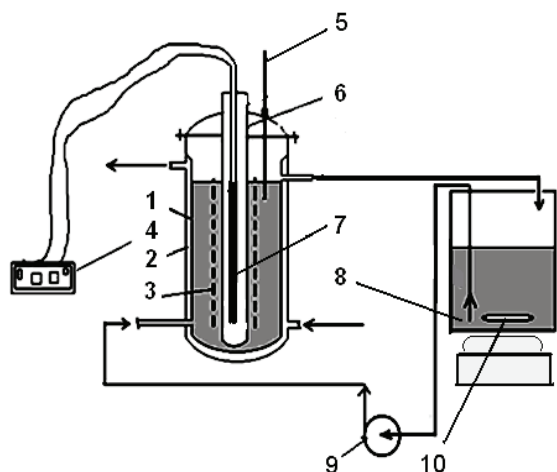


Fig. 1. Laboratory photo-catalytic reactor with continuous recirculation (1-photo-catalytic reactor; 2-cooling jacket; 3-steel wire mesh, cylindrical shape; 4-UV lamp source; 5-thermometer; 6-quartz tube; 7-UV lamp; 8-recirculation reservoir; 9-recirculation pump; 10-magnetic stirrer)

High-performance liquid chromatography (HPLC) analyses were done using an Ultimate 3000 "Diode Array" chromatograph, detector UVD-3000, C18 Acclaim 120 DIONEX, pump LPG-3400A. The separation column used was C18 Acclaim 120 with a length of 250 mm and 4 mm diameter. The working conditions were: mobile phase of 0.0035M H_2SO_4 , column temperature $40^\circ C$, flow rate 0.6 mL/min, wavelength 210 nm.

Liquid chromatography coupled with mass spectrometry (LC-MS) analyses were done using an Agilent 1200 Series chromatograph equipped with detector MS 6120 Qudrupole and autosampler. The working conditions were: mobile phase of acetonitrile/water = 10/90 (w/w), column temperature $25^\circ C$, flow rate 1.25 mL/min, injection volume 10 μL . Detection was performed in the MDC SIM, positive polarization (MM-ACDI) and MM-ES APCI ionization.

The pH of the solution was measured using an ION check 10 (Radiometer Analytical) pH-meter. Fe^{2+}/Fe^{3+} analyses were performed by spectrometric methods based on the spectral properties of $Fe(II)$ and $Fe(III)$ complexes, using a Cecil CE 1011 series spectrophotometer. Fe^{2+} concentration was determined at $\lambda=510$ nm using an orto-phenantroline reagent and Fe^{3+} concentration was determined at $\lambda=620$ nm using a tiron reagent.

3. Results and discussion

The experimental data concerning the influence of the reaction time on the organic substrate concentration, expressed as COD/COD_0 and TOC/TOC_0 values, are presented in Fig. 2. For the reaction time interval of 0-30 min, the oxidation process takes place with high reaction rate. At the same time interval, TOC/TOC_0 value decreases with a lower rate comparing with COD/COD_0 value,

indicating the formation of intermediate organic compounds.

Furthermore, the significant decrease of the pH values (Fig. 3) indicates the acidic nature of these compounds.

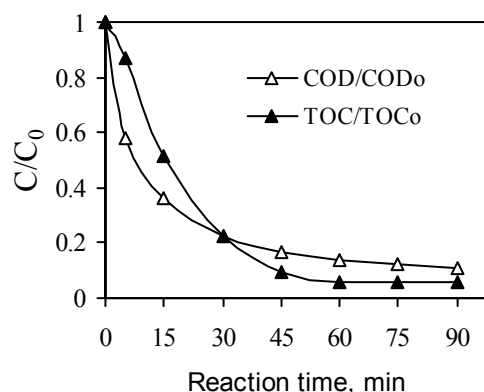


Fig. 2. Organic substrate concentration function of reaction time

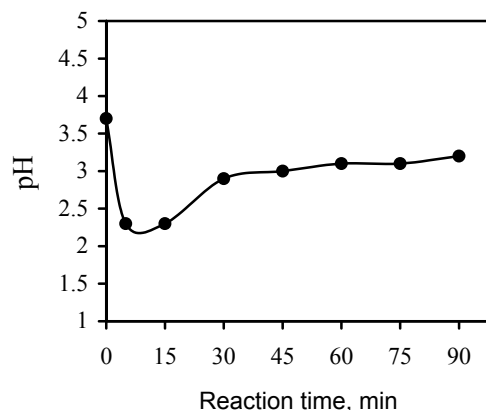


Fig. 3. Solution pH variation function of reaction time

Inorganic (HCl) and/or organic acids react with the Fe from steel wire mesh forming into the reaction medium small amounts of Fe^{2+} which acts as a photo-catalyst, in accordance with the classic homogeneous photo-Fenton process.

HPLC analysis of solution samples collected at reaction time of 15 min and 90 min (Figs. 4 and 5) have revealed the presence of acetic acid at approximately 3.07 min retention time. The peak height and the peak area (Table 1) show that the quantity of acetic acid formed into the solution is relatively similar for a reaction time of 15 min and 90 min. This means that the acetic acid is formed as an intermediate reaction and as a result, can lead to leaching out the Fe^{2+} ions from steel wire mesh into the solution. Also, the acetic acid remains in solution at higher reaction times, certifying a high resistance to the oxidation process. The formic acid has not been identified in the samples collected at reaction time of 15 min or 90 min. LC-MS analyses of the solution samples collected at different reaction times have revealed the formation of several intermediate

organic compounds whose concentration changes during the oxidation process.

Table 1. Retention characteristics of acetic acid HPLC analysis

| Sample | Reaction time (min) | Retention time (min) | Peak height (mAu) | Peak area (mAu min) |
|--------|---------------------|----------------------|-------------------|---------------------|
| 4-CP | 15 | 3.067 | 77.432 | 15.3779 |
| | 90 | 3.075 | 78.943 | 16.0012 |

The oxalic acid (retention time of approximately 0.39 min for standard sample, Fig. 6) was not identified in samples collected at reaction time of 15 min and 90 min.

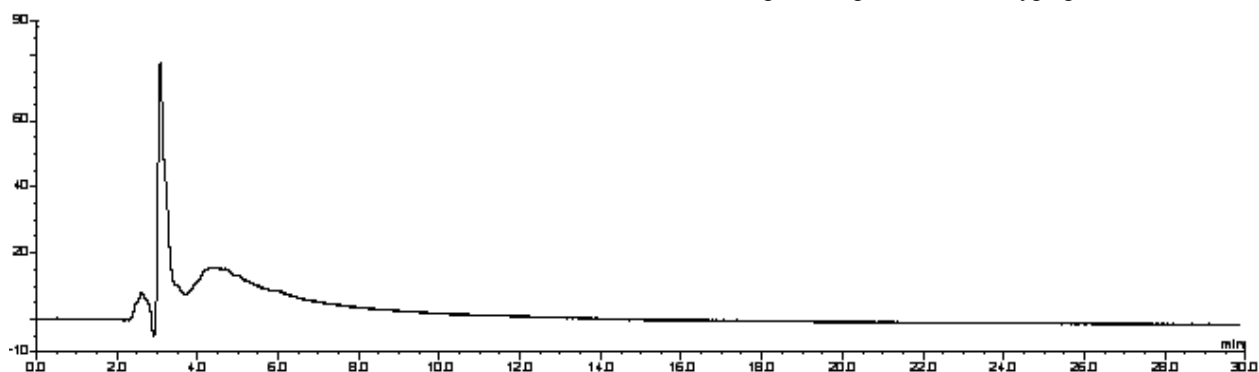


Fig. 4. HPLC analysis for acetic acid (sample collected at 15 min reaction time)

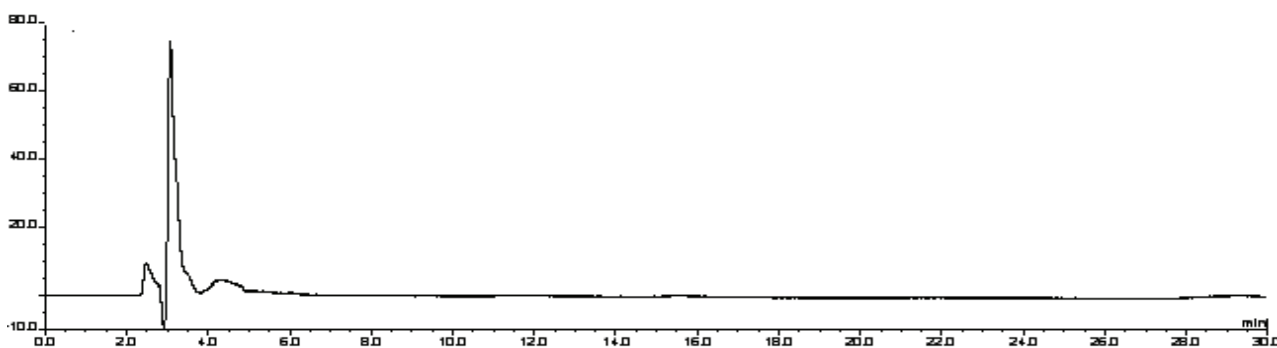


Fig. 5. HPLC analysis for acetic acid (sample collected at 90 min reaction time)

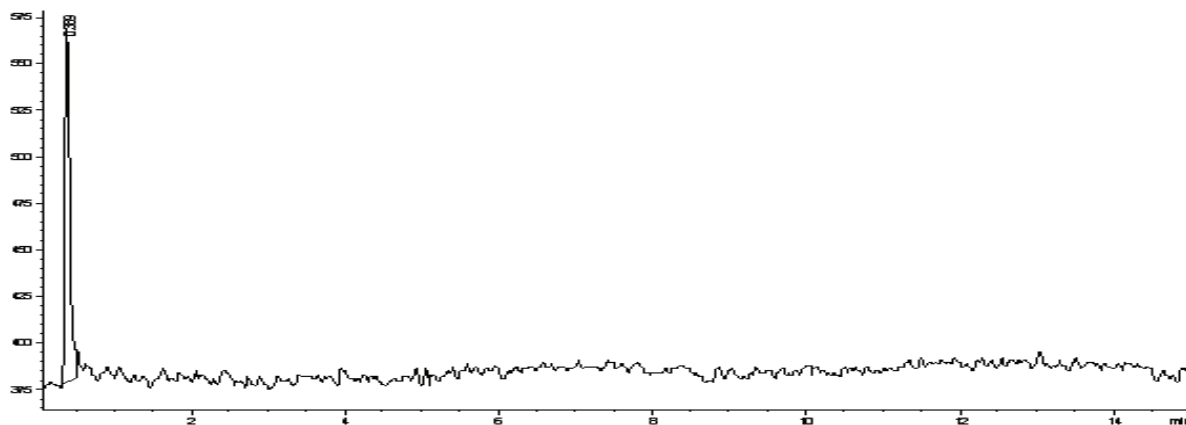


Fig. 6. LC-MS analysis for oxalic acid (standard sample)

The characteristic peaks, recorded at higher retention times (Fig. 7), can be attributed to organic acids with higher molecular weight, such as malonic, maleic, succinic or muconic acids (Li et al., 2005). At the beginning of the process, Fe^{2+} concentration increased gradually, reaching a maximum value after 30 minutes of reaction time (Fig. 8).

After 15 min reaction time, the solution pH increases due to some organic acids mineralization and to HO^- ions formation by Fe^{2+} oxidation to Fe^{3+} in the presence of H_2O_2 and UV radiation (Eq. 1).



Thus, at higher reaction time, the pH of the reaction medium reaches at value of about 3, which is the optimum pH for Fenton type processes.

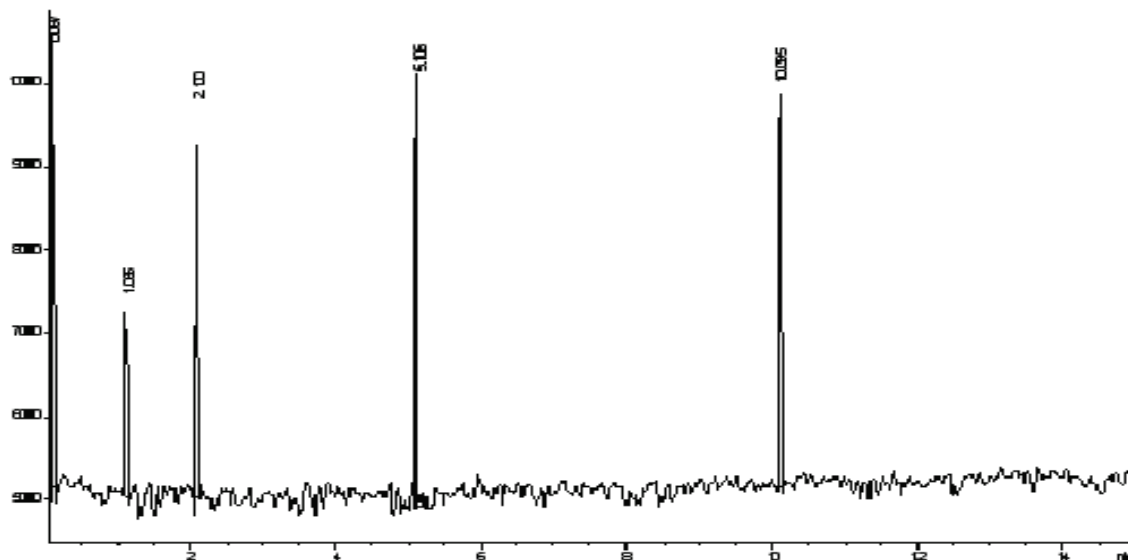


Fig. 7. LC-MS analysis (sample collected at 15 min reaction time)

Due to the high oxidation potential of the reaction medium, Fe(II) and Fe(III) oxides and oxyhydroxides species (such as FeO, Fe₂O₃, Fe₃O₄ and FeOOH) can be formed on the surface of the steel wire mesh. These compounds have photo-catalytic properties and a high reactivity in the oxidation process of organic pollutants (Leland and Bard, 1987; Moura et al., 2005; 2006; Nie et al., 2008). As result, the high reaction rate may be explained by the fact that the 4-CP oxidation can occur simultaneously by both homogeneous and heterogeneous photo-Fenton processes.

After 30 min reaction time, the oxidation process takes place with a slow reaction rate due to low molecular weight organic acids (such as acetic acid) which are more resistant towards the oxidation process. Also, the change of the Fe(II)/Fe(III) molar ratio (Fig. 8 and 9) is an important factor which controls the rate of the oxidation process.

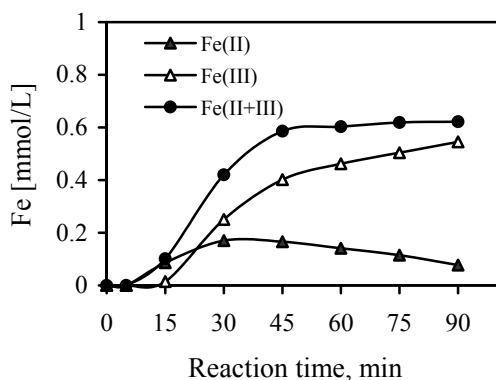


Fig. 8. Fe(II) and Fe(III) concentrations function of reaction time

The decrease of the oxidation rate in this stage may be explained also by the progressive Fe²⁺ disappearance from the solution. The steel wire mesh allows the access of UV radiations into entire photo-catalytic reactor volume and acts as a catalyst source in the sense that, during the oxidation process, it

continuously generates Fe²⁺ into the reaction medium. The ferrous ions, in the presence of hydrogen peroxide and UV radiation, play an important role in the catalytic oxidation process, according to the specific reaction mechanism of the classic homogeneous photo-Fenton process.

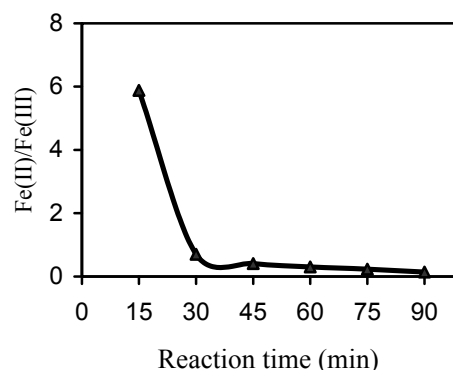


Fig. 9. Fe(II)/Fe(III) molar ratio function of reaction time

Also, the steel wire mesh acts as a heterogeneous photo-catalyst due to Fe⁰/Fe^(II,III) species formed on the surface. As consequence, the oxidation can take place both by homogeneous and heterogeneous photo-Fenton processes.

It is not easy to determine if the degradation of the organic substrate is due to the oxidation process by hydroxyl radicals coming from the breakage of H₂O₂ catalyzed by the iron species formed on the surface of the steel wire mesh (heterogeneous photo-Fenton process) or by the Fe²⁺ ions leached out into the reaction medium (homogeneous photo-Fenton process). The concentration control of Fe²⁺ leached out into the solution may be done by limiting the reaction time and by changing the solution recirculation ratio and the steel wire mesh characteristics (wire thickness, wire mesh size, height and diameter of cylinder etc.).

The advantage of the new photo-Fenton procedure is given by the fact that, into the reaction

medium, no additional other substances or materials with catalytic activity (such as FeSO_4 , $\text{Fe}_2(\text{SO}_4)_3$, FeCl_3 , $\text{Fe}(\text{NH}_3)_2(\text{SO}_4)_2$, $\text{Fe}(\text{NO}_3)_2$ or other compounds of Fe(II) or Fe(III)) are necessary and no longer must be corrected the initial pH of the solution. In the case of wastewaters containing non-biodegradable or low biodegradable organic pollutants (chlorophenols as example), this procedure can be successfully applied as a pre-treatment method by combining with biological treatment.

4. Conclusions

The new photo-Fenton procedure proposed for the oxidative degradation of organic compounds from wastewater is based on the homogeneous photo-Fenton process modified by using a photo-catalytic reactor equipped with a steel wire mesh which allows the access of UV radiations and acts as source for the Fe^{2+} catalyst generation into the reaction medium and as a heterogeneous catalyst, by photo-catalytic active iron oxy-hydroxyl compounds formation on the surface.

The oxidation rate of 4-chlorophenol (4-CP), used as low biodegradable testing compound in the experimental study, is higher at the beginning of the process and then slows down, being controlled by the nature of the intermediate oxidation products and by Fe(II)/Fe(III) molar ratio changing into the solution.

The photo-Fenton procedure, based on in situ Fe^{2+} catalyst generation, is simple but effective, combining the advantages of homogeneous and heterogeneous photo-Fenton processes.

Acknowledgements

Authors recognize financial support from the European Social Fund through POSDRU/89/1.5/S/54785 project: "Postdoctoral Program for Advanced Research in the Field of Nanomaterials".

References

- Assadi A., Eslami A., (2010), Comparison of phenol photodegradation by UV/ H_2O_2 and Photo-Fenton processes, *Environmental Engineering and Management Journal*, **9**, 807-812
- Du Y., Zhou M., Lei L., (2006), Role of the intermediates in the degradation of phenolic compounds by Fenton-like process, *Journal of Hazardous Materials*, **136**, 859-865.
- Duarte F., Madeira L.M., (2010), Fenton- and Photo-Fenton-Like Degradation of a Textile Dye by Heterogeneous Process with Fe/ZSM-5 Zeolite, *Separation Science and Technology*, **45**, 1512-1520.
- Feng J., Hu X., Yue P.L., (2005), Discoloration and mineralization of Orange II by using a bentonite clay-based Fe nanocomposite film as a heterogeneous photo-Fenton catalyst, *Water Research*, **39**, 89-96.
- Gogate P.R., Pandit A.B., (2004), A review of imperative technologies for wastewater treatment II: hybrid methods, *Advances in Environmental Research*, **8**, 553-597.
- He J., Ma W., Song W., Zhao J., Qian X., Zhang S., Yu J.C., (2005), Photoreaction of aromatic compounds at a- $\text{FeOOH}/\text{H}_2\text{O}$ interface in the presence of H_2O_2 : evidence for organic-goethite surface complex formation, *Water Research*, **39**, 119-128.
- Herney-Ramirez J., Vicente M.A., Madeira L.M., (2010), Heterogeneous photo-Fenton oxidation with pillared clay-based catalysts for wastewater treatment: A review, *Applied Catalysis B: Environmental*, **98**, 10-26.
- Kavitha V., Palanivelu K., (2004), The role of ferrous ion in Fenton and photo-Fenton processes for the degradation of phenol, *Chemosphere*, **55**, 1235-1243.
- Leland J.K., Bard A.J., (1987), Photochemistry of colloidal semiconducting iron oxide polymorphs, *Journal of Physical Chemistry*, **91**, 5076-5083.
- Li X.Y., Cui Y.H., Feng Y.J., Xie Z.M., Gu J.D., (2005), Reaction pathways and mechanisms of the electrochemical degradation of phenol on different electrodes, *Water Research*, **39**, 1972-1981.
- Moura F.C.C., Araujo M.H., Costa R.C.C., Fabris J.D., Ardisson J.D., Macedo W.A.A., Lago R.M., (2005), Efficient use of Fe metal as an electron transfer agent in a heterogeneous Fenton system based on $\text{Fe}^0/\text{Fe}_3\text{O}_4$ composites, *Chemosphere*, **60**, 1118-1123.
- Moura F.C.C., Oliveira G.C., Araujo M.H., Ardisson J.D., Macedo W.A.A., Lago R.M., (2006), Highly reactive species formed by interface reaction between Fe^0 -iron oxides particles: An efficient electron transfer system for environmental applications, *Applied Catalysis A: General*, **307**, 195-204.
- Nie Y., Hu C., Zhou L., Qu J., (2008), An efficient electron transfer at the Fe^0 /iron oxide interface for the photoassisted degradation of pollutants with H_2O_2 , *Applied Catalysis B: Environmental*, **82**, 151-156.
- Orbeci C., Untea I., Dancila M., Stefan D.S., (2010), Kinetics considerations concerning the oxidative degradation by Photo-Fenton process of some antibiotics, *Environmental Engineering and Management Journal*, **9**, 1-5.
- Ortiz de la Plata G.B., Alfano O.M., Cassano A.E., (2010), Decomposition of 2-chlorophenol employing goethite as Fenton catalyst. I. Proposal of a feasible, combined reaction scheme of heterogeneous and homogeneous reactions, *Applied Catalysis B: Environmental*, **95**, 1-13.
- Pera-Titus M., Garcia-Molina V., Banos M.A., Gimenez J., Esplugas S., (2004), Degradation of chlorophenols by means of advanced oxidation processes: a general review, *Applied Catalysis B: Environmental*, **47**, 219-256.
- Vinita M., Dorathi R.P.J., Palanivelu K., (2010), Degradation of 2,4,6-trichlorophenol by photo Fenton's like method using nano heterogeneous catalytic ferric ion, *Solar Energy*, **84**, 1613-1618.
- Wang H., Wang J., (2007), Electrochemical degradation of 4-chlorophenol using a novel Pd/C gas-diffusion electrode, *Applied Catalysis B-Environmental*, **77**, 58-65.
- Zazo J.A., Casas J.A., Mohedano A.F., Gilarranz M.A., Rodriguez J.J., (2005), Chemical Pathway and Kinetics of Phenol Oxidation by Fenton's Reagent, *Environmental Science and Technology*, **39**, 9295-9302.



Review

Effect of a modified photo-Fenton procedure on the oxidative degradation of antibiotics in aqueous solutions

Cristina Orbeci^{a,*}, Ion Untea^a, Gheorghe Nechifor^a, Adina Elena Segneanu^b, Mihaela Emanuela Craciun^a^a "Politehnica" University of Bucharest, Faculty of Applied Chemistry and Materials Science, 1-7 Gh. Polizu Street, 011061 Bucharest, Romania^b National Institute of Research and Development for Electrochemistry and Condensed Matter, 144 A.P. Podeanu Street, 300569 Timisoara, Romania

ARTICLE INFO

Article history:

Received 7 January 2013

Received in revised form 13 November 2013

Accepted 15 November 2013

Available online 23 November 2013

Keywords:

Photo-Fenton

In situ Fe²⁺ generation

Oxidation

Antibiotics

Ampicillin

Penicillin G

ABSTRACT

The aim of this study was to evaluate a modified photo-Fenton procedure as a suitable advanced oxidative process to degrade antibiotics in aqueous solutions. The classical photo-Fenton procedure was modified using a photo-catalytic reactor with continuous recirculation, which was equipped with a high pressure cylindrically shaped mercury lamp centrally and coaxially positioned and surrounded by iron mesh. The oxidation of the organic substrate could occur simultaneously through homogeneous and heterogeneous photocatalytic mechanisms due to Fe²⁺ ions from the solution and Fe⁰/Fe^{2+/3+} species formed on the surface of the iron mesh. The antibiotic degradation process was studied by monitoring the organic substrate concentration using chemical oxygen demand (COD), total organic carbon (TOC), high-performance liquid chromatography (HPLC) and Liquid chromatography coupled with mass spectrometry (LC-MS) analyses, in connection with monitoring the solution pH and the Fe^{2+/3+} concentration as function of the reaction time. During the oxidative process, the formation of iron oxy-hydroxyl species on the surface of the iron mesh and iron ionic species in the solution was observed. The efficiency of the antibiotics degradation, obtained using the modified photo-Fenton procedure is similar to that obtained through the classical photo-Fenton procedure. The advantage of this method is that it is a simple and inexpensive procedure. In addition, no additional materials with photo-catalytic activity are necessary for the procedure, and the initial pH of the solution no longer needs to be corrected.

© 2013 Elsevier B.V. All rights reserved.

Contents

| | |
|--|-----|
| 1. Introduction | 291 |
| 2. Materials and methods | 291 |
| 2.1. Materials | 291 |
| 2.2. The laboratory photocatalytic reactor | 292 |
| 2.3. The working procedure | 292 |
| 2.4. Analytical methods | 292 |
| 3. Results and discussion | 292 |
| 3.1. Efficiency of antibiotics oxidation through photo-Fenton like processes | 292 |
| 3.2. First stage of the oxidative process | 293 |
| 3.3. Second stage of the oxidative process | 294 |
| 3.4. Third stage of the oxidative process | 294 |
| 4. Conclusions | 296 |
| Acknowledgement | 296 |
| References | 296 |

* Corresponding author. Tel.: +40 721259875.

E-mail addresses: cristina27ccc@yahoo.com (C. Orbeci), i.untea@yahoo.com (I. Untea), doru.nechifor@yahoo.com (G. Nechifor), s_adinaelena@yahoo.com (A.E. Segneanu), me.craciun@gmail.com (M.E. Craciun).

1. Introduction

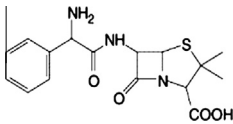
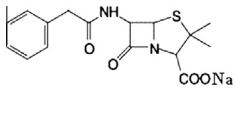
The extent to which antibiotics can be metabolised by human beings and animals is variable. Depending on the quantities of antibiotics used and their rates of excretion, antibiotics can be released into effluents and can reach sewage treatment plants [1–3]. Data available on antibiotics (from the ampicillin, erythromycin, tetracycline and penicilloyl groups) indicate their capability to exert toxic effects on living organisms, such as bacteria and algae, even at very low concentrations. These antibiotics are practically non-biodegradable and have the potential to survive sewage treatment, which leads to the persistence of these compounds in the environment and the potential for bio-accumulation [4]. The presence of antibiotics in the environment has favoured the emergence of antibiotic-resistant bacteria, increasing the possibility of infections, as well as the need to find new and more powerful antibiotics. As expected, antibiotic-contaminated water is incompatible with conventional biological water treatment technologies [5].

Antibiotics have the potential to affect the microbial community in sewage systems and can affect bacteria in the environment, there by disturbing the natural elemental cycles [3]. If the antibiotics are not eliminated during the purification process, they pass through the sewage system and may end up in the environment, primarily in the surface water. This outcome is of special importance because the surface water is a possible source of drinking water [6]. The degradation of the antibiotics by advanced oxidative processes has been demonstrate to be reasonably suited and quite feasible for application as a pretreatment method by combining it with the biological treatment [4]. The pretreatment of effluents containing penicillin by advanced oxidative processes based on O_3 and H_2O_2/O_3 did not completely remove the toxic procaine penicillin G from the effluents, which can lead to serious inhibition of the treatment of activated sludge [7]. One of the novel technologies for treating polluted sources of industrial wastewater and drinking water is the photo-Fenton process, in which hydroxyl radicals are generated in the presence of the H_2O_2 , Fe^{2+} catalyst and UV radiation.

Advanced oxidative processes of the Fenton and photo-Fenton type can be used for the degradation of antibiotics in wastewater [8] or for increasing their biodegradability in biological wastewater treatment [9]. Unlike the complete amoxicillin degradation, the mineralisation of the organic compounds from solution is not complete in the Fenton oxidative process, due to formation of refractory intermediates [10]. The degradation of amoxicillin by the photo-Fenton process that use the iron species as catalysts ($FeSO_4$ and a potassium ferrioxalate complex) and solar radiation reduces the bactericide effect of the amoxicillin but the toxicity may persist, due to the intermediates formed during the oxidative process. The toxicity decreases significantly when these intermediaries are converted to short chain carboxylic acids, which subsequently allows further conventional treatment [11]. The homogeneous photo-Fenton process is limited by its narrow working pH range (2.5–4) and requires the correction of the solution pH for iron precipitation and catalyst separation and recovery. Otherwise, high amounts of metal-containing sludge can be formed and the catalytic metals can be lost in this sludge. Due to these disadvantages, several attempts have been made to develop a heterogeneous photo-Fenton procedure by immobilising active iron species on solid supports. Because iron is relatively inexpensive and nontoxic, it has been widely used in various environmental treatment processes [12,13].

In the heterogeneous photo-Fenton process, various iron-containing catalysts can be used, such as iron bulk catalysts (iron oxy-hydroxyl compounds: hematite, goethite and magnetite) or iron-supported catalysts (zeolites, clays, bentonite, glass, active carbon and polymers) [13–15].

Table 1
Characteristics of antibiotics.

| Antibiotics | Ampicillin (AMP) | Penicillin G (PEN G) |
|------------------|---|---|
| Chemical formula | $C_{16}H_{19}N_3O_4S$ | $C_{16}H_{17}N_2O_4SNa$ |
| Molecular mass | 349.41 g/mol | 356.4 g/mol |
| Structure |  |  |

The heterogeneous photo-Fenton process requires that the catalyst have a high catalytic activity and a high stability in the reaction medium. At high concentrations of the iron-containing catalyst, an important decrease of the UV radiation effect may occur due to the turbidity (small particles are suspended in solution). A relevant fraction of the incident radiation can be lost via scattering; therefore, it is no longer available to induce the photo-Fenton process [12].

The pH of the reaction medium affects the photocatalytic performance (for pH values greater than 3 the oxidative efficiency decreases significantly) but it also affects the leaching of Fe from the support (for pH values less than 3 a higher amount of Fe is released into the solution) [12,14].

The advanced oxidative processes, or even the hybrid methods, may not be useful in degrading large quantities of effluent economically and it is therefore advisable to use these methods for reducing the toxicity of the pollutant stream to a certain level below which the biological oxidation can achieve the complete mineralisation of the biodegradable products [16].

The aim of this study was to evaluate a modified photo-Fenton procedure as a suitable advanced oxidative process to degrade certain antibiotics, such as ampicillin and penicillin G, in aqueous solutions.

The new proposed photo-Fenton procedure uses a photocatalytic reactor equipped with a high pressure mercury lamp and an iron mesh (cylindrically shaped, as well as centrally and coaxially positioned) as a precursor of active photocatalytic iron species.

2. Materials and methods

2.1. Materials

The antibiotics used in this work (Table 1) were ampicillin (AMP) and penicillin G (PEN G), in the form of crystalline powder

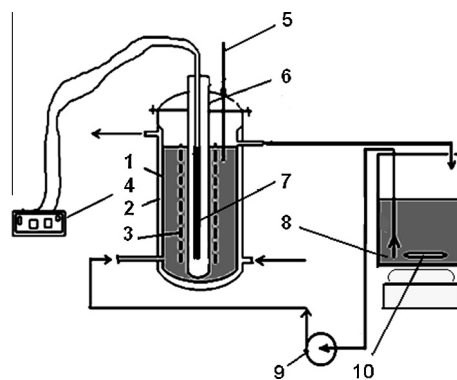


Fig. 1. Photo-Fenton procedure: diagram of work installation. (1–Photo-catalytic reactor; 2–Cooling jacket; 3–Iron mesh, cylindrical shape; 4–UV lamp source; 5–Thermometer; 6–Quartz tube; 7–UV lamp; 8–Recirculation reservoir; 9–Recirculation pump; 10–Magnetic stirrer).

of pharmaceutical grade. The hydrogen peroxide, a solution stock of 30% (w/w) was an analytical reagent from SC COMCHIM SA (Bucharest, RO). Other chemical substances used in this work were analytical reagents grade purchased from Aldrich.

2.2. The laboratory photocatalytic reactor

The classical photo-Fenton procedure was modified by the *in situ* generation of the $\text{Fe}^{2+/3+}$ catalyst using an annular photocatalytic reactor equipped with an iron mesh (cylindrically shaped, 70 mm in diameter, with a height of 350 mm, a wire thickness of 0.23 mm, 30 mesh/cm² and an initial mass of 25.2773 g) and a high pressure mercury lamp, of 120 W power, centrally and coaxially positioned (Fig. 1). The volume of the photocatalytic reactor was 1.5 L, the volume of the total solution 4.0 L and the recirculation flow rate was 1.5 L/min.

2.3. The working procedure

The experiments were performed at 30 ± 2 °C using synthetic solutions of 250 mg/L ampicillin (with an initial COD of 320 mg O₂/L and a TOC of 130.8 mg C/L) and 280 mg/L penicillin G (with an initial COD of 340 mg O₂/L and a TOC of 121.9 mg C/L). In each experiment, the initial concentration of the hydrogen peroxide was of 500 mg/L and the initial pH of the solution was not modified by adding other acidic compounds.

In the case of the classical photo-Fenton procedure, the comparative experimental data were obtained in the absence of the iron mesh and in the presence of the Fenton reagent (a solution of $\text{FeSO}_4 \cdot 7\text{H}_2\text{O}$ and H_2O_2). The experiments were performed for an initial solution pH of 3 ± 0.1 , a H_2O_2 concentration of 500 mg/L and a Fe^{2+} concentration of 0.8 mM.

The antibiotic degradation process was studied by monitoring the changes in the organic substrate concentration using chemical oxygen demand (COD), total organic carbon (TOC), high-performance liquid chromatography (HPLC) and liquid chromatography coupled with mass spectrometry (LC-MS) analyses, in connection with monitoring the solution pH and the $\text{Fe}^{2+/3+}$ concentration as function of the reaction time. The collected samples were stabilized using MnO_2 crystalline powder so that the unreacted H_2O_2 could quickly decompose, and then they were filtered. For the COD analysis, the samples were corrected in terms of the pH using a NaOH solution 40% (w/w) for the Fe ions precipitation, and then they were filtered.

2.4. Analytical methods

Chemical oxygen demand analyses (COD) were performed through a standard method (SR ISO 6060/1996) using a Digester

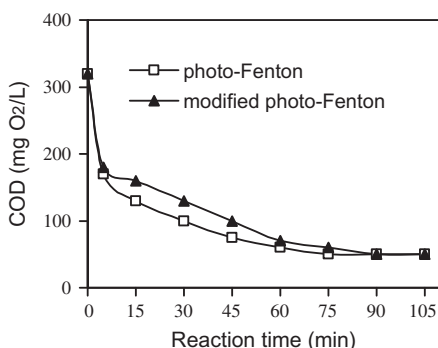


Fig. 2. The oxidative degradation of AMP through photo-Fenton like processes.

DK6. Total organic carbon (TOC) analyses were performed using a Multi N/C 2100 (Analytik Jena) TOC-analyzer.

High-performance liquid chromatography (HPLC) analyses were applied using an Ultimate 3000 “Diode Array” chromatograph, a UVD-3000 detector, a C18 Acclaim 120 DIONEX, and a LPG-3400A pump. The separation column used was C18 Acclaim 120 with a length of 250 mm and a 4 mm diameter. The working conditions were the following: a mobile phase of 0.0035 M H_2SO_4 , a column temperature of 40 °C, a flow rate of 0.6 mL/min, and a wavelength of 210 nm.

The acetic acid could be identified in the samples through comparing it with a HPLC chromatogram recorded for the standard sample of acetic acid.

Liquid chromatography, coupled with mass spectrometry (LC-MS) analyses were applied using an Agilent 1200 Series chromatograph equipped with an MS 6120 Quadrupole detector and an autosampler. The working conditions were the following: a mobile phase of acetonitrile/water = 10/90 (w/w), a column temperature of 25 °C, a flow rate of 1.25 mL/min, and an injection volume of 10 μL . Detection was performed in the MDC SIM, positive polarisation (MM-ADDI) and MM-ES APCI ionisation.

The oxalic acid could be identified in the samples through comparing it with a LC-MS chromatogram recorded for the standard sample of oxalic acid. The pH of the solution was measured using an ION check 10 pH-meter (Radiometer Analytical).

$\text{Fe}^{2+}/\text{Fe}^{3+}$ analyses were performed using spectrometric methods based on the spectral properties of the Fe(II) and Fe(III) complexes, using a Cecil CE 1011 series spectrophotometer. The Fe^{2+} concentration was determined at $\lambda = 510$ nm using an ortho-phenanthroline reagent, while the Fe^{3+} concentration was determined at $\lambda = 620$ nm using a tiron reagent.

3. Results and discussion

3.1. Efficiency of antibiotics oxidation through photo-Fenton like processes

Using the photocatalytic reactor presented in Fig. 1 and following the working procedure presented in subsection 2.3, comparative experimental data concerning the efficiency of the oxidative degradation of ampicillin and penicillin G antibiotics (Figs. 2 and 3) were obtained in the presence of an iron mesh (the modified photo-Fenton procedure) and in the absence of the iron mesh but in the presence of a Fenton reagent (the classical photo-Fenton procedure).

The first remark to be made is that in both cases there is a progressive and pronounced degradation of the antibiotics, certifying the oxidative efficiency of the photo-Fenton process.

Concerning the dependence of the COD values on time, notice that there is a difference between the two photo-Fenton proce-

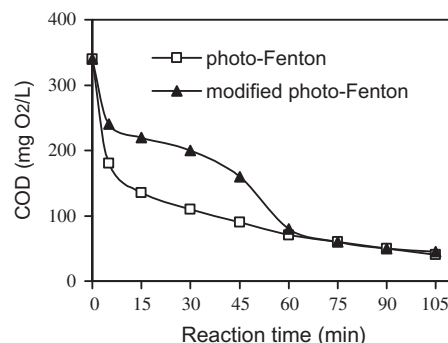


Fig. 3. The oxidative degradation of PEN G through photo-Fenton like processes.

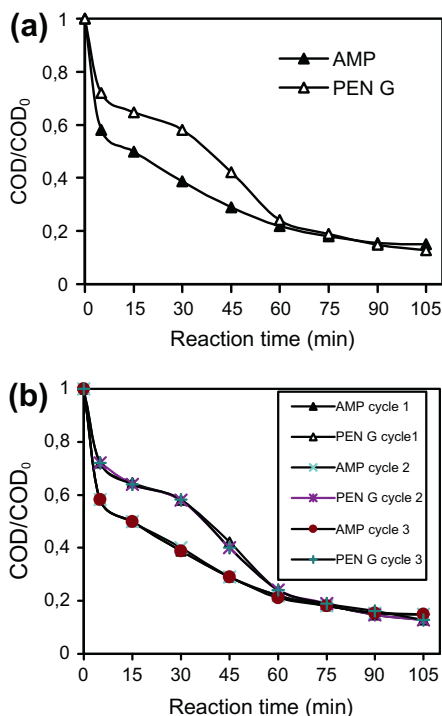


Fig. 4. (a) Kinetics data expressed as time dependence of COD/COD₀ values, (b) kinetics data expressed as time dependence of COD/COD₀ values (successive tests).

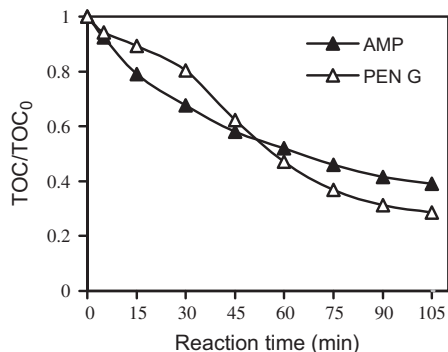


Fig. 5. Kinetics data expressed as time dependence of TOC/TOC₀ values.

dures regarding the rate of the antibiotics oxidation, especially for a reaction time interval of 10–60 min. Also, there is a higher oxidation rate in the case of the penicillin G (Fig. 3) than in the case of the ampicillin (Fig. 2). This suggests that, at least for this reaction time interval, different processes or mechanisms occur in the case of the modified photo-Fenton procedure and also, that they are influenced by the structure of the antibiotic.

Figs. 4a, b and 5 present the experimental data obtained in the case of the photo-Fenton procedure modified by the in situ generation of the Fe²⁺ catalyst and expressed as the influence of the reaction time and the structure of the antibiotic on the value of the COD/COD₀ and TOC/TOC₀ ratios.

In what concerns the antibiotics oxidation, Fig. 4b shows the kinetics data expressed as dependence of COD/COD₀ values on time, obtained in three successive stages of testing in identical conditions. They demonstrate the reproducibility of the analyses and the viability of the modified photo-Fenton procedure.

The overall oxidative process is relatively similar for the ampicillin and the penicillin G, involving three hypothetical successive stages.

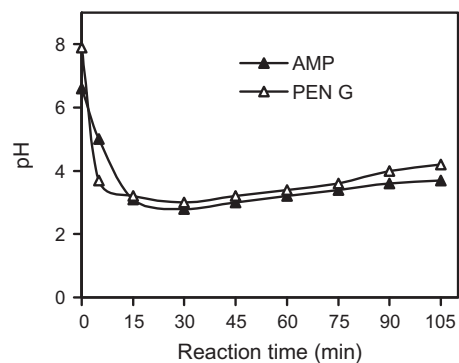


Fig. 6. pH values profile with time.

3.2. First stage of the oxidative process

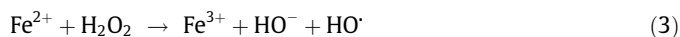
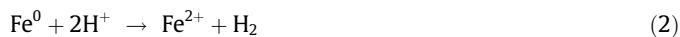
In the first stage (a reaction time interval of 0–10 min) the COD/COD₀ values show that the degradation process takes place with a high reaction rate for both antibiotics. The high oxidative rate for the ampicillin and the penicillin G in this stage may be explained by the presence of the HO[•] radicals formed by the direct photolysis of H₂O₂ in the presence of the UV radiation (Eq. (1)):



The COD/COD₀ and TOC/TOC₀ values have different slopes of degradation, as can be seen in Figs. 4 and 5.

The significant decrease in the value of the solution pH (Fig. 6) indicates the acidic nature of these compounds. The initial pH of the solution and its variation in time depends on the nature of the antibiotic. The penicillin G solution has a higher initial pH (pH = 7.9) as compared with the ampicillin solution (pH = 6.6). Penicillin G has one less amino group but it is in the form of a sodium salt and, therefore, it triggers a higher pH in aqueous solutions.

The acidic compounds formed through the oxidation of the antibiotics react with the Fe⁰ from the iron mesh (Eq. (2)) generating small amounts of Fe²⁺ in the aqueous phase, which acts as a main factor for the generation of hydroxyl radicals (Eq. (3)).



Due to the high oxidative potential of the reaction medium, Fe(II) and Fe(III) oxides and oxy-hydroxides species (FeO, Fe₂O₃, Fe₃O₄ and FeOOH) can be formed on the surface of the solid phase [13,15], which is represented by the iron mesh in our study.

Literature data [13] have recently shown that a composite structure based on a zero-valent iron with the iron oxide (Fe⁰/Fe₂O₃, Fe⁰/Fe₃O₄) has a high reactivity in the oxidative process applied to organic pollutants. Moreover, the scientific paper [15] has proved that the oxides and oxy-hydroxides such as α-Fe₂O₃, γ-Fe₂O₃, α-FeOOH, β-FeOOH and γ-FeOOH have photocatalytic properties and oxidize organic compounds.

The experimental data obtained by Nie et al. [13] indicate that the hydrogen peroxide functions as a driving force in the electron transfer from Fe²⁺ to Fe³⁺, while the degradation of the organic pollutants increases the electron transfer at the interface of Fe⁰/iron oxide due to their reaction with the hydroxyl radicals.

For the reaction time interval of 0–10 min, Fe(II) or Fe(III) ions were not detected in the reaction medium. As a consequence, the oxidative process in this stage may be due to the hydroxyl radicals formed by the H₂O₂ direct photolysis in the presence of the UV radiation, as well as to a photocatalytic effect of the Fe⁰/Fe(II, III)

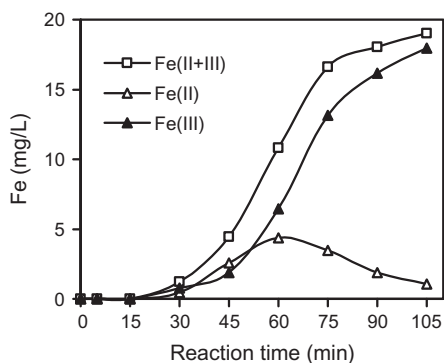


Fig. 7. Fe(II) and Fe(III) concentration profile with time (AMP).

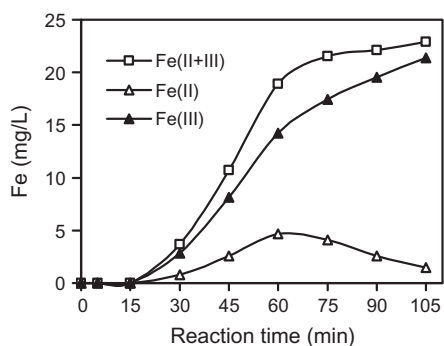


Fig. 8. Fe(II) and Fe(III) concentration profile with time (PEN G).

species formed on the surface of the iron mesh. In this stage the oxidation cannot take place through the homogeneous photocatalysis process, because the Fe^{2+} concentration in the reaction medium is practically zero and the value of the solution pH is greater than 4.

3.3. Second stage of the oxidative process

In the second stage (a reaction time interval of 10–60 min) the oxidative process takes place with a moderate reaction rate, and the oxidation efficiency for AMP is higher than PEN G (Fig. 4).

For a 10–30 min reaction time interval, the pH of the solution further decreases until it reaches a minimum value of approximately 3, which is the optimum value for the homogeneous photo-Fenton processes. Note that the pH of the penicillin G solution has a slightly higher value than the pH of the penicillin solution, and it is in correlation with the different efficiency of the oxidative process (Figs. 4 and 6).

In this stage, the Fe^{2+} and Fe^{3+} are formed in the reaction medium, being leached from the iron mesh. The concentration of the Fe^{2+} reaches a maximum value for 60 min reaction time then it tends to decrease by oxidation to Fe^{3+} . After 30 min reaction time, the total content of Fe in the solution increases significantly (Figs. 7 and 8).

The decrease in the COD and TOC values of the solution is associated with a partial mineralisation of the intermediate organic compounds formed in the first oxidative stage. The iron mesh plays a double role: it provides Fe^{2+} ions in the solution and acts as a heterogeneous photo-catalyst due to the $\text{Fe}^0/\text{Fe(II, III)}$ species formed on the surface.

As a consequence, the oxidation can take place both through homogeneous and heterogeneous photo-Fenton processes. The effective contribution of a heterogeneous or homogeneous photo-Fenton process is hard to measure, given that the Fe(II, III) species formed on the surface and the amount of Fe leached from the iron mesh vary with the reaction time. In the case of the heterogeneous photo-Fenton process, it is difficult to establish whether the degradation of the organic substrate is due to the oxidation through hydroxyl radicals (coming from the breakage of H_2O_2 catalyzed by the iron-supported catalysts) or through the Fe ions leached into the solution [12].

3.4. Third stage of the oxidative process

In the third stage (a reaction time of more than 60 min) the oxidative process occurs with a slow reaction rate probably due to the organic acids of a low molecular weight which are more resistant to the oxidative process. In the case of amoxicillin oxidation through the Fenton processes, some literature studies [10,11] have revealed that the mineralisation is not complete due to the formation of refractory intermediaries.

HPLC analyses of solution samples collected for a reaction time of 15 min and 90 min have revealed the presence of the acetic acid for both antibiotics (Table 2). A typical chromatogram is presented in Fig. 9. As can be seen in Table 2, for a greater reaction time (90 min), the amount of acetic acid formed in the solution is much greater than for a low reaction time (15 min). The formic acid has not been identified in the samples collected for a reaction time of 15 min or 90 min, for both ampicillin and penicillin G antibiotics.

LC-MS analyses of the solution samples collected at different reaction times have revealed the formation of several intermediate organic compounds whose concentration changes during the oxidative process. The oxalic acid has been identified with certainty for both ampicillin and penicillin G antibiotics at a retention time of approximately 0.39 min. In this respect, a typical chromatogram is presented in Fig. 10.

The typical peaks, recorded at higher retention times, can be attributed to organic acids with higher molecular weight, such as the malonic, maleic, succinic or muconic acids.

The formation of organic acids with a low molecular weight determines, on the one hand, an increase in the overall oxidative rate due to the higher concentration of the Fe^{2+} in the liquid phase, as a result of their leaching from the iron mesh. On the other hand, however, the presence of these acids in the liquid phase leads to a decrease of the overall efficiency of the oxidation, given their resistance to the oxidative process.

For a reaction time interval of 45–105 min, the pH of the solution increases gradually due to the disappearance of certain organic acids through complete mineralisation, as well as to the HO^-

Table 2
Characteristics of acid acetic peaks obtained through HPLC analysis.

| Sample | Reaction time (min) | Retention time (min) | Peak height (mAu) | Peak area (mAu min) |
|--------|---------------------|----------------------|-------------------|---------------------|
| AMP | 15 | 3.036 | 14.836 | 2.8129 |
| | 90 | 3.687 | 72.105 | 13.8454 |
| PEN G | 15 | 3.026 | 36.028 | 6.9354 |
| | 90 | 3.245 | 101.180 | 22.2613 |

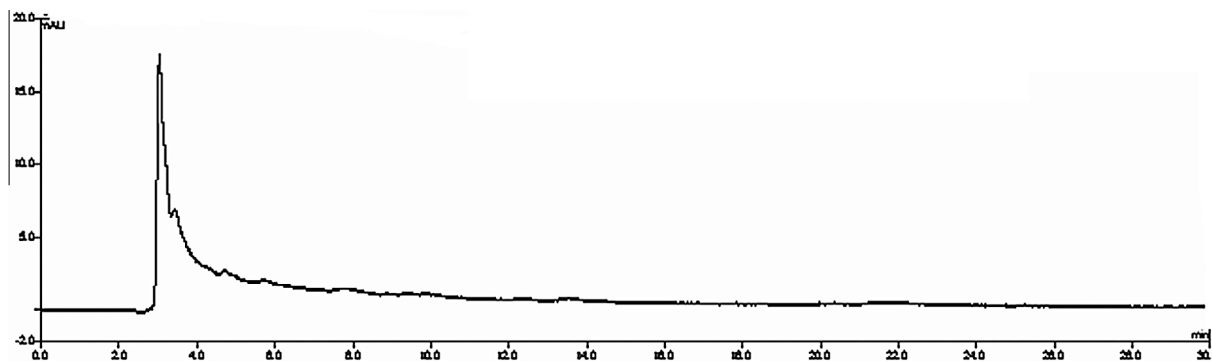


Fig. 9. HPLC analysis for acetic acid (AMP sample collected at 15 min reaction time).

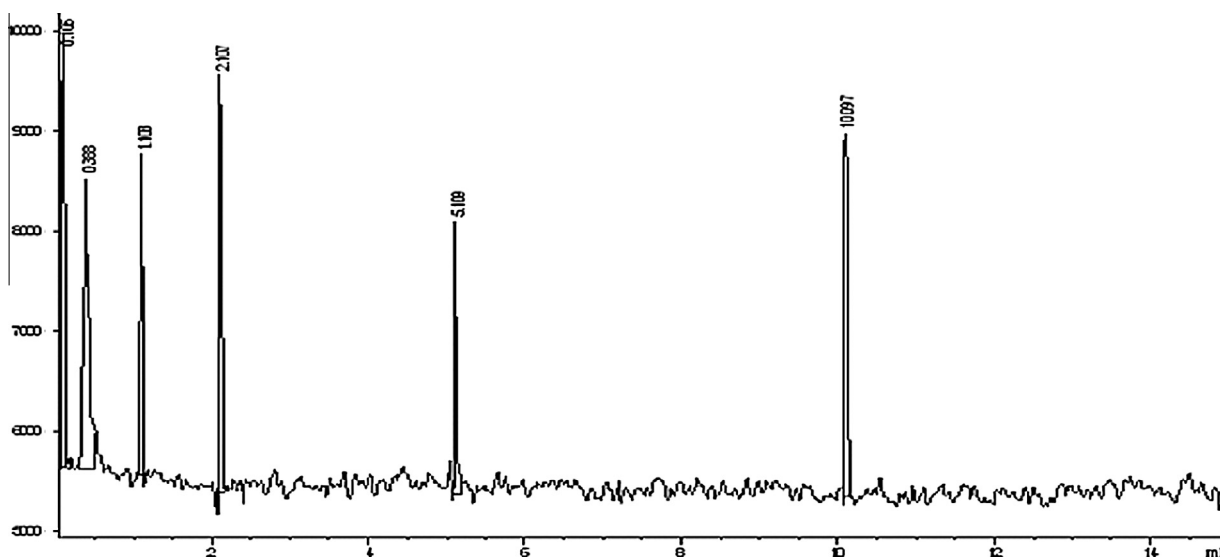


Fig. 10. LC-MS analysis for oxalic acid (AMP sample collected at 15 min reaction time).

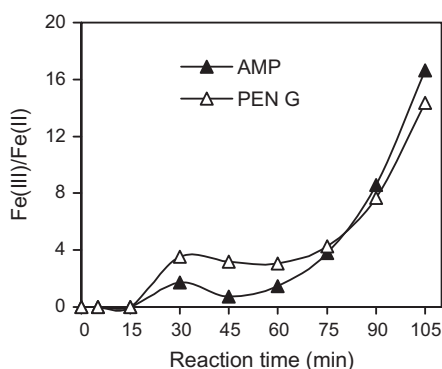


Fig. 11. Fe(III)/Fe(II) molar ratio function of reaction time.

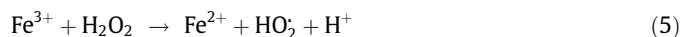
ions generated through the oxidation of Fe^{2+} to Fe^{3+} in the presence of H_2O_2 (Eq. (3)) and HO^\cdot radicals (Eq. (4)).



For the entire reaction time interval, the variation of the Fe(III)/Fe(II) molar ratio in the reaction medium is presented in Fig. 11.

The Fe^{2+} oxidation to Fe^{3+} according to reactions (3) and (4) is the main cause for the increase in the molar ratio Fe(III)/Fe(II) for a reaction time greater than 60 min. As a result, the decrease in

the oxidation rate for a higher reaction time may be explained by the progressive disappearance of the Fe^{2+} from the solution. In the presence of the UV radiation and the hydrogen peroxide, the ferric ion generated in reaction (3) is reduced to a ferrous ion (Eq. (5)):



Given that the rate of reaction (5) is much slower than the rate of reaction (3), the ferrous ions are quickly consumed, but slowly regenerated. As a consequence, the oxidative process slows down due to the low concentration of the ferrous ions.

Controlling the excessive increase in the concentration of Fe ions in the reaction medium may be done by changing the characteristics of the iron mesh (the initial mass, the height and diameter of the cylinder, the thickness of the wire or the mesh size), and by limiting the recirculation flow rate and the reaction time.

The advantage of the new photo-Fenton procedure is that, in the reaction medium, no additional substances or materials with photocatalytic activity are necessary and the initial pH of the solution no longer needs to be corrected.

Even if the oxidation of the ampicillin and the penicillin G does not completely occur in a reasonable reaction time, their toxicity and bactericidal effect may be greatly reduced through converting them to short chain carboxylic acids [11].

The experimental data, obtained through the oxidative degradation of ampicillin and penicillin G type antibiotics from water using

the photo-Fenton process modified by the in situ generation of the Fe^{2+} catalyst, certify that this procedure may be used as a feasible process to be applied as a pre-treatment method by combining it with the biological treatment.

4. Conclusions

The oxidative degradation of ampicillin and penicillin G type antibiotics from water using the photo-Fenton procedure modified by the in situ generation of the Fe^{2+} catalyst occurs following three hypothetical successive stages.

In the first oxidation stage (a reaction time interval of 0–10 min) the degradation process takes place with a high reaction rate due to the hydroxyl radicals formed by the direct photolysis of H_2O_2 in the presence of the UV radiation and to a photocatalytic effect of the $\text{Fe}^0/\text{Fe(II, III)}$ species formed on the surface of the iron mesh.

In the second stage (a reaction time interval of 10–60 min), the oxidative process takes place with a moderate reaction rate. In this stage, the Fe^{2+} and Fe^{3+} are formed in the reaction medium, being leached from the iron mesh due to the acidic compounds from the solution. The oxidative process is controlled by the hydroxyl radicals as a result of the photocatalytic effect of the $\text{Fe}^0/\text{Fe(II, III)}$ species formed on the surface of the iron mesh (homogeneous photo-Fenton process) and the photocatalytic effect of the Fe^{2+} leached into the solution (homogeneous photo-Fenton process).

In the third stage (a reaction time of more than 60 min) the oxidative process takes place with a slow reaction rate due to the organic acids of a low molecular weight (such as the oxalic and acetic acids) which are more resistant to the oxidative process and also due to the progressive disappearance of the Fe^{2+} catalyst from the solution.

The efficiency of the degradation of ampicillin and penicillin G antibiotics obtained using the photo-Fenton procedure modified by the in situ generation of the Fe^{2+} catalyst is relatively similar to that obtained through the classical photo-Fenton procedure. The advantage of the new procedure is that it is simple and cheap. Moreover, no additional substances or materials with photocatalytic activity are necessary, and the initial pH of the solution no longer needs to be corrected.

Acknowledgement

Authors recognize financial support from the European Social Fund through POSDRU/89/1.5/S/54785 project: “Postdoctoral Program for Advanced Research in the field of Nanomaterials”.

References

- [1] R. Alexy, T. Kumpel, K. Kümmerer, Assessment of degradation of 18 antibiotics in the closed bottle test, *Chemosphere* 57 (2004) 505–512.
- [2] J.P. Bound, N. Voulvoulis, Pharmaceuticals in the aquatic environment – a comparison of risk assessment strategies, *Chemosphere* 56 (2004) 1143–1155.
- [3] K. Kümmerer, Antibiotics in the aquatic environment – a review – Part I, *Chemosphere* 75 (2009) 417–434.
- [4] I. Arslan-Alaton, S. Dogruel, E. Baykal, G. Gerone, Combined chemical and biological oxidation of penicillin formulation effluent, *J. Environ. Manage.* 73 (2) (2004) 155–163.
- [5] O. Rozas, D. Contreras, M.A. Mondaca, M. Pérez-Moya, H.D. Mansilla, Experimental design of Fenton and photo-Fenton reactions for the treatment of ampicillin solutions, *J. Hazard. Mater.* 177 (2010) 1025–1030.
- [6] S. Kaniou, K. Pitarakis, I. Barlagianni, I. Poullos, Photocatalytic oxidation of sulfamethazine, *Chemosphere* 60 (2005) 372–380.
- [7] I. Arslan-Alaton, A.E. Caglayan, Toxicity and biodegradability assessment of raw and ozonated procaine penicillin G formulation effluent, *Ecotoxicol. Environ. Saf.* 63 (2006) 131–140.
- [8] C. Orbeci, I. Untea, M. Dancila, D.S. Stefan, Kinetics considerations concerning the oxidative degradation by photo-Fenton process of some antibiotics, *Environ. Eng. Manage. J.* 9 (1) (2010) 1–5.
- [9] E. Elmolla, M. Chaudhuri, Degradation of the antibiotics amoxicillin, ampicillin and cloxacillin in aqueous solution by photo-Fenton process, *J. Hazard. Mater.* 172 (2009) 1476–1481.
- [10] F. Ay, F. Kargi, Advanced oxidation of amoxicillin by Fenton' reagent treatment, *J. Hazard. Mater.* 179 (2010) 622–627.
- [11] A.G. Trovó, R.F.P. Nogueira, A. Agüera, A.R. Fernandez-Alba, S. Malato, Degradation of the antibiotic amoxicillin by photo-Fenton process – chemical and toxicological assessment, *Water Res.* 45 (2011) 1394–1402.
- [12] J. Herney-Ramirez, M.A. Vicente, L.M. Madeira, Heterogeneous photo-Fenton oxidation with pillared clay-based catalysts for wastewater treatment: a review, *Appl. Catal. B – Environ.* 98 (2010) 10–26.
- [13] Y. Nie, C. Hu, L. Zhou, J. Qu, An efficient electron transfer at the $\text{Fe}^0/\text{iron oxide}$ interface for the photoassisted degradation of pollutants with H_2O_2 , *Appl. Catal. B – Environ.* 82 (2008) 151–156.
- [14] J. Feng, X. Hu, P.L. Yue, Discoloration and mineralization of Orange II by using a bentonite clay-based Fe nanocomposite film as a heterogeneous photo-Fenton catalyst, *Water Res.* 39 (2005) 89–96.
- [15] J. Chun, H. Lee, S.H. Lee, S.W. Hong, J. Lee, C. Lee, J. Lee, Magnetite/mesocellular carbon foam as a magnetically recoverable Fenton catalyst for removal of phenol and arsenic, *Chemosphere* 89 (2012) 1230–1237.
- [16] P.R. Gogate, A.B. Pandit, A review of imperative technologies for wastewater treatment II: hybrid methods, *Adv. Environ. Res.* 8 (2004) 553–597.

Biomass Extraction Methods

Adina-Elena Segneanu, Florentina Cziplu, Paulina Vlazan,
Paula Sfirloaga, Ioan Grozescu and Vasile Daniel Gherman

Additional information is available at the end of the chapter

<http://dx.doi.org/10.5772/55338>

1. Introduction

Biomass represents an extremely valuable potential to obtain new clean energy sources and natural structurally complex bioactive compounds. Renewable energy can be produced from any biological feedstock, that contains appreciable amounts of sugar or materials that can be converted into sugar (e.g. starch or cellulose). Lignocellulose's biomass—dendromass and phytomass is natural based material consisting of complex of heterogenic macromolecules with cell structure (celluloses, hemicelluloses and lignin) as well as numerous organic and inorganic structures with low molecule weight (Sun, 2002).

Long-term economic and environmental concerns have resulted in a great amount of research in the past couple of decades on renewable sources of liquid fuels to replace fossil fuels. Producing of cellulose and alcohol from biomass is important technological process. Conversion of abundant lignocellulosic biomass to biofuels as transportation fuels presents a viable option for improving energy security and reducing greenhouse emissions. Lignocellulosic materials such as agricultural residues (e.g., wheat straw, sugarcane bagasse, corn stover), forest products (hardwood and softwood), and dedicated crops (switchgrass, salix) are renewable sources of energy. These raw materials are sufficiently abundant and generate very low net greenhouse emissions. The use of biomass with low economic value, the waste from agriculture, forestry and wild flora as sources of clean energy, is a viable way to avoid potential conflicts with the biomass production for food, which represent the main concern of UE regarding the biofuels production from biomass.

The presence of lignin in lignocelluloses leads to a protective barrier that prevents plant cell destruction by fungi and bacteria for conversion to fuel. For the conversion of biomass to fuel, the cellulose and hemicellulose must be broken. The digestibility of cellulose present in lignocellulosic biomass is hindered by many physicochemical, structural, and compositional factors. The lignocellulosic biomasses need to be treated prior to fuel production to expose

cellulose. In present, there is many different type of pretreatment of lignocelluloses materials. Pretreatment uses various techniques, including ammonia fiber explosion, chemical treatment, biological treatment, and steam explosion, to alter the structure of cellulosic biomass to make cellulose more accessible. The purpose of the pretreatment is to remove lignin and hemicellulose, reduce cellulose crystallinity, and increase the porosity of the materials. Then, acids or enzymes can be used to break down the cellulose into its constituent sugars. Enzyme hydrolysis is widely used to break down cellulose into its constituent sugars. Pretreatment can be the most expensive process in biomass-to-fuels conversion but it has great potential for improvements in efficiency and lowering of costs through further research and development. Cellulose chains can also be broken down into individual glucose sugar molecules by enzymes known as cellulase. Cellulase refers to a class of enzymes produced by fungi, bacteria, and protozoans that catalyze the hydrolysis of cellulose. But, one of the main drawn back of convention chemical methods used in ethanol formation process is degradation of carbohydrates and formation of undesirable by-products, which severely inhibition of ethanol during the fermentation process: furfural, 5-hydroxymethylfurfural, uronic acid, levulinic acid, acetic acid, formic acid, hydroxybenzoic acid, vanillin, phenol, cinnamaldehyde, formaldehyde, and so (Nenkova et.al., 2011). Some inhibitors such as terpene compounds are present in the biomass–dendromass.

Lignin is a complex reticulated phenolic polymer that occurs in xylem of most terrestrial plants and is the second most abundant biopolymer in nature, corresponding to around 30% of the biosphere organic carbon. This macromolecule is one of the biggest wood components and also one of the most important. Even the lignin has a significant role in technology, in the bioethanol production process valuable chemical properties and functions from lignin and hemicelluloses are not fully recovery, the black liquor result from process being using specially for energy recovery. About half of wood components are dissolved into this black liquor. The dissolved organic compounds consist mainly in degraded lignin and also hemicelluloses and cellulose degradation products. Also, phenols derived from biomass are valuable and useful chemicals, due to their pharmacological properties including antiviral inhibitor (anti-HIV). These compounds with good antioxidant activity can be used to preserve food from lipid peroxidation and oxidative damage occurring in living systems (Martínez et.al., 1996; Mahugo Santana et.al., 2009; Nenkova, et.al.2011). Antioxidants can also prevent the loss of food color, flavor and active vitamins content, providing the stabilization of the molecules involved in such characteristics. They can also be used for the production of adhesives and for the synthesis of polymer.

It is well known that, biomass also contains many other natural products: waxes and fatty acids, polyacetylenes, terpenoids (e.g., monoterpenoids, iridoids, sesquiterpenoids, diterpenoids, triterpenoids), steroids, essential oils, phenolics, flavonoids, tannins, anthocyanins, quinones, coumarins, lignans, alkaloids, and glycosidic derivatives (e.g., saponins, glycosides, flavonoid glycosides) (Alonso et.al., 1998; Japón-Luján et.al., 2006; Faustino, 2010; Fang et.al., 2009; Gallo, 2010; Carro, 1997; Kojima, 2004). In this regards, are needed more studies to recover these important compounds from biomass for use in pharmaceutical industry, food industry, and so.

2. Extraction techniques

Actually, there are known many different techniques used for biomass extraction: liquid-solid extraction, liquid-liquid extraction, partitioning, acid-base extractions, ultrasound extraction (UE), microwave assisted extraction (MAE). The capability of a number of extraction techniques have been investigated, such as solvent extraction (J.A. Saunders, D.E. Blume, 1981) and enzyme-assisted extraction (B.B. Li, B. Smith, M.M. Hossain, 2006). However, these extraction methods have drawbacks to some degree.

The choice of extraction procedure depends on the nature of the natural material and the components to be isolated. The main conventional extraction procedures are liquid-liquid extraction and liquid-solid extraction. For liquid-liquid extraction is using two different solvents, one of which is always water, (water-dichloromethane, water-hexane, and so). Some of the disadvantages of this method are: cost, toxicity and flammability (Kaufmann 2002; McCabe, 1956; Perry, 1988; Sarker et. al., 2006).

Solid-phase extraction (SPE) can be used to isolate analytes dissolved or suspended in a liquid mixture are separated from a wide variety of matrices according to their physical and chemical properties. Conventional methods include: soxhlet extraction, maceration, percolation, extraction under reflux and steam distillation, turbo-extraction (high speed mixing) and sonication. Although these techniques are widely used, have several shortcomings: are very often time-consuming and require relatively large quantities of polluting solvents, the influence of temperature which can lead to the degradation of thermo labile metabolites (Kaufmann 2002; McCabe, 1956; Sarker et. al., 2006; Routray, 2012).

Supercritical fluid extraction (SFE), microwave-assisted extraction (MAE) and pressurised solvent extraction (PSE) are fast and efficient unconventional extraction methods developed for extracting analytes from solid matrixes.

2.1. Supercritical fluid extraction

Supercritical fluid extraction (SFE) is one of the relatively new efficient separation method for the extraction of essential oils from different plant materials. The new products, extracts, can be used as

a good base for the production of pharmaceutical drugs and additives in the perfume, cosmetic, and food industries. Use of SFE under different conditions can allow selecting the extraction of different constituents. The main reason for the interest in SFE was the possibility of carrying out extractions at

temperature near to ambient, thus preventing the substance of interest from incurring in thermal denaturation.

Supercritical fluid extraction has proved effective in the separation of essential oils and its derivatives for use in the food, cosmetics, pharmaceutical and other related industries, producing high-quality essential oils with commercially more satisfactory compositions

(lower monoterpenes) than obtained with conventional hydro-distillation (Ehlers et al., 2001; Diaz-Maroto et al., 2002; Ozer et al., 1996). Also, extraction with supercritical fluids requires higher investment but can be highly selective and more suitable for food products. This plays a mechanistic role in supercritical fluid chromatography (SFC), where it contributes to the separation of the solutes that are injected into the chromatographic system.

Supercritical fluid extraction is an interesting technique for the extraction of flavouring compounds from vegetable material. It can constitute an industrial alternative to solvent extraction and steam distillation processes (Stahl, E. and Gerard, D. 1985). SFE allows a continuous modification of solvent power and selectivity by changing the solvent density (Nykanen, I. et al., 1991). Nevertheless, the simple SFE process, consisting of supercritical CO₂ extraction and a one-stage subcritical separation, in many cases does not allow a selective extraction because of the simultaneous extraction of many unwanted compounds.

2.2. Ultrasound-assisted solvent extraction

Ultrasound assisted extraction is very efficient extraction procedure. Sonication induces cavitation, the process in which bubbles with a negative pressure are formed, grown, oscillated, and may split and implode. By this process different chemical compounds and particles can be removed from the matrix surface by the shock waves generated when the cavitation bubbles collapse. The implosion of the cavities creates microenvironments with high temperatures and pressures. Shock waves and powerful liquid micro jets generated by collapsing cavitation bubbles near or at the surface of the sample accelerate the extraction (R. Kellner et al., 2004). Ultrasonic assisted extraction has many advantages since it can be used for both liquid and solid samples, and for the extraction of either inorganic or organic compounds (S.L. Harper et al., 1983). If extracted from solid samples, different problems can occur: there is a possibility of the decomposition of the analyte which could be trapped inside of the collapsing cavitation bubbles. The ultrasound extraction system can be also applied as a dynamic system in which the analytes are removed as soon as they are transferred from the solid matrix to the solvent. In this process, furthermore, the sample is continuously exposed to the solvent (I. Rezić' et al., 2008).

This is a modified maceration method where the extraction is facilitated by the use of ultrasound (high-frequency pulses, 20 kHz). Ultrasound is used to induce a mechanical stress on the cells of biomass solid samples through the production of cavitations in the sample. The cellular breakdown increases the solubilization of metabolites in the solvent and improves extraction yields. The efficiency of the extraction depends on the instrument frequency, and length and temperature of sonication. Ultrasonification is rarely applied to large-scale extraction; it is mostly used for the initial extraction of a small amount of material. It is commonly applied to facilitate the extraction of intracellular metabolites from plant cell cultures (Kaufmann, 2002; Sarker, 2006).

2.3. Pressurized Solvent Extraction (PSE)

Pressurized solvent extraction or “accelerated solvent extraction,” employs temperatures that are higher than those used in other methods of extraction, and requires high pressures to maintain the solvent in a liquid state at high temperatures. It is best suited for the rapid and reproducible initial extraction of a number of samples. The solid biomass sample is loaded into an extraction cell, which is placed in an oven. The solvent is then pumped from a reservoir to fill the cell, which is heated and pressurized at programmed levels for a set period of time. The cell is flushed with nitrogen gas, and the extract, which is automatically filtered, is collected in a flask. Fresh solvent is used to rinse the cell and to solubilize the remaining components. A final purge with nitrogen gas is performed to dry the material. High temperatures and pressures increase the penetration of solvent into the material and improve metabolite solubilization, enhancing extraction speed and yield. Moreover, with low solvent requirements, pressurized solvent extraction offers a more economical and environment-friendly alternative to conventional approaches

As the material is dried thoroughly after extraction, it is possible to perform repeated extractions with the same solvent or successive extractions with solvents of increasing polarity. An additional advantage is that the technique can be programmable, which will offer increased reproducibility. However, variable factors, e.g., the optimal extraction temperature, extraction time, and most suitable solvent, have to be determined for each sample (Kaufmann, 2002; Tsubaki, 2010; Sarker, 2006).

Microwave-assisted extraction (MAE) or simply microwave extraction is a relatively new extraction technique that combines microwave and traditional solvent extraction. The microwave energy has been investigated and widely applied in analytical chemistry to accelerate sample digestion, to extract analytes from matrices and in chemical reactions. Application of microwaves for heating the solvents and plant tissues in extraction process, which increases the kinetic of extraction, is called microwave-assisted extraction. Microwave energy is a non-ionizing radiation that causes molecular motion by migration of ions and rotation of dipoles, without changing the molecular structures if the temperature is not too high. Nonpolar solvents, such as hexane and toluene, are not affected by microwave energy and, therefore, it is necessary to add polar additives. Microwave-assisted extraction (MAE) is an efficient extraction technique for solid samples which is applicable to thermally stable compounds accepted as a potential and powerful alternative to conventional extraction techniques in the extraction of organic compounds from materials. The microwave-assisted extraction technique offers some advantages over conventional extraction methods.

Compared to conventional solvent extraction methods, the microwave-assisted extraction (MAE) technique offers advantages such as improved stability of products and marker compounds, increased purity of crude extracts, the possibility to use less toxic solvents, reduced processing costs, reduced energy and solvent consumption, increased recovery and purity of marker compounds, and very rapid extraction rates.

The use of MAE in natural products extraction started in the late 1980s, and through the technological developments, it has now become one of the popular and cost-effective

extraction methods available today, and several advanced MAE instrumentations and methodologies have become available, e.g., pressurized microwave-assisted extraction (PMAE) and solvent-free microwave-assisted extraction (SFMAE).

Comparison between conventional and MAE extraction method

This technique has been used successfully for separation of phenolic compounds from types of biomass, polyphenols derivatives, pyrimidine glycosides, alkaloids, terpenes, and so.

In most cases, the results obtained suggested that the microwave assisted method was more convenient even compared to the ultrasound extraction method.

Pyrimidine glycosides

The studies regarding the microwave extraction of vicine and convicine (toxic pyrimidine glycosides) from *Vicia faba* using a methanol: water mixture (1:1 v/v) involves two successive microwave irradiations (30 s each) with a cooling step in between. No degradation could be observed under these conditions, but further irradiation was found to decrease the yield of vicine and convicine. The yield obtained was 20% higher than with the conventional Soxhlet extraction method.

Alkaloids Sparteine, a lupine alkaloid, was extracted from *Lupinus mutabilis*, with methanol: acetic acid (99:1, v/v) in a common microwave oven and the microwave irradiation program used one to five cycles of 30 s with a cooling step in between and conduct to 20% more sparteine than was obtained with a shaken-flask extraction using the same solvent mixture for 20 min.

Terpenes Five terpenic compounds: linalool, terpineol, citronellol, nerol and geraniol, associated with grape (*Vitis vinifera*) aroma, was extracted from must samples by MAE (Carro et al., 1997). Was investigated the influence of the parameters: extracting solvent volume, extraction temperature, and amount of sample and extraction time. Several conditions were fixed, such as the extraction time (10 min) and the applied power (475 W). The solvent volume appeared to be the only statistically significant factor, but was limited to 15 mL by the cell size. The highest extraction yield was obtained with both the solvent volume and the temperature at their maximum tested values. In contrast, the sample amount had to be minimized in order to obtain the best recoveries. The final optimized extraction conditions were as follows: 5 mL sample amounts extracted with 10 mL of dichloromethane at a temperature of 90°C for 10 min with the microwave power set at 50% (475 W).

Steroids Recently, was demonstrated that only 30–40 s were sufficient to extract ergosterol quantitatively by MAE using 2 mL methanol and 0.5 mL 2 M sodium hydroxide. Microwave irradiation was applied at 375W for 35 s and the samples were cooled for 15 min before neutralization with 1 M hydrochloric acid followed by pentane extraction. The yield was similar to or even higher than that obtained with the traditional methanolic extraction followed by alkaline saponification and pentane extraction.

Alkaloids The extraction of two alkaloids cocaine and benzoylecgonine by focused MAE was optimized by taking into account several parameters such as the nature of the extracting solvent, particle size distribution, sample moisture, applied microwave power and radiation time. MAE was found to generate similar extracts to those obtained by conventional SLE but in a more efficient manner. Indeed, 30s were sufficient to extract cocaine quantitatively from leaves, using methanol as solvent and a microwave power of 125 W. (Kaufmann, 2002).

Phenolic compounds

In recent years, synthetic antioxidants were reported to have the adverse effects such as toxicity and carcinogenicity and this situation has forced scientists to search for new natural antioxidants from herbs or the other materials. Phenolic compounds, the most important bioactive compounds from plant sources, are among the most potent and therapeutically useful bioactive substances, providing health benefits associated with reduced risk of chronic and degenerative disease (Luthria, 2006; Tsubaki et al., 2010; Proestos, 2008).

Extraction is one of the most imperative steps in the evaluation of phenolic compounds from plant. Often is done a saponification prior to the extraction step because is necessary to cleave the ester linkage to the cell walls (Robbins, 2003).

The capability of a number of extraction techniques have been investigated, such as solvent extraction and enzyme-assisted extraction. However, these extraction methods have drawbacks to some degree. For example, solvent extraction is time consuming and enzyme in enzyme assisted extraction is easy to denature. In the case of Soxhlet extraction, the extraction time vary from 1 minute to 6 h. Ultrasonic is one of the most industrially used methods to enhance mass transfer phenomena (Japón-Luján et.al. 2006; Luthria, 2006; Pérez-Serradilla, 2007). Meanwhile, microwave assisted extraction heats the extracts quickly and significantly accelerates the extraction process (Martínez, 1996; Kojima, 2004; Patsias, 2009). Simultaneous ultrasonic/microwave assisted extraction (UMAE) coupled the advantage of microwave and ultrasonic, presenting many advantages (Kojima, 2004).

Extraction of phenolic compounds from solid samples is usually carried out by stirring (Luthria, 2006; Nepote, 2005), although the use of auxiliary energies has demonstrated to accelerate the process (Japón-Luján, et.al.2006; Pérez-Serradilla, 2007). Microwave-assisted extraction (MAE) is the process by which microwave energy is used to heat polar solvents in contact with solid samples and to partition compounds of interest between the sample and the solvent, reducing both extraction time and solvent consumption.

The conventional liquid–solid extraction techniques, such as heat reflux extraction (HRE), ultrasonic extraction (UE) and maceration extraction (ME), are discommodious, laborious, time-consuming and require large volumes of toxic organic solvents. So increasing attention is paid to the development of more efficient extraction methods for the rapid extraction of active compounds from materials.

The current analytical methods used to extract phenolic compounds from liquid samples are based on *liquid-liquid extraction* (LLE). Although this technique offers efficient and precise results, it is relatively time-consuming, possibly harmful due the use of large volume of organic solvents (frequently toxic) and highly expensive. For these reasons, there is an increasing tendency to replace LLE by solid-phase extraction (SPE) for liquid samples. SPE was developed in the 1980s, and has emerged as a powerful tool for chemical isolation and purification. This methodology is an alternative extraction to LLE due to it reduces organic solvents consumption, the length of analysis and it can be automated (Martínez, et. al., 1996; Kojima, 2004; Patsias, et.al., 2009).

Although most attention has been focused on the determination of phenolic compounds in aqueous samples, more substituted phenols, such as pentachlorophenol, show limited transport in water and they are more likely absorbed in sediments and soils. This fact contributes to the persistent of these compounds in the environment and it results in high concentrations of them that could affect aquatic and earth organism. For extraction, Soxhlet extraction is one of the most popular techniques for isolating phenolic compounds from solid samples, due to its simplicity, inexpensive extraction apparatus. Despite the good results obtained with this methodology, Soxhlet extraction makes the analysis procedure excessive time consuming. Moreover, it requires large amount of hazardous organic solvents.

Ultrasonic extraction is another conventional technique to extract analytes from solid samples. Although sonication is faster than Soxhlet extraction, it also requires large volumes of toxic and expensive organic solvents.

The studies show that the compounds are extracted more effectively when the energy provided by microwave is employed (Perez-Serradilla, 2011).

3. Experimental studies

The efficiencies of different solvents (water, acid and alcohol) in the extraction of caffeine and phenols from leaves of white, black, green and red tea in different solvents: ethanol, isopropanol, methanol and water. Extraction was performed comparative by ultrasonic and by MAE. Determination of the total amount of phenolic compounds was studied comparative using different extraction times 5, 15 and respectively 30 minutes. The microwave irradiation shortens time necessary to extract phenols and caffeine from tea samples (between 30 and 50 seconds). The results of the comparison investigation are presented in the figure 1.

4. Conclusion

Chromatographic determination of phenolic compounds isolated from the tea samples by ultrasonic and MAE extraction is comparable. The difference between the two methods of extraction consists in extraction time and amount of solvents used. Also, the yield for MAE was about 20% is 20% higher than that of the ultrasonic extraction.

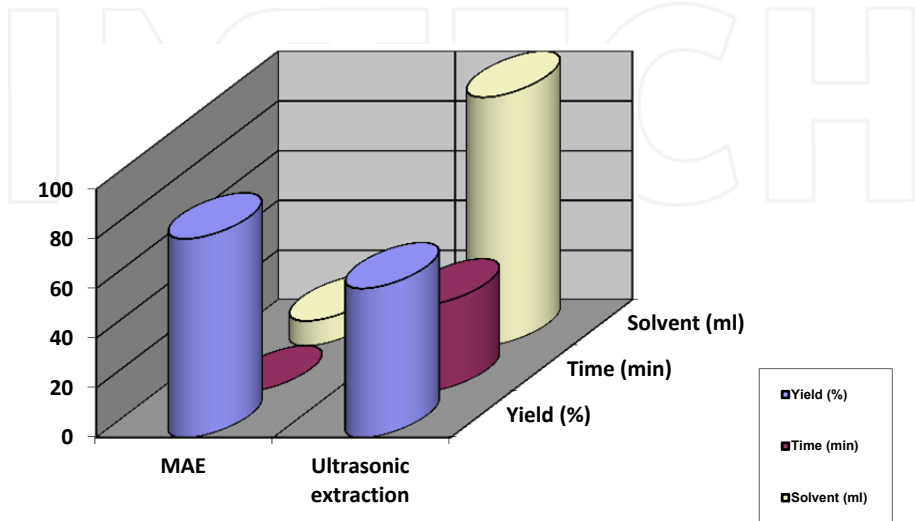


Figure 1. Comparison between the two extraction methods

Author details

Adina-Elena Segneanu, Paulina Vlazan,
Paula Sfirloaga and Ioan Grozescu

*National Institute of Research and Development for Electrochemistry and Condensed Matter –
INCENM Timisoara, Romania*

Florentina Czipl

Eftimie Murgu University, Resita, Romania

Vasile Daniel Gherman

Politehnica University of Timisoara, Romania

5. References

- Alonso M.C., Puig D., Silgoner I., Grasserbauer M., Barcelo' D., (1998), Determination of priority phenolic compounds in soil samples by various extraction methods followed by liquid chromatography–atmospheric pressure chemical ionisation mass spectrometry, *Journal of Chromatography A*, 823, 231–239;
- Carro,N., GarciaC.M., Cela R., (1997), Microwave-assisted extraction of monoterpenols in must samples, *Analyst*, 122 (4), 325–330;
- Diaz-Maroto MC, Perez-Coello MS, Cabezudo MD. Supercritical carbon dioxide extraction of volatiles from spices – comparison with simultaneous distillation – extraction. *J. of Chromatography A*, 947, 23-29, 2002.
- Ehlers D, Nguyen T, Quirin KW, Gerard D. Anaylsis of essential basil oils-CO₂ extracts and steam-distilled oils. *Deutsche Lebensmittel-Rundschau*, 97, 245-250, 2001.
- Fang X., Wang J., Zhou H., Jiang X., Zhu L., Gao X.(2009), Microwave-assisted extraction with water for fast extraction and simultaneous RP-HPLC determination of phenolic acids in Radix Salviae Miltiorrhizae, *J. Sep. Sci.*, 32, 2455 – 2461;
- Faustino H., Gil N., Baptista C., Duarte A.P., (2010), Antioxidant Activity of Lignin Phenolic Compounds Extracted from Kraft and Sulphite Black Liquors, *Molecules*, 15, 9308-9322;
- Gallo M., Ferracane R., Graziani G., Ritieni A. Fogliano V. (2010), Microwave Assisted Extraction of Phenolic Compounds from Four Different Spices, *Molecules*, 15, 6365-6374;
- Harper S.LWalling, J.F., Holland D.M., Pranger L.J., *Anal. Chem.* 55 (1983) 1553.
- Japón-Luján, R., Luque-Rodríguez, J.M., & Luque de Castro, M. D. (2006), Multivariate optimization of the microwave-assisted extraction of oleuropein and related biophenols from olive leaves, *Analytical and Bioanalytical Chemistry*, 385, 753–759;
- Kaufmann B., Christen P., (2002), Recent extraction techniques for natural products: microwave-assisted extraction and pressurised solvent extraction, *Phytochemical Analysis*, Vol.13, 2, 105–113;
- Kellner R., Mermet J., Otto M., Valcarel M., Widmer H.M., *Analytical Chemistry*, second ed., Wiley-VCH, Germany, 2004.
- Kojima, M., Tsunoi, S., Tanaka, M., (2004), High performance solid-phase analytical derivatization of phenols for gas chromatography–mass spectrometry, *J. Chromatogr. A* 1042,1-7;
- Li X.; Zeng, Z.; Zhou, J. (2004), High thermal-stable sol–gel-coated calix[4]arene fiber for solid-phase microextraction of chlorophenols, *Anal. Chim. Acta* 509, 27-37;
- Li B.B., Smith B. Hossain M.M., *Separation and Purification Technology* 48 (2006) 189.
- Luthria, D.L., Mukhopadhyay, S., Kwansa, A.L. (2006), A systematic approach for extraction of phenolic compounds using parsley (*Petroselinum crispum*)

- flakes as a model substrate, *Journal of the Science of Food and Agriculture*, 86, 1350–1358;
- Mahugo Santana C., Sosa Ferrera Z., Torres Padrón M. E., Santana Rodríguez J.J., (2009), Methodologies for the Extraction of Phenolic Compounds from Environmental Samples: New Approaches, *Molecules*, 14, 298-320;
- McCabe, W. L., and J. C. Smith, *Unit Operations of Chemical Engineering*, McGraw- Hill, 1956;
- Martínez, D., Pocurull, E., Marcé, R.M., Borrull, F., Calull M., (1996), Comparative study of the use of high-performance liquid chromatography and capillary electrophoresis for determination of phenolic compounds in water samples, *Chromatographia*, 43, 619-624;
- Nenkova S., Radoykova T., Stanulov K., (2011), Preparation and antioxidant properties of biomass low molecular phenolic compounds (review), *Journal of the University of Chemical Technology and Metallurgy*, 46, 2, 109-120;
- Nepote, V., Grosso, N.R., Guzman, C.A. (2005), Optimization of extraction of phenolic antioxidants from peanut skins, *Journal of the Science of Food and Agriculture*, 85, 33–38;
- Nykanen, I., Nykanen, L. and Alkio, M. (1991) *J. Essential Oil Res.* 3, 229.
- Ozer EO, Platin S, Akman U, Hortasçsu O. Supercritical Carbon Dioxide Extraction of Spearmint Oil from Mint-Plant Leaves. *Can. J. Chem. Eng.*, 74, 920-928, 1996.
- Patsias, J., Papadopoulou-Mourkidou, E. (2009), Development of an automated on-line solid-phase extraction–high-performance liquid chromatographic method for the analysis of aniline, phenol, *Molecules*, 14, 315;
- Perry, R. H., and D. Green, *Perry's Chemical Engineers' Handbook*, 6th Edition, McGraw-Hill, 1988;
- Pérez-Serradilla, J.A., Japón-Luján, R., Luque de Castro, M.D. (2007), Simultaneous microwave-assisted solid–liquid extraction of polar and nonpolar compounds from Alperuja, *Analytica Chimica Acta*, 602, 82–88;
- Proestos C., Komaitis M., (2008), Application of microwave-assisted extraction to the fast extraction of plant phenolic compounds, *LWT* 41, 652–659;
- Rezic I., Krstic D., Bokic Lj., Ultrasonic extraction of resins from an historic textile, *Ultrasonics Sonochemistry* 15 (2008) 21–24
- Robbins, R. J. (2003), Phenolic Acids in Foods: An Overview of Analytical Methodology, *J. Agric. Food Chem.*, 51, 2866-2887;
- Routray W., Orsat V., (2012), Microwave-Assisted Extraction of Flavonoids:A Review, *Food Bioprocess Technol.* 5, 409–424;
- Sarker S.D., Latif Z., Gray A. I.,(2006), *Natural Products Isolation* Second Edition, *Humana Press Inc.*;
- Saunders J.A., Blume D.E., *Journal of Chromatography A* 205 (1981) 147.
- Stahl, E. and Gerard, D. (1985) *Perfumer Flavorist* 10, 29.

Sun, Y., Cheng, J. (2002), Hydrolysis of lignocellulosic materials for ethanol production: a review. *Bioresource Technology*, 83, 1–11;

Tsubaki S., Sakamoto M., Azuma J., (2010), Microwave-assisted extraction of phenolic compounds from tea residues under autohydrolytic conditions, *Food Chemistry*, 123, 1255–1258;

INTECH

INTECH

Combined Microwave - Acid Pretreatment of the Biomass

Adina-Elena Segneanu, Corina Amalia Macarie,
Raluca Oana Pop and Ionel Balcu
*National Institute of Research and Development for
Electrochemistry and Condensed Matter, Timisoara
Romania*

1. Introduction

Bioethanol represents an important alternative for the fossil fuels. The limited fossil fuel stock, the growth of the energy necessary all over the world and the environmental safety lead to an increasing interest in alternative fuels [Balat et al., 2008]. One of the most important renewable energy sources is the lignocellulosic biomass, including wood and crop residues, and that may have applications in the energetic field (both thermal energy and biofuels). There are four main steps in the conversion process of lignocellulosic biomass to ethanol: pretreatment, enzymatic hydrolysis, fermentation and separation [Petersen et al., 2009]. One of the key factors that influence the obtaining of bioethanol is the pretreatment stage. Biomass composition consists in 70-85% cellulosic materials (cellulose and hemicelluloses) and 15-30% lignins. For a corresponding capitalization of biomass, the removal of the lignin content and the transformation of cellulose and its derivatives in sugars are required.

Pretreatment of the lignocellulosic biomass is an important preliminary step that is performed in order to improve the yield of the hydrolysis reaction of cellulosic derivatives in fermentable sugars. The goal of the pretreatment stage consists in changes that are made in the lignocellulosic materials structure, in order to facilitate the access of enzymes in the hydrolysis reaction (Soccol, 2010). A corresponding pretreatment stage must fulfill the following conditions (Balat et al., 2008; Del Campo, 2006; Balat, 2010):

- to improve the sugar formation or the capacity to subsequently obtain sugars by hydrolysis
- to prevent degradation or the loss of carbohydrates
- to prevent the obtaining of possible inhibitory by-products in the hydrolysis and fermentation stages
- costs efficiency
- to avoid the destroy of cellulose and hemicelluloses
- the use of a minimum amount of chemical products

The above-mentioned characteristics represent the basis for the comparisons among various pretreatment methods that are used in the bioethanol industry. A number of different methodologies have been developed in order to accomplish the first stage of the lignocellulosic biomass to ethanol, namely the pretreatment of the biomass.

2. Pretreatment methods of the lignocellulosic biomass

2.1 Acid pretreatment

The main objective of the acid pretreatment is the solubilization of the hemicellulosic fraction of the biomass, in order to increase the accessibility of the enzymes in the enzymatic hydrolysis reaction (Alvira et al., 2010). Inorganic acids like H_2SO_4 , HCl and H_3PO_4 have been used for the pretreatment of the lignocellulosic biomass, in order to improve the enzymatic hydrolysis. There may be used both concentrated and diluted inorganic acids. Pretreatment of the biomass with concentrated acids, at ambient temperature, will lead to higher yields of fermentable sugars and to the hydrolysis of both cellulose and hemicelluloses. There are frequently used acids like H_2SO_4 72%, HCl 41% and trifluoroacetic acid 100%. In this case, a necessary step is the recovery of the acid, in order to lower the economic costs of the process (Girio et al, 2010). The method has the advantage not to use enzymes for saccharification in the further stage, but there are also a number of drawbacks: energy consumption, the use of equipment that is resistant to corrosion, a longer reaction time and the necessary operation of acid recovery (Talebnia et al., 2010).

Pretreatment with diluted acids presents many advantages for an industrial use and it may be applied to different types of biomass. The pretreatment stage may occur at higher temperatures (180°C) for a shorter time, or at lower temperatures (120°C) and a longer residence time. Pretreatment with dilute acid shows the advantage of hemicellulose solubilization, but also of the conversion of the solubilized hemicellulose in fermentable sugars. Pretreatment with diluted acids leads to the obtaining of a fewer degradation products than the pretreatment with concentrated acids (Alvira et al., 2010). The highest yields of the hydrolysis reaction have been recorded after treating the lignocellulosic material with dilute sulfuric acid. Usually, sulfuric acid concentrations are in the range 0.5-1.5%, and the working temperatures are 120-160°C (Alvira et al., 2010).

Organic acids (fumaric acid, maleic acid) appear as alternatives for the improving of the hydrolysis yield of the lignocellulosic biomass. Maleic acid is proven to be more efficient than the fumaric acid, and has the advantage to lead to the obtaining of lower amounts of furfural (compared to the dilute sulfuric acid) (Kootstra et al., 2009). Another pretreatment method with dilute acids uses H_2CO_3 (obtained through the absorption of CO_2 in aqueous solutions) (van Walsum and Shi, 2004).

2.2 Alkaline pretreatment

Pretreatment with alkaline solutions increases the digestibility of cellulose and favors the solubilization of lignins (Alvira, 2010). It may occur at room temperature and reaction time may vary from seconds to days. It leads to a smaller degradation of sugars than in the case of acid pretreatment, but is proven to be more efficient for crop residues than for lignocellulosic biomass (Kumar and Wyman, 2009). For the optimization of the pretreatment conditions, the possibility of losing the fermentable sugars and the formation of some inhibitory compounds must be taken into account.

Reagents that are frequently used for the alkaline pretreatment are NaOH , KOH , $\text{Ca}(\text{OH})_2$, $(\text{NH}_4)_2\text{OH}$. Among them, most widely used is NaOH . For example, pretreatment with NaOH solutions leads to swelling and the increasing of internal surface of cellulose (Alvira et al., 2010). The same authors mentioned that pretreatment with NaOH of hardwood increases the digestibility by the decreasing to 20% of the lignin content.

Although alkaline pretreatments show great efficiency as regards the lignin solubilization, they are less efficient concerning the solubilization of cellulose and hemicelluloses (Girio, 2010).

A widely spread alkaline pretreatment method of the biomass is represented by the ARP (Ammonia Recycle Percolation) procedure (Wu and Lee, 1997). It consists in the use of aqueous ammonia at temperatures around 170°C (Kim and Lee, 2005). The solubilization of hemicelluloses in an oligomeric form occurs within 40-60% range (Girio et al., 2010). The cellulosic fraction is hardly degraded, but in the following steps of the hydrolysis the yields are closed to the theoretic ones (Kim and Lee 2005, Kim et al. 2008). The mechanism of the reaction with aqueous ammonia is very similar to the pretreatment with $\text{Ca}(\text{OH})_2$ and NaOH, especially as regarding the swelling of biomass and the breakdown of the ester and ether bonds of the carbohydrates that exist in lignin (Girio et al, 2010). The advantages of the use of NH_3 are: swelling of the lignocellulosic material, a selective reaction for the removal of lignin, low interaction with carbohydrates, high volatility. One of the known reactions of aqueous NH_3 with lignin is represented by the breakdown of the C-O-C bonds from lignin, as well as of the etheric and esteric bonds from the complex lignin-carbohydrates (Stavrinos et al., 2010). As a result of ARP pretreatment, 60-85% from the entire lignin content is removed (Kim et al., 2008).

Another procedure that uses ammonia for the pretreatment of biomass is the AFEX (Ammonia Fiber Explosion) process. It consists in the contact of biomass with liquid ammonia at elevated temperatures and under pressure for a certain time, followed by a fast decompression (Zheng et al., 2009). The method proved to be less efficient in the case of hardwood and softwood residues (Zheng et al., 2009)

2.3 Organosolv pretreatment

In the Organosolv process, there are used a number of organic or aqueous solvents (methanol, ethanol, acetone, ethylene glycol) in order to solubilize the lignin and to obtain a corresponding treated cellulose for the hydrolysis process (Chum et al., 1988). The advantage of the Organosolv procedure consists in the recovery of lignin as secondary product. The maximum working temperature is 205°C, regarding the used solvent. The economicity of the process depends on the recovery of the organic solvent (Zhao et al., 2009).

The main advantages of the Organosolv pretreatment are: organic solvents can be easily removed by distillation and they can be reused; lignin may be isolated as solid materials (solids) and the carbohydrates are isolated as syrup (Zhao et al., 2009; Kim et al., 2008).

Disadvantages: the pretreated solids need to be initially washed with organic solvents in order to prevent reprecipitation of the dissolved lignin. Also, the process must be strictly controlled, due to the volatility of the organic solvents (Zhao et al., 2009).

Regarding the economy of the process, recovery of the solvents is necessary, even though high amounts of energy are needed. Due to these considerations, Organosolv pretreatment has no applications at industrial level.

The Organosolv pretreatment undergoes both in the presence or absence of a catalyst, at temperatures in the range 185-210°C. The yields of delignification process are improved if mineral acids like HCl, H_2SO_4 or H_3PO_4 or organic acids like formic, oxalic or acetylsalicylic acid (Sun and Cheng, 2002) are used. After pretreatment with Organosolv, three fractions are obtained: dry lignin, an aqueous hemicellulosic phase and a cellulosic fraction (Duff and Murray, 1996).

The most frequently used is the Organosolv pretreatment with aliphatic alcohols (especially methanol and ethanol), mostly due to their low price. Among the alcohols with higher

boiling points, mostly used are polyhydroxylic alcohols like ethylene glycol and glycerol. The main advantage is the fact that the process could occur at atmospheric pressure. Pretreatment with aqueous glycerol leads to the removal of the lignin, but also to a significant loss of cellulose (Kucuk, 2005).

2.4 Pretreatment with solid superacids

The solid acid catalysts appeared as a consequence of the developing of a new, eco-friendly process for the obtaining of bioethanol. Particles of solid acid can be separated by the liquid products through decantation or filtration, and the catalyst may be reused without further processing stages to be necessary.

Solid superacids are made from a solid medium treated with Lewis or Bronsted acids (Zhao et al., 2009). They have the great advantage of being non-toxic, non-corrosive and safe for the environment. They are better donors than pure sulfuric acid and show a higher selectivity in the hydrolysis reaction and require low temperatures and atmospheric pressure (Zhao et al., 2009; Yamaguchi and Hara). Some of the superacids used in the process of the obtaining of bioethanol are: niobic acid ($\text{Nb}_2\text{O}_5 \cdot n\text{H}_2\text{O}$), zeolite, Amberlyst-15, amorphous C that contains SO_3H , COOH and OH groups (Zhao et al., 2009).

Another superacid used for the selective conversion of cellulose to glucose is the heteropoly acid $\text{H}_3\text{PW}_{12}\text{O}_{40}$ (Tian et al., 2010). The selectivity of the pretreatment method is very high (around 90%) and requires mild reaction conditions (160-180°C). Another advantage of this method is the possibility to reuse the catalyst, which can be recycled by extraction with diethyl ether (Tian et al., 2010).

2.5 Ionic liquids

The main advantage of using ionic liquids for the bioethanol production is represented by the possibility of a complete solubilization of the lignocellulosic biomass. Swatloski et al. suggested that solubilization is due to the breakdown of the H bonds of the polysaccharides by the anion of the ionic liquids. In the present, the process cannot be applied at industrial level due to the high costs of the ionic liquids (Swatloski et al., 2002).

A variant of the pretreatment with ionic liquids is represented by the microwave-assisted pretreatment of lignocellulosics in ionic liquids (Zhang and Zhao, 2009; Zhu et al., 2006). The method is characterized by shorter reaction time (due to the microwave irradiation) and a better solubilization of the biomass. According to Zhu et al., the raw lignocellulosic material is directly solubilized in the ionic liquid in the presence of microwaves and cellulose is precipitated by adding water. The other organic compounds (like lignins) remain in solution. Experimental results (Zhu et al., 2006) showed that the yields in ethanol are very similar to the ones obtained through steam explosion or chemical pretreatment.

2.6 Hydrothermal methods of pretreatment

The hydrothermal reactions for the pretreatment of biomass are new, eco-friendly pretreatment methods. They consist in the contact of the lignocellulosic materials with water at elevated temperature and pressure. During the process, hemicelluloses are hydrolyzed to sugars. The reaction time is very short (seconds) in order to avoid degradation of the sugars (<http://www.ecn.nl/units/bkm/biomass-and-coal/transportation-fuels-and-chemicals/transportation-fuels/biomass-pre-treatment-fractionation/>).

A variant of the hydrothermal pretreatment consists in the use of catalytic hydrothermal reaction that uses a solid catalyst (for example, amorphous carbon that contains $-\text{SO}_3\text{H}$ groups) and results in higher amounts of fermentable sugars (Onda et al., 2009).

2.7 Ozonolysis

Pretreatment with ozone occurs in mild conditions (room temperature, atmospheric pressure) and results in a strong delignification of the biomass (Sun and Cheng, 2002). The major drawback of the process is represented by the high costs, due to the large quantity of ozone that is needed during the pretreatment (Sun and Cheng, 2002).

2.8 Combined methods of pretreatment

2.8.1 Pretreatment with alkaline peroxides, followed by steam explosion

The procedure combines the advantages of alkaline pretreatment and steam explosion. It will lead to an efficient delignification and to the chemical swelling of the lignocellulosics fibers (Zhao et al., 2009). Use of a combined process (steam explosion and NaOH 10%) led to a significant increase of the free sugars concentration towards the pretreatment with H_2O_2 1% and NaOH 1% (Chen and Qiu, 2010).

2.8.2 Pretreatment with ionic liquids coupled with steam explosion

Pretreatment of the lignocellulosics biomass with ionic liquids coupled with steam explosion led to the degradation of hemicelluloses in fermentable sugars (Chen and Qiu, 2010). Lignin with high molecular mass is insoluble in ionic liquids, so it can be separated from cellulose.

2.8.3 Biological pretreatment

For the biological pretreatment of the lignocellulosic biomass there are used both microorganisms (fungi and bacteria) and enzymes (Mtui, 2009; Balat, 2011). There are used white, brown and soft-rot fungi for the solubilization of hemicelluloses and also for the lignin degradation (Mtui, 2009; Balat, 2011). For the enzymatic pretreatment of the biomass, different cellulases (endoglucanases, exoglucanases and β -glucosidases) are used (Sun and Cheng, 2002).

3. Studies regarding the determination of the optimum parameters of the microwave-assisted dilute acid pretreatment of lignocellulosic biomass

Lignocellulosics biomass has three main components: cellulose (40-50%), hemicelluloses (25-35%), lignin (15-20%) and also small amounts of proteins, lipids, acids, mineral salts. As it was mentioned before, the aim of the pretreatment stage is the removal of hemicelluloses and lignin. Also, the cellulose structure is altered in order to facilitate the enzymatic attack.

From all the pretreatment methods presented in the former chapter, pretreatment with dilute mineral acids (especially H_2SO_4) combined with microwave irradiation has been chosen. The advantages of this process are the reaction conditions (that does not involve corrosion problems, or volatility or very high temperatures issues) and the low economic costs. Also, the use of microwave irradiation leads to shorter reaction time and also provides a uniform heating of the reaction mixture.

Experimental part: three types of sawdust (hardwood (oak) and softwood (fir) essences and herbs (hemp)) were treated with dilute sulfuric acid (for different concentrations: 0.55, 0.82, 1.23 and 1.64%) and heated (in the presence of microwaves) at three different temperatures: 120, 140 and 160°C, for 15 and 30 minutes, in order to perform an extensive study on the pretreatment in acid medium. The concentration in sugars (expressed as free glucose) of the solutions obtained after the hydrolysis reactions was considered in order to establish the best pretreatment method.

After cooling, the suspension was neutralized with CaCO_3 until a pH value of 5.5-6, for the removal of sulfates. Pretreated sawdust were filtered and washed with water, in order to remove the entire amount of sugars.

Determination of the total amount of carbon hydrates after performing dilute acid pretreatment on different types of sawdust was made by the colorimetric method with 3,5-dinitrosalicylic acid. 5 milliliters from the solution obtained after pretreatment were treated with DNS 1%, boiled for 15 minutes on a water bath and then cooled. Extinction was measured (against blank) at 575 nm.

Results of the pretreatment method with dilute sulfuric acid (H_2SO_4 0.55%) at 120°C, for 15 and 30 minutes, are presented in the table below:

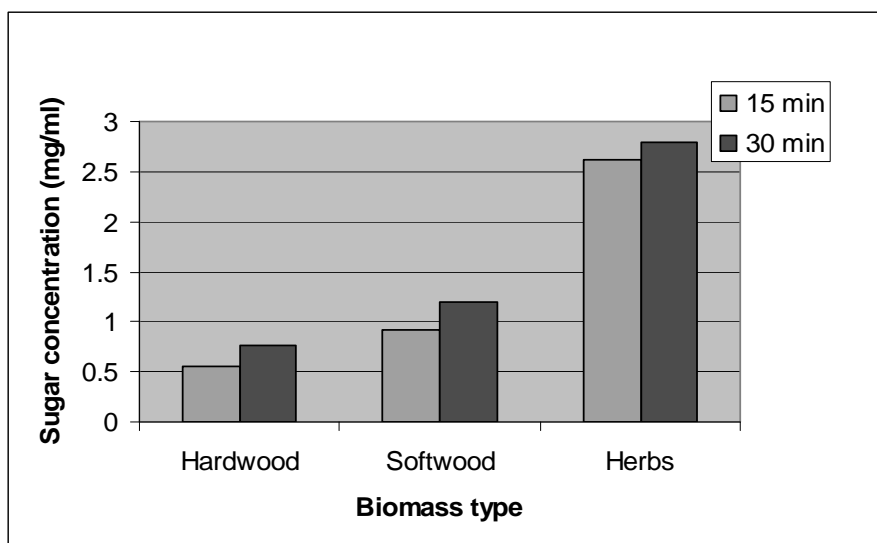


Fig. 1. Pretreatment of the biomass with H_2SO_4 0.55% at 120°C

As it may be seen, best results are obtained for the sawdust from herbaceous plants (in our case, hemp). The amount of sugars (expressed as free glucose) obtained after pretreatment is almost three times higher in the case of hemp sawdust than in the case of hardwood sawdust.

Pretreatment with the same acid solution (H_2SO_4 0.55%) at 140 and 160°C, respectively, led to the following results:

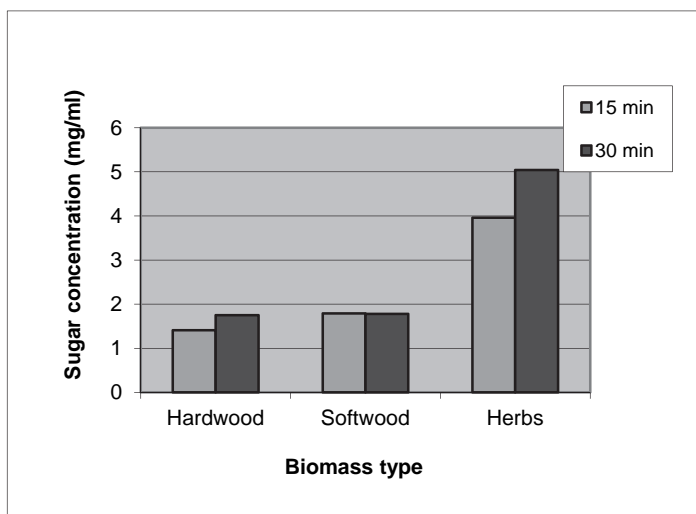


Fig. 2. Pretreatment of the biomass with H_2SO_4 0.55% at 140°C

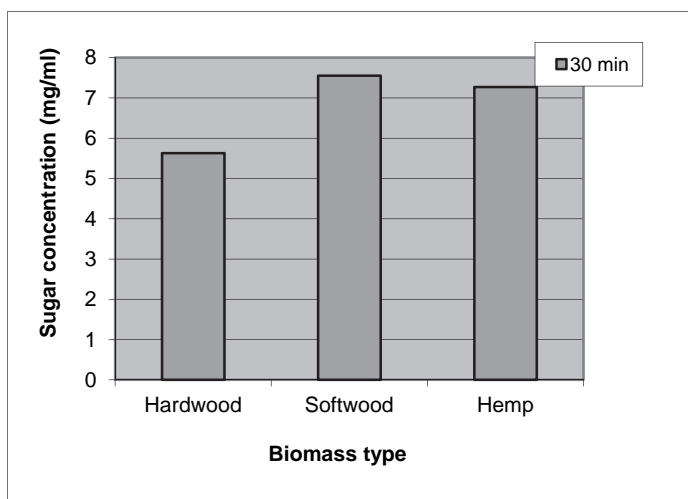


Fig. 3. Pretreatment of the biomass with H_2SO_4 0.55% at 160°C

In the case of the pretreatment with H_2SO_4 0.55% at 140°C , an increase of the reaction (pretreatment) time has significant consequences only in the case of hemp sawdust, when higher concentration of free sugars are obtained when the pretreatment time is 30 minutes instead of 15 minutes. For the hardwood (oak) and softwood (fir) sawdust, an increase of the pretreatment time does not lead to a significant improvement of the free sugars yield.

In the case of pretreatment with dilute acid at 160°C , our previous studies showed that there is no difference between the results of the pretreatment process at 15 or 30 min. Taking into

account that in the other pretreatment methods best results have been obtained when the pretreatment lasted 30 minutes, the same period was chosen for the hydrolysis with H_2SO_4 0.55% at 160°C.

All the presented results show that, best results are obtained when pretreatment at 160°C is performed. The highest yields in free sugars are obtained for softwood and herbaceous sawdust, respectively, so it may be said that the softwood and herbaceous sawdust structure is more easily attacked than the hardwood sawdust structure during the acid hydrolysis.

The same pretreatment method with dilute sulfuric acid (0.82%) combined with microwave irradiation was used for the same types of sawdust (hardwood-oak, softwood-fir, herbaceous-hemp) at three different temperatures. The experiments were carried out in the same conditions as mentioned before, the only change being the different concentration of the acid. The aim of the study was to establish if an increase of the acid concentration leads to an increase of the amount of obtained sugars in the same temperatures conditions or, as a result, much of the already formed sugars will be degraded. The results are presented in the figures below:

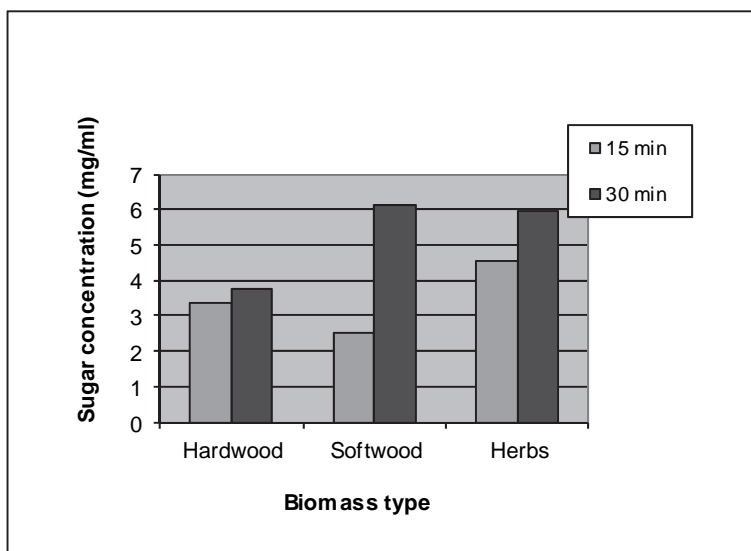


Fig. 4. Pretreatment of the biomass with H_2SO_4 0.82% at 120°C

According to these results, a slight concentrated solution of sulfuric acid has better results regarding the concentration in fermentable sugars of the solutions obtained after pretreatment. Good results are obtained especially for the fir sawdust, the level of sugars is almost 5 times higher when treated with H_2SO_4 0.82% at 120°C for 30 minutes than with H_2SO_4 0.55% for an identical time and temperature. Also the results of hardwood sawdust pretreatment are improved, the concentration of final solutions after pretreatment in free sugars is almost three times higher than in the case when H_2SO_4 0.55% was used. The results of the pretreatment are much poorer for the oak (hardwood) sawdust than for the fir (softwood) and herbaceous (hemp) sawdust.

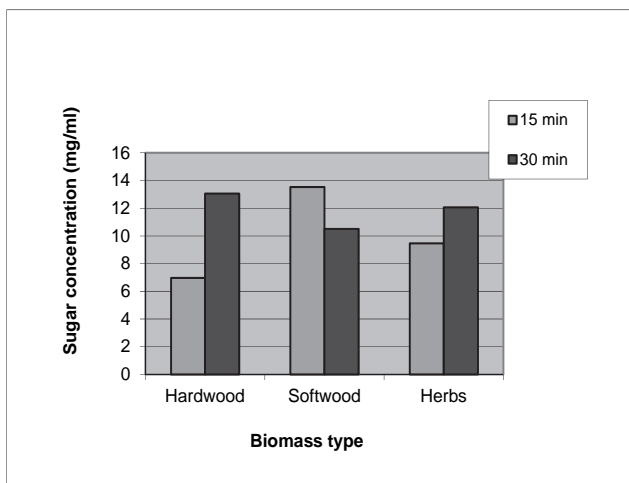


Fig. 5. Pretreatment of the biomass with H_2SO_4 0.82% at 140°C

Pretreatment with sulfuric acid 0.82% at 140°C led to the obtaining of very similar results for all the sawdust types used in the study. Except the softwood sawdust, when best results were obtained for a shorter reaction time (15 minutes), pretreatment with H_2SO_4 0.82% at 140°C for 30 minutes is more efficient than the similar one with H_2SO_4 0.55%.

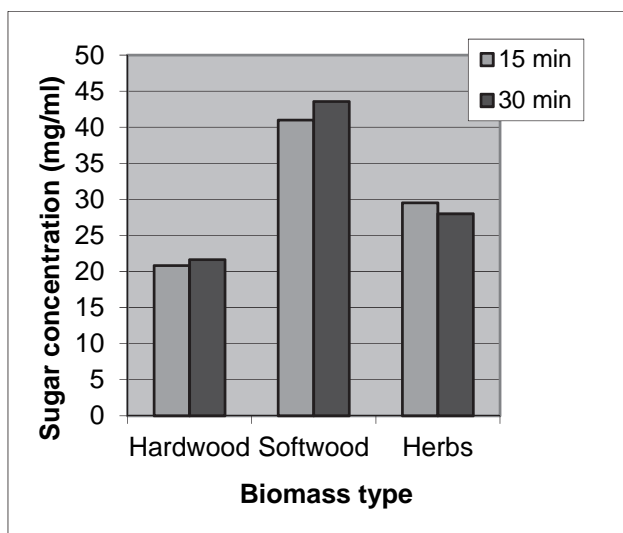


Fig. 6. Pretreatment of the biomass with H_2SO_4 0.82% at 160°C

When temperature is increased to 160°C , much higher concentrations of fermentable sugars are obtained. It may be observed that, at this temperature, there are almost no differences

between the results of the 15 minutes and 30 minutes pretreatment. The pretreatment method shows its efficiency especially as regards the fir sawdust, followed by the hemp sawdust. As happened in all of the previous cases, poorer concentrations in fermentable sugars are obtained for the oak sawdust.

Same pretreatment method was used for the three types of sawdust, but in this case a solution of H_2SO_4 1.23% was used. The results are presented below in a graphic form:

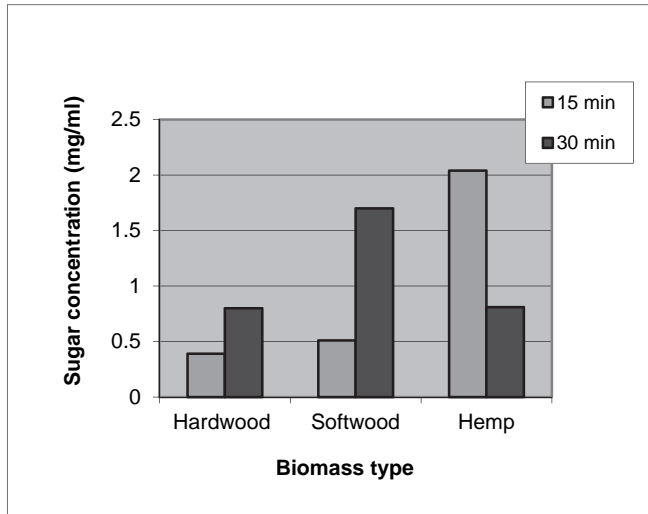


Fig. 7. Pretreatment of the biomass with H_2SO_4 1.23% at 120°C

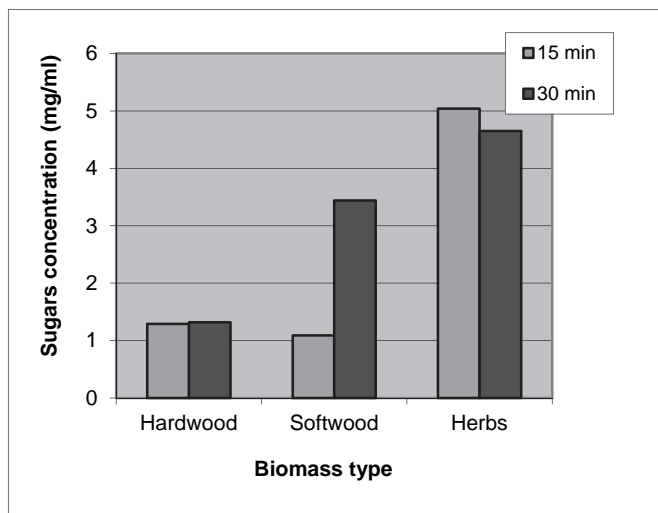


Fig. 8. Pretreatment of the biomass with H_2SO_4 1.23% at 140°C

It may be seen that the results of the pretreatment with a solution of sulfuric acid 1.23% in the same conditions of temperature and residence time result in much poorer results than in the above-mentioned case, when sulfuric acid 0.82% was used. A possible explanation consists in the fact that, at higher concentrations of acidic solution, the already formed sugars to be destroyed and degraded.

Taking into account the similarity of the results of the pretreatment with H_2SO_4 0.82% at 160°C for 15 and 30 minutes respectively, reaction of the sawdust with H_2SO_4 1.23% at 160°C was carried out only for 30 minutes. The results are presented below:

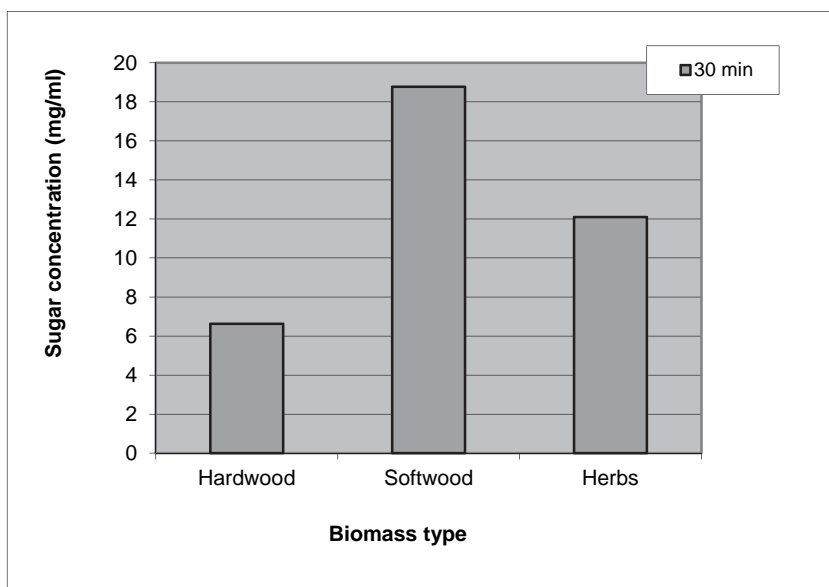


Fig. 9. Pretreatment of the biomass with H_2SO_4 1.23% at 160°C

Unlike the pretreatment with H_2SO_4 0.55%, it may be observed that in the case of herbaceous sawdust (hemp), an increased reaction time leads to smaller amounts of fermentable sugars. A stronger acid and a longer pretreatment time have better results only for the softwood (fir) sawdust, while as regarding the herbaceous sawdust it appears that a shorter reaction time leads to an increase yield in fermentable sugars. Data presented in Figures... show that the best results are obtained for the fir sawdust, and, as in the previous case (H_2SO_4 0.55%), the pretreatment method gives the poorer results for the hardwood sawdust. It appears that a prolonged acid pretreatment, with a slight acidic solution (than the concentrations of H_2SO_4 used before, namely 0.55% and 0.82%) is not benefic for the herbaceous sawdust, being possible that a great part of the already formed fermentable sugars to be simultaneously degraded during the pretreatment time.

In order to see if a more concentrated acid has a positive influence on the acid hydrolysis of the lignocellulosic materials, a solution of H_2SO_4 1.64% was employed for the pretreatment of the three types of sawdust, at the same temperatures (120 , 140 and 160°C) and 15 and 30 minutes reaction time, respectively. The results are the following:

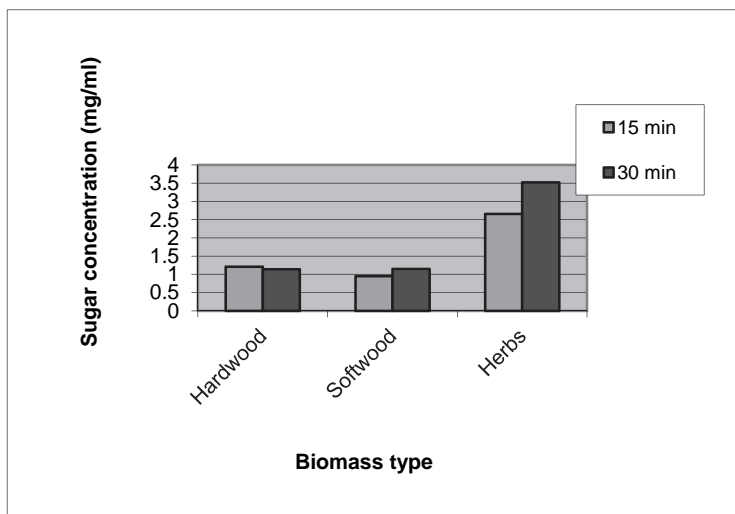


Fig. 10. Pretreatment of the biomass with H₂SO₄ 1.64% at 120°C

The results show that hemp sawdust is favored by this pretreatment method, but the concentrations in fermentable sugars are lower than the ones obtained in the same conditions, but when H₂SO₄ 0.82% was used.

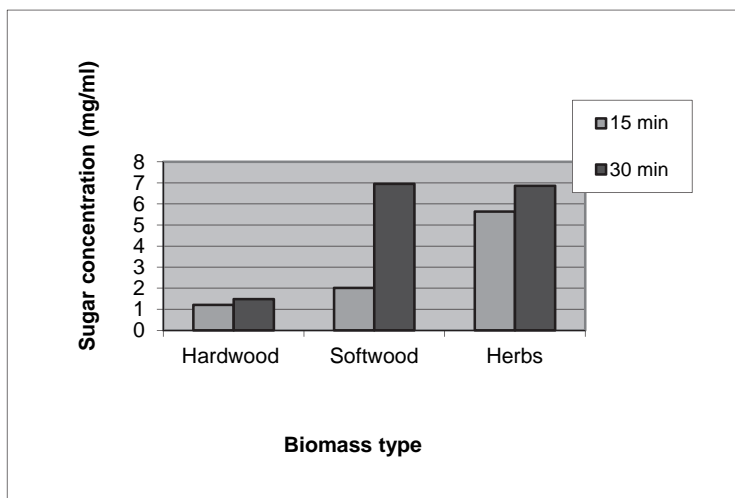


Fig. 11. Pretreatment of the biomass with H₂SO₄ 1.64% at 140°C

An increase of the temperature leads to a higher concentrations in free sugars, but only for fir and hemp sawdust, respectively. Elevated residence time led to considerably improved results, especially as regarding the hemp sawdust.

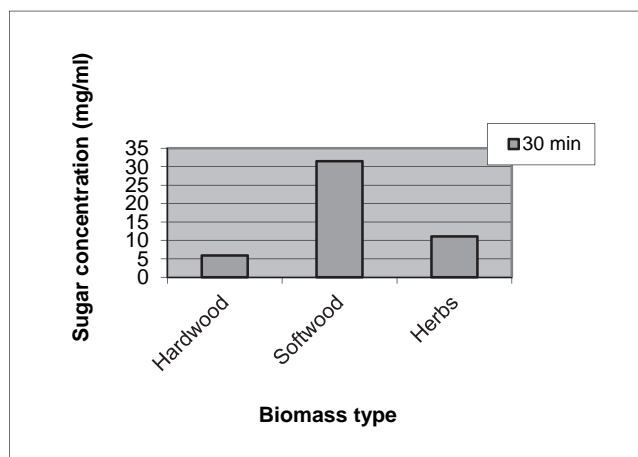


Fig. 12. Pretreatment of the biomass with H_2SO_4 1.64% at 160°C

The profile of the results is, somewhat, similar to the pretreatment with H_2SO_4 0.82% in the same conditions. It may be observed that, quantitatively, pretreatment at higher temperatures and longer time leads to better results. The amount of fermentable sugars increases with the acid concentration and with the residence time. Best results are obtained for the fir sawdust, when pretreated with H_2SO_4 1.64% at 160°C . Poorer results are obtained for the herbaceous sawdust (hemp) and hardwood sawdust, respectively. It appears that harsh conditions are required for a corresponding pretreatment in the case of fir sawdust (30 minutes residence time and 140 or 160°C).

Best results are obtained for the fir sawdust, when pretreated with H_2SO_4 0.82% at 160°C , with no significant difference due to the residence time (15 or 30 minutes).

As regarding the hemp sawdust, the best results are obtained when pretreatment with H_2SO_4 0.82% at 160°C for 15 minutes is employed. It can be said that a corresponding hydrolysis of the lignocellulosics from herbaceous sawdust requires less harsh conditions than the acid hydrolysis of softwood sawdust.

Concerning the hardwood sawdust, it may be said that pretreatment with dilute acids at temperatures in the range 120 - 160°C is not suitable. In all of the cases, only small amounts of free, fermentable sugars are obtained after the pretreatment. From all the pretreatment variant presented, it appears that the most suitable is the method that uses H_2SO_4 0.82% at 160°C for 15 minutes (the differences are very small between results of the 15 minutes and 30 minutes pretreatment, respectively).

It may be said that a corresponding microwave-assisted pretreatment of oak, fir and hemp sawdust is achieved by means of dilute sulfuric acid (0.82%) at 160°C , for 15 minutes.

In order to determine the pretreatment severity, the combined severity factor (CSF) that includes acid concentration, temperature and pretreatment time was used (Hsu et al., 2010).

$$\text{CSF} = \log \left\{ t \cdot \exp \left[(T_H - T_R) 14.75 \right] \right\} - \text{pH}$$

Where: t - time (minutes), T_H - temperature of the process, T_R - reference temperature (100°C), pH - pH of the dilute sulfuric acid.

| Pretreatment conditions | Acid concentration (%) | CSF |
|-------------------------|------------------------|------|
| 120°C, 15' | 0.55 | 0.65 |
| | 0.82 | 0.80 |
| | 1.23 | 0.95 |
| | 1.64 | 1.10 |
| 120°C, 30' | 0.55 | 0.95 |
| | 0.82 | 1.10 |
| | 1.23 | 1.25 |
| | 1.64 | 1.40 |
| 140°C, 15' | 0.55 | 1.25 |
| | 0.82 | 1.40 |
| | 1.23 | 1.55 |
| | 1.64 | 1.65 |
| 140°C, 30' | 0.55 | 1.55 |
| | 0.82 | 1.70 |
| | 1.23 | 1.85 |
| | 1.64 | 1.95 |
| 160°C, 30' | 0.55 | 2.10 |
| | 0.82 | 2.30 |
| | 1.23 | 2.45 |
| | 1.64 | 2.55 |

Table 1. The combined severity factor (CSF) of the different variants of the microwave-assisted dilute acid hydrolysis process

4. A study concerning the possibility of using lyophilization as an efficient pretreatment method of the lignocellulosic residues

Experimental part: a suspension of sawdust and NaOH 1% and H₂SO₄ 1% solution (1:10 w/v) was lyophilized at -52°C for 24 hours. The pretreated suspensions were filtered, washed with ultrapure water and the filtrate was neutralized with a solution of H₂SO₄ 0.82% (the alkaline ones) and with CaCO₃ (the acid ones). The concentration in free, fermentable sugars was determined using the colorimetric method with 3,5-dinitrosalicylic acid.

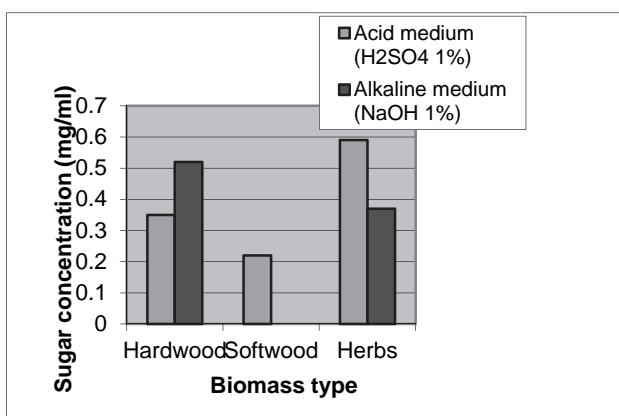


Fig. 13. Results of the alkaline and acid lyophilization pretreatment

The concentrations of free sugars are much poorer compared to the ones obtained after the combined pretreatment of microwave irradiation and dilute acid hydrolysis. No detectable concentrations of fermentable sugars were obtained for fir sawdust, when treated with an alkaline solution. A comparison between the two proposed methods is clearly in the favor of the microwave-assisted acid hydrolysis, which requires much less time and lower economic costs.

5. Conclusions

The results of the microwave-assisted acid pretreatment of the lignocellulosic biomass show that for good results in free sugars concentration there are not necessary elevated temperatures and high acid concentration. As results from the performed study, very efficient seems to be the pretreatment with sulfuric acid 0.82% at a temperature of 140°C, conditions that are characterized by a combined severity factor of 1.7. As regarding the possibility of using lyophilization in acid or alkaline medium, the obtained results are very poor and do not stand for the use of lyophilization as a viable pretreatment method.

6. References

- Alvira, P., Tomas-Pejo, E., Ballesteros, M., Negro, M. J. (2010). Pretreatment technologies for an efficient bioethanol production process based on enzymatic hydrolysis: A review. *Bioresource Technology*, Vol. 101, pp. 4851-4861
- Balat, M. (2011). Production of bioethanol from lignocellulosic materials via the biochemical pathway: A review. *Energy Conversion and Management*, Vol. 52, pp. 858-875
- Balat, M., Balat, H., Oz, C. (2008). Progress in bioethanol processing. *Progress in Energy and Combustion Science*, Vol. 34, pp. 551-573
- Chen, H., Qiu, W. (2010). Key technologies for bioethanol production from lignocellulose. *Biotechnology Advances*, Vol.28, pp. 556-562
- Chum, H. L., Johnson, D. K., Black, S., Baker, J., Grohmann, K., Sarkanen, K. V., Wallace, K., Schroeder, H. A. (1988). Organosolv pretreatment for enzymatic hydrolysis of poplars: I. Enzyme hydrolysis of cellululosic residues. *Biotechnology and Bioengineering*, Vol. 31, pp. 643-649
- Del Campo, I. et al. (2006). Diluted acid hydrolysis pretreatment of agri-food wastes for bioethanol production. *Industrial Crops and Products*, Vol. 24, pp. 214-221
- Duff, S. J. B., Murray, W. D. (1996). Bioconversion of forest products industry waste cellulose to fuel ethanol: A review. *Bioresource Technology*, Vol. 55, pp. 1-33
- Girio, F. M., Fonseca, C., Carvalheiro, F., Duarte, L. C., Marques, S., Bogel-Lucasik, R. (2010). Hemicelluloses for fuel ethanol: A review. *Bioresource Technology*, Vol. 101, pp. 4775-4800
- Hsu, T.-C., Guo, G.-L., Chen, W.-H., Hwang, W.-S. (2010). Effect of dilute acid pretreatment of rice straw on structural properties and enzymatic hydrolysis. *Bioresource Technology*, Vol. 101, pp. 4907-4913
- Inoue, H., Yano, S., Endo, T., Sakaki, T., Sawayama, S. (2008). Combining hot-compressed water and ball milling pretreatments to improve the efficiency of the enzymatic hydrolysis of eucalyptus. *Biotechnology for Biofuels*, 1:2
- Kim, J.-S., Kim, H., Lee, J.-S., Lee, J.-P., Park, S.-C. (2008). Pretreatment characteristics of waste oak wood by ammonia percolation. *Appl. Biochem. Biotechnol.*, Vol. 148, pp. 15-22
- Kim, T. H., Lee, Y. Y. (2005). Pretreatment and fractionation of corn stover by ammonia recycle percolation. *Process. Bioresource Technology*, Vol. 96, No. 18, pp. 2007-2013

- Kootstra, A. M. J., Beeftink, H. H., Scott, E. L., Sanders, J. P. M. (2009). Optimization of the dilute maleic acid pretreatment of wheat straw. *Biotechnology for Biofuels*, Vol. 2, No. 31
- Kucuk, M. M. (2005). Delignification of biomass using alkaline glycerol. *Energ. Source*, Vol. 27, pp.1245-1255
- Kumar, R., Wyman, C. E. (2009) Does change in accesibility with conversion depend on both the substrate and pretreatment technology? *Bioresource Technology*, Vol. 100, pp. 4193-4202
- Mtui, G. Y. S. (2009). Recent advances in pretreatment of lignocellulosic wastes and production of value added products. *African J. of Biotechnology*, Vol.8, No.8, pp. 1398-1415
- Onda, A., Ochi, T., Yanagisawa, K. (2009). Hydrolysis of cellulose selectively into glucose over sulfonated activated-carbon catalyst under hydrothermal conditions. *Top Catal.*, Vol. 52, pp. 801-807
- Soccol, C. R. et al. (2010). Bioethanol from lignocelluloses: Status and perspectives in Brazil. *Bioresource Technology*, Vol. 101, pp. 4820-4825
- Stavrinides, A. J., Phipps, D. A., Al-Shamma'a, A. (2010). Review: Current and developing lignocellulosic pretreatment methods for bioethanol production, Available from: www.ljmu.ac.uk/.../Amended_PROCEEDINGS_BEAN_2010_WEB_VERSION_24.pdf
- Swatloski, R. P., Spear, S. K., Holbrey, J. D., Rogers, R. D.(2002). Dissolution of cellose with ionic liquids. *J. Am. Chem. Soc.*, Vol. 124, pp. 4974-4975
- Sun, Y., Cheng, J. (2002). Hydrolysis of lignocellulosic materials for ethanol production: a review. *Bioresource Technology*, Vol. 83, pp. 1-11
- Talebna, F., Karakashev, D., Angelidaki, I. (2010). Production of bioethanol from wheat straw: An overview on pretreatment, hydrolysis and fermentation. *Bioresource Technology*, Vol. 101, pp. 4744-4753
- Tian, J., Wang, J., Zhao, S., Jiang, C., Zhang, X., Wang, X. (2010). Hydrolysis of cellulose by the heteropoly acid $H_3PW_{12}O_{40}$. *Cellulose*, Vol. 17, pp. 587-594
- Van Walsum, G. P., Shi, H. (2004). Carbonic acid enhancement of hydrolysis in aqueous pretreatment of corn stover. *Bioresource Technology*, Vol. 93, No. 3, pp. 217-226
- Wu, Z., Lee, Y. Y. (1997). Ammonia recycled percolation as a complementary pretreatment to the dilute-acid process. *Applied Biochemistry and Biotechnology*, Vol. 63-65, No. 1, pp. 21-34
- Yamaguchi, D., Hara, M. (2010). Optimization of hydrolysis of cellulosic materials by a solid acid catalyst. Available from: www.iis.org/CDs2010/CD2010IMC/ICEME_2010/.../FB297UD.pdf
- Zhao, X., Cheng, K., Liu, D. (2009). Organosolv pretreatment of lignocellulosic biomass for enzymatic hydrolysis. *Appl. Microbiol. Biotechnol.*, Vol. 82, pp. 815-827
- Zhang, Z., Zhao, Z. K. (2010). Solid acid and microwave-assisted hydrolysis of cellulose in ionic liquid. *Carbohydrate Research*, Vol. 344, pp. 2069-2072
- Zheng, Y., Pan, Z., Zhang, R. (2009). Overview of biomass pretreatment for cellulosic ethanol production. *Int. J. Agric. & Biol. Eng.*, Vol. 2, No. 3, pp. 51
- Zhu, S. et al. (2006). Dissolution of cellulose with ionic liquids and its application: a mini-review. *Green Chem.*, Vol. 8, pp. 325-327
- <http://www.ecn.nl/units/bkm/biomass-and-coal/transportation-fuels-and-chemicals/transportation-fuels/biomass-pre-treatment-fractionation/>

MAGNETIC COBALT FERRITE NANOPARTICLES: SYNTHESIS AND SURFACE FUNCTIONALIZATION WITH NATURALLY SMALL PEPTIDE

A.E. SEGNEANU, P. VLAZAN, P. SVERA, I. GROZESCU, P. SFIRLOAGA*
*National Institute of R&D for Electrochemistry and Condensed Matter -
INCEMC Timisoara, I Plautius Andronescu, 300224 Timisoara, Timis*

The aim of the present study was to prepare inorganic-organic hybrid material for biomedical potential application. The cobalt-ferrite (CoFe_2O_4) magnetic nanoparticles (MNPs) obtained by sol-gel method and treated at 200 °C were immobilized in a small peptide. Covalent and non-covalent attachment of proteins with MNPs provides access to functional hybrid systems with applications in biotechnology, medicine and catalysis. The crystalline phases, morphology and chemical composition of the particles were characterized by GC-MS, NMR, TEM/EDX, BET and FT-IR.

(Received December 11, 2013; Accepted June 18, 2014)

Keywords: Magnetic nanomaterials, Surface functionalization, Peptide, Inorganic-organic

1. Introduction

Magnetic nanoparticles (MNPs) have an additional advantage of being easily manipulated by permanent magnets or electromagnets, independent of normal microfluidic or biological processes. A variety of nanoparticles (NPs) with various shapes such as spheres, nanotubes, nano-horns and nano-cages, made of different materials, from organic dendrimers, liposomes, gold, carbon, semiconductors, silicon to iron oxide, have already been fabricated and explored in many scientific fields, including chemistry, material sciences, physics, medicine and electronics [1].

Advances in nanotechnology play an important role in designing nanomaterials with specific functional properties that can address the shortcomings in the area of diagnostics and therapeutics. The potential of nanomaterials has sparked enormous interest in the drug industry and has envisaged several applications, as can be evidenced by the exponential growth of activities in this field. The advantages of the nanoparticles are mainly due to their nanoscale size and large surface area with the ability to get functionalized with targeting ligands, therapeutic moieties and biomolecules [2].

The phase structure and microstructure of the nanoparticles determine their physical properties. Nanoparticle syntheses utilizing biomimetic approaches have advanced in recent years. Peptides, with their ability to influence inorganic crystal growth, are a topic of great interest. The peptide influences the phase as well as the microstructure and therefore, the magnetic properties of the particles [3].

The chemical coating of these nanoparticles may also be linked to molecules compatible, that specifically targeting a area such as an organ, a disease or a particular biological system [4].

In the last decade, magnetic NPs are used in bio-applications, including magnetic bio-separation and detection of biological entities (cell, protein, nucleic acids, enzyme, bacterial, virus, etc.), clinic diagnosis and therapy (such as MRI (magnetic resonance image) and MFH (magnetic fluid hyperthermia)), targeted drug delivery and biological labels [5].

* Corresponding author: psfirloaga@yahoo.com

Nanotechnology presents very promising characteristics for its application in the biomedicine area. By now the most advanced application of nanoparticles in medicine is the use of iron oxide nanoparticles embedded in biocompatible polymers as magnetic resonance imaging (MRI) contrast agents. Until now have been studied various synthesis techniques for the preparation of CoFe_2O_4 nanoparticles, such as co precipitation [6], hydrothermal [7] micro emulsion [8], but the principal difficulty of these methods is that the obtained nanoparticles are agglomerated, having limited control over dimensional distribution, thus restricting their applications [9]. For early detection of tumors by MRI were used iron oxide bond with various types of ligands such as proteins, peptides and small molecules demonstrate active targeting of tumors via specific molecular recognition[10]. Bio-sensing strategies based on magnetic nanoparticles (MNPs) have recently received considerable attention.

The chemical synthesis of multimaterial nanocrystal heterostructures combining sections of oxide, metal and semiconductor materials in a single multifunctional nanoscale object represents a challenging research direction along which nanochemistry research is investing substantial efforts [11]. Multi-functional nanomaterials possessing fluorescent and magnetic properties may be used in a number of biomedical applications in nanobiotechnology, such as bioimaging, bio- and chemo-sensing, cell tracking and sorting, bioseparation, drug delivery and therapy systems in nanomedicine [12]. The therapeutic applications of oxide and hybrid nanostructures strongly depend on their physicochemical properties such as permeability, stability, morphology (size, shape and functionality) and biocompatibility. These physicochemical properties are dictated by the types, structures and orientations of the materials that comprise the oxide and hybrid nanostructures [13]. The bio-functionalization of monodisperse magnetic nanoparticles (NPs) of size 10-20 nm is of great interest as it would enable the ultra-sensitive magnetic detection of both proteins and nucleic acids. Given their extremely small size and high magnetization, such nanoparticles could also be used to bind and transport proteins, nucleic acids, and other biomolecules through microfluidic networks and, following introduction into a living organism, they could provide a means of monitoring and influencing cellular processes [14].

The present study investigates a new and easily synthetic route of preparation of inorganic-organic hybrid material with potential application in biomedicine. A proper characterization methodology was developed for this hybrid material.

2. Materials and Methods

All used reagents are analytical grade. Iron (III) nitrate hexahydrate, cobalt (II) nitrate hexahydrate, ammonium hydroxide and polyvinyl alcohol, triethylamine, dichloromethane and *N,N'*-dicyclohexylcarbodiimide were purchased from Merck. Amino acids were acquired from Applichem and Alfa Aesar (USA).

2.1. Peptide synthesis:

Boc-protected dipeptide (Boc-Ser-Val-OMe) was obtained from valine methyl ester hydrochloride, *N*-BOC-*L* serine, triethylamine and *N,N'*-dicyclohexylcarbodiimide in a molar ratio of 1:1:1.1:1.1. The *N*-*tert*-butyloxycarbonyl group was removed using 50% TFA/dichloromethane. The dipeptide was afforded in 75.8 % yield.

2.2. Nanoparticles synthesis and functionalization

Spinel cobalt ferrites were prepared by sol-gel method using iron and cobalt nitrates as precursors. The preparation protocol included the following steps: (1) dissolution of metal nitrates in bi-distilled water; (2) addition of polyvinyl alcohol (PVA) to first solution for obtain a colloid; (3) increase pH to about 8 by addition of NH_4OH solution; (4) stirring at 80°C ; (5) drying the gel at 140°C ; (6) and finally the dried gel was treated at 200°C . The solid product thus obtained was incorporated in dipeptide in mass ratio 1:1 and 1:4. The mixture was dissolved in dichloromethane and ultrasonic for one hour at 40°C , in an ultrasonic bath equipped with thermostat and timer.

The hybrid material obtained was characterized using following methods: GC-MS, TEM/EDX, and BET analysis.

2.3. Materials Characterization

Qualitative analysis of dipeptide was performed on a GC-MS 7890A-5975C system (Agilent Germany) using the EZ: faast GC-MS free amino acids kit and ZB-AAA GC column (Phenomenex, Torrance, CA, USA). The used analysis conditions were the standard conditions written on the kit.

GC-MS separation conditions: the standard analysis conditions were the instructions from the kit: Oven: 30°C (hold 1 min) to 40°C at 30°C/min (hold 10 min) to 360°C (hold 1 min); Equilibration time: 1 min; Injection: split 1: 15; 250°C; 2 μ L; Carrier Gas: Helium 1.1mL/min; 110°C; Inlet pressure: 5.824 kPa/min; Detector: MS; Mode: Scan Transfer Line Temperature: 250°C; Analyzer Type: Electron Energy: 70eV.

¹H NMR spectra were recorded on a Varian Mercury 300 spectrometer operating at 299.97 MHz.

The surface morphology of the materials obtained was observed using a transmission electron microscope (TECNAL, F30 G2) with linear resolution 1 Å and a punctual resolution of 1.4 Å and elemental analysis was performed with Energy Dispersive X Ray (EDX) spectrum.

The nanomagnetic compound and the hybrid material specific surface area (BET) were determined by Brunauer-Emmet-Teller (BET) method, based on adsorption/desorption isotherms of nitrogen at 77 K obtained with NOVA 2200 apparatus. The pore size distribution (PSD) was calculated from the adsorption isotherms using BJH (Barrett-Joyner- Halenda) method [15].

The Fourier transformed infrared spectrum was recorded in KBr pellet on a Bruker FT/IR-Vertex 70 instrument (resolution 4 cm⁻¹) in spectral range 4000-400 cm⁻¹ (32 scans).

3. Results and Discussions

3.1 GC-MS analysis

As a first step were prepared the hybrid material precursors: MNPs and the dipeptide. The synthesis of the dipeptide was provided by a conventional solution method, according to a procedure previously described by our research team [17-19]. For the synthesis of peptide was selected two amino acids that are found in natural products, especially in medicinal herbs, namely: *L*-serine and *L*-valine. The formation of the dipeptide was investigation by GC-MS method. The obtained chromatograms are shown in the Figure 1.

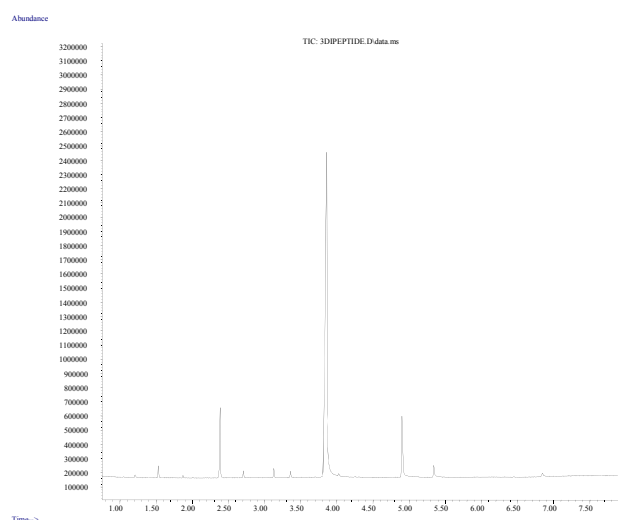


Fig. 1. GC-MS chromatogram for dipeptide

The mass spectra of the component from the GC-MS chromatogram was compared with the spectra from the NIST/NBS spectral database, and was identified the presence of dipeptide *L*-serin-*L*-valine.

3.2 H-NMR analysis

^1H -NMR (D_2O , δ , ppm): 1.16 d, 2.39m, 4.19t, 4.32m, 4.42m, 4.54m, 4.71s, 6.51s, 7.46s, 8.75s. The assigned ^1H NMR signals confirmed the serin-valine formation. The assigned ^1H NMR signals demonstrate the serin-valine formation.

3.3 TEM/EDX analysis

MNPs synthesis was carried out by sol-gel method. This approach present the advantage that by imposition of certain values of the reaction parameters (pH, temperature, etc) it can be controlled the size (at about 30 nm) and shape of spinel cobalt ferrites nanoparticles [20-24].

The morphology of obtained hybrid material was evaluated by comparative analyzing of inorganic material before and after the functionalization.

In Figures 2 (a) and 2 (b) are shown TEM images of the CoFe_2O_4 nanoparticles before assembly and after with dipeptide assembly, demonstrating their structures from the nanoscale level up to the aggregate particles.

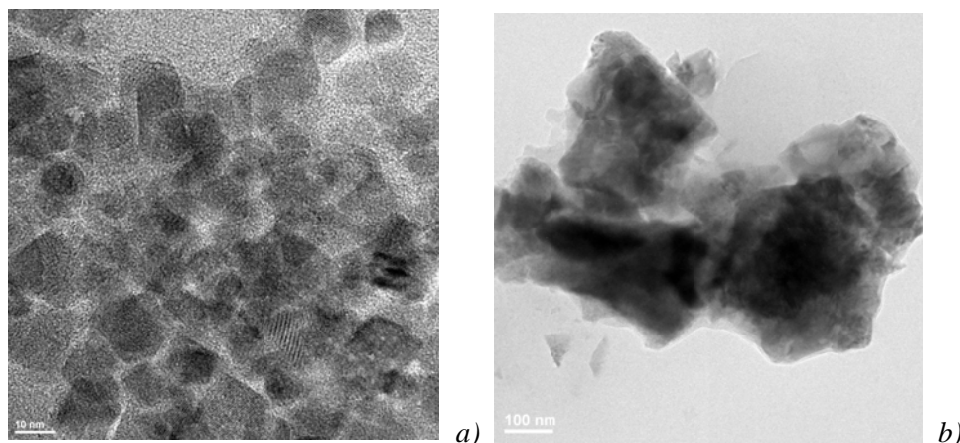


Fig. 2. TEM images for CoFe_2O_4 (a) and CoFe_2O_4 /dipeptide (b)

Also can be seen the TEM image for the CoFe_2O_4 /dipeptide where are showed structures that covers matrix of the nanoparticle, and suppose that belong of the dipeptide structures assembled. These lamellar self-assembled structures are similar to the βCD crystals described previously in the literature [16], confirming the presence of the dipeptide in the ferrite matrix.

The EDX spectrum presents the elemental composition of the sample in which Co, Fe, O₂ are the majority elements and currently Cu in the sample is due to grid – support (Figure 3).

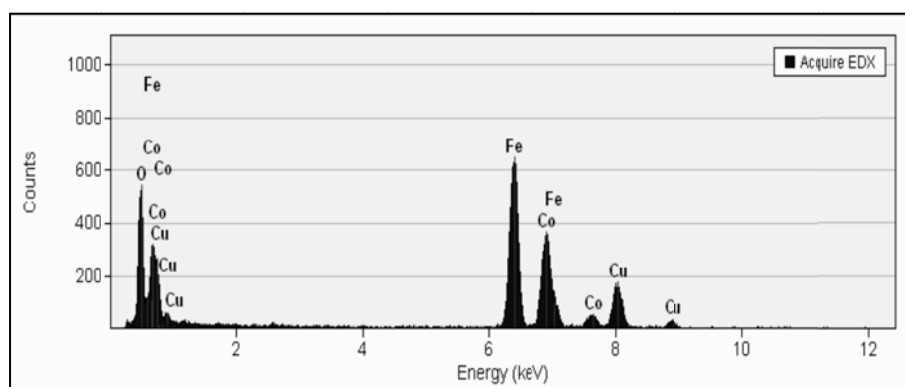


Fig. 3. EDX spectrum for CoFe_2O_4

3.4 BET analysis

Many properties of nanoparticles are improved with reducing size, so it is very important to determine their surface area.

The isotherm data obtained in partial pressure range of 0.05 to 0.3 (**Figure 4**) is plugged into the Langmuir adsorption isotherm, to obtain the BET plot.

Table 1. BET results for CoFe_2O_4 and $\text{CoFe}_2\text{O}_4/\text{dipeptide}$

| BET CoFe_2O_4 | | | BET $\text{CoFe}_2\text{O}_4/\text{dipeptide}$ | | |
|-------------------------------|----------------------------|------------------|--|----------------------------|------------------|
| p/p^* | $\text{cm}^3/\text{g STP}$ | $1/x[(p^*/p)-1]$ | p/p^* | $\text{cm}^3/\text{g STP}$ | $1/x[(p^*/p)-1]$ |
| 0.0577 | 0.313 | 0.1956 | 0.0577 | 1.3601 | 0.04505 |
| 0.1128 | 0.3766 | 0.3378 | 0.1126 | 2.1129 | 0.04601 |
| 0.1755 | 0.3949 | 0.539 | 0.1758 | 2.5434 | 0.08385 |
| 0.238 | 0.3935 | 0.7937 | 0.238 | 2.7805 | 0.11233 |
| 0.3005 | 0.3677 | 1.1683 | 0.3006 | 2.9192 | 0.14723 |

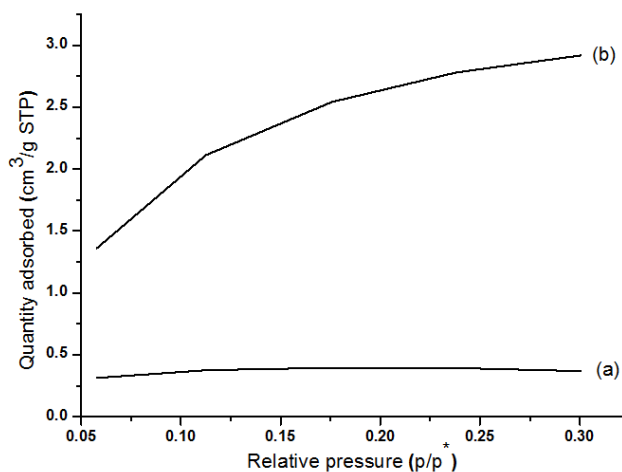


Fig. 4. The BET isotherms of the CoFe_2O_4 (a) and $\text{CoFe}_2\text{O}_4/\text{dipeptide}$ (b)

In figure 5 is presented BET plot of IRMOF-13 using points collected at the pressure range 0.05 to 0.3 by the equation used to determine the surface area.

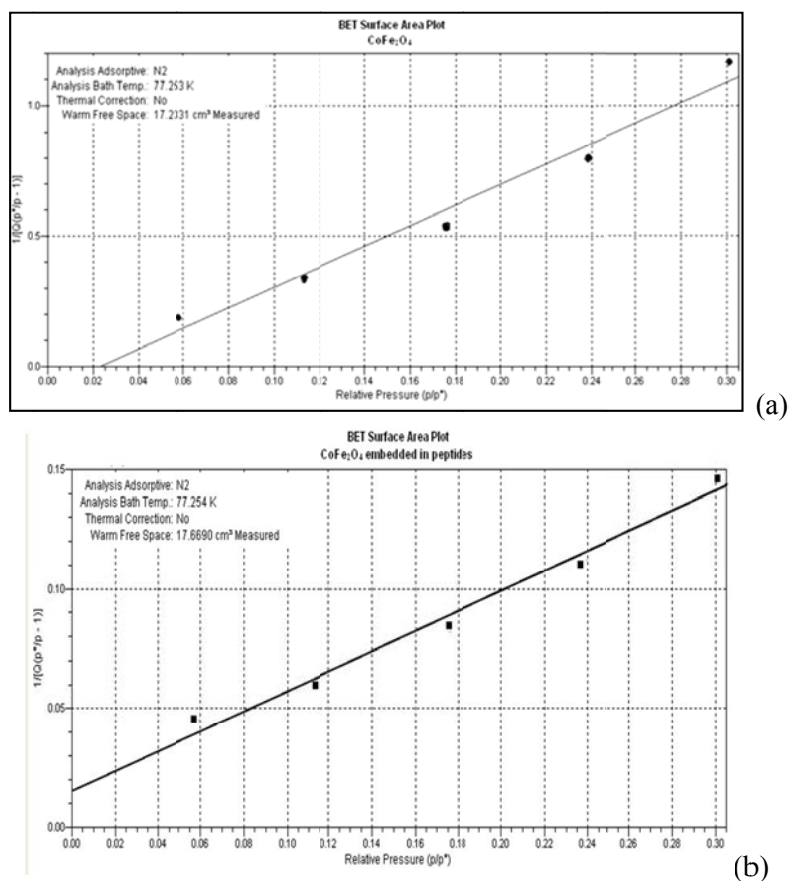


Fig. 5. BET plot using points collected at the pressure range 0.05 to 0.3 by the BET equation used to determine the surface area for CoFe₂O₄ (a) and CoFe₂O₄/dipeptide (b)

BET surface area and pore volume analysis were examined to confirm the surface modification. Figure 5 shows nitrogen adsorption isotherms of CoFe₂O₄ nanoparticle (a) before assembly and (b) after assembly of the dipeptide at 77°K, with corresponding pore-size distribution calculated by BJH method from desorption. Before assembly, the cobalt ferrite nanoparticles have a BET surface area of 1.1301m²/g and warm free space 17.2331 measured. After dipeptide assembly, the values are 9.9801m²/g and warm free space 17.6690 measured. From the result of BET analysis, we can find that the BET surface area increase after the layer-by-layer assembly.

Confirmation of MNPs functionalization was carried out also by FTIR spectroscopy. In this regard was recorded IR spectrum for hybrid material (figure 7) and for comparison, are included also spectres of precursors. Investigation of IR spectra dates of final products showed presence of wavelength characteristic to Fe – O bonds at approximate 567 cm⁻¹, C=O bond at 1617 cm⁻¹, amide bond at 1354 cm⁻¹, CN stretching at 1472 cm⁻¹. The strong signal at 1587 cm⁻¹ is attributed amide band from dipeptide. The peak at 3400 cm⁻¹ corresponds for hydroxyl group –OH. According to these results the functionalization of MNPs with targeting dipeptide was successfully accomplished.

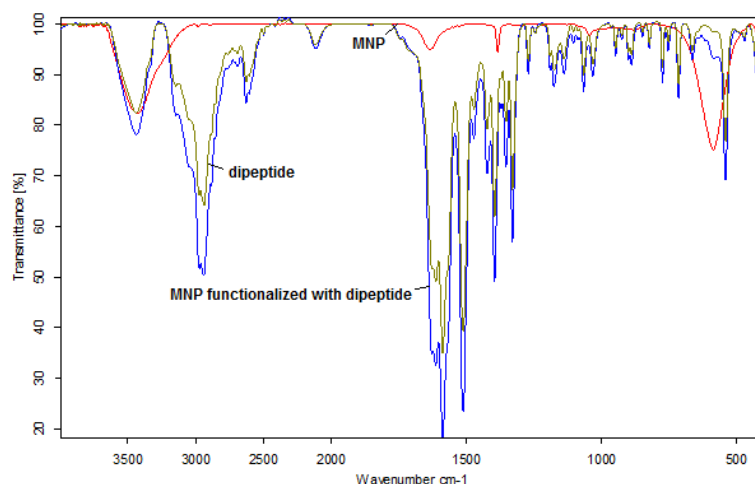


Fig. 6. Overlapping IR spectra for hybrid inorganic-organic material and precursors

4. Conclusions

Hybrid magnetic nanoparticles based on cobalt ferrite and serin-valine were prepared through a simple, effective method. The chemical structure of organic compound was evaluated by GC-MS and NMR analysis. Investigation of the specific surface of hybrid material crystalline phases, morphology and chemical composition of the final compound and precursors proved the confirmed obtaining of the hybrid system. The final product present interesting potential application in biomedicine, due to the fact that shows both features of magnetic nanoparticles and total synthesis of a natural dipeptide. Obtaining of inorganic-organic hybrid material was proven by TEM/EDAX, FT-IR and BET analysis.

This MNPs functionalization with a naturally small peptide can be considered as just a first step in design of new inorganic –organic hybrid materials with interesting features for development of new and improved nanotechniques especially for medical area.

Acknowledgements

This study was supported by Bilateral project RO-SI - 535/2011 “*Innovative design of new biologically active peptide systems with specific properties*”.

References

- [1] A. S.de Dios, M. E. Díaz-García, *Analytica Chimica Acta* **666**, 1–22. (2010).
- [2] H. Maeda, J. Wu, T. Sawa, Y. Matsumura, K. Hori, *J. Control. Rel.* **65**, 271 (2000).
- [3] A. Wolff, K. Frese, M. Wißbrock, K. Eckstadt, I. Ennen, W. Hetaba, S. Löffler, A. Regtmeier, P. Thomas, N. Sewald, P. Schattschneider, A. Hutten, *J Nanopart Res.* **14**,1161 (2012).
- [4] C. Corot, P. Robert, J.M. Idée, M. Port, *Advanced Drug Delivery Reviews*, **58**, 1471 (2006)
- [5] W. Wu, Q. He, C. Jiang, *Nanoscale Res Lett*, **3**, 397 (2008).
- [6] Y. Kim, D. Kim, C. Sub Lee, *Physica B* **337**, 42 (2003).
- [7] D. Zhao, X. Wu, H. Guan, E. Han, *J. of Supercritical Fluids*, **42**, 226 (2007).
- [8] C. Liu, A. J. Rondinone, Z. J. Zhang, *Pure Appl. Chem.*, **72**, 37 (2000),
- [9] S.Y. Zhao, D.K. Lee, C.W. Kim, H.G. Cha, Y.H. Kim, Y.S. Kang, *Bull Korean Chem Soc*, **27**, 237 (2006).
- [10] H. Shao, C. Min, D. Issadore, M. Liong, T.J. Yoon, R. Weissleder, H. Lee, *Magnetic Nanoparticles and microNMR for Diagnostic Applications, Theranostics*, **2**(1.) 55 (2012),

- [11] L. Carbone., P. D. Cozzoli, *Nano Today* **5**, 449 (2010),
- [12] S.A. Corr, Y.P. Rakovich, Y.K. Gunko, *Nanoscale Res Lett* **3**, 87 (2008),
- [13] S. Chandra, K.C. Barick, D. Bahadur, *Advanced Drug Delivery Reviews* **63**, 1267 (2011).
- [14] S.G. Grancharov, H. Zeng, S. Sun, S.X. Wang, S. O'Brien, C.B. Murray, J.R. Kirtley, G.A. Held, *J. Phys. Chem. B* **109**, 13030 (2005).
- [15] S. Lowell, et al., *Characterization of Porous Solids and Powders: Surface Area, Pore Size and Density*, Kluwer Academic Publishers, Dordrecht/Boston/ London; (2004),
- [16] A.M.L., De Sousa F.B., Passos J.J., Guatimosim F.C., Barbosa K.D., Burgos A.E., Castro de Oliveira F., da Silva J.C., Neves B.R.A, Mohallem, N.D.S. Sinisterra R.D., Beilstein *J Org Chem.* **8**, 1867 (2012).
- [17] I. Grozescu, A. Bebeselea, A. Segneanu, *Digest Journal of Nanomaterials and Biostructures* **7(4)**, 1689 (2012).
- [18] A.E. Segneanu, M. Milea, I. Grozescu, *Optoelectron. Adv. Mater.-Rapid Commun.* **6(5-6)**, 656-659; (2012).
- [19] A.E. Segneanu, Use of organic carbonates for protection of group amino and activation of carboxyl group from amino acids in peptide synthesis, PhD thesis de, Ed. Politehnica Timișoara, ISSN: 1842-8444, ISBN: 978-973-625-431-4; (2007),
- [20] M. Goodarz Naseri, E.B.Saion, H. Abbastabar Ahangar, A. H. Shaari, M.Hashim, Simple Synthesis and Characterization of Cobalt Ferrite Nanoparticles by a Thermal Treatment Method, *Journal of Nanomaterials*, Article ID 604241, 11 page; (2010).
- [21] M. Faraji, Y. Yamini, M. Rezaee, *Magnetic Nanoparticles: Synthesis, Stabilization, Functionalization, Characterization, and Applications*, *J. Iran. Chem. Soc.*, **7(1)**, 1 (2010).
- [22] S. A. Popescu;, P. Vlazan;, P. V Notingher., , S. Novaconi;, I. Grozescu, , A. Bucur, P., Sfirloaga, *Synthesis, Morphology and Magnetic Characterization of Zn Ferrite Powders*, *Communications & Network*; **2(4)**, 598 (2010).
- [23] P. Vlazan, M. Vasile, *Optoelectron. Adv. Mater.-Rapid Commun.* **4(9)**, 1307 (2010).
- [24] P. Vlazan, *Nanocrystalline cobalt ferrites obtained by alternative methods: Structure, properties and potential applications*, PhD Thesis, Ed University "Politehnica" Timisoara, ISBN 978-606-554-477-2. (2012),

A simple and rapid method for calixarene-based selective extraction of bioactive molecules from natural products

Adina-Elena Segneanu, Daniel Damian, Iosif Hulka, Ioan Grozescu & Athanasios Salifoglou

Amino Acids

The Forum for Amino Acid, Peptide and Protein Research

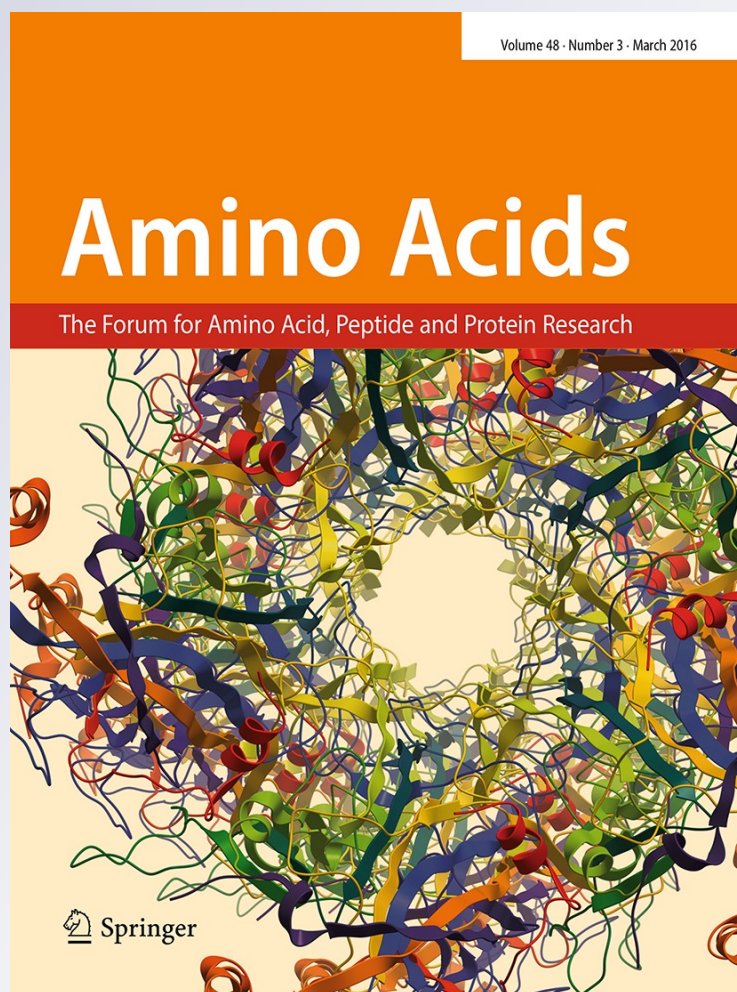
ISSN 0939-4451

Volume 48

Number 3

Amino Acids (2016) 48:849-858

DOI 10.1007/s00726-015-2132-9



Your article is protected by copyright and all rights are held exclusively by Springer-Verlag Wien. This e-offprint is for personal use only and shall not be self-archived in electronic repositories. If you wish to self-archive your article, please use the accepted manuscript version for posting on your own website. You may further deposit the accepted manuscript version in any repository, provided it is only made publicly available 12 months after official publication or later and provided acknowledgement is given to the original source of publication and a link is inserted to the published article on Springer's website. The link must be accompanied by the following text: "The final publication is available at link.springer.com".

A simple and rapid method for calixarene-based selective extraction of bioactive molecules from natural products

Adina-Elena Segneanu¹ · Daniel Damian^{1,2} · Iosif Hulka² · Ioan Grozescu^{1,2} · Athanasios Salifoglou^{1,3}

Received: 5 April 2015 / Accepted: 4 November 2015 / Published online: 23 November 2015
© Springer-Verlag Wien 2015

Abstract Natural products derived from medicinal plants have gained an important role in drug discovery due to their complex and abundant composition of secondary metabolites, with their structurally unique molecular components bearing a significant number of stereo-centers exhibiting high specificity linked to biological activity. Usually, the extraction process of natural products involves various techniques targeting separation of a specific class of compounds from a highly complex matrix. Aiding the process entails the use of well-defined and selective molecular extractants with distinctly configured structural attributes. Calixarenes conceivably belong to that class of molecules. They have been studied intensely over the years in an effort to develop new and highly selective receptors for biomolecules. These macrocycles, which display remarkable structural architectures and properties, could help usher a new approach in the efficient separation of specific classes of compounds from complex matrices in natural products. A simple and rapid such extraction method is presented herein, based on host–guest interaction(s) between a calixarene synthetic receptor, 4-tert-butyl-calix[6]arene, and natural biomolecular targets (amino acids and peptides) from *Helleborus*

purpurascens and *Viscum album*. Advanced physicochemical methods (including GC–MS and chip-based nanoESI–MS analysis) suggest that the molecular structure and specifically the calixarene cavity size are closely linked to the nature of compounds separated. Incorporation of biomolecules and modification of the macrocyclic architecture during separation were probed and confirmed by scanning electronic microscopy and atomic force microscopy. The collective results project calixarene as a promising molecular extractant candidate, facilitating the selective separation of amino acids and peptides from natural products.

Keywords Calixarene · Host–guest interaction · Selective extraction · Chip-based nanoESI–MS analysis · Scanning electronic microscopy · Atomic force microscopy

Introduction

Phytoconstituents, generally isolated from medicinal plants, represent a mixture of biomolecules from different chemical classes (sterols, quinones, alkaloids, carbohydrates, terpenes, flavones, proteins, etc.) (Gutsche 2008; Karpagasundari and Kulothungan 2014; Sikorka et al. 2000). Two of the most popular medicinal plants (a) containing such bioactive components, and (b) used for centuries in traditional phytotherapeutical formulations, due to their remarkable therapeutic properties (immunostimulant, antitumor, etc.), are *Helleborus purpurascens* and *Viscum album*. Research on the chemical composition of these plants has shown that, in addition to their ordinary phytoconstituents, special peptide derivatives with high biological activity (thioneins, viscotoxins, viscumamide, lectins) were also present (Ikeda and Shinkai 1997). Although, several methods

Handling Editor: T. Langer.

✉ Athanasios Salifoglou
salif@auth.gr

¹ National Institute of Research and Development for Electrochemistry and Condensed Matter INCHEM Timisoara, 1 Plautius Andronescu, 300224 Timisoara, Romania

² University Politehnica Timisoara, 2 Piata Victoriei, 30006 Timisoara, Romania

³ Department of Chemical Engineering, Aristotle University of Thessaloniki, 54124 Thessaloniki, Greece

exist for the extraction and isolation of bioactive metabolites from natural sources, pronounced interest for new methods exhibiting high selectivity continues to be on the rise (Bart and Pilz 2011; Fiehn et al. 2000; Neda et al. 2012; Popescu et al. 2011; Vaszilcsin et al. 2010). Poised to pursue and develop such methods, studies were launched focusing on calixarenes, synthetic macrocycles, able to act as selective and efficient natural product molecular extractants in various separation processes. These cyclic oligomers are well known through their extensive application in various fields, as very flexible ligands binding metal ions, amines, amino acids and proteins (Gutsche 2008; Ikeda and Shinkai 1997; Koh et al. 1995; Mutihac et al. 2005; Shimojo et al. 2004). In fact, numerous studies in the specific field have focused on the design of selective ionic receptors in metal recognition and extraction processes (Atwood and Steed 2004; Gutsche 2008; Hassen et al. 2007; Ikeda and Shinkai 1997; Koh et al. 1995; Ludwig 2005; Ludwig and Thi Kim Dzung 2002; Oshima et al. 2002; Shimojo et al. 2004; Sirit and Yilmaz 2009; Stone et al. 2002). Logically, therefore, research on host–guest interactions between synthetic receptors and biomolecules rises as a topic of great interest due to a plethora of emerging applications in the natural product field. Owing to their very special features, including the chemical structure and molecular design (cavity size), calixarenes could be successfully used for the selective separation of amino acids and small peptides (Shimojo et al. 2004; Sirit and Yilmaz 2009; Stone et al. 2002; Mutihac et al. 2005). In such a process, incorporation of a biomolecule into the calixarene cavity leads to modification of the ligand structure symmetry (Koh et al. 1995; Mutihac et al. 2005). Hence, the study and establishment of interactions between the supramolecular ligands and specific amino acids (and small peptides) are undoubtedly paramount in the chemistry of natural products, meriting further in-depth perusal.

In an effort to study the nature and exploit the relevant interactions emerging through such processes, thereby developing a simple, rapid and efficient natural product extraction method, research was launched in our labs to probe the capacity of calix[6]arene to act as a selective extractant for the separation of amino acids from two different medicinal plant extracts: *H. purpurascens* (S_1) and *V. album* (V_1). Identification of the biomolecules incorporated into the calixarene cavity was pursued through several key high performance analytical techniques: gas chromatography coupled to mass spectrometry (GC–MS), chip-based nanoelectrospray ionization mass spectrometry (nanoESI chip MS), scanning electron microscopy (SEM), and atomic force microscopy (AFM).

Materials and methods

Reagents

All chemicals used were of analytical grade purity. The solvents ethanol, methanol and dichloromethane were purchased from VWR (Austria). 4-Tert-butyl-calix[6]arene (calixarene) was obtained from InnoChemTech GmbH (Germany). All MS reagents used in this study were also of analytical grade purity. Distilled and deionized water were obtained from Milli-Q water systems (Millipore, Bedford, MA, USA).

GC–MS techniques

Detection of free amino acids and peptides was performed on a GC–MS 7890A-5975C system (Agilent, Germany) using the EZ:faast GC–MS free amino acids kit and ZB-AAA GC column (Phenomenex, Torrance, CA, USA). The analysis conditions employed were the standard conditions proposed by the kit manufacturer.

Mass spectrometry

MS experiments were conducted on a High Capacity Ion Trap Ultra (HCT Ultra, PTM discovery) mass spectrometer from Bruker Daltonics, Bremen, Germany. All mass spectra were acquired in the positive ion mode, in a mass range of 100–2500 m/z , with a scan speed of 8000 m/z per second. The m/z scale of all mass spectra was externally calibrated using G2421A electrospray “tuning mix” from Agilent Technologies (Santa Rosa, CA, USA) as a calibration standard. The reference in the positive ion mode provided a spectrum with a fair ionic coverage of the m/z range covered in a full scan MS. Following calibration, the obtained mass accuracy was within the normal range of an HCT MS instrument.

Scanning electron microscopy (SEM)

SEM images were acquired using a FEI Inspect S PANalytical model coupled with an energy dispersive X-ray analysis detector (EDX) at an accelerated voltage of 30 kV.

Atomic force microscopy (AFM)

Atomic force microscopy measurements were performed with a Nanosurf® easyScan 2 Advanced Research AFM (Switzerland). Surface imaging was run under ambient conditions, with samples deposited onto pure silica plates by slow evaporation of the solvent $\text{CH}_3\text{CH}_2\text{OH}$. For recording measurements, a stiff ($450 \times 50 \times 2 \mu\text{m}$) piezoelectric

ceramic cantilever (spring constant of 0.2 N m^{-1}) was used, with an integral tip oscillated near its resonance frequency of about 13 kHz. AFM images were obtained in contact mode.

General experimental procedures

Plant material

Helleborus purpurascens (rhizome) and *V. album* (mistletoe leaves and young twigs from *Robinia pseudoacacia*) were obtained from a collection taken in December 2013 in Costei, Timis, and identified by Dr. Dana Bobit (Romanian Ethnopharmacology Society, Dacia Plant SRL Brasov, Romania). A voucher sample for each plant (ID No. O0186 and O0187) was deposited at the herbarium of the Cluj-Napoca Botanical Garden, Romania.

Extraction methodology

Phase I

Plant samples (*H. purpurascens* and *V. album*) were ground in a ball mill. Two samples from each plant (2.59 g) were placed in a 50 mL volumetric flask containing 30 mL of distilled water. The mixtures were sonicated for 30 min at $60 \text{ }^\circ\text{C}$, with a frequency of 50 kHz. Subsequently, each sample solution was filtered through a $0.45 \text{ }\mu\text{m}$ filter.

Phase II

0.10 g of calixarene was dissolved in 15 mL of dichloromethane. The organic solution was mixed for 1 h with an equal volume of the aqueous plant fraction (15 mL). Following phase separation, the solvent of the organic phase was removed under vacuum and the residues S_I (hellebore extract) and V_I (viscum extract) were analyzed by spectroscopic, chromatographic and microscopy techniques.

Chromatographic analysis

GC-MS separation conditions

The standard analysis conditions were described in the instructions on the kit: oven: $30 \text{ }^\circ\text{C}$ (hold 1 min) to $40 \text{ }^\circ\text{C}$ at $30 \text{ }^\circ\text{C min}^{-1}$ (hold 10 min) to $360 \text{ }^\circ\text{C}$ (hold 1 min); equilibration time: 1 min; injection: split 1:15; $250 \text{ }^\circ\text{C}$; $2 \text{ }\mu\text{L}$; carrier gas: helium 1.1 mL min^{-1} ; $110 \text{ }^\circ\text{C}$; inlet pressure:

$5.824 \text{ kPa min}^{-1}$; detector: MS; mode: scan transfer line temperature: $250 \text{ }^\circ\text{C}$; analyzer type: electron energy: 70 eV . A Phenomenex-Zebron ZB-AAA 10 m X 0.25 mm capillary GC column was used.

NanoESI chip MS spectroscopy

Prior to chip-based nanoESI mass spectrometry analysis, all sample solutions were centrifuged for 30 min in a SIGMA 2–16 model centrifuge from Sartorius GmbH (Göttingen, Germany). Fully automated chip-based nanoelectrospray was performed on a NanoMate robot, incorporating ESI 400 Chip technology (Advion BioSciences, Ithaca, USA), controlled and manipulated by ChipSoft 7.1.1 software operating on Windows. The robot was coupled to the HCT Ultra mass spectrometer via an in-laboratory made interface. $10 \text{ }\mu\text{L}$ aliquots of the working sample solutions were loaded onto a NanoMate 96-well plate. The robot was programmed to a) aspirate $5 \text{ }\mu\text{L}$ of the sample, followed by $2 \text{ }\mu\text{L}$ of air, into the pipette tip to prevent dripping, and subsequently b) deliver the sample on to the inlet side of the 400 microchip. The NanoMate HCT MS system was tuned to operate in the positive ion mode at 0.30 kV ESI potential, 0.80 p.s.i. nitrogen back pressure, and 50 V capillary exit. The source block, maintained at the constant temperature of $80 \text{ }^\circ\text{C}$, provided an optimal desolvation of the generated droplets with no need of desolvation gas. Following sample infusion and MS analysis, the pipette tip was ejected and a new tip and nozzle were used for each sample, thus preventing any cross-contamination or carryover. Each chip nozzle had an internal diameter of $2.5 \text{ }\mu\text{m}$, which under the specific conditions delivered a working flow rate of $\sim 100 \text{ nL min}^{-1}$. Mass spectra were calibrated using sodium iodide as a calibrating agent. Accurate determination of the average mass was 20 ppm, with a resolution of about 4000. Samples were dissolved in methanol at a concentration of $\sim 5 \text{ pmol}/\mu\text{L}$. At the acquisition time of 2 min, the required volume of sample was $\sim 2 \text{ pmol}$, a value reflecting very high sensitivity in the specific analysis. All samples were measured under identical solution and instrumental parametric conditions. Moreover, the samples were simultaneously loaded onto the NanoMate microtiter plate and infused contiguously in a high-throughput mode, following the same measurement methodology. All mass spectra were processed through Data Analysis 3.4 software from Bruker Daltonics (Bremen, Germany), which allows signal extraction, smoothing and subtraction. Proposals for molecular ion composition were pursued through exact mass calculation. All mass spectra were acquired in the mass range $100\text{--}2900 \text{ m/z}$, with a scan speed of 2.1 scans per second.

Results and discussion

Studies on calixarenes used for immobilization of various bioactive molecules, especially enzymes, have been previously reported, emphasizing the successful incorporation of the guest molecule in the macrocyclic cavity. As a further consequence, these macrocyclic derivatives facilitated the separation and purification of a target biocompound from a complex mixture. The importance of such macrocycles can be attested to by the fact that they, in view of their structural and physicochemical attributes, can act as synthetic receptors able to sustain stability, bioactivity and enantioselectivity of the guest compound, even when the latter pertains to high molecular mass proteins and enzymes (Yilmaz and Erdemir 2013). The advantageous reactivity properties, therefore, of calixarenes could be useful to natural products research, where a dire necessity exists for the development of efficient separation techniques enabling isolation of a specific bioactive compound, not unlike the ones mentioned above. Further delving into the specific area of research reveals that intimately associated with efficient separation processes from natural products are analytical techniques, contributing to the identification of the separated biomolecules (Neda et al. 2012; Popescu et al. 2011; Vaszilcsin et al. 2010). Presently, GC–MS represents one of the most useful analytical tools for the structural elucidation of compounds emerging from natural complex matrices (Leonards et al. 2011; Xu et al. 2009). Nevertheless, a derivatization step is usually required prior to GC analysis to increase volatility, decrease reactivity and enhance detectability of phytochemicals. Silylation is considered to be the most widely used derivatization method, although the presence of moisture causes dramatic decrease of the yield. It should be borne in mind, however, that silylated derivatives of amino acids exhibit low stability, thereby necessitating the discovery of new derivatization chemistries far more suitable and efficient (Villas-Bôas et al. 2011).

Poised to peruse the aforementioned area of natural products research, a comparative study was carried out on the utility of calixarene (Fig. 1) as a specific molecular platform for the selective extraction and recognition of amino acids from two plants extracts (*H. purpurascens* and *V. album*) using EZ:faast amino acids analysis. The involved approach presents clear advantages over the traditionally employed silylation method, i.e. rapidity, simplicity and reliability (with no interference problems), with the results showing that calixarene can (a) incorporate in its cavity amino acids, small and even relatively large peptides (8 amino acids), and (b) serve as a very selective extractant for amino acids from natural plant extracts (*H. purpurascens* and *V. album*).

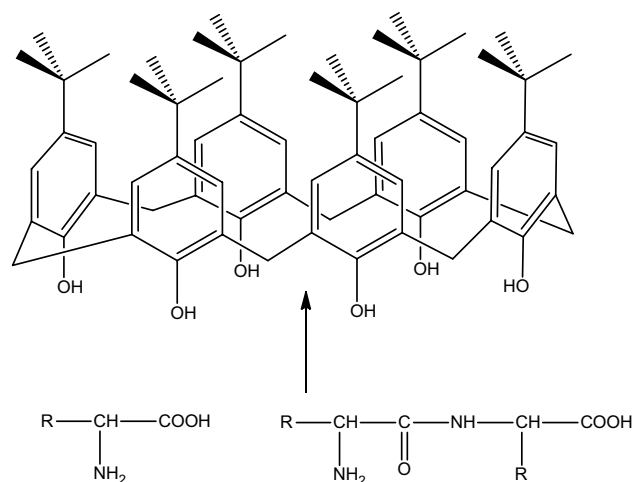


Fig. 1 Scheme of proposed of biomolecule incorporation in calixarene

GC–MS analysis

Molecular recognition of biomolecules extracted into the calixarene cavity was pursued by GC–MS analysis. Spectral data obtained from the peaks aided in the identification of the amino acid derivatives. The obtained total ion chromatograms (TIC) are shown in Figs. 2 and 3.

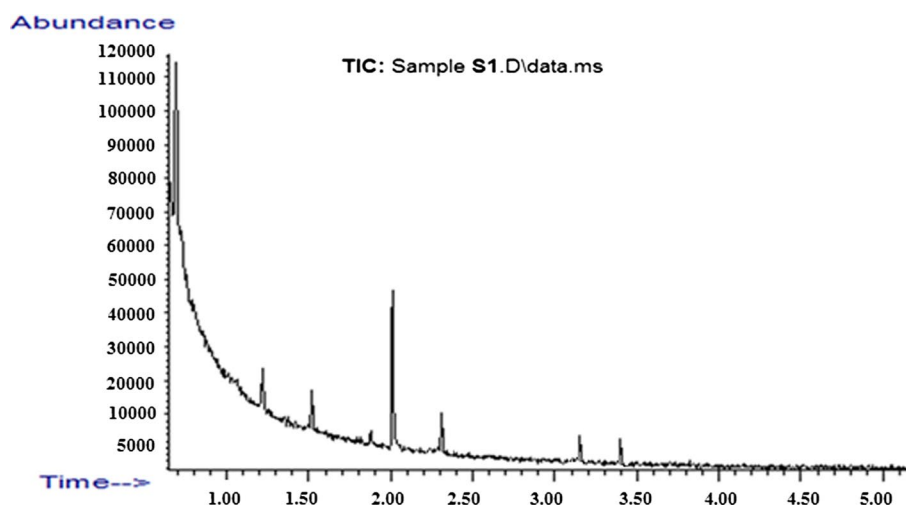
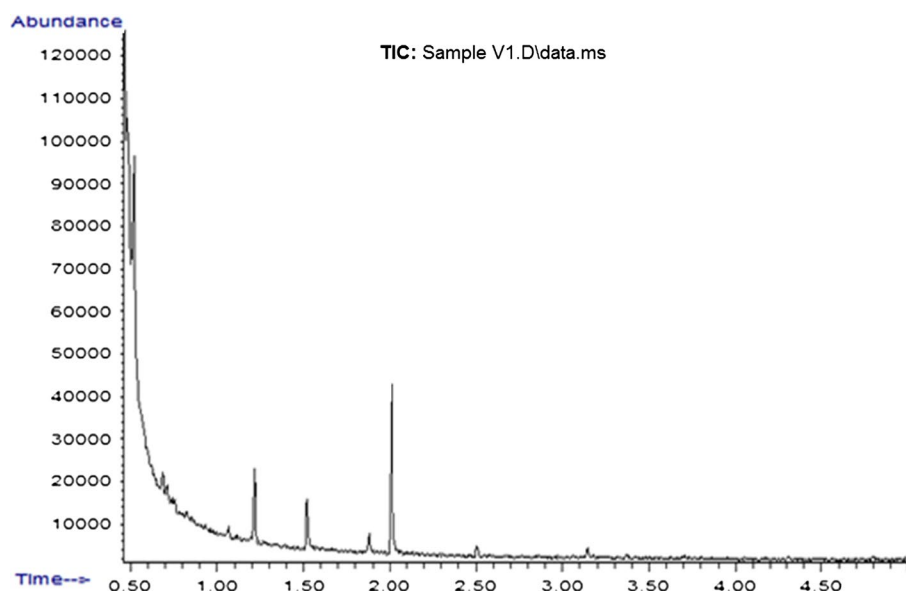
Component mass spectra extracted from the total ion chromatogram were compared with spectra in the NIST/NBS spectral database. The identified amino acids and peptides are presented in Table 1.

The results indicate that regardless of the nature of the plant extract, calixarene practically extracted the same amino acids from hellebore (S_I) and viscum (V_I). The sole difference between the samples appears to be the intensity of the TIC signals.

NanoESI chip MS analysis

To elucidate the chemical composition and nature of molecules extracted with calixarene, a novel mass spectrometry method was developed and applied, based on the fully automated nanoESI high-capacity ion trap (HCT). To this end, both extract samples and calixarene were submitted to high-throughput positive nanoESI chip MS screening under identical solution conditions and instrumental parameters. The full scan mass spectra generated under the employed conditions are shown in Figs. 4, 5 and 6, with the assignment of the detected ions and their corresponding amino acid and peptide structure(s) listed in Table 2.

Ostensibly, the results obtained by mass spectrometry confirmed the chemical structures detected by

Fig. 2 TIC of S_I extract**Fig. 3** TIC of V_I extract

chromatographic techniques. Although, the developed chromatographic analysis method provided information on almost all of the chemical species present in S_I and V_I , mass spectrometry provided an even larger collection of data, reflecting upon the complexity of the peptide structures found in the studied biomolecules associated with the calixarene cavity. Moreover, through positive mode nanoESI chip MS, we were able to identify peptide chains encompassing up to 8 amino acids (Table 2). To further highlight the existence of a selective binary interaction between host amino acids from the natural products (plant extract) in *V. album* and *H. purpurascens*, physical methods were also employed, including scanning electron microscopy and atomic force microscopy (Latterini and Tarpani 2012; Ludwig 2000; Ludwig and Thi Kim Dzung 2002).

Scanning electron microscopy

Scanning electron microscopy (SEM) was employed and specifically optimized to study the topography and host-guest complex assembly (calixarene–amino acids or peptides from plant extracts), with the emerging results being compared to the host molecule (calixarene). SEM was used to obtain more direct information on the host molecule morphology and final topography of the host-guest complex for both types of plant extracts. In this regard, the secondary electron image offers good resolution and provides detailed information about the host-guest complex surface morphology. Exemplifying the aforementioned thesis, Fig. 7a–e shows the amorphous structure of the host molecule (Fig. 7a) before and after the interaction with biomolecules from both plant extracts.

Table 1 Amino acids identified in S_I and V_I extracts

| Extract sample | Proposed structure | Abbreviation | SIM ^a |
|----------------|--------------------|--------------|------------------|
| S_I | Valine | Val | 72; 158 |
| | Cystine | C–C | 41; 42 |
| | Threonine | Thr | 101; 160 |
| | Leucine | Leu | 86; 162 |
| | Glycine | Gly | 74; 116 |
| | Glutamic acid | Glu | 38; 40 |
| | Phenylalanine | Phe | 59; 60 |
| V_I | Glutamic acid | Glu | 38; 40 |
| | Cystine | C–C | 41; 42 |
| | Phenylalanine | Phe | 59; 60 |
| | Glycine | Gly | 74; 116 |
| | Threonine | Thr | 101; 160 |
| | Valine | Val | 72; 158 |
| | Leucine | Leu | 86; 162 |

^a Selected-ion monitoring chromatogram

Accordingly, the amorphous structure of the host molecule (Fig. 7a) changes completely as a result of the (a) interaction with plant extracts and selective embedding of biomolecules in its cavity, and (b) formation of micron particles of polyhedral shape, with lengths of $\sim 6 \mu\text{m}$ and a width of $0.7 \mu\text{m}$ (Fig. 7b, c), corresponding to the *H. purpurascens* sample. The modification of the macrocyclic architecture upon incorporation of guest biomolecules from the hellebore extract(s) and host–guest complex formation can be seen in both Fig. 7b, c. The same behavior applies

to the viscum extract (Fig. 7d, e). In this case, the secondary electron images show formation of micron particles of polyhedral shape with lengths of $\sim 8 \mu\text{m}$ and a width of $0.5 \mu\text{m}$, throughout the amorphous structure of calixarene. Therefore, SEM analysis provides significant information about the (a) surface of the host molecule, and (b) morphology and topography of the guest compounds on a micro-metric scale, thereby confirming the selective interaction between the host and biomolecules from *V. album* and *H. purpurascens*.

Atomic force microscopy

Atomic force microscopy (AFM) analysis was performed to investigate the topography of the surface and architecture of the host and final products—compounds, specifically focusing on each host–guest complex (calixarene and biomolecules from plant extracts) (Latterini and Tarpani 2012). The emerging AFM images showed the surface geometry of calixarene and the resulting host–guest complex. The data obtained from AFM-3D representations provide significant information about the topography of the host–guest complex, and geometry of the macrocyclic synthetic receptor and biomolecules corresponding to each plant extract (S_I and V_I). In this sense, the derived AFM topography images of the macrocyclic compound (calixarene) and natural biomolecules (amino acids and small peptides) from each plant sample provide new knowledge about the interaction between the host and guest compounds as well as the architecture of the final products. In this regard, AFM-3D representations

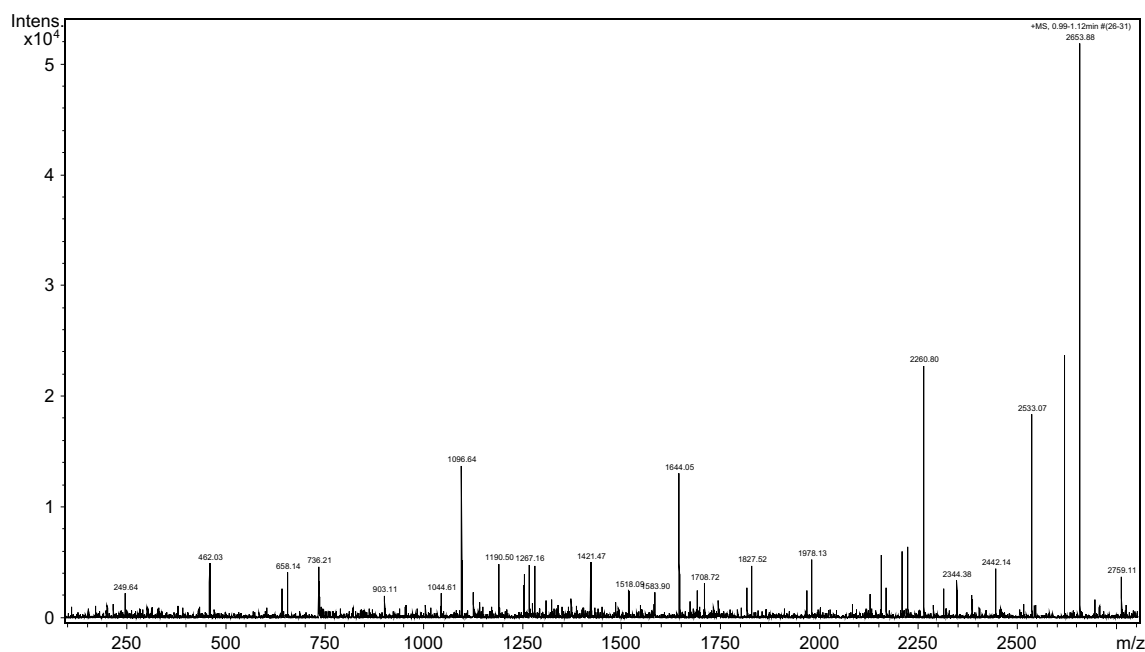


Fig. 4 Positive ion mode NanoESI chip MS of S_I extract

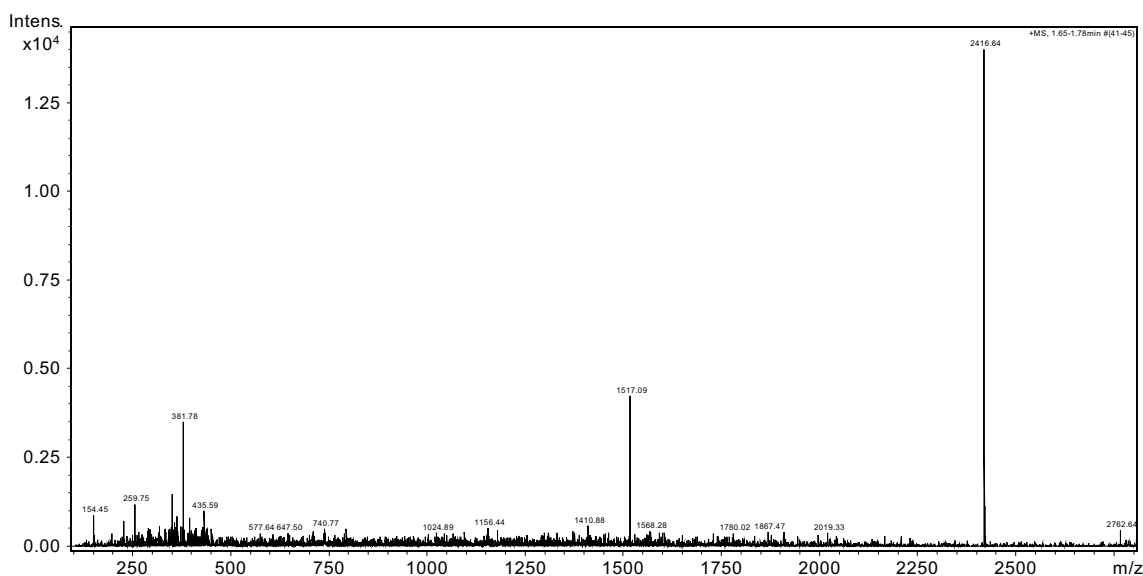


Fig. 5 Positive ion mode NanoESI chip MS of V_I extract

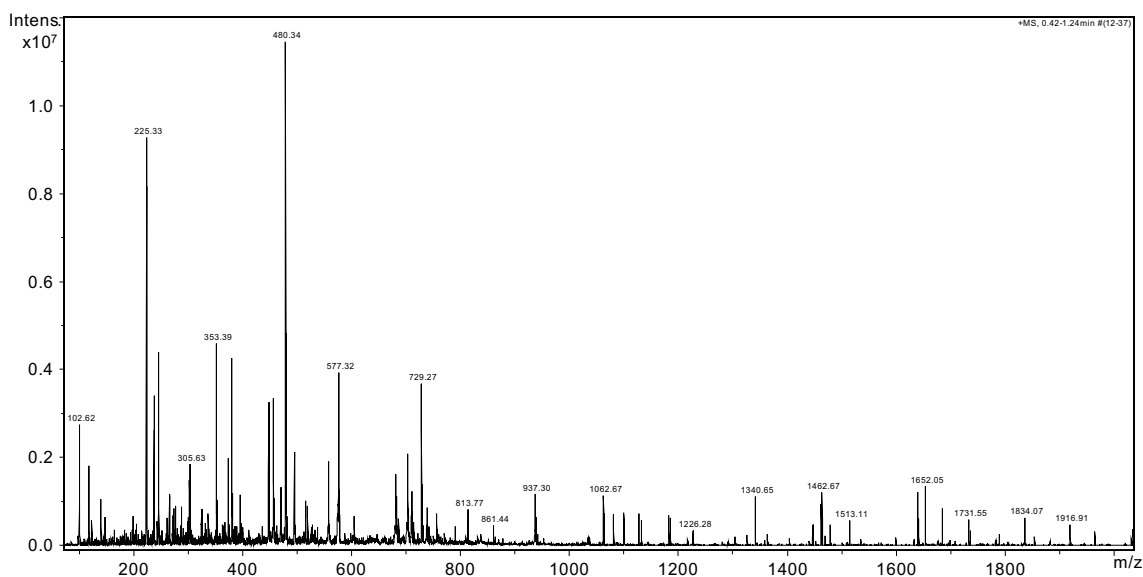


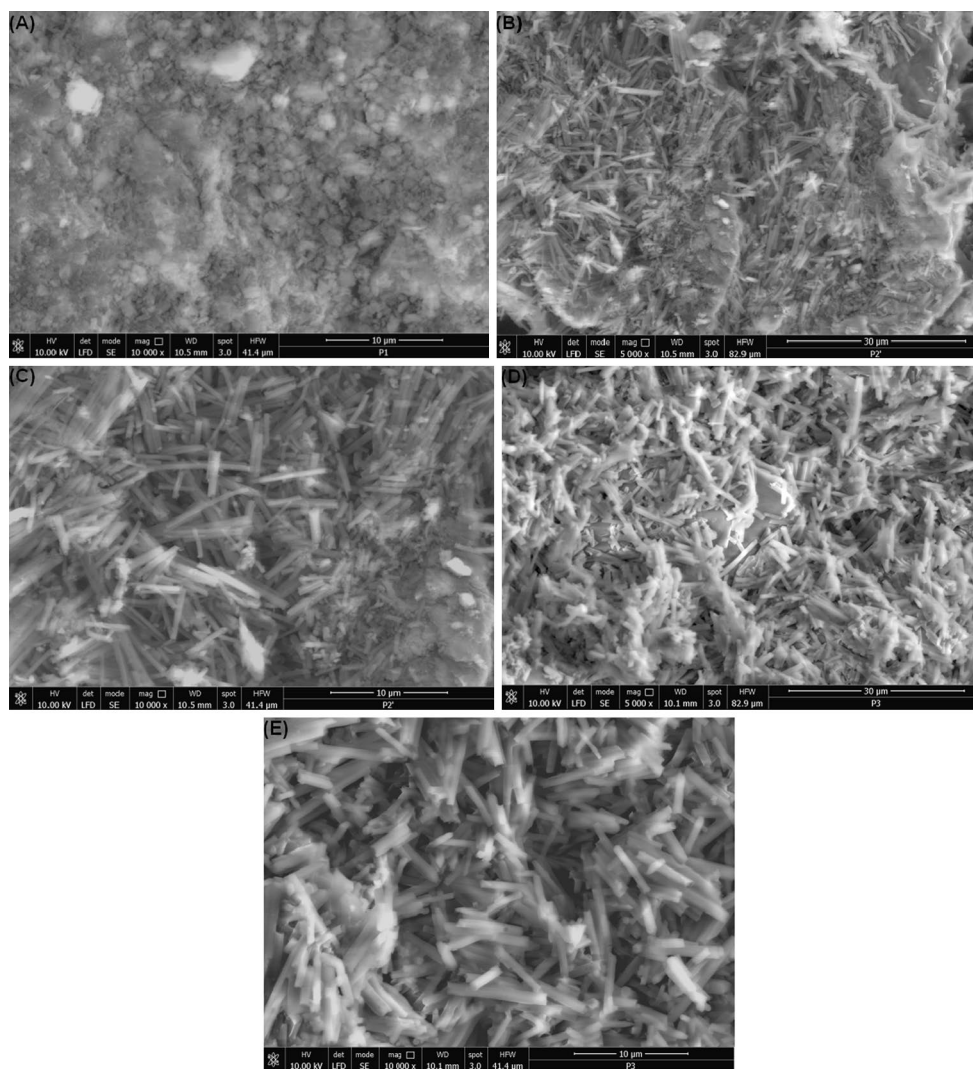
Fig. 6 Positive ion mode NanoESI chip MS of 4-tert-butyl-calix[6]arene

can clearly reveal an important modification of the host molecule surface topography ascribed to biomolecules isolated from the plant extracts. Figure 8a shows the topography of the host calixarene molecule prior to the interaction with biomolecules from the plant extracts. Figure 8b, c presents the topography of the final host–guest complex corresponding to S_I and V_I samples, respectively. The interaction between the calixarene derivative and biomolecules is easily discernible, as that can be attested to by the presence of well-defined shapes embedded in the host molecule structure, thereby exemplifying host–guest molecule interactions.

The same geometry of the guest compounds is also visible in Fig. 8b, c samples, exhibiting prominent forms of regular shape, with the guest species embedded in the host molecule structure alongside individual less defined sections or irregular formations. Analysis of the AFM representation, in terms of dimensionality, can lead to the observation of a small difference between the geometric dimensions of the two guest compounds. This can be explained by the existence of two types of biomolecules (amino acids and peptide) interacting with calixarene. Analysis of the AFM-3D representations (Fig. 8a–c)

Table 2 Amino acid and peptide species in plant extracts detected by MS

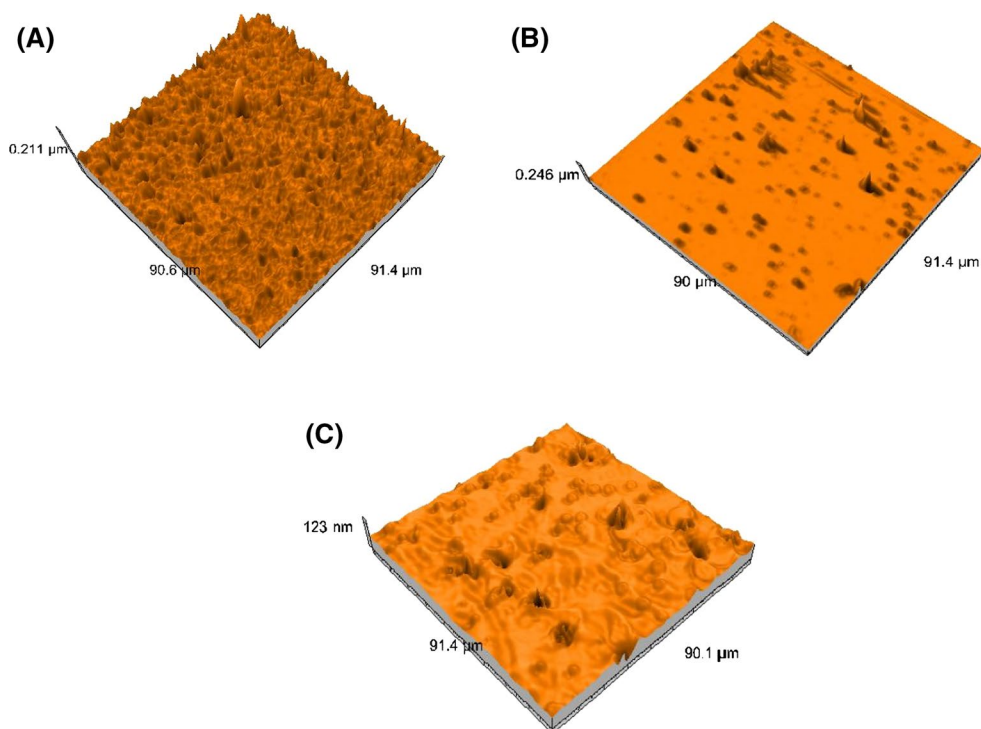
| Extract sample | Type of molecular ion | m/z detected | m/z calculated | Proposed structure |
|----------------|-----------------------|--------------|----------------|---------------------------------|
| S_I | $[M+H_2O+H]^+$ | 249.64 | 249.23 | Thr-Glu |
| | $[M+NH_3]^+$ | 462.03 | 461.56 | C-C-Phe-Gly |
| | $[M+H_2O+2H]^{2+}$ | 658.14 | 658.74 | Phe-Thr-Gly-Val-Phe |
| | $[M+H_2O+2H]^{2+}$ | 736.21 | 736.57 | C-C-Glu-Thr-Phe-Val |
| | $[M+H_2O+2H]^{2+}$ | 903.11 | 903.2 | Leu-Cys-Phe-Cys-Thr-Cys-Val-Leu |
| V_I | $[M+NH_3]^+$ | 259.75 | 259.38 | Leu-Glu |
| | $[M+2H]^{2+}$ | 381.78 | 381.45 | Cys-Phe-Glu |
| | $[M+H_2O+H]^+$ | 435.59 | 435.56 | Cys-Leu-Thr-Val |
| | $[M+H_2O+H]^+$ | 647.5 | 647.5 | C-C-Phe-Leu-Gln |
| | $[M+2H]^{2+}$ | 740.77 | 740.01 | Leu-Cys-Phe-Cys-Leu-Thr-Gly |

Fig. 7 SEM micrographs showing host molecule surface morphology before and after interaction with plant extract biomolecules

reveals significant modification of calixarene topography and the presence of guest structural formations arranged in an orderly fashion in the host molecule, thus demonstrating that the actual effect is due to the interaction between

the synthetic receptor (calixarene) and the natural biomolecules. The specific results were corroborated by SEM (Fig. 7a-e).

Fig. 8 AFM-3D images showing host molecule surface topography before and after interaction with plant extract biomolecules



Conclusions

The presented study investigated the selective extraction capability of 4-tert-butyl-calix[6]arene (calixarene) toward amino acids and small peptides from complex mixtures of two highly important medicinal herbs (hellebore and viscum). The natural biomolecules separated from plant extracts were identified through modern analytical methodologies involving chromatography (GC–MS) and chip-based nanoESI mass spectrometry. The presence of interactions between the synthetic receptor (calixarene) and the natural biomolecules was demonstrated by scanning electronic microscopy and atomic force microscopy. The collective results suggest that incorporation of natural biomolecules into the calixarene cavity is due both to the molecular construction (cavity size) and compatibility of the host molecule with suitable guests, selectively and efficiently interacting with amino acids and peptides from natural products, thereby justifying further applied research and development of host–guest technology in the specific field.

Acknowledgments The study was supported by Romania–China Bilateral Grant nr. 628/2013: BIOSIM—“*Study on Activity and Potential Drug Interactions of Immunomodulating Natural Products*”. We would like to thank Dr. A. D. Zamfir, I. Neda and Dr. M. Birdeanu (INCEMC Timisoara) for their contribution to this paper.

Compliance with ethical standards

Conflict of interest The authors declare that they have no conflict of interest.

References

- Atwood JL, Steed JW (2004) Encyclopedia of Supramolecular Chemistry vol.1, CRC Press
- Bart HJ, Pilz S (2011) Industrial scale natural products extraction, 1st edn. Wiley-VCH Verlag GmbH & Co. KGaA, Weinheim
- Fiehn O, Kopka J, Trethewey RN, Willmitzer L (2000) Identification of uncommon plant metabolites based on calculation of elemental compositions using gas chromatography and quadrupole mass spectrometry. *Anal Chem* 72:3573–3580
- Gutsche CD (2008) Calixarenes: an introduction, monographs in supramolecular chemistry. Royal Society of Chemistry, Cambridge
- Hassen WM, Martelet C, Davis F, Higson SPJ, Abdelghani A, Helali S, Jaffrezic-Renault N (2007) Calix[4]arene based molecules for amino-acid detection. *Sens Actuators B* 124:38–45
- Ikeda A, Shinkai S (1997) Novel cavity design using calix[n]arene skeletons: towards molecular recognition and metal binding. *Chem Rev* 97:1713–1734
- Karpagasundari C, Kulothungan S (2014) Analysis of bioactive compounds in *Physalis minima* leaves using GC MS, HPLC, UV-VIS and FTIR techniques. *J Pharmacogn Phytochem* 3:196–201
- Koh K, Araki K, Shinkai S, Asfari Z, Vicens J (1995) Cation binding properties of a novel 1,3-alternate calix[4]bis crown formation of 1:1 and 1:2 complexes and unique cation tunneling across a calix[4]arene cavity. *Tetrahedron Lett* 36:6095–6098
- Latterini L, Tarpani L (2012) AFM measurements to investigate particulates and their interactions with biological macromolecules. In: Frewin C (ed) Atomic force microscopy investigations into biology—from cell to protein. InTech, Rijeka, pp 87–98
- Leonards PEG, Brix R, Barceló D, Lamoree M (2011) Advanced GC–MS and LC–MS tools for structure elucidation in effect-directed analysis. In: Brack W (ed) Effect-directed analysis of complex environmental contamination, the handbook of environmental chemistry, vol 15. Springer, Berlin, pp 143–165

- Ludwig R (2000) Calixarenes in analytical and separation chemistry. *Fresenius J Anal Chem* 367:103–128
- Ludwig R (2005) Calixarenes for biochemical recognition and separation. *Microchim Acta* 152:1–19
- Ludwig R, Thi Kim Dzung N (2002) Calixarene-based molecules for cation recognition. *Sensors* 2:397–416
- Mutihac L, Buschmann HJ, Mutihac RC, Schollmeyer E (2005) Complexation and separation of amines, amino acids and peptides by functionalized calix[n]arenes. *J Incl Phenom Macrocyclic Chem* 51:1–10
- Neda I, Vlazan P, Pop RO, Sfirloaga P, Grozescu I, Segneanu AE (2012) Peptide and amino acids separation and identification from natural products. In: Krull IS (ed) *Analytical chemistry*. InTech, Rijeka, pp 135–146
- Oshima T, Goto M, Furusaki S (2002) Extraction behavior of amino acids by calix[6]arene carboxylic acid derivatives. *J Incl Phenom Macrocyclic Chem* 43:77–86
- Popescu C, Fitigău F, Segneanu AE, Martagiu R, Vaszilcsin CG (2011) Separation and characterization of anthocyanins by analytical and electrochemical methods. *Environ Eng Manag J* 10(5):697–701
- Shimojo K, Oshima T, Goto M (2004) Calix[6]arene acetic acid extraction behavior and specificity with respect to nucleobases. *Anal Chim Acta* 521:163–171
- Sikorka M, Matlawska I, Glowniak K, Zgorka G (2000) Qualitative and quantitative analysis of phenolic acids in *Asclepias Syriaca* L. *Acta Pol Pharm Drug Res* 57:69–72
- Sirit A, Yilmaz M (2009) Chiral calixarenes. *Turk J Chem* 33:159–200
- Stone MM, Franz AH, Lebrilla CB (2002) Non-covalent calixarene amino acid complexes formed by MALDI-MS. *J Am Soc Mass Spectr* 13:964–974
- Vaszilcsin CG, Segneanu AE, Balcu I, Fitigău F, Mirica MC (2010) Eco-friendly extraction and separation methods of capsaicines. *Environ Eng Manag J* 9(7):971–976
- Villas-Bôas SG, Smart K, Sivakumaran S, Lane GA (2011) Alkylation or silylation for analysis of amino and non-amino organic acids by GC-MS? *Metabolites* 1:3–20
- Xu JZ, Shen J, Cheng Y, Qu H (2009) GC-MS analysis of amino acids in extract of *Cornus Caprae* hircus. *Chem Res Chin Univ* 25:812–816
- Yilmaz M, Erdemir S (2013) Calixarene-based receptors for molecular recognition. *Turk J Chem* 37:558–585

Waste Water Treatment Methods

Adina Elena Segneanu, Cristina Orbeci, Carmen Lazau,
Paula Sfirloaga, Paulina Vlazan, Cornelia Bandas and Ioan Grozescu

Additional information is available at the end of the chapter

<http://dx.doi.org/10.5772/53755>

1. Introduction

The last decades have shown a reevaluation of the issue of environmental pollution, under all aspects, both at regional and at international level. The progressive accumulation of more and more organic compounds in natural waters is mostly due to the development and extension of chemical technologies for organic synthesis and processing.

Population explosion, expansion of urban areas increased adverse impacts on water resources, particularly in regions in which natural resources are still limited. Currently, water use and reuse has become a major concern. Population growth leads to significant increases in default volumes of waste water, which makes it an urgent imperative to develop effective and affordable technologies for wastewater treatment.

The physico-chemical processes common treatment (coagulation and flocculation) using various chemical reagents (aluminum chloride or ferric chloride, polyelectrolytes, etc.) and generates large amounts of sludge. Increasing demands for water quality indicators and drastic change regulations on wastewater disposal require the emergence and development of processes more efficient and more effective (ion exchange, ultrafiltration, reverse osmosis and chemical precipitation, electrochemical technologies). Each of these treatment methods has advantages and disadvantages.

Water resources management exercises ever more pressing demands on wastewater treatment technologies to reduce industrial negative impact on natural water sources. Thus, the new regulations and emission limits are imposed and industrial activities are required to seek new methods and technologies capable of effective removal of heavy metal pollution loads and reduction of wastewater volume, closing the water cycle, or by reusing and recycling water waste.

Advanced technologies for wastewater treatment are required to eliminate pollution and may also increase pollutant destruction or separation processes, such as advanced oxidation

methods (catalytic and photocatalytic oxidation), chemical precipitation, adsorption on various media, etc.. These technologies can be applied successfully to remove pollutants that are partially removed by conventional methods, e.g. biodegradable organic compounds, suspended solids, colloidal substances, phosphorus and nitrogen compounds, heavy metals, dissolved compounds, microorganisms that thus enabling recycling of residual water. (Zhou, 2002) Special attention was paid to electrochemical technologies, because they have advantages: versatility, safety, selectivity, possibility of automation, environmentally friendly and requires low investment costs (Chen, 2004; Hansen et. al., 2007).

The technologies for treating wastewater containing organic compounds fall within one of the following categories:

- Non-destructive procedures – based on physical processes of adsorption, removal, stripping etc.
- Biological destructive procedures – based on biological processes using active mud.
- Oxidative destructive processes – based on oxidative chemical processes which, in their turn, can fall within one of the following categories:
 - Incineration;
 - WO - "Wet Oxidation", operating in conditions of high temperature and pressure, with the versions:
 - WAO - "Wet Air Oxidation" (wet oxidation with O₂ air oxidative agent);
 - CWAO - "Catalytic Wet Air Oxidation" (catalytic wet oxidation with O₂ air oxidative agent);
 - SWA - "Supercritical Water Oxidation" (oxidation with O₂ air oxidative agent in supercritical conditions).
 - Liquid oxidation: AOPs - "Advanced Oxidation Processes", operating in conditions of temperature and pressure and use as oxidative agents O₃, H₂O₂ and even O₂, catalysts and/ or UV radiations.

2. Advanced oxidation processes

Advanced oxidation processes (AOPs) are widely used for the removal of recalcitrant organic constituents from industrial and municipal wastewater. In this sense, AOP type procedures can become very promising technologies for treating wastewater containing non-biodegradable or hardly biodegradable organic compounds with high toxicity. These procedures are based on generating highly oxidative HO radicals in the reaction medium.

- H₂O₂
 - H₂O₂ + UV (direct photolysis)
 - H₂O₂ + Fe^{2+/3+} (classic, homogeneous Fenton)
 - H₂O₂ + Fe/support (heterogeneous Fenton)
 - H₂O₂ + Fe^{2+/3+} + UV (VIS) (Photo-Fenton)

- O₃
 - O₃ (direct ozone feeding)
 - O₃ + UV (photo-ozone feeding)
 - O₃ + catalysts (catalytic ozone feeding)
- H₂O₂ + O₃
 - TiO₂ (heterogeneous catalysis)
 - TiO₂ + UV (photo-catalysis)

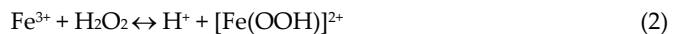
The preferential use of H₂O₂ as oxidative agent and HO radicals generator is justified by the fact that the hydrogen peroxide is easy to store, transported and used, and the procedure is safe and efficient.

The technologies developed so far indicate the use of zeolites, active coal, structured clay, silica textures, Nafion membranes or Fe under the form of goethite (α -FeOOH), as support materials for the catalytic component.

The AOPs (Advanced Oxidation Processes) can be successfully used in wastewater treatment to degrade the persistent organic pollutants, the oxidation process being determined by the very high oxidative potential of the HO· radicals generated into the reaction medium by different mechanisms (*Pera-Titus et al., 2004*).

AOPs can be applied to fully or partially oxidize pollutants, usually using a combination of oxidants. Photo-chemical and photocatalytic advanced oxidation processes including UV/H₂O₂, UV/O₃, UV/H₂O₂/O₃, UV/H₂O₂/Fe²⁺(Fe³⁺), UV/TiO₂ and UV/H₂O₂/TiO₂ can be used for oxidative degradation of organic contaminants. A complete mineralization of the organic pollutants is not necessary, being more worthwhile to transform them into biodegradable aliphatic carboxylic acids followed by a biological process (*Wang and Wang, 2007*).

The oxidation process is determined by the very high oxidative potential of the HO· radicals generated into reaction medium by different mechanisms. In the case of the AOPs Fenton-type procedure (hydrogen peroxide and Fe²⁺ as catalyst), the generation of hydroxyl radicals takes place through a catalytic mechanism in which the iron ions play a very important role (*Andreozzi et al., 1999; Esplugas, et al., 2002*) the main reactions involved being presented in equations (1) – (4):



In the presence of UV radiations (photo-Fenton process), an additional number of HO· radicals are produced both through direct H₂O₂ photolysis and through UV radiations interaction with the iron species in aqueous solutions (eq. 5-7) (*Spacek et al., 1995; Pignatello, J.J., 1992*):



The main parameters which determine the efficiency of the oxidation process are: the structure of the organic compounds, the hydrogen peroxide and the catalyst concentrations, the wave length and intensity of UV radiations, the initial solution pH and the reaction contact time.

As recalcitrant organic pollutants continue to increase in air and wastewater streams, environmental laws and regulations become more stringent (Gayaa et al, 2008). The main causes of surface and groundwater contamination are industrial effluents (even in small amounts), excessive use of pesticides, fertilizers (agrochemicals) and domestic waste landfills. Wastewater treatment is usually based on physical and biological processes. After elimination of particles in suspension, the usual process is biological treatment (natural decontamination), but unfortunately, some organic pollutants, classified as bio-recalcitrant, are not biodegradable. In this way advanced oxidation processes (AOPs) may become the most widely used water treatment technologies for organic pollutants not treatable by conventional techniques due to their high chemical stability and/or low biodegradability (Munoz et al.2005). Advanced oxidation processes are indicated for removal of organic contaminants such as halogenated hydrocarbons (trichloroethane, trichlorethylene), aromatics (benzene, toluene, and xylene), pentachlorophenol (PCP), nitrophenol, detergents, pesticides, etc. These processes can also be applied to oxidation of inorganic contaminants such as cyanides, sulfides and nitrites (Munter, 2001). A general classification of advanced oxidation processes based on source allowing radicals. This classification is presented in Figure 1.

Heterogeneous photocatalysis has proved to be of real interest as efficient tool for degrading both aquatic and atmospheric organic contaminants because this technique involved the acceleration of photoreaction in presence of semiconductor photocatalyst (Guillard, 1999). Thus these processes can be classified in: advanced oxidation processes based on ozone based advanced oxidation processes H₂O₂, photocatalysis, POA "hot" technologies based on ultrasound, electrochemical oxidation process, oxidation processes with electron beam. These processes involve generation and subsequent reaction of hydroxyl radicals (·OH), which are one of the most powerful oxidizing species. Photocatalytic reaction is initiated when a photoexcited electron is promoted from the filled valence band of semiconductor photocatalyst to the empty conduction band as the absorbed photon energy, h_ν, equals or exceeds the band gap of the semiconductor photocatalyst leaving behind a hole in the valence band. Thus in concert, electron and hole pair (e⁻-h⁺) is generated (Horvath, 2003). An ideal photocatalyst for photocatalytic oxidation is characterized by the following attributes: photo-stability, chemically and biologically inert nature, availability and low cost

(Carp et al., 2004). Many semiconductors such as TiO_2 (Lazau, 2011), ZnO (Daneshvar et al., 2007), ZrO_2 (Lopez et al. 2007), CdS (Yingchun, 2011), MoS_2 (Kun Hong, 2011), Fe_2O_3 (Seiji, 2009) and WO_3 (Yuji, 2011) have been examined and used as photocatalysts for the degradation of organic contaminants. TiO_2 is most preferred one due to its chemical and biological inertness, high photocatalytic activity, photodurability, mechanical robustness and cheapness. Thus, these materials were used in the degradation of phenol, 1,4-dichlorobenzene (Papp et al., 1993), methanol (Nobuaki et al., 2007), azo dye (Daneshvar, 2003), trichloromethane, hexachloro cyclohexane (Byrappa et al., 2002), trichloroethylene and dichloropropionic acid (Nikola, 2001). To avoid the problem of filtration, many methods were proposed to immobilize the photocatalysts, but in these conditions the photocatalyst is expected to be used for a relatively long time, especially for industrial applications (Venkata, 2004). Various substrates have been used as a catalyst support for the photocatalytic degradation of polluted water. For example glass materials: glass mesh, glass fabric, glass wool, glass beads and glass reactors were very commonly used as a support for titania. Other uncommon materials such as microporous cellulosic membranes, alumina clays, ceramic membranes, monoliths, zeolites, and even stainless steel were also experimented as a support for TiO_2 (Gianluca, 2008).

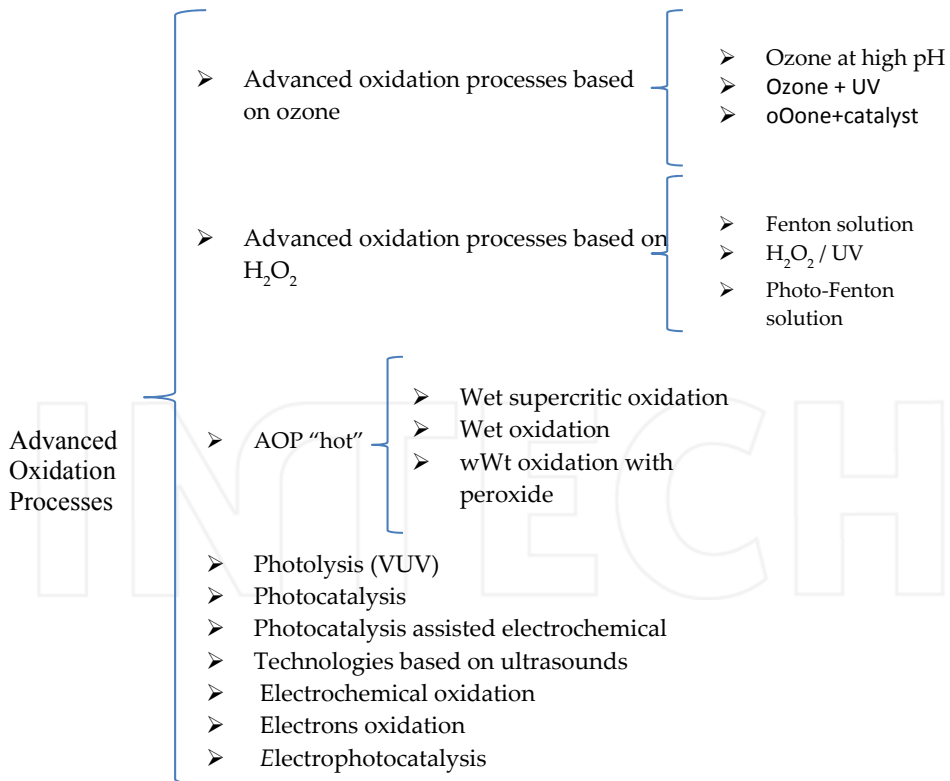


Figure 1. Classification of advanced oxidation processes

Advanced oxidation processes (AOPs) and electrochemical oxidation is based on the in-situ generation of OH radicals, which allow its non-selective reaction with organics allowing organics mineralization by its conversion into CO₂. The electrochemical methods are very promising alternatives for organics degradation because of their environmental compatibility, versatility, simplicity, and easy possibility of automation. The electrochemical oxidation performance depends strongly on the electrode material. To generate OH radicals by electrooxidation, several types of anodes with high overpotential for oxygen potential are suitable, i.e., DSA-type, PbO₂, boron-doped diamond (BDD) electrodes etc. Recently, electrochemical oxidation with a boron-doped diamond electrode is one of the most promising technologies in the treatment of the industrial effluents containing organics. BDD electrode exhibited a very good chemical stability and its application in the electrooxidation of organics led to complete mineralization into CO₂ in relation with applied potential or current density. A major drawback of the electrochemical oxidation consists of the high energy consumption to the mineralization. The presence of a catalyst in the electrical field or combined and direct photoelectrochemical application can enhance the treatment efficiency with lower energy consumption (Ratiu et. al., 2010).

Electrochemical and photochemical technologies may offer an efficient means of controlling pollution. Their effectiveness is based on the generation of highly reactive and non-selective hydroxyl radicals, which are able to degrade many organic pollutants. Electrolysis, heterogeneous photocatalysis, or photo-assisted electrolysis may be regarded as advanced oxidation processes (AOPs) and used in the supplementary treatment of wastewaters. The efficiency of the electrochemical oxidation depends on the anode material and the operating conditions, e.g., current density or potential. In general, in most applications of photoelectrocatalysis in the degradation of organics, the applied anodic bias potential is lower than the oxidation potential of organics on the electrode, due to direct electro-oxidation does not complicate the photocatalytic mechanism (Ratiu et. al.,2011).

The efficiency of photoelectrochemical degradation for organic pollutants depends not only on the selection of a suitable supporting electrolyte and pH values, but also on the electrode potential and preparation conditions of the semiconductors involved. In a photoelectrochemical system, photoelectrons and photoholes can be separated under the influence of an applied electric field. The problem of the separation of semiconductor particles from the treated solution, so persistent in heterogeneous photolysis, is not an issue in photoelectrochemical systems. There are numerous semiconductors which can be used as photoelectrocatalytic materials, such as TiO₂, WO₃, SnO₂, ZnO, CdS, diamond, and others (Hepel 2005).

2.1. Particular aspects

In the case of the chlorinated phenols, the number and the position on aromatic ring of the chlorine atoms modifies the oxidation efficiency (Pera-Titus et al., 2004).

The oxidation rate constant decreases linearly with increasing number of chlorine content on the aromatic ring. Also, the increase of chlorine content will block some favorable positions susceptible to hydroxyl radical attack.

The oxidation process is also controlled by the presence of another species in reaction medium (intermediate products) in the sense that they interact with the catalyst component in a different manner. The species of reductive character accelerate the oxidation process because they reduce Fe^{3+} (inactive) to Fe^{2+} (active) and thus the generation of $\text{OH}\cdot$ radicals intensifies (Du et al. 2006; Riga, A., et al, 2007). The acid type species lower the pH of the reaction medium and can form stable complexes with Fe^{3+} or Fe^{2+} ions, strongly slowing the oxidation process. The presence into reaction medium of the inorganic ionic species (Cl^- , ClO_4^- , NO_3^- , HCO_3^- , CO_3^{2-} , SO_4^{2-} , H_2PO_4^-) modifies the rate of the oxidation of the organic compounds as function of their nature and concentration. The inorganic anions can change the overall efficiency of the system by different ways. The influence of ClO_4^- and NO_3^- ions is less pronounced than another anions because they do not form complexes with Fe(II) and Fe(III) and do not react with $\text{HO}\cdot$ (Lu et al., 1997; Siedlecka, E. M., 2007). Cl^- , SO_4^{2-} and H_2PO_4^- anions decrease the rate of decomposition of H_2O_2 by forming ferric unreactive complexes and react with hydroxyl radicals forming $\text{Cl}_2\cdot^-$, $\text{SO}_4\cdot^-$ and $\text{H}_2\text{PO}_4\cdot$ radicals who are less or much less reactive than $\text{HO}\cdot$ (Siedlecka, E. M., 2007; De Laet et al., 2004). The influence of Cl^- is in correlation with the solution pH and its concentration, being insignificant at low concentration (<5 mM) but becomes very important at higher concentration values (>28 mM) (Kwon et al., 1999). As function of the nature of the inorganic anions, at higher concentration of 0.1 M, the inhibition order of the oxidation rate is the following: $\text{H}_2\text{PO}_4^- > \text{Cl}^- > \text{HCO}_3^- > \text{CO}_3^{2-} > \text{SO}_4^{2-} > \text{NO}_3^-$ (Riga, A., et al., 2007).

The presence of the inorganic species inside the reaction medium influences the rate of the oxidation process as function of their nature and concentration. The inorganic anionic species reduce the 4-CP oxidation efficiency by Fe(II) and Fe(III) complexes forming, $\text{HO}\cdot$ radicals scavenging or iron precipitate forming.

NO_3^- induces a small influence on 4-CP oxidation efficiency. This may be explained by the absence of the interactions between NO_3^- and the catalyst ($\text{Fe}^{2+/3+}$) and hydroxyl radicals. The anions Cl^- , SO_4^{2-} and PO_4^{3-} modify drastically the 4-CP oxidation efficiency, especially at high concentration into reaction medium. They interact with Fe^{2+} and Fe^{3+} forming chloro-, sulfato- and phosphate-iron complexes which are inactive in $\text{HO}\cdot$ generation mechanism. Also, Cl^- , SO_4^{2-} and H_2PO_4^- anions interact with hydroxyl radicals (scavenging process), forming less reactive species ($\text{Cl}_2\cdot^-$, $\text{SO}_4\cdot^-$ and $\text{H}_2\text{PO}_4\cdot$) into reaction medium.

The decrease of the 4-CP oxidation degree by the photo-Fenton procedure is correlated with the nature of the anions as following: $\text{Cl}^- > \text{PO}_4^{3-} > \text{SO}_4^{2-} \gg \text{NO}_3^-$ (Orbeci et al., 2008).

The presence of the insoluble inorganic species (bentonite) modifies the 4-CP oxidation efficiency in different manner. Into reaction medium, 4-CP can be adsorbed by the bentonite substratum or can be destruct by oxidation, both processes increasing the 4-CP removal degree from the solution. The presence of the insoluble inorganic species (bentonite) modifies the oxidation efficiency by additional 4-CP and UV sorption processes, especially at high solution turbidity values (Orbeci et al., 2008).

The efficiency of the various AOPs depends both on the rate of generating the free radicals and the extent of contact between the radicals and the organic compound. Also, the pH has a significant role in determining the efficiency of Fenton and photo-Fenton oxidation processes (Gogate and Pandit, 2004). Limitations due to the use of homogeneous catalysts, such as limited pH range, production of Fe containing sludge, and deactivation could be overcome by heterogeneous catalysts.

The optimum pH range in the case of homogeneous photo-Fenton process is 2.5-4, a correction of solution pH being necessary. Also, at the end of the oxidation process, iron precipitation and catalyst separation and recovery are necessary. These disadvantages can be avoided using the heterogeneous photo-Fenton procedure by immobilization of active iron species on small particulate solid supports. In this case, different iron-containing catalysts can be used, such as the iron bulk catalysts (iron oxy-hydroxyl compounds: hematite, goethite, magnetite) or iron supported catalysts (zeolites, clays, bentonite, glass, active carbon, polymers etc.) (Duarte and Madeira, 2010; Feng et al., 2005; He et al., 2005; Leland and Bard, 1987; Nie et al., 2008; Ortiz de la Plata et al., 2010; Vinita et al. 2010).

The use of the heterogeneous photo-Fenton procedure in the catalytic component version (Fe in various oxidation states) precipitated on solid support presents several drawbacks:

- catalyst's relatively high cost – associated with the cost of the so-called support, with the cost of the Fe compounds and with the operations necessary for Fe compounds to fix on the support;
- decrease in the efficiency of the UV radiations due to their partial adoption on the solid support;
- progressive solubility of the catalytic component (Fe) during oxidative processes and as a result of a progressive loss of catalytic activity.

In the case of the heterogeneous photo-Fenton process, a relevant fraction of the incident UV radiation can be lost via scattering, due to particulate solid support suspended into the reaction medium. As a consequence, the photo-Fenton process may be seriously affected (Herney-Ramirez et al., 2010). Also, the solution pH affects the iron leaching from the support, at pH values less than 3 a higher amount of iron being released into the solution (Duarte and Madeira, 2010). By using a zero-valent iron with iron oxide composite catalysts, the oxidation process proceeds via hydroxyl radicals generated from $\text{Fe}^{2+}(\text{surf})$ species and H_2O_2 in a Fenton like mechanism. The $\text{Fe}^{2+}(\text{surf})$ species are formed by electron transfer from Fe^0 to Fe^{3+} at the interface metal/oxide (Moura et al., 2005, 2006). The experimental data (Nie et al., 2008) indicate that the hydrogen peroxide provides a driving force in the electron transfer from Fe^{2+} to Fe^{3+} , while the degradation of organic pollutants increases the electron transfer at the interface of Fe^0 /iron oxide due to their reaction with hydroxyl radicals.

The degradation of organic pollutants using photo-Fenton processes occurs by intermediate oxidation products formation. In the case of phenol oxidation by Fenton reagent, a series of intermediates were identified, corresponding mainly to ring compounds and short-chain organic acids (Zazo et al., 2005). Most significant among the former were catechol,

hydroquinone, and *p*-benzoquinone; the main organic acids were maleic, acetic, oxalic, and formic, with substantially lower amounts of muconic, fumaric, and malonic acids. Oxalic and acetic acid appeared to be fairly refractory to the Fenton oxidation process. In the Fenton process, carboxylic acids like acetic and oxalic acid may be formed as end products during the degradation of phenol while in photo-Fenton process, both these acids were identified during the early stages of phenol degradation and were oxidized almost completely at the end of the process (Kavitha and Palanivelu, 2004). The chlorophenols are common persistent organic contaminants, which show low biodegradability, posing serious risks to the environment once discharged into natural water (Du *et al.*, 2006).

Studying the degradation of 4-chlorophenol by an electrochemical advanced oxidation process, several authors (Wang and Wang, 2007) have proposed the following possible pathways: (a) 4-chlorophenol dechlorination to phenol; (b) hydroxylation of phenol to hydroquinone; (c) dehydrogenation of hydroquinone to benzoquinone; (d) oxidation of benzoquinone (with aromatic ring cleavage) to aliphatic carboxylic acids such as maleic acid, fumaric acid, malonic acid; (e) oxidation of maleic and fumaric acids to oxalic acid, formic acid and finally, to carbon dioxide and water.

The main intermediate products detected by HPLC analyses were chlorocatechol and benzoquinone after 60 min reaction time and aliphatic carboxylic acids after 120 min reaction time. Benzoquinone and hydroquinone-like intermediates such as catechol, hydroquinone and 4-chlorocatechol can reduce the ferric ion to ferrous ion and the oxidation process becomes faster (Du *et al.*, 2006). It is not necessary to degrade 4-chlorophenol to the final products of CO₂ and H₂O, being more worthwhile to treat to the biodegradable stage-aliphatic carboxylic acids followed by a biological process (Wang and Wang, 2007). The photocatalytic processes may be used as a pre-treatment of toxic chemicals, including chlorophenols, in order to convert them into fully biodegradable compounds.

Recently, a series of pharmaceuticals such as analgesics, antibiotics, steroids etc. have been detected in the water feeding systems of several countries in Europe, the USA and Australia (Bound and Voulvoulis, 2004; Kaniou *et al.*, 2005). Unless antibiotics are removed from wastewaters through specific purification processes, they can affect the microbial communities in filtering systems using active sludge and, in general, the bacteria found in water, and, as a result, they can disturb the natural elementary cycles. The accumulation of antibiotics in surface waters represents a potential danger in the case in which they are used as sources of drinking water. Photocatalytic oxidation of antibiotics in aqueous solution is based on the oxidative potential of the HO radicals (2.80 V) generated in the reaction medium through photocatalytic mechanisms, in the presence of H₂O₂ and UV radiations. Through the photo-Fenton procedure, the efficiency of the oxidation is controlled by the nature and the structure of the organic substrate, the initial pH of the solution, the concentration of H₂O₂ and of the catalytic component (Fe²⁺) as well as by the time the reaction medium stands in the area where UV radiations act.

The kinetic assessment of the oxidative degradation process applied to antibiotics of the type amoxicillin, ampicillin and streptomycin (pseudo 1st degree Lagergren kinetic model)

suggests that the oxidative process occurs in two successive steps, with the formation of reaction intermediates. The ratio of the 1st degree kinetic constant values corresponding to the two oxidation stages depends on the structure of the antibiotics and indicates a marked decrease in the oxidation rate in the second stage. This decrease can be attributed to the formation of reaction intermediates such as inferior organic acids with a high stability in regard to oxidation and/or blocking active catalytic centers through the formation of compounds of the $\text{Fe}^{2+/3+}$ species with the reaction intermediates, compounds which are inactive in the process of generating HO radicals (Orbeci *et al.*, 2010).

Advanced oxidation processes of Fenton and photo-Fenton type can be used for antibiotics degradation from wastewater (Orbeci *et al.*, 2010) or for increasing their biodegradability in biological wastewater treatment (Elmolla and Chaudhuri, 2009). Unlike complete amoxicillin degradation, the mineralization of the organic compounds from solution is not complete in the Fenton oxidation process due to formation of refractory intermediates (Ay and Kargi, 2010).

The photo-Fenton process degradation of amoxicillin by using iron species as catalyst (FeSO_4 and potassium ferrioxalate complex) and solar radiation reduces the bactericide effect of amoxicillin but the toxicity may persist due to intermediates formed during the oxidation process. The toxicity decreases significantly when these intermediates are converted into short chain carboxylic acids, allowing further conventional treatment (Trovó *et al.*, 2011). The homogeneous photo-Fenton process is limited by the narrow working pH range (2.5-4) and requires the correction of solution pH for iron precipitation and catalyst separation and recovery. Otherwise, high amounts of metal-containing sludge can be formed and the catalytic metals are lost in these sludge. Because of these disadvantages, several attempts have been made to develop heterogeneous photo-Fenton procedure by immobilization of active iron species on solid supports. Since iron is relatively inexpensive and nontoxic, it has been widely used in different environmental treatment processes (Herney-Ramirez *et al.*, 2010; Nie *et al.*, 2008). In the heterogeneous photo-Fenton process, different iron-containing catalysts can be used, such as the iron bulk catalysts (iron oxy-hydroxyl compounds: hematite, goethite, magnetite) or iron supported catalysts (zeolites, clays, bentonite, glass, active carbon, polymers etc.) (Feng *et al.*, 2005; He *et al.*, 2005; Leland and Bard, 1987; Nie *et al.*, 2008; Ortiz de la Plata *et al.*, 2010; Vinita *et al.* 2010).

Antibiotics can be more or less extensively metabolized by humans and animals. Depending on the quantities used and their rate of excretion, they are released in effluents and reach sewage treatment plants (Alexy *et al.*, 2004; Bound and Voulvoulis, 2004; Kümmerer, 2009).

Available data on antibiotics (ampicillin, erythromycin, tetracycline and penicilloyl groups) indicate their capability to exert toxic effects to living organisms (bacteria, algae etc.), even at very low concentration. These antibiotics are practically non-biodegradable having the potential to survive sewage treatment, leading to a persistence of these compounds in the environment and a potential for bio-accumulation (Arslan-Alaton *et al.*, 2004). The presence of antibiotics in the environment has favored the emergence of antibiotic-resistant bacteria, increasing the likelihood of infections as well as the need to find new and more powerful

antibiotics. As expected, antibiotic-contaminated water is incompatible with conventional biological water treatment technologies (Rozas *et al.*, 2010). Antibiotics have the potential to affect the microbial community in sewage systems and can affect bacteria in the environment and thus disturb natural elementary cycles (Kümmerer, 2009). If they are not eliminated during the purification process, they pass through the sewage system and may end up in the environment, mainly in the surface water.

This is of special importance, since surface water is a possible source of drinking water (Kaniou *et al.*, 2005). The antibiotics degradation by advanced oxidation processes has proven to be reasonably suited and quite feasible for application as a pre-treatment method by combining with biological treatment (Arslan-Alaton *et al.*, 2004). The pre-treatment of penicillin formulation effluent by advanced oxidation processes based on O_3 and H_2O_2/O_3 did not completely remove the toxicity of procaine penicillin G from the effluents, leading to serious inhibition of the treatment of activated sludge (Arslan-Alaton *et al.*, 2006). One of the novel technologies for treating polluted sources of industrial wastewater and drinking water is the photo-Fenton process by which hydroxyl radicals are generated in the presence of H_2O_2 , Fe^{2+} catalyst and UV radiation.

The advanced oxidation processes or even the hybrid methods may not be useful in degrading large quantity of the effluent with economic efficiency and hence it is advisable to use these methods for reducing the toxicity of the pollutant stream to a certain level beyond which biological oxidation can ensure the complete mineralization of the biodegradable products (Gogate and Pandit, 2004).

Removal of organic compounds in wastewater is a very important subject of research in the field of environmental chemistry. In this sense, photocatalysis is a handy promising technology, very attractive for wastewater treatment and water potabilization (Nikolaki *et al.*, 2006; Lim *et al.*, 2009). Using titanium dioxide for water splitting after UV irradiation, it has been shown that this can encompass a wide range of reactions, especially the oxidation of organic compounds. The study of the photodegradation for a large series of substances such as halogenated hydrocarbons, aromatics, nitrogenated heterocycles, hydrogen sulfide, surfactants and herbicides, and toxic metal ions, among others has clearly shown that the majority of organic pollutants present in waters can be mineralized or at least partially destroyed. The photocatalytic treatment of many organic compounds has been successfully achieved. The photocatalytic activity is dependent on the surface and structural properties of the semiconductor such as crystal composition, surface area, particle size distribution, porosity, band gap and surface hydroxyl density (Ahmed *et al.*, 2010).

A variety of semiconductor powders (oxides, sulfides etc.) acting as photocatalysts have been used. Most attention has been given to TiO_2 because of its high photocatalytic activity having a maximum quantum yields, its resistance to photo-corrosion, its biological immunity and low cost. There are two types of reactors: reactors with TiO_2 suspended in the reaction medium and reactors with TiO_2 fixed on a carrier material (Lim *et al.*; 2009, Mozia, 2010; Li *et al.*, 2009). A very promising method for solving problems concerning the separation of the photocatalyst from the reaction medium is the application of

photocatalytic membrane reactors (PMRs), having other advantages such as the realization of a continuous process and the control of a residence time of molecules in the reactor (Mozia, 2010). In case of polymer membranes, there is a danger for the membrane structure to be destroyed by UV light or hydroxyl radicals. The investigations described (Chin *et al.*, 2006; Molinari *et al.*, 2000) show that the lowest resistance exhibit membranes prepared from polypropylene, polyacrylonitrile, cellulose acetate and polyethersulfone, UV light leading to a breakage in the chemical bonds of the methyl group. The least effect of the UV/oxidative environment on the membrane stability was observed in case of polytetrafluoroethylene and polyvinylidene fluoride membranes (Chin *et al.*, 2006).

The self-assembly of TiO₂ nanoparticles was established through coordinance bonds with –OH functional groups on the membrane surface, improving reversible deposition, hydrophilicity and flow and diminishing the irreversible fouling (Mansourpanah *et al.*, 2009). TiO₂-functionalized membranes may be obtained by several methods, but the sol-gel process is ubiquitous because it has many advantages such as purity, homogeneity, control over the microstructure, ease of processing, low temperature and low cost (Alphonse *et al.*, 2010).

The advanced oxidation processes based on the photo-activity of semiconductor-type materials can be successfully used in wastewater treatment for destroying the persistent organic pollutants, resistant to biological degradation processes. TiO₂ is the most attractive semiconductor because of its higher photocatalytic activity and can be used suspended into the reaction medium (slurry reactors) or immobilized as a film on solid material. A very promising method for solving problems concerning the photocatalyst separation from the reaction medium is to use the photocatalytic reactors in which TiO₂ is immobilized on support. The immobilization of TiO₂ onto various supporting materials has largely been carried out via physical or chemical route.

The application of photocatalysis in water and wastewater treatment has been well established, particularly in the degradation of organic compounds into simple mineral acids, carbon dioxide and water (Pera-Titus *et al.*, 2004; Cassano and Alfano, 2000). Titanium dioxide (TiO₂), particularly in the anatase form is a photocatalyst under ultraviolet (UV) light. A reactor refers to TiO₂ powder which is suspended in the water to be treated, while the immobilized catalyst reactor has TiO₂ powder attached to a substrate which is immersed in the water to be treated. Immobilised TiO₂ has become more popular due to the complications in the TiO₂ suspension systems (Hoffmann *et al.*, 1995).

The TiO₂ immobilisation procedure developed not long ago can be used in determining a suitable immobilization procedure, particularly if economical and simple equipment is necessary. The overall performance of the TiO₂ coating can be affected by various factors depending on the coating methods. In addition, it is also difficult to evaluate the photocatalytic efficiency of the coatings through photocatalytic activity (Augugliaro *et al.*, 2008). Invariably, the TiO₂ was immobilized using the sol-gel technique (Addamo *et al.*, 2008). In this case, some problems are noted: decrease of surface area; potential loss of TiO₂; decreased adsorption of organic substances on the TiO₂ surface; mass transfer limitations.

No polymeric support was considered to immobilise TiO_2 since the polymeric material can undergo photo-oxidative degradation by illuminated TiO_2 (Cassano and Alfano, 2000; Augugliaro et al., 2008).

Researchers have used photocatalytic oxidation to remove and destroy many types of organic pollutants. After photocatalysis was recognized to be a great oxidation mechanism, researchers began testing it on many different compounds, and in many different processes (Cassano and Alfano, 2000; Hoffmann et al., 1995; Addamo et al., 2008).

Phenolic compounds, a kind of priority pollutants, often occur in the aqueous environment due to their widespread use in many industrial processes such as the manufacture of plastics, dyes, drugs, antioxidants, and pesticides. Phenols, even at concentrations below 1 lg/L , can affect the taste and odor of the water (Pera-Titus et al., 2004). Therefore, the identification and monitoring of these compounds at trace level in drinking water and surface waters are imperative. Chlorophenols represent an important class of very common water pollutants. 4-chlorophenol is a toxic and non-biodegradable organic compound and can often be found in high quantity in the waste waters from various industrial sectors (Pera-Titus et al., 2004; Augugliaro et al., 2006). A severe toxicity of 4-chlorophenol requires the development of a simple, sensitive and reliable analytical method.

Among the advanced oxidation processes investigated in the last decades, photocatalysis in the presence of an irradiated semiconductor has proven to be very effective in the field of environment remediation. The use of irradiation to initiate chemical reactions is the principle on which heterogeneous photocatalysis is based; in fact, when a semiconductor oxide is irradiated with suitable light, excited electron-hole pairs result that can be applied in chemical processes to modify specific compounds. The main advantage of heterogeneous photocatalysis, when compared with the chemical methods, is that in most cases it is possible to obtain a complete mineralization of the toxic substrate even in the absence of added reagents. The radical mechanism of photocatalytic reactions, which involve fast attacks of strongly oxidant hydroxyl radicals, determines their unselective features.

Environmental applications of photocatalysis using TiO_2 have attracted an enormous amount of research interest over the last three decades (Hoffmann et al., 1995; Linsebigler et al., 1995; Mills and Le Hunte, 1997; Stafford et al., 1996). It is well established that slurries of TiO_2 illuminated with UV light can degrade to the point of mineralization almost any dissolved organic pollutant. Nevertheless, photocatalysis, particularly in aqueous media, has still not found widespread commercial implementation for environmental remediation. The main hurdle appears to be the cost, which is high enough to prevent the displacement of existing and competing technologies by photocatalysis. TiO_2 research has progressed on multiple tiers, whereby the study of fundamental processes promotes material development, allowing no repeated uses that promise to play a larger and larger role in engineering sustainable technologies.

TiO_2 is the most used semiconductor because of its higher photocatalytic activity, resistance to the photocorrosion process, absence of toxicity, biological immunity and the relatively

low cost (Nikolaki *et al.*, 2006; Han *et al.*, 2009). TiO₂ crystalline powder can be used suspended into a reaction medium (slurry reactors) or immobilized as a film on a carrier material. The anatase form of TiO₂ is reported to give the best combination of photoactivity and photostability. An ideal photocatalyst for oxidation is characterized by the following attributes: photostability; chemically and biologically inert nature; availability and low cost; capability to adsorb reactants under efficient photonic activation (Bideau *et al.*, 1995, Pozzo *et al.*, 1997, Balasubramanian *et al.*, 2004, Gaya and Abdullah, 2008, Siew-Teng Ong *et al.*, 2009, Hanel *et al.*, 2010). The support must have the following characteristics: (a) transparent to irradiation; (b) strong surface bonding with the TiO₂ catalyst without negatively affecting the reactivity; (c) high specific surface area; (d) good absorption capability for organic compounds; (e) separability; (f) facilitating mass transfer processes and (g) chemically inert (Pozzo *et al.*, 1997). As solid support, different materials were investigated: natural or synthetic fabrics, polymer membranes, activated carbon, quartz, glass, glass fiber, optical fibers, pumice stone, zeolites, aluminum, stainless steel, titanium metal or alloy, ceramics (including alumina, silica, zirconia, titania), red brick, white cement etc. (Bideau *et al.*, 1995, Rachel *et al.*, 2002, Balasubramanian *et al.*, 2004, Kemmitt *et al.*, 2004, Gunlazuardi and Lindu, 2005, Hunoh *et al.*, 2005, Chen *et al.*, 2006, Medina-Valtierra *et al.*, 2006, Gaya and Abdullah, 2008, Lim *et al.*, 2009, Siew-Teng Ong *et al.*, 2009, Hanel *et al.*, 2010, Zita *et al.*, 2011).

The immobilization of TiO₂ on different supporting materials has largely been carried out via a physical or chemical route: dip coating, porous material impregnation, sol-gel method, reactive thermal deposition, chemical vapor deposition, electron beam evaporation, spray pyrolysis, electrophoresis, electro-deposition (Rachel *et al.*, 2002, Gunlazuardi and Lindu, 2005, Medina-Valtierra *et al.*, 2006, Hanel *et al.*, 2010, Zita *et al.*, 2011).

The methods most commonly used for deposition of TiO₂ on supports are sputtering and sol-gel dip-coating or spin-coating. Often the fixation of TiO₂ on solid supports reduces its efficiency due to various reasons such as reduction of the active surface, a more difficult exchange with solution, introduction of ionic species etc. A degree of 60–70% reduction in performance is reported in aqueous systems for immobilized TiO₂ as compared to the unsupported catalyst (Gaya and Abdullah, 2008), the best results being obtained by the immobilization of TiO₂ on glass fiber (Rachel *et al.*, 2002, Lim *et al.*, 2009). The separation and/or removal technologies based on membrane and photocatalytic processes have a great potential for application in advanced wastewater treatment. Separation membranes have become essential parts of the human life because of their growing industrial applications in high technology such as biotechnology, nanotechnology and membrane based separation and purification processes. Available technologies to deal with chlorophenolic compounds include the advanced oxidation processes (AOPs) based on the formation of hydroxyl radicals with high oxidation potential.

The hybrid method consists in a photocatalytic procedure using a reactor equipped with TiO₂-functionalized membrane (cylindrical shape) and high pressure mercury lamp for UV radiations generation, centrally and coaxially positioned. The TiO₂-functionalized membranes have been obtained by sol-gel method synthesis of TiO₂ (from

tetrabutylortotitanate) as nanoparticles, formed directly in porous membrane regenerated cellulose type. Solutions of methyl, ethyl and propyl alcohols have been used as reaction medium. The experiments were performed at $30\pm 2^{\circ}\text{C}$ using synthetic solutions of 4-CP (analytical grade reagent). The amount of hydrogen peroxide (30% w/w) used was calculated at 1.5 time $\text{H}_2\text{O}_2/4\text{-CP}$ stoichiometric ratio. The degradation process was studied by monitoring the organic substrate concentration changes function of reaction time using chemical oxygen demand analysis (COD).

The experimental data show the catalytic role of TiO_2 -functionalized membranes in the oxidation process. The oxidation is preceded by an adsorption process and the transfer of 4-chlorophenol from the solution to the photocatalytic reaction zone through the functionalized membrane. Titanium dioxide, deposited on the membrane, acts as a photocatalyst in the presence of UV radiations leading to a higher efficiency of the oxidation process in a short reaction time. The catalytic activity of TiO_2 -functionalized membranes is influenced by the nature of the alcohol used in obtaining them. This can be explained by the crystallite size of TiO_2 and their dispersion on membrane. However, at a higher reaction time, the determined solution COD values tend to increase, indicating that the TiO_2 -functionalized membranes become unstable. This can be attributed to a partial solubilization process of membrane into reaction medium with a strong oxidizing potential.

The presence of phenol and phenolic derivatives in water induces toxicity, persistence and bioaccumulation in plant and animal organisms and is a risk factor for human health. The technologies of separation and/or removal of phenolic derivatives based on membrane and photocatalytic processes play an important role.

Available technologies to deal with phenolic compounds include the advanced oxidation processes, based on the formation of very active hydroxyl radicals, which react quickly with the organic contaminant. Among the AOPs, the photocatalytic process is one of the most attractive methods because the reagent components are easy to handle and environmentally benign.

3. Wastewater decontamination by processes of adsorption

Rapid development of industry and society led to serious environmental problems such as contamination of groundwater and surface chemical treatment with organic compounds coming from agriculture (pesticides, herbicides, other.) or inorganic compounds in industry (pigments, heavy metals, etc.)

A method used for the wastewater decontamination is the contaminants adsorption on the catalyst surface. The most known adsorbent substances cleansing practice are: activated carbon, silica gel, discolored soils, molecular sieves, cotton fibers etc.

After the manner in which the contact is realized between wastewater and adsorbent is distinguished static and dynamic adsorption. In the first case finely adsorbent divided is stirred with water and after a time it's separated by decantation or filtration. In the dynamic adsorption case, wastewater passes through a fixed, mobile or a fluidized adsorbent layer with a continuous flow.

Another alternative to the wastewater treatment is the use of technologies based on magnetic nanomaterials AB_2O_4 type ($A = \text{Co, Ni, Cu, Zn}$, $B = \text{Fe}^{3+}$) used as catalysts for degradation of organic compounds or adsorbents to retain the surface pollutants heavy metals (mercury, arsenic, lead and others). Their importance and complexity led to research programs development on magnetic materials, with new or improved properties in last decades. These properties are dependent on chemical composition and microstructural characteristics, which can be controlled in the fabrication and synthesis processes.

These materials must have a relatively high surface area, a smaller particle size, and porous structure. In particular, the magnetic properties of the powders makes them to be easily recovered by magnetic separation technology after adsorption or regeneration, which overcomes the disadvantage of separation difficulty of common powdered adsorbents (Qu, et.al, 2008).

Challenges in synthesis of nanostructured catalysts are that many reactions employ mixed catalysts consisting of different oxide metals, and that the function of active centers is not only determined by the constituent atoms but also by the surrounding crystal or surface structures; it is thus necessary to accurately control the synthesis of nanostructured catalysts (Rickerby, et.al, 2007).

Magnetite nanoparticles have highest saturation magnetization of 90 emu/g among iron oxides. Therefore, magnetite nanoparticles can be used to adsorb arsenic ions followed by magnetic decantation. Other iron oxides and hydroxides have been reported to have arsenic ability (Hai, et. al, 2009). Oxidation resistance is an important factor for arsenic removal under atmospheric conditions.

By diverse synthesis methods (hydrothermal, ultrasonic hydrothermal, sol-gel, coprecipitation and other), was obtained ferrite nanomaterials derived from magnetite (FeO , Fe_2O_3) substituting the Fe^{2+} ion in different concentrations (0.5, 0.8, 1, 1.2, 1.5) with Co^{2+} , Cu^{2+} , Ni^{2+} , Zn^{2+} ions (Vlazan, 2010; Fannin, et.al, 2011).

4. Membrane oxidative processes in water treatment

This topic gives an overview of the hybrid photocatalysis-membrane processes and their possible applications in water and wastewater treatment. Different configurations of photocatalytic membrane reactors (PMRs) are described and characterized. They include PMRs with photocatalyst immobilized on/in the membrane and reactors with catalyst in suspension. The advantages and disadvantages of the hybrid photocatalysis-membrane processes in terms of permeate flow, membrane fouling and permeate quality are discussed. Moreover, a short introduction to the heterogeneous photocatalysis and membrane processes as unit operations is given.

The detailed mechanism of the photocatalytic oxidation of organic compounds in water has been discussed widely in the literature and will be presented here in brief only. The overall process can be divided into the following steps.

1. Diffusion of reactants from the bulk liquid through a boundary layer to the solution-catalyst interface (external mass transfer).
2. Inter-and/or intra-particle diffusion of reactants to the active surface sites of the catalyst (internal mass transfer).
3. Adsorption of at least one of the reactants.
4. Reactions in the adsorbed phase.
5. Desorption of the product(s).
6. Removal of the products from the interface of the bulk solution.

A photocatalyst should be characterized by: (I) high activity, (II) resistance to poisoning and stability in prolonged at elevated temperatures, (III) mechanical stability and resistance to attrition, (IV) non-selectivity in most cases, and (V) physical and chemical stability under various conditions. Moreover, it is desirable for the photocatalyst to be able to use not only UV, but also visible light and to be inexpensive. Different semiconducting materials, such as oxides (TiO_2 , ZnO , CeO_2 , ZrO_2 , WO_3 , V_2O_5 , Fe_2O_3 , etc.) and sulfides (CdS , ZnS , etc.) have been used as photocatalysts.

Recently, numerous investigations have been focused on different modifications of TiO_2 in order to improve its activity under UV irradiation or to reduce the band gap energy so that it is able to utilize the visible light. The best photocatalytic performances with maximum quantum yields have been always obtained with TiO_2 . Anatase is the most active allotropic form of TiO_2 among the various ones available. Unfortunately, due to a wide band gap (about 3.2 eV), TiO_2 is inactive under visible light.

The most important operating parameters which affect the efficiency of the photocatalytic oxidation process can be summarized as follows: reactor design; light wavelength and intensity; loading of the photocatalyst; initial concentration of the reactant; temperature; pH of reaction medium; oxygen content; the presence of inorganic ions (*Moziá, 2005; Gogate and Pandit, 2004; Herrmann, 2006*). The photocatalytic reactors can be divided into two main groups:

- i. Reactors with TiO_2 suspended in the reaction mixture: in the case of reactors with TiO_2 suspended in the reaction mixture (I), the photocatalyst particles have to be separated from the treated water after the oxidation process.
- ii. Reactors with TiO_2 fixed on a carrier material (glass, quartz, stainless steel, pumice stone, titanium metal, zeolites, pillared clays, membranes etc.).

A very promising method for solving problems concerning separation of the photocatalyst as well as products and by-products of photo-oxidation process from the reaction mixture is application of photocatalytic membrane reactors (PMRs). PMRs are hybrid reactors in which photo-catalysis is coupled with a membrane process. The membrane would play both the role of a simple barrier for the photocatalyst and of a selective barrier for the molecules to be degraded. Membrane processes are separation techniques which are widely applied in various sectors of industry including food, chemical and petrochemical, pharmaceutical,

cosmetics and electronic industries, water desalination, water and wastewater treatment and many others. The main advantages of membrane processes are: low energy consumption; low chemicals consumption; production of water of stable quality almost independent on the quality of the treated water; automatic control and steady operation allowing performance of a continuous operation; low maintenance costs; easy scale up by simple connecting of additional membrane modules

Synthetic membranes may be: organic or inorganic materials; homogeneous or heterogeneous; symmetrical or asymmetrical; porous or dense; electrically neutral or charged.

In this sense, the driving forces are: pressure difference; concentration difference; partial pressure difference or electrical potential difference.

Most of the PMRs described in the literature combine photo-catalysis with pressure driven membrane processes such as:

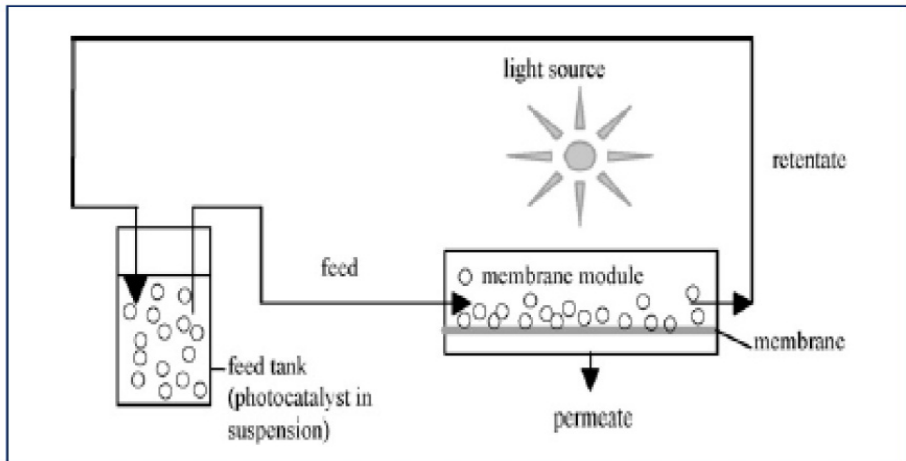
- Micro-Filtration (MF)
- Ultra-Filtration (UF)
- Nano-Filtration (NF)
- Dialysis
- Pervaporation (PV)
- Direct Contact Membrane Distillation (DCMD)

Hybrid photocatalysis-membrane processes are conducted in the installations often called "photocatalytic membrane reactors". However, in the literature, other names for these configuration can be also found, including "membrane chemical reactor" (MCR), "membrane reactor", "membrane photoreactor", or, more specific, "submerged membrane photocatalysis reactor" and "photocatalysis-ultrafiltration reactor"(PUR). For the hybridization of photocatalysis with membrane process it will be useful to apply a general term of "photocatalytic membrane reactor".

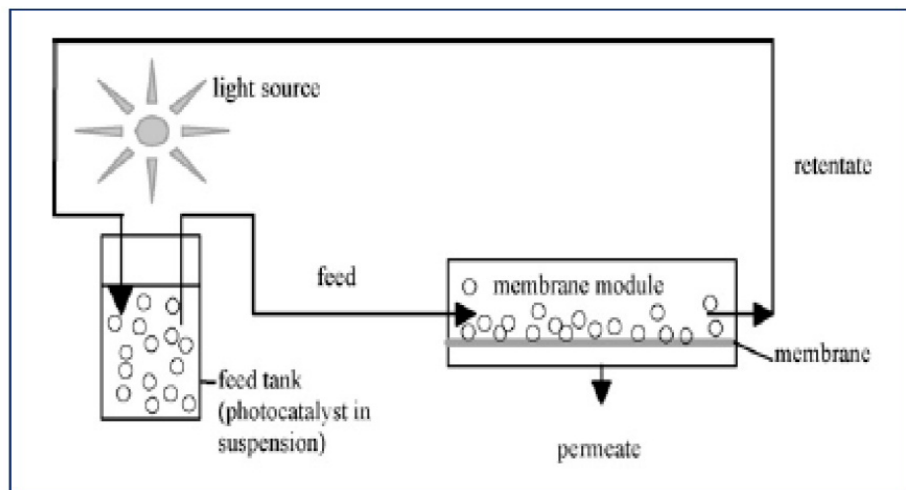
Photocatalytic membrane reactors design show in figure 2 (a, b).

Photocatalytic membranes for the PMRs can be prepared from different materials and indifferent ways. Figure 3 presents two possible types of asymmetric photocatalytic membranes (Bosc *et al.*, 2005). In the first case, photoactive separation layer is deposited on a non-photoactive porous support (Fig. 3a) the photoactive layer, being also the separation layer (skin) is formed on a porous non-photoactive support. In the second case, a non-photoactive separation layer is deposited on a photoactive porous support (Fig. 3b) the separation layer is non-photoactive and is deposited on a porous active support.

The main advantage of PMRs with photocatalytic membranes is that this configuration allows one to minimize the mass transfer resistances between the bulk of the fluid and the semiconductor surface.



(a)



(b)

Figure 2. a. PMR utilizing photo-catalyst in suspension: irradiation of the membrane module (Mozia S., 2010), b. PMR utilizing photo-catalyst in suspension: irradiation of the feed tank (Mozia S., 2010)

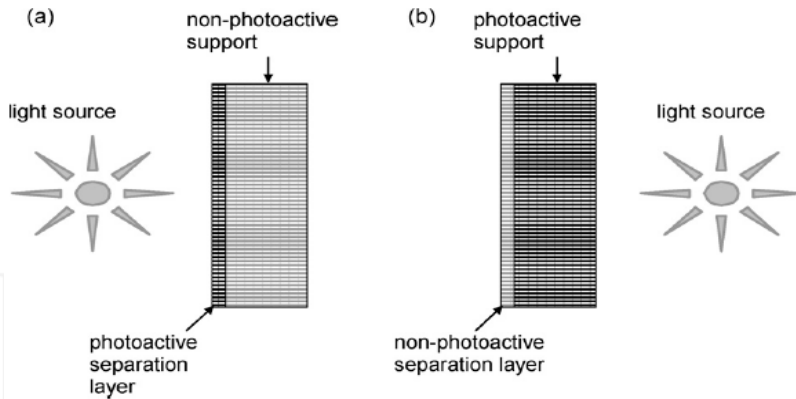


Figure 3. Asymmetric photocatalytic membranes (Bosc *et al.*, 2005)

5. Conclusion

Choosing the most suitable method of wastewater treatment studies require both increasing the effectiveness and economic efficiency (operating and investment costs).

Advanced oxidation processes (AOPs) are good alternatives for removal the toxic compounds from wastewater. The AOPs can be successfully used in wastewater treatment to degrade the persistent organic pollutants, the oxidation process being determined by the very high oxidative potential of the HO· radicals generated into the reaction medium by different mechanisms. AOPs can be applied to fully or partially oxidize pollutants, usually using a combination of oxidants. Photo-chemical and photo-catalytic advanced oxidation processes including UV/H₂O₂, UV/O₃, UV/H₂O₂/O₃, UV/H₂O₂/Fe²⁺(Fe³⁺), UV/TiO₂ and UV/H₂O₂/TiO₂ can be used for oxidative degradation of organic contaminants. A complete mineralization of the organic pollutants is not necessary, being more worthwhile to transform them into biodegradable aliphatic carboxylic acids followed by a biological process. The efficiency of the various AOPs depend both on the rate of generation of the free radicals and the extent of contact between the radicals and the organic compound.

Photocatalytic oxidation in water treatment has proved its efficiency at many pilot-scale applications. However, wide marketing of commercially available solar detoxification systems is obstructed by the general market situation: a new water treatment procedure has an opportunity to be implemented only when its cost is at least two-fold lower than the cost of a procedure currently in use. Photocatalysis, also called the "green" technology, represents one of the main challenges in the field of treatment and decontamination systems, especially for water and air. Its operating principle is based on the simultaneous action of the light and a catalyst (semi-conductor), which allows for pollutant molecules to be destroyed without damaging the surrounding environment.

In recent years, applications to environmental remediation have been one of the most active subjects in photocatalysis.

Author details

Adina Elena Segneanu, Carmen Lazau, Paula Sfirloaga, Paulina Vlazan,
Cornelia Bandas and Ioan Grozescu*
National Institute for Research and development in Electrochemistry and Condensed Matter –
INCEMC Timisoara, Romania

Cristina Orbeci
Politehnica University Bucuresti, Romania

6. References

- Addamo, M., Augugliaro, V., Di Paola, A., García-López, E., Loddo, V., Marci, G., Palmisano, L., (2008), Photocatalytic thin films of TiO₂ formed by a sol-gel process using titaniumtetraisopropoxide as the precursor, *Thin Solid Films* 516, pp. 3802–3807.
- Ahmed, S., Rasul, M. G., Martens, W. N., Brown R., Hashib, M. A., (2010), “Heterogeneous photocatalytic degradation of phenols in wastewater: A review on current status and developments”, *Desalination*, 261(1-2), pp. 3-18.
- Alexy, R., Kumpel, T., Kümmerer, K., (2004), Assessment of degradation of 18 antibiotics in the Closed Bottle Test. *Chemosphere* 57, 505-512.
- Alphonse, P., Varghese A., Tendero, C., (2010), “Stable hydrosols for TiO₂ coatings”, *Journal of Sol-Gel Science and Technology*, 56(3), 250-263.
- Andreozzi R.; Caprio V.; Insola A.; Marotta R. (1999), Advanced oxidation processes (AOP) for water purification and recovery, *Catalysis Today*, 53 (1), 51-59
- Anita Rachel, Machiraju Subrahmanyam, Pierre Boule, (2002), Comparison of photocatalytic efficiencies of TiO₂ in suspended and immobilised form for the photocatalytic degradation of nitrobenzenesulfonic acids, *Applied Catalysis B: Environmental* 37(4), 301–308.
- Arslan-Alaton, I., Caglayan, A.E., (2006), Toxicity and biodegradability assessment of raw and ozonated procaine penicillin G formulation effluent. *Ecotox. Environ. Safe.* 63, 131-140.
- Arslan-Alaton, I., Dogruel, S., Baykal, E., Gerone, G., (2004), Combined chemical and biological oxidation of penicillin formulation effluent. *J. Environ. Manag.* 73, 155-163.
- Augugliaro, V., Litter, M., Palmisano, L., Soria, J., (2006), The combination of heterogeneous photocatalysis with chemical and physical operations: A tool for improving the photoprocess performance, *Journal of Photochemistry and Photobiology C: Photochemistry Reviews* 7, 127–144.
- Ay, F., Kargi, F., (2010), Advanced oxidation of amoxicillin by Fenton’ reagent treatment. *J.Hazard.Mater.* 179, 622-627.

* Corresponding Author

- Balasubramanian G., Dionysiou D.D., Suidan M.T., Baudin I., Laîné J.M., (2004), Evaluating the activities of immobilized TiO₂ powder films for the photocatalytic degradation of organic contaminants in water. *Applied Catalysis B: Environmental*, 47(2), 73-84.
- Bideau, M., Claudel, B., Dubien, C., Faure, L., Kazouan H., (1995), On the "immobilization" of titanium dioxide in the photocatalytic oxidation of spent waters, *Journal of Photochemistry & Photobiology A: Chemistry*, 91(2), 137-144.
- Bosc, F., Ayrat, A., Guizard, C., (2005), Mesoporous Anatase Coatings for Coupling Membrane Separation and Photocatalyzed Reactions" *J. Membr. Sci.* 265, 13-19.
- Bound, J.P., Voulvoulis, N., (2004), Pharmaceuticals in the aquatic environment – a comparison of risk assessment strategies. *Chemosphere* 56, 1143-1155.
- Byrappa, K., Rai, K.M.L., Yoshimura, M. (2002), "Hydrothermal preparation of TiO₂ and photocatalytic degradation of hexachloro cyclohexane and dichlorodiphenyl trichloromethane", *Journal of Environmental Science and Technology*, 21, pp 1085–1090;
- Cassano, A. E., Alfano, O. M. (2000) "Reaction Engineering of Suspended Solid Heterogeneous Photocatalytic Reactors", *Catalysis Today*, 58(2-3), pp. 167-197.
- Carp, O., Huisman, C.L., Reller, A., (2004), Photoinduced reactivity of titanium dioxide, *Prog. Solid State Chem.* 32(1-2), 33-177.
- Chakinala, A.G., Gogate, P.R., Burgess, A.E., Bremner, D.H., (2009), Industrial wastewater treatment using hydrodynamic cavitation and heterogeneous advanced Fenton processing. *Chemical Engineering Journal*, 152, 498-502.
- Chen S.Z, Zhang P.Y, Zhu W.P., Chen L, Sheng-Ming Xu, (2006), Deactivation of TiO₂ photocatalytic films loaded on aluminium: XPS and AFM analyses, *Appl. Surf. Sci.* 252 (20), 7532-7538.
- Chin, S. S., Chiang, K., Fane, A. G., (2006), "The stability of polymeric membranes in a TiO₂ photocatalysis process", *Journal of Membrane Science*, 275(1-2), pp. 202-211.
- Daneshvar N., Salari D., Khataee A.R., (2003), Photocatalytic degradation of azo dye acid red 14 in water: investigation of the effect of operational parameters, *Journal of Photochemistry and Photobiology A: Chemistry*, 157 111–116;
- Daneshvar N., Aber S., Seyed Dorraji M. S., Khataee A. R., Rasoulifard M. H., (2007), Preparation and Investigation of Photocatalytic Properties of ZnO Nanocrystals: Effect of Operational Parameters and Kinetic Study, *World Academy of Science, Engineering and Technology* 29;
- Daneshvar N., D. Salari, A.R. Khataee, (2003), Photocatalytic degradation of azo dye acid red 14 in water: investigation of the effect of operational parameters, *Journal of Photochemistry and Photobiology A: Chemistry* 157, 111–116.
- De Laat J., Truong Le G., Legube B., (2004), A comparative study of the effects of chloride, sulfate and nitrate ions on the rates of decomposition of H₂O₂ and organic compounds by Fe(II)/H₂O₂ and Fe(III)/H₂O₂. *Chemosphere*, 55(5):715-23.
- Du Y., Zhou M., Lei L., (2006), Role of the intermediates in the degradation of phenolic compounds by Fenton-like process, *Journal of Hazardous Materials*, 136, 859-865.

- Duarte F., Madeira L.M., (2010), Fenton and Photo-Fenton-Like Degradation of a Textile Dye by Heterogeneous Process with Fe/ZSM-5 Zeolite, *Separation Science and Technology*, 45, 1512-1520.
- Elmolla, E., Chaudhuri, M., (2009), Degradation of the antibiotics amoxicillin, ampicillin and cloxacillin in aqueous solution by photo-Fenton process. *J. Hazard. Mater.* 172, 1476-1481.
- Esplugas, S., Gimenez, J., Contreras, S., Pascual, E., Rodriguez M., (2002), Comparison of different advanced oxidation processes for phenol degradation, *Water Res.*, 36, p. 1034-1042
- Fang Han, Venkata Subba Rao Kambala, Madapusi Srinivasan, Dharmarajan Rajarathnam, Ravi Naidu, (2009), Tailored titanium dioxide photocatalysts for the degradation of organic dyes in wastewater treatment: A review. *Applied Catalysis A, General*, 359 (1-2), 2009, 25-40.
- Fannin P.C., Marin C.N., Malaescu I., Stefu N., Vlăzan P., Novaconi S., Popescu S., (2011), Effect of the concentration of precursors on the microwave absorbent properties of Zn/Fe oxide nanopowders; *Journal of Nanoparticle Research*; 13, 311-319.
- Feng J., Hu X., Yue P. L., (2005), Discoloration and mineralization of Orange II by using a bentonite clay-based Fe nanocomposite film as a heterogeneous photo-Fenton catalyst, *Water Research*, 39, 89-96.
- Gao, Y., Liu, H., (2005), Preparation and catalytic property study of a novel kind of suspended photocatalyst of TiO₂-activated carbon immobilized on silicone rubber film, *Mater. Chem. Phys.* 92(2-3), 604-608.
- Gayaa U. I., Abdullaha A. H., (2008), Heterogeneous photocatalytic degradation of organic contaminants over titanium dioxide: A review of fundamentals, progress and problems, *Journal of Photochemistry and Photobiology C: Photochemistry Reviews* 9, 1-12.
- Getoff N., (2001), Comparison of radiation and photoinduced degradation of pollutants in water: synergistic effect of O₂, O₃ and TiO₂. A Short Review, *Research on Chemical Intermediates*, Vol. 27, Numbers 4-5, 343-358.
- Li Puma G., Bonob A., Krishnaiah D., Collin J.G.,(2008) Preparation of titanium dioxide photocatalyst loaded onto activated carbon support using chemical vapor deposition: A review paper, *Journal of Hazardous Materials* 157. 209-219.
- Gogate P. R., Pandit A. B., (2004), A review of imperative technologies for wastewater treatment II: hybrid methods, *Advances in Environmental Research*, 8, 553-597.
- Guillard C.; Disdier J.; Herrmann J.-M.; Lehaut C.; Chopin T.; Malato S.;Blanco J., 1999, Comparison of various titania samples of industrial origin in the solar photocatalytic detoxification of water containing 4-chlorophenol, *Catalysis Today*, 54, (2,-3), 217-228.
- Hänel, A., Moren, P., Zaleska, A., Hupka, J. (2010), Photocatalytic activity of TiO₂immobilized on glass beads, *Physicochem. Probl. Miner. Process.* 45, 49-56
- Hansen H. K., Nunez P., Raboz D., Schippacasse I., Grandon R., (2007), Electrocoagulation in wastewater containing arsenic: Comparing different process designs, *ScienceDirect, Electrochimica Acta* 52, 3464-3470.

- Hai N. H., Phu N. D., 25 (2009), Arsenic removal from water by magnetic $\text{Fe}_{1-x}\text{Co}_x\text{Fe}_2\text{O}_4$ and $\text{Fe}_{1-y}\text{Ni}_y\text{Fe}_2\text{O}_4$ nanoparticles; *VNU Journal of Science, Mathematics - Physics* 15-19.
- He J., Ma W., Song W., Zhao J., Qian X., Zhang S., Yu J. C., (2005), Photoreaction of aromatic compounds at $\alpha\text{-FeOOH}/\text{H}_2\text{O}$ interface in the presence of H_2O_2 : evidence for organic-goethite surface complex formation, *Water Research*, 39, 119–128.
- Hepel M., Hazelton S., (2005), Photoelectrocatalytic degradation of diazo dyes on nanostructured WO_3 electrodes, *Electrochimica Acta* 50. 5278–5291.
- Hoffmann, M. R., Martin, S. T., Choi, W., Bahnemann, D. W., (1995) „Environmental Applications of Semiconductor Photocatalysis”, *Chemical Reviews*, 95, pp. 69-96.
- Hu, K.H., Yong Kui Cai Y.K., Li S., (2011), Photocatalytic Degradation of Methylene Blue on $\text{MoS}_2/\text{TiO}_2$ Nanocomposite, *Advanced Materials Research*, Volumes 197 – 198.
- Hua, Zi-Le, Shi, Jian-Lin, Zhang, Wen-Hua, Huang, Wei-Min, (2002), Direct synthesis and characterization of Ti-containing mesoporous silica thin films, *Materials Letters* 53(4-5), 299-304.
- Kaniou, S., Pitarakis, K., Barlagianni, I., Poullos, I., (2005), Photocatalytic oxidation of sulfamethazine. *Chemosphere* 60, 372-380.
- Jarnuzi Gunlazuardi, Winarti Andayani Lindu, (2005), Photocatalytic degradation of pentachlorophenol in aqueous solution employing immobilized TiO_2 supported on titanium metal, *Journal of Photochemistry and Photobiology A: Chemistry*, 173(1), 51-55.
- Jiří Zita, Josef Krýsa, Urh Černigoj, Urška Lavrenčič-Štangar, Jaromír Jirkovský, Jiří Rathouský, (2011), Photocatalytic properties of different TiO_2 thin films of various porosity and titania loading, *Catalysis Today*, 161 (1), 29-34.
- João Rocha, Artur Ferreira, Zhi Lin, Michael W. Anderson, (1998), Synthesis of microporous titanasilicate ETS-10 from TiCl_3 and TiO_2 : a comprehensive study, *Micropor. Mesopor. Mater.*, 23(5-6), 253-263.
- Jorge Medina-Valtierra, Manuel Sánchez-Cárdenas, Claudio Frausto-Reyes, Sergio Calixto, (2006), Formation of smooth and rough TiO_2 thin films on fiberglass by sol-gel method, *J. Mex. Chem. Soc.*, 50(1), 8-13.
- Kavitha V., Palanivelu K., (2004), The role of ferrous ion in Fenton and photo-Fenton processes for the degradation of phenol, *Chemosphere*, 55, 1235-1243.
- Kakuta S., Abe T., (2009), Photocatalysis for water oxidation by Fe_2O_3 nanoparticles embedded in clay compound: correlation between its polymorphs and their photocatalytic activities, *Journal of Materials Science*, Vol. 44, Number 11 2890-2898.
- Khelifa A., Moulay S., Naceur A.W., (2005), Treatment of metal finishing effluents by the electroflotation technique, *Desalination* 181, 27-33.
- Kondo Y., Fujihara S., (2011), Solvothermal Synthesis of WO_3 Photocatalysts and their Enhanced Activity, *Key Engineering Materials (Volume 485)* 283-286.
- Hu K.H., Yong Kui Cai , Sai Li, (2011), Photocatalytic Degradation of Methylene Blue on $\text{MoS}_2/\text{TiO}_2$ Nanocomposite, *Advanced Materials Research* , vol 197 – 198, 996-999;
- Kümmerer, K., (2009), Antibiotics in the aquatic environment - A review - Part I. *Chemosphere* 75, 417-434.

- Kwon, B. G., Lee, D. S., Kang, N., Yoon, J., (1999), Characteristics of p-chlorophenol oxidation by Fenton's reagent. *Water Res.* 33 (9), 2110-2118.
- Lazau C., Ratiu C., Orha C., R. Pode, F. Manea, (2011), Photocatalytic activity of undoped and Ag-doped TiO₂-supported zeolite for humic acid degradation and mineralization, *Materials Research Bulletin* 46, 11, Pages 1916–1921.
- Leland J. K., Bard A. J., (1987), Photochemistry of colloidal semiconducting iron oxide polymorphs, *Journal of Physical Chemistry*, 91, 5076–5083.
- Li Puma G., Bonob A, Krishnaiah D., Collin J.G., (2008), Preparation of titanium dioxide photocatalyst loaded onto activated carbon support using chemical vapor deposition: A review paper, *Journal of Hazardous Materials*, 157 209–219.
- Li, J.-H., Xu, Y.-Y., Zhu, L.-P., Wang, J.-H., Du, and C.-H., (2009), Fabrication and characterization of a novel TiO₂ nanoparticle self-assembly membrane with improved fouling resistance, *Journal of Membrane Science*, 326(2), pp. 659-666.
- Li, X.Y., Cui, Y.H., Feng, Y.J., Xie, Z.M., Gu, J.D., (2005), Reaction pathways and mechanisms of the electrochemical degradation of phenol on different electrodes. *Water Res.* 39, 1972-1981.
- Lim, L. L. P., Lynch, R. J., In, S. I. (2009), Comparison of simple and economical photocatalyst immobilisation procedures, *Applied Catalysis A: General*, 365(2): 214–221.
- Liu Xincheng. Kerry Thomas. J., (1996), Synthesis of microporous titanosilicates ETS-10 and ETS-4 using solid TiO₂ as the source of titanium, *Chem. Commun.*, 12, 1435-1436.
- Lopez T., M. Alvarez, F. Tzompantzi, M. Picquart, Photocatalytic degradation of 2,4-dichlorophenoxyacetic acid and 2,4,6-trichlorophenol with ZrO₂ and Mn/ZrO₂ sol-gel materials, *J Sol-Gel Sci Techn* (2006) 37: 207–211.
- Lu M. C., Chen J. N., Chang C. P., (1997), Effect of inorganic ions on the oxidation of dichlorvos insecticide with Fenton's reagent. *Chemosphere*, 35(10), 2285–2293.
- Mansourpanah, Y., Madaeni, S. S., Rahimpour, A., Farhadian, A., Taheri, A. H. (2009), Formation of appropriate sites on nanofiltration membrane surface for binding TiO₂ photo-catalyst: Performance, characterization and fouling-resistant capability", *Journal of Membrane Science*, 330(1-2), pp. 297-306.
- Molinari, R., Mungari, M., Drioli, E., Di Paola, A., Loddo, V., Palmisano L., Schiavello, M., (2000), Study on a photocatalytic membrane reactor for water purification", *Catalysis Today*, 55(1-2), pp. 71-78.
- Moura F. C. C., Araujo M. H., Costa R. C. C., Fabris J. D., Ardisson J. D., Macedo W. A. A., Lago R. M., (2005), Efficient use of Fe metal as an electron transfer agent in a heterogeneous Fenton system based on Fe⁰/Fe₃O₄ composites, *Chemosphere*, 60, 1118-1123.
- Moura F. C. C., Oliveira G. C., Araujo M. H., Ardisson J. D., Macedo W. A. A., Lago R. M., Highly reactive species formed by interface reaction between Fe-iron oxides particles: An efficient electron transfer system for environmental applications, *Applied Catalysis A: General*, 307, (2006), 195-204.

- Mozia, S., (2010), "Photocatalytic membrane reactors (PMRs) in water and wastewater treatment. A review", *Separation and Purification Technology*, 73(2), pp. 71-91.
- Munoz I., Rieradevall J., Torrades F., Peral J., Domenech X., (2005), Environmental Assessment of Different Solar Driven Advanced Oxidation Processes", *Sol. Energy*, 79, p. 369.
- Munter R., (2001), Advanced Oxidation Processes – Current Status and Prospects, *Proc. Estonian Acad. Sci. Chem.* 50(2) p. 59.
- Nie Y., Hu C., Zhou L., Qu J., (2008), An efficient electron transfer at the Fe⁰/iron oxide interface for the photoassisted degradation of pollutants with H₂O₂, *Applied Catalysis B: Environmental*, 82, 151-156.
- Nikolaki, M. D., Malamis, D., Pouloupoulos, S. G., Philippopoulos, C. J. (2006), Photocatalytical degradation of 1,3-dichloro-2-propanol aqueous solutions by using an immobilized TiO₂ photoreactor, *Journal of Hazardous Materials* 2006, 137(2), 1189–1196.
- Oh S.H., Kim J.S., Chung J.S., Kim E.J., Hahn S. H., (2005), Crystallization and Photoactivity of TiO₂ Films Formed on Soda Lime Glass by a Sol-Gel Dip-Coating Process, *Chem. Eng. Comm.* 192 (3), 327-335.
- Ong S.T., Lee C.K., Zainal Z., Keng P.S. Ha S.T., (2009), Photocatalytic degradation of basic and reactive dyes in both single and binary systems using immobilized TiO₂, *Journal of Fundamental Sciences*, 5(2), 88-93.
- Orbeci, C., Untea, I., Kopsiaftis, G., (2008), The influence of inorganic species on oxidative degradation of 4-chlorophenol by photo-Fenton type process, *Revista de Chimie* 59(9), 952-955.
- Orbeci, C., Untea, I., Dancila, M., Stefan, D.S., (2010), Kinetics considerations concerning the oxidative degradation by photo-Fenton process of some antibiotics. *Environ. Eng. Manage. J.*, 9, 1-5.
- Ortiz de la Plata G. B., Alfano O. M., Cassano A. E., (2010), Decomposition of 2-chlorophenol employing goethite as Fenton catalyst. I. Proposal of a feasible, combined reaction scheme of heterogeneous and homogeneous reactions, *Applied Catalysis B: Environmental*, 95, 1-13.
- Papp J., Shen H.S., Kershaw R, Dwight K., Wold A., (1993), Titanium(IV) Oxide Photocatalysts with Palladium, *Chem. Mater.* 5, 284;
- Pera-Titus M., Garcia-Molina V., Banos M. A., Gimenez J., Esplugas S., (2004), Degradation of chlorophenols by means of advanced oxidation processes: a general review, *Applied Catalysis B: Environmental*, 47, 219-256.
- Pignatello, J.J., (1992), Dark and photoassisted Fe³⁺ catalyzed degradation of chlorophenoxy herbicides by hydrogen peroxide, *Environ.Sci.Technol.* 26, 944–951.
- Qu J., (2008), Research progress of novel adsorption processes in water purification: A review; *Journal of Environmental Sciences* 201–13.
- Ratiu C., Manea , F. Lazau, C., Grozescu, I. Radovan C., Schoonman, J., Electrochemical oxidation of p-aminophenol from water with boron-doped diamond anodes and assisted photocatalytically by TiO₂-supported zeolite, *Desalination* 260 (2010) 51–56.

- Ratiu C., Manea , F. Lazau, C., Orha, C., Burtica, G., Grozescu, I., Schoonman, J., Photocatalytically-assisted electrochemical degradation of p-aminophenol in aqueous solutions using zeolite-supported TiO₂ catalyst, *Chemical Papers* 65 (3) 289–298 (2011).
- Riga, A., Soutsas, K., Ntampeglotis, K., Karayannis, V., Papapolymerou G., (2007), Effect of System Parameters and of Inorganic Salts on the Degradation Kinetics of Procion Hexl Dyes. Comparison of H₂O₂/uv, Fenton, and photo-Fenton, TiO₂/UV and TiO₂/UV / H₂O₂ processes, *Desalination*, 211, 72-86.
- Pozzo, R., Baltanás, M., Cassano, A., Supported titanium oxide as photocatalyst in water decontamination: *State of the art, Catalysis Today*, 39 (3), 1997, 219-231.
- Rozas, O., Contreras, D., Mondaca, M.A., Pérez-Moya, M., Mansilla, H.D., (2010), Experimental design of Fenton and photo-Fenton reactions for the treatment of amplicillin solutions. *J. Hazard. Mater.* 177, 1025-1030.
- Shimizu N., Ogino C., Farshbaf Dadjour M., Murata T., (2007), Sonocatalytic degradation of methylene blue with TiO₂ pellets in water, *Ultrasonics Sonochemistry*, 14, 184–190.
- Siedlecka, E. M., Wieckowska, A., Stepnowski, P. (2007), Influence of inorganic ions on MTBE degradation by Fenton's reagent, *Journal of Hazardous Materials*, 147, 497–502.
- Spacek, W., Bauer, R., Heisler, G., (1995), Heterogeneous and homogeneous wastewater treatment Comparison between photodegradation with TiO₂ and the photo-Fenton `reaction, *Chemosphere* 30, 477–484.
- Trovó, A.G., Nogueira, R.F.P., Agüera, A., Fernandez-Alba, A.R., Malato, S., (2011), Degradation of the antibiotic amoxicillin by photo-Fenton process – Chemical and toxicological assessment. *Water Res.* 45, 1394-1402.
- Venkata K., Rao S., Subrahmanyam M., Boule P., (2004), Immobilized TiO₂ photocatalyst during long-term use: decrease of its activity, *Applied Catalysis B: Environmental* 49 239–249.
- Vinita M., Dorathi R. P. J., Palanivelu K., (2010), Degradation of 2,4,6-trichlorophenol by photo Fenton's like method using nano heterogeneous catalytic ferric ion, *Solar Energy*, 84, 1613-1618.
- Vlazan P., Vasile M., (2010), Synthesis and characterization CoFe₂O₄ nanoparticles prepared by the hydrothermal method; *Optoelectronics and Advanced Materials-Rapid Communications*; 4; 1307-1309;
- Xu, Hongwu, Zhang, Yiping, Navrotsky, Alexandra, (2001), Enthalpies of formation of microporous titanosilicates ETS-4 and ETS-10, *Microporous and Mesoporous Materials*, 47, 2-3, 285-291.
- Zhou H., Smith, D.W., (2002), Advanced technologies in water and wastewater treatment, *J. Environ. Eng. Sci.* 1: 247–264.
- Zazo J. A., Casas J. A., Mohedano A. F., Gilarranz M. A., Rodríguez J. J., (2005), Chemical Pathway and Kinetics of Phenol Oxidation by Fenton's Reagent, *Environmental Science and Technology*, 39, 9295-9302.
- Wang H., Wang J., (2007), Electrochemical degradation of 4-chlorophenol using a novel Pd/C gas-diffusion electrode, *Applied Catalysis B; Environmental*, 77, 58-65.

Yu Y., Ding Y., Zuo S., Liu J., (2011) Photocatalytic Activity of Nanosized Cadmium Sulfides Synthesized by Complex Compound Thermolysis, *International Journal of Photoenergy*, 1-5;

INTECH

INTECH